UNIVERSIDADE ESTADUAL PAULISTA
"JÚLIO DE MESQUITA FILHO"
Câmpus de São José do Rio Preto

MARCIO AUGUSTO RIBEIRO SANCHES

Valorização do bagaço de malte usando ultrassom e peróxido de hidrogênio: um estudo visando sua estabilização, processamento e conversão em produtos de valor agregado

São José do Rio Preto - SP
2024

MARCIO AUGUSTO RIBEIRO SANCHES

Valorização do bagaço de malte usando ultrassom e peróxido de hidrogênio: um estudo visando sua estabilização, processamento e conversão em produtos de valor agregado

Tese apresentada como parte dos requisitos para obtenção do título de Doutor em Engenharia e Ciência de Alimentos, junto ao Programa de Pós-graduação em Alimentos, Nutrição e Engenharia de Alimentos, do Instituto de Biociências, Letras e Ciências Exatas da Universidade Estadual Paulista “Júlio de Mesquita Filho”, Câmpus de São José do Rio Preto.

Financiadora: CAPES e FAPESP

Orientador: Dr. Javier Telis Romero
Coorientador: Dr. Tiago Carregari Polachini
Coorientador: Dr. Pedro Esteves Duarte Augusto

São José do Rio Preto - SP
2024

S211v

Sanches, Marcio Augusto Ribeiro

Valorização do bagaço de malte usando ultrassom e peróxido de hidrogênio: um estudo visando sua estabilização, processamento e conversão em produtos de valor agregado / Marcio Augusto Ribeiro Sanches. -- São José do Rio Preto, 2024

194 p. : il., tabs.

Tese (doutorado) - Universidade Estadual Paulista (UNESP), Instituto de Biociências Letras e Ciências Exatas, São José do Rio Preto

Orientador: Javier Telis Romero

Coorientador: Tiago Carregari Polachini

1. Brewer's spent grain (BSG). 2. Subproduto agroindustrial. 3. Estabilização. 4. Pré-tratamento. 5. Tecnologias não convencionais. I. Título.

Sistema de geração automática de fichas catalográficas da Unesp. Biblioteca da Universidade Estadual Paulista (UNESP), Instituto de Biociências Letras e Ciências Exatas, São José do Rio Preto. Dados fornecidos pelo autor(a).

Essa ficha não pode ser modificada.

MARCIO AUGUSTO RIBEIRO SANCHES

Valorização do bagaço de malte usando ultrassom e peróxido de hidrogênio: um estudo visando sua estabilização, processamento e conversão em produtos de valor agregado

Tese apresentada como parte dos requisitos para obtenção do título de Doutor em Engenharia e Ciência de Alimentos, junto ao Programa de Pós-graduação em Alimentos, Nutrição e Engenharia de Alimentos, do Instituto de Biociências, Letras e Ciências Exatas da Universidade Estadual Paulista "Júlio de Mesquita Filho", Câmpus de São José do Rio Preto.

Financiadora: CAPES e FAPESP

COMISSÃO EXAMINADORA

Prof. Dr. Javier Telis Romero
UNESP – Universidade Estadual Paulista "Júlio de Mesquita Filho"
Campus de São José do Rio Preto
Orientador

Prof. Dr. Roger Darros Barbosa
UNESP – Câmpus de São José do Rio Preto

Prof. Drª. Christianne Elisabete da Costa Rodrigues
USP – Universidade de São Paulo – Campus de Pirassununga

Prof. Drª. Márcia Cristina Teixeira Ribeiro Vidigal
UFV – Universidade Federal de Viçosa – Campus de Viçosa

Prof. Dr. Jefferson Luiz Gomes Corrêa
UFLA – Universidade Federal de Lavras

São José do Rio Preto - SP
02 de maio de 2024

AGRADECIMENTOS

Agradeço primeiramente a Deus, pela força, fé e por me cercar de pessoas especiais, que me dão força, me apoiam e acreditam em mim.

À minha família, em especial aos meus pais, Marcio e Luciane, minha gratidão pelo exemplo de união, caráter, simplicidade e amor que sempre demonstraram. Agradeço por todo o apoio e incentivo, que foram fundamentais para que eu pudesse chegar até aqui. À minha irmã, Marcela, meu sincero agradecimento por estar sempre ao meu lado, independentemente das circunstâncias. Amo muito vocês.

Agradeço ao meu orientador, Prof. Dr. Javier Telis Romero, por ser não apenas um excelente professor e orientador, mas também por ser um grande amigo ao longo de toda essa trajetória. Você é uma inspiração tanto como profissional quanto como ser humano, e espero um dia poder ser um orientador como você tem sido para mim.

Aos meus coorientadores, Dr. Tiago e Dr. Pedro, minha sincera gratidão pelos ensinamentos e pelo constante apoio desde o início dessa jornada. Agradeço também pela confiança, amizade e motivação que sempre me proporcionaram.

Agradeço a todos os meus amigos pelo apoio e pela presença constante ao longo desta jornada. Em especial, aos amigos da graduação e que continuam ao meu lado, agora também nas pós-graduações espalhadas pelo país: Callebe, Karolyna (mulatta), Eulália e Noadia. Onze anos de amizade significam muito mais do que apenas tempo; são laços que construímos juntos e que guardarei com carinho para sempre.

Aos meus amigos da Unesp/Ibilce, em especial, a Mari, André, Maria Júlia, Carol, Cleberyanne, Rodrigo, Micael, Bianca, Maria Fernanda, Oneide, Marcelo e Adilson, por bons momentos dentro e fora da universidade. Saibam que cada gesto de amizade foi fundamental e será sempre lembrado com carinho.

Aos alunos de iniciação científica (Vitor, Gustavo, Thamires, Nathalia, Beatriz e Emanuelle) que tive oportunidade de coorientar. Aprendi muito com vocês.

A todos os professores e funcionários do Departamento de Engenharia e Tecnologia de Alimentos (DETA-UNESP) por toda dedicação, empenho, conhecimentos transmitidos e por contribuírem para a nossa formação como profissionais, e principalmente, como pessoas. Em especial, agradeço ao professor Dr. Roger, pela oportunidade de acompanhá-lo nas disciplinas de Operações Unitárias III e Laboratório de Engenharia de Processos, por todos os ensinamentos e pela experiencia única na minha carreira como docente. Agradeço também a professora Dra. Andrea, pelo apoio e incentivo constantes, tanto no mestrado quanto no doutorado. Sou profundamente grato por sua amizade e pela energia positiva que sempre me transmitiu.

Gostaria de expressar minha sincera gratidão pelo apoio financeiro concedido pela Fundação de Amparo à Pesquisa do Estado de São Paulo

(FAPESP), por meio do projeto “Emprego do ultrassom de potência para intensificação da conversão de resíduos da indústria cervejeira em produtos de valor agregado”, Processo n° 2022/05272-8. Agradeço também a Coordenação de Aperfeiçoamento de Pessoal de Nível Superior - Brasil (CAPES), pela bolsa de doutorado, cujo Código Financeiro é 001. Esses recursos foram fundamentais para viabilizar este estudo e contribuíram para o seu desenvolvimento e conclusão.

À Universidade Estadual Paulista “Júlio de Mesquita Filho” (UNESP), ao Departamento de Engenharia e Tecnologia de Alimentos (DETA) e a todos que de alguma forma contribuíram com esse trabalho.

RESUMO

O bagaço de malte (BSG) é um coproduto que representa a maior parte dos resíduos gerados pela indústria cervejeira, totalizando cerca de 85%. A fim de maximizar o aproveitamento dessa biomassa e promover a economia circular, é fundamental abordar os desafios que permeiam desde sua estabilização inicial até o uso final desse recurso. Entre esses desafios, destaca-se a necessidade de aprimorar as etapas de pré-tratamento para viabilizar a conversão do BSG em produtos de valor agregado. Nesse contexto, a presente tese de doutorado tem como objetivo geral avaliar os diversos processos envolvidos desde a estabilização até os pré-tratamentos utilizando peróxido de hidrogênio alcalino (AHP) e/ou ultrassom de alta intensidade (US), visando melhorar a extração de proteínas e aumentar a acessibilidade do BSG pré-tratado para facilitar sua sacarificação subsequente. Inicialmente, foram investigadas as propriedades de sorção de água do BSG, com o intuito de preparar e estabilizar a biomassa para as etapas seguintes. Em seguida, analisou-se o efeito do processamento com diferentes concentrações de AHP (1–8%) e BSG (2–8%), submetidos a diferentes tempos de processamento (0–12 h), na composição química, morfologia, cristalinidade, modificações de grupos funcionais e comportamento reológico das suspensões de BSG ao longo do processamento. Posteriormente, avaliou-se a extração de proteínas do BSG utilizando ultrassom (1200 W) e peróxido de hidrogênio alcalino (3%), bem como seu impacto no rendimento da extração, propriedades estruturais (morfologia por SEM; estruturas secundárias por FTIR e tamanho dos cristais por DRX do concentrado proteico) e tecno-funcionais (capacidade de retenção de água e de óleo, capacidade de formação e estabilidade da emulsão e de espuma e cor instrumental). Em relação as propriedades de adsorção de água do BSG obtido do processo cervejeiro à base de malte de cevada (“Lager” – BSGL) e de trigo (“Weiss” – BSGW), o aumento da umidade relativa e a redução da temperatura levaram a um aumento na umidade de equilíbrio dos BSGs. As propriedades de ligação à água foram ligeiramente prejudicadas pelos maiores teores de proteína observados em BSGW. O modelo GAB foi eficaz na descrição das isotermas de adsorção, fornecendo informações sobre a umidade da monocamada em uma ampla faixa de temperatura. As análises termodinâmicas evidenciaram que os processos de

adsorção foram impulsionados pela entalpia e não ocorreram espontaneamente. Uma umidade relativa de 40% foi identificada como ideal para o armazenamento dos BSGs. No que diz respeito ao processamento com AHP, observou-se que o aumento da concentração de AHP e o tempo de processamento melhoraram a remoção de proteínas, lignina e extrativos do BSG, resultando em mudanças morfológicas que indicam um aumento da acessibilidade do material. Além disso, as suspensões de BSG apresentaram comportamento não newtoniano, com aumento da resistência ao fluxo devido ao incremento da concentração de AHP, BSG e, principalmente, tempo de processamento, o que estão relacionadas com as mudanças estruturais das partículas. Por sua vez, as diferentes estratégias envolvendo ultrassom e AHP demonstraram melhorias no rendimento de extração e impactaram positivamente as propriedades estruturais e tecno-funcionais dos concentrados proteicos. A utilização dessas abordagens promissoras mostra-se como uma maneira eficaz de intensificar a extração de proteínas e aumentar a acessibilidade do BSG pré-tratado, podendo facilitar sua subsequente sacarificação. Em conclusão, o uso de AHP e/ou US apresenta-se como uma abordagem promissora para melhorar a extração de proteínas e aumentar a acessibilidade do BSG pré-tratado, contribuindo para sua utilização eficiente e agregando valor a esse coproduto da indústria cervejeira.

Palavras-chave: Conservação**,** Armazenamento**,** Proteínas, Açúcares, Biorrefinaria, Biomassa lignocelulósica, Pré-tratamento.

ABSTRACT

Brewer's spent grain (BSG) is a co-product that represents the majority of waste generated by the brewing industry, totaling around 85%. In order to maximize the use of this biomass and promote the circular economy, it is essential to address the challenges that permeate from its initial stabilization to the final use of this resource. Among these challenges, the need to improve the pre-treatment steps to enable the conversion of BSG into value-added products stands out. In this context, the general aim of this doctoral thesis is to evaluate the various processes involved, from stabilization to pre-treatments using alkaline hydrogen peroxide (AHP) and/or high-intensity ultrasound (US), aiming to improve protein extraction and increase the accessibility of pretreated BSG to facilitate its subsequent saccharification. Initially, the water sorption properties of BSG were investigated, with the aim of preparing and stabilizing the biomass for the following steps. Next, the effect of processing with different concentrations of AHP (1–8%) and BSG (2–8%), subjected to different processing times (0–12 h), on the chemical composition, morphology, crystallinity, functional group modifications, and rheological behavior of BSG suspensions throughout the processing was analyzed. Subsequently, the extraction of proteins from BSG was evaluated using ultrasound (1200 W) and alkaline hydrogen peroxide (3%), as well as their impact on extraction yield, structural properties (morphology by SEM; secondary structures by FTIR and size of crystals by XRD of the protein concentrate) and techno-functional (water and oil holding capacity, emulsion capacity and stability, foam capacity and stability, instrumental color). Regarding the water adsorption properties of BSG obtained from the brewing process based on barley malt (“Lager” – BSGL) and wheat (“Weiss” – BSGW), the increase in relative humidity and the reduction in temperature led to an increase in the equilibrium moisture of BSGs. The water-binding properties were slightly impaired by the higher protein contents observed in BSGW. The GAB model was effective in describing the adsorption isotherms, providing information about the monolayer moisture over a wide temperature range. Thermodynamic analyses showed that the adsorption processes were driven by enthalpy and did not occur spontaneously. An environment with relative humidity of 40% was identified as ideal for the storage of BSGs. With regard to alkaline processing with hydrogen

peroxide (AHP), it was observed that increasing AHP concentration and processing time improved the removal of proteins, lignin, and extractives from BSG, resulting in morphological changes that indicate increased accessibility of the material. Furthermore, the BSG suspensions showed non-Newtonian behavior, with increased resistance to flow due to the increase in the concentration of AHP, BSG, and, mainly, processing time, which are related to the structural changes of the particles. In turn, the different strategies involving ultrasound and AHP demonstrated improvements in extraction yield and positively impacted the structural and techno-functional properties of protein concentrates. The use of these promising approaches proves to be an effective way to intensify protein extraction and increase the accessibility of pretreated BSG, which can facilitate its subsequent saccharification. In conclusion, the use of alkaline hydrogen peroxide (AHP) and/or high intensity ultrasound (US) presents itself as a promising approach to improve protein extraction and increase the accessibility of pretreated BSG, contributing to its utilization efficient and adding value to this co-product of the brewing industry.

Keywords: Conservation, Storage, Proteins, Sugars, Biorefinery, Lignocellulosic biomass, Pre-treatment.

LISTA DE FIGURAS

LISTA DE TABELAS

SUMÁRIO

1. INTRODUÇÃO GERAL

O bagaço de malte (BSG) é um resíduo agroindustrial de grande potencial e necessidade de tratamento, uma vez que representa 85% do total de resíduos gerado na indústria cervejeira (Borel et al., 2018). Ele é constituído pela parte sólida de casca e do endosperma amiláceo residual dos grãos de malte obtidos após a filtração do mosto (Mello and Mali, 2014). O BSG é um coproduto rico, principalmente em celulose (15-25%; base seca - bs), hemicelulose (20-40; bs), proteínas (15-25%; bs), lignina (10-20; bs) e compostos bioativos com atividade antioxidante (Agrawal et al., 2023) – fato que o caracteriza como fonte de compostos de interesse comercial. Enquanto a fração proteica vem apresentando grande interesse como ingrediente de fonte vegetal de inúmeras funcionalidades e aplicabilidades, o resíduo fibroso representa um matéria-prima viável para produção de etanol de segunda geração.

Embora o BSG seja um material rico em frações de interesse industrial, são necessárias abordagens adequadas para estabilizá-lo antes do seu tratamento e uso. Revisões sobre o assunto relataram que os principais desafios para o correto aproveitamento do BSG são a composição e a alta umidade. Esses fatores o tornam suscetível ao crescimento e deterioração microbiana, além de elevam os custos de transporte do BSG úmido e/ou os custos de secagem (Pabbathi et al., 2022). Dessa forma, os estudos devem ser inicialmente direcionados para otimizar essas etapas.

Para tanto, algumas informações são necessárias para o correto dimensionamento dos equipamentos e processos de secagem, bem como para escolher a melhores condições de armazenamento e prever a estabilidade do coproduto. As isotermas de sorção de água relacionam a umidade de equilíbrio do produto (X_{eq}) e sua correspondente atividade de água (a_w), em cada temperatura, fornecendo informações sobre a disponibilidade e interações entre as moléculas de água e os componentes da matriz sólida (Freitas et al., 2016). Além das isotermas, as propriedades termodinâmicas resultantes também se mostram relevantes para projetar os secadores, determinar a energia necessária no processo de secagem, avaliar a microestrutura do alimento, estudar a água

adsorvida e fenômenos físicos que ocorrem na superfície do alimento (Corrêa et al., 2017).

Após a estabilização do BSG, o próximo desafio é superar o caráter recalcitrante da biomassa lignocelulósica do BSG que impede a extração de compostos ou sua própria despolimerização. Devido à complexa matriz de lignocelulose, formada principalmente por uma estrutura espessa de hemicelulose e lignina que envolve as moléculas de celulose (Saravanan et al., 2022), o acesso dos reagentes e/ou enzimas é dificultado. Nesse sentido, etapas adequadas e eficientes de pré-tratamento são exigidas para possibilitar o melhor aproveitamento do resíduo com menor impacto ambiental.

Na literatura, os métodos de pré-tratamento para melhorar a acessibilidade do material lignocelulósico podem ser categorizados em quatro grupos: métodos físicos, químicos, físico-químicos e biológicos (Kumar et al., 2020). Atualmente, estes métodos são combinados de forma a melhorar e intensificar o rendimento e produtividade (Hassan et al., 2018).

O peróxido de hidrogênio alcalino (AHP) é um método químico que tem despertado interesse como pré-tratamento de diversas biomassas lignocelulósica. Além de ser capaz de sacarificar diferentes biomassas (Ho et al., 2019), o pré-tratamento com AHP pode promover o aumento da solubilidade de proteínas (Yoshida and Prudencio, 2020). No entanto, antes de explorar a conversão do BSG em produtos de valor agregado, é essencial realizar estudos para avaliar o impacto do tempo de processamento alcalino com peróxido de hidrogênio (AHP) na composição química, estrutura do BSG e propriedades reológicas das suspensões resultantes. Essa análise prévia é fundamental para entender o efeito do AHP no aproveitamento do BSG.

A atuação do AHP pode ser ainda mais intensificada pela utilização de tecnologias combinadas. O ultrassom de potência (US), por exemplo, é um pré-tratamento físico emergente que vem sendo usado para reduzir o tamanho de partícula da biomassa e aumentar área de superfície de contato do material (Kumari and Singh, 2018). Por consistirem em ondas sonoras em uma frequência acima de 20 kHz e intensidades acima de 1 W/cm² (Bhargava et al., 2021), sua energia é suficiente para romper ligações intermoleculares. Esse efeito é capaz de alterar propriedades estruturais e favorecer reações químicas (Villamielet al. 2017), intensificando a quebra das ligações éteres entre a hemicelulose e a

lignina e atuando como intensificador de reações secundárias ocorrendo simultaneamente.

Dessa forma, o pré-tratamento combinado com AHP e US pode facilitar a penetração de reagentes e/ou enzimas na estrutura do BSG e, assim, melhorar a extração de proteínas e/ou a hidrólise enzimática do BSG para liberação de açucares fermentescíveis. No entanto, é importante salientar que, no que diz respeito às proteínas, embora essas técnicas combinadas possam aumentar o rendimento da extração, ainda existem incertezas sobre os efeitos delas nas propriedades estruturais e tecnológico-funcionais das proteínas extraídas.

2. OBJETIVOS

2.1. Objetivo geral

O objetivo geral desta tese de doutorado foi avaliar os diferentes estágios envolvidos no processo, desde a estabilização inicial do bagaço de malte até os pré-tratamentos utilizando peróxido de hidrogênio alcalino (AHP) e/ou ultrassom de alta intensidade (US), com o propósito de melhorar a extração de proteínas e aumentar a acessibilidade do BSG pré-tratado para facilitar sua sacarificação subsequente.

2.2. Objetivos específicos

Como parte do desenvolvimento do objetivo geral, a tese buscou especificamente:

• Caracterizar quimicamente bagaços de malte de duas indústrias cervejeiras, resultantes do processamento de cerveja tipo “Pilsen” e cerveja tipo “Weissbier”.

• Determinar as isotermas de sorção e propriedades termodinâmicas do bagaço de malte em condições aplicadas durante o armazenamento e secagem;

• Avaliar o impacto do processamento alcalino com diferentes concentrações de BSG (2–8%), AHP (1–8%) em diferentes tempos de processamento (0–12 h) na composição química, estrutura e propriedades reológicas das suspensões de BSG;

• Avaliar a eficiência das diferentes condições de pré-tratamento com peróxido de hidrogênio alcalino (AHP) e ultrassom de alta intensidade (US) no rendimento de extração, propriedades estruturais e tecno-funcionais das proteínas do bagaço de malte.

3. ORGANIZAÇÃO DA TESE

A Figura 1 apresenta o plano de trabalho de acordo com as etapas iniciais da tese de doutorado até a sua conclusão. A tese foi constituída de quatro capítulos que abordaram desde a revisão da literatura até a obtenção dos produtos de valor agregado. No Capítulo 1 foram apresentados os principais desafios encontrados para o aproveitamento integral do bagaço de malte e sua conversão em produtos de valor agregado através de uma revisão bibliográfica da literatura.

Nos Capítulos 2 e 3 foram estudadas as etapas e ferramentas essenciais para a gestão e o aproveitamento do bagaço de malte, a fim de fornecer informações úteis para seu manejo até o processamento. O Capítulo 2, especificamente, apresenta a composição química (celulose, hemicelulose, lignina, proteínas, extrativos, cinzas) e as propriedades de sorção de água do bagaço de malte proveniente de dois tipos de processamento de cerveja. Foram determinadas as isotermas de sorção de água avaliando condições de armazenamento (5-40 °C) e de secagem (50-90 °C), bem como suas propriedades termodinâmicas de sorção de água (pressão de espalhamento, área de superfície de sorção, calor de sorção, entalpia, entropia e avaliação da teoria da compensação). No Capítulo 3, investigou-se o impacto do processamento alcalino com peróxido de hidrogênio (AHP) na composição química, estrutura e propriedades reológicas do bagaço de malte. Suspensões com diferentes concentrações de BSG (2–8%) e AHP (1–8%) foram submetidas a diferentes tempos de processamento (0–12 h). A composição química, morfologia, cristalinidade, modificações de grupos funcionais e comportamento reológico do BSG foram avaliados ao longo do processamento.

Por fim, foi estudado no Capítulo 4 o impacto do pré-tratamento combinado com peróxido de hidrogênio alcalino e ultrassom de potência para extração de proteínas do bagaço de malte, além dos efeitos em suas propriedades estruturais e tecno-funcionais.

Figura 1. Organização dos capítulos da presente tese de doutorado.

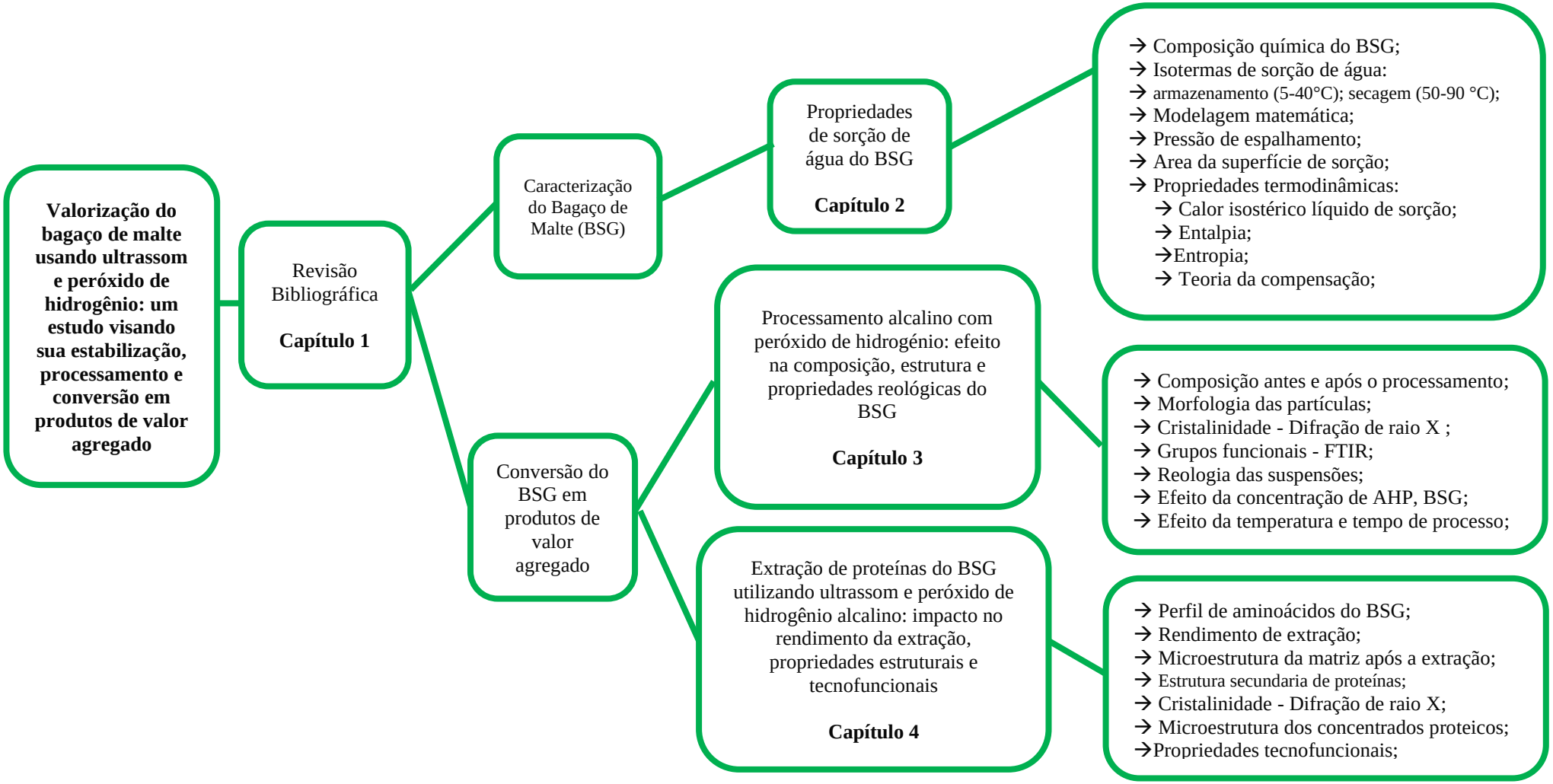

CAPÍTULO 1

Além da alimentação animal: novas fronteiras na conversão do bagaço de malte em produtos de valor agregado

Artigo de Revisão

Será elaborada uma versão em inglês para submissão ao periódico.

Marcio Augusto Ribeiro-Sanches[1*], Pedro Esteves Duarte Augusto[2], Tiago Carregari Polachini[1], Javier Telis-Romero[1]

[1]Food Engineering and Technology Department, São Paulo State University, Institute of Biosciences, Humanities and Exact Sciences (Ibilce), Campus São José do Rio Preto, São Paulo, 15.054-000, Brazil.

[2]Université Paris-Saclay, CentraleSupélec, Laboratoire de Génie des Procédés et Matériaux, Centre Européen de Biotechnologie et de Bioéconomie (CEBB), 3 rue des Rouges Terres 51110 Pomacle, France.

*Author to whom correspondence may be addressed. E-mail address: mar.sanches@unesp.br (Marcio Augusto Ribeiro Sanches).

RESUMO

O bagaço de malte (BSG), principal subproduto da indústria cervejeira, é composto principalmente por carboidratos (celulose e hemicelulose), proteínas e lignina. Apesar de sua abundância e potencial como matéria-prima, o BSG atualmente é subutilizado, sendo destinado principalmente à alimentação animal ou aterros sanitários. No entanto, seu baixo custo, alto volume e composição tornam-no uma fonte promissora e renovável para o desenvolvimento de biorrefinarias. Neste contexto, esta revisão aborda o processo de produção de cerveja, a geração do BSG, suas características e os principais desafios

enfrentados para sua preservação. Além disso, são destacadas algumas etapas de pré-tratamento destinadas a melhorar a acessibilidade dos componentes do material. A revisão também enfatiza potenciais aplicações em alimentos processados para consumo humano, visando a reformulação de produtos com propriedades funcionais, a recuperação de compostos bioativos, proteínas e a conversão da fração lignocelulósica em açúcares fermentescíveis, além de explorar outras aplicações biotecnológicas. São abordados tanto métodos convencionais quanto emergentes, todos voltados para a valorização do BSG e a garantia da máxima recuperação de recursos.

Keywords: Subproduto agroindustrial; Recuperação de recursos; Estabilização; Pré-tratamento; Tecnologias não convencionais.

1. INTRODUÇÃO

A cerveja é uma das bebidas mais consumidas e apreciadas em todo o mundo (Leichtweis et al., 2021; Yang and Gao, 2021; Yang et al., 2021b). Ela é tradicionalmente feita com apenas quatro ingredientes básicos: água, malte, lúpulo e fermento (Gasiński et al., 2021). Em 2018, a produção mundial de cerveja foi de aproximadamente 1,9 bilhão de litros (Yang and Gao, 2021; Yang et al., 2021b). Grande parte destas cifras tem sido atribuída à crescente popularidade das cervejas artesanais nos últimos anos. A cerveja artesanal é definida como cerveja produzida em “qualquer pequena cervejaria independente, que adere às práticas e ingredientes tradicionais da fabricação de cerveja” (Jaeger et al., 2020). Esse tipo de cervejaria tem se concentrado na produção de cervejas diferenciadas, autênticas e de alta qualidade, com características sensoriais diferentes das cervejas produzidas por grandes indústrias disponíveis no mercado consumidor (Nunes Filho et al., 2021).

Independente se a produção é industrial ou artesanal, o malte, sem dúvida, é um dos ingredientes responsável por características sensoriais como cor, sabor e aroma característico da bebida, além de ser essencial para a produção de cerveja (Machado et al., 2020). Comumente confundido com outros alimentos, o malte é originado a partir de qualquer tipo de cereal como o trigo, centeio, arroz, milho e a própria cevada.

O processo de malteação garante que o grão desenvolva as enzimas necessárias para a conversão do endosperma amiláceo do cereal em açúcares fermentescíveis, tais como as amilases. Este processo se dá por meio da germinação, de qualquer cereal, sob condições controladas (Carvalho et al., 2018). Os grãos devem passar por uma captação inicial de água para quebrar a dormência do cereal, seguido de germinação parcial ou completa sob baixas temperaturas. Quando o nível de germinação desejado é alcançado, o cereal germinado (malte verde) passa por secagem para preservar e estabilizar suas enzimas (Guimarães et al., 2020). Após a secagem, a radícula e o caulículo são retirados, dando origem ao malte que será usado pela indústria cervejaria.

O bagaço de malte representa 85% do total de resíduos gerados na indústria cervejeira (Borel et al., 2018). Ele é principalmente constituído pela casca e endosperma amiláceo residual do malte (Mello and Mali, 2014). Cerca de 20 kg de bagaço de malte úmido são gerados para cada 100 litros de cerveja produzida (Lynch et al., 2016). Visto que em 2018 a produção mundial de cerveja foi de aproximadamente 1,9 bilhão de litros (Yang and Gao, 2021; Yang et al., 2021b), é esperado uma produção de resíduos do malte em torno de 200 mil toneladas.

2. GERAÇÃO DO BAGAÇO DE MALTE

Após a obtenção do malte, o processo de produção de cerveja pode ser dividido em três fases: a) Produção do mosto - onde envolve a moagem do malte, mosturação, filtração, fervura e clarificação do mosto; b) Processo fermentativo – subdividido em fermentação e maturação; c) Acabamento da cerveja – envolve operações de filtração, carbonatação e pasteurização (Aquarone et al., 2001).

A etapa inicial de produção do mosto é a fase responsável pela geração do bagaço de malte. Na moagem, tem-se por objetivo triturar o malte, expondo o endosperma amiláceo à ação enzimática. Posteriormente, as matérias-primas cervejeiras (água, malte, lúpulo) são submetidas à etapa de mosturação, cuja finalidade é extrair para o mosto os extratos solúveis e as enzimas contidas no malte. A mosturação consiste em submeter o mosto a três diferentes faixas de temperatura.

Figura 1. Fluxograma do processamento industrial de cerveja.

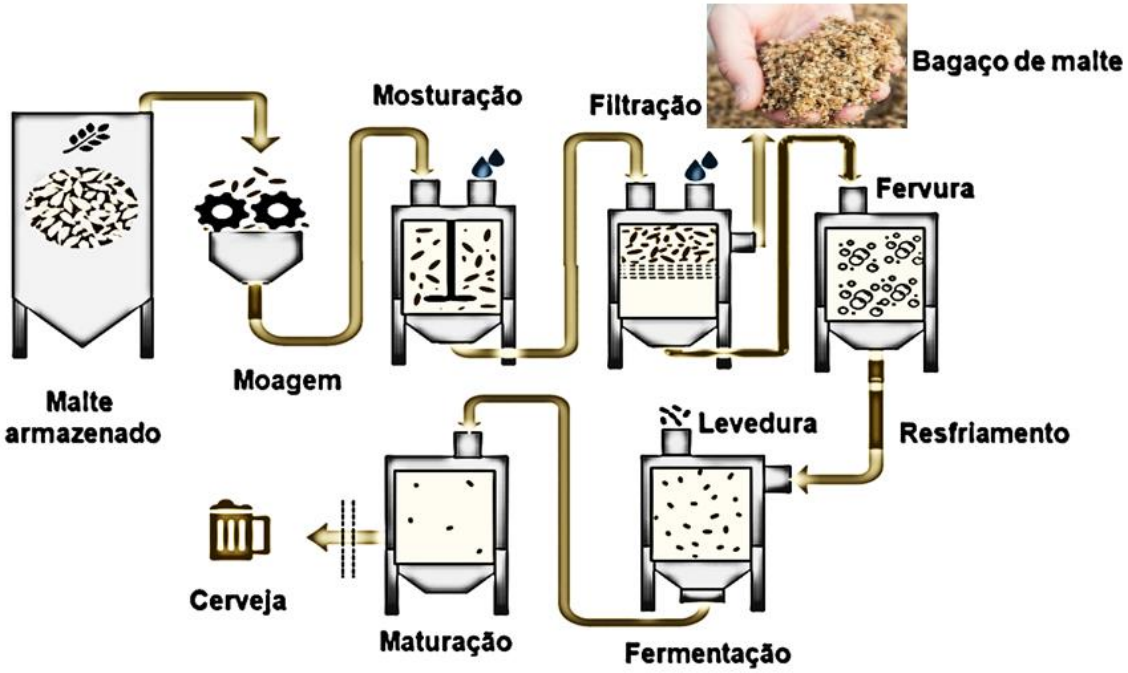

Fonte: Adaptado de Qazanfarzadeh et al. (2023).

Inicialmente o mosto começa a ser extraído a 40 °C. Posteriormente, a temperatura do mosto é elevada para 52-54 °C. Após um breve período, a temperatura é elevada novamente até a mistura atingir 65°C. Uma cocção final elevará a temperatura do mosto a 73-76 °C. Esta sequência de temperaturas proporciona ótimas condições para a hidrólise das proteínas do grão em aminoácidos metabolizáveis pelas leveduras (40-54 °C), para a hidrólise do amido, pelas amilases, (54-65 °C) e finalmente (73-76 °C) para a separação do mosto. Após a mosturação, a fração líquida do mosto deve ser separado da parte sólida insolúvel através da etapa de filtração. Neste momento, a torta de filtro é recuperada na forma de um coproduto, comumente chamado de bagaço de malte (BSG) úmido. Após essa etapa, o mosto segue para as etapas subsequentes até a obtenção da cerveja.

3. CARACTERÍSTICAS DO BAGAÇO DE MALTE

A Tabela 1 apresenta os componentes do BSG conforme relatado por diferentes estudos. Por apresentar alta umidade (~70–80% (Lynch et al., 2016)) e alta quantidade de matéria orgânica, o bagaço de malte apresenta alguns obstáculos para o seu reaproveitamento.

Tabela 1. Composição química de diferentes bagaços de malte (BSG).

Amido (% db)	Neutral detergent fiber (% bs)	Acid detergent fiber (% bs)	Celulose (% bs)	Hemicelulose (% bs)	Lignina (% bs)	Proteínas (% bs)	Lipídeos (% bs)	Cinzas (% bs)	Extrativos (% bs)	Umidade (% bu)	Referências
ND	ND	ND	15.4 – 15.8	28.1 – 28.4	19.6 - 20.6	21.4 - 24.1	ND	3.6 – 3.8	8.3	ND	(Sanches et al., 2023a)
ND	ND	ND	18.4	15.1	27.4	22.3	10.0	3.6	ND	ND	(Cassoni et al., 2023a)
ND	ND	ND	28.7	17.5	16.9	21.4	ND	3.7	13.1	ND	(Sibhatu et al., 2021a)
20.88	ND	ND	17.52	25,31	ND	22,65	ND	ND	ND	76.43	(Parchami et al., 2021a)
ND	44.7	19.8	ND	ND	11.3	22.9	8.5	4.3	ND	ND	(He et al., 2019)
33.1	32.3	5.9	ND	ND	ND	18,7	6,3	3,2	ND	77.1	(Jin et al., 2022)
ND	ND	ND	ND	ND	15.0	23.0	11.0	4.0	ND	ND	(Rommi et al., 2018)
4.10	ND	ND	14.0	32.0	20.8	22.1	6.2	3.3	14.5	ND	(Alonso-Riaño et al., 2023)
ND	ND	ND	16.44	25.81	12.36	15.52	3.58	2.42	ND	ND	(Santos et al., 2024)

*ND = Não determinado; bs = base seca; bu = base úmida.

A alta umidade do bagaço eleva os custos de transporte e, juntamente com sua composição, o torna suscetível ao crescimento e deterioração microbiana. Dessa forma, a secagem e estabilização desse bagaço úmido devem ser realizadas de forma a garantir sua qualidade e reduzir custos ao longo da cadeia de suprimento.

O bagaço de malte é considerado um produto heterogêneo devido principalmente às variações de formulações entre as cervejarias e os próprios tipos de cervejas. Sua composição depende de fatores como a variedade e quantidade do cereal, tipo de lúpulo adicionado, a época da colheita, condições de maltagem, maceração e se adjuvantes foram empregados (Ibarruri et al., 2019; Parchami et al., 2021b).

No geral, estudos mostraram que o bagaço de malte apresenta composição variável em termo de: proteínas (15,5–24.1%), lignina (15,0–27,4%), cinzas (2,4–4,3%), carboidratos (80,5–79,3%), fibras (3,3%), lipídios (2,5–10,6%), sendo os resultados expressos em base seca. Do percentual de carboidratos, pode-se considerar a presença de celulose (14,0–28,7%), hemicelulose (15,1–32,0%), além de outros polissacarídeos como o próprio amido não hidrolisado (Lynch et al., 2016; Roth et al., 2019).

Embora esse resíduo seja altamente rico em proteínas e polissacarídeos, ele é atualmente utilizado na alimentação animal com baixo valor de mercado (Buffington, 2014). Além disso, a oferta como ração para gado muitas vezes pode superar a demanda, resultando em um alto volume de bagaço excedente (Lynch et al., 2016). Devido à sua abundância e suas características de composição supracitadas, o bagaço de malte apresenta-se como potencial matéria-prima a ser avaliada para conversão em produtos de valor agregado a partir de processos adequados. Além de se mostrar uma importante fonte de proteínas de origem vegetal, os polissacarídeos presentes também podem ser utilizados como matéria-prima para produção de biocombustíveis como o etanol de segunda geração, embalagens sustentáveis de alimentos (Qazanfarzadeh et al., 2023), síntese de xilitol e produção de enzimas por microrganismos; A lignina, um biopolímero subutilizado, também tem se mostrado como matéria prima interessante para a recuperação de compostos antioxidantes e antimicrobianos (Bajwa et al., 2019) e produção de polímeros (polietileno, polipropileno, poliuretano, ácido polilático e, etc.) (Cassoni et al., 2023a). Tais utilizações

contribuem para suprir a atual demanda pela produção de alimentos de origem vegetal e biocombustíveis renováveis, bem como para incentivar a economia circular.

4. PRINCIPAIS DESAFIOS ENCONTRADOS PARA PRESERVAR O BSG

Para utilizar o bagaço de malte em escala industrial e convertê-lo em produtos de valor agregado, é necessário o projeto de um processo de biorrefinaria eficaz e de baixo custo. Para isso, existem vários desafios relacionados ao processo de conversão. Um dos principais desafios é o seu conteúdo inicial de água, que geralmente se encontra entre 70–85% (Lynch et al., 2016; M. V. Santos et al., 2024), tornando-o um coproduto extremamente instável, que se deteriora rapidamente devido a ação microbiana. Robertson et al. (2010) avaliaram a variação da composição química e microbiológica do bagaço de malte de 10 cervejarias. Os resultados mostram que uma microflora residente de bactérias aeróbicas principalmente termofílicas ($<10^7$ UFC/g^{-1} de peso fresco) persiste no BSG. Esta população microbiana é suscetível a mudanças rápidas após a geração do BSG, indicando que o BSG deve ser estabilizado e armazenado em condições adequadas para ser posterior utilização.

Alguns estudos abordaram diferentes métodos de conservação para prolongar o tempo de armazenamento do bagaço de malte. O estudo de Al-Hadithi, Muhsen & Yaser (1985) avaliou a possibilidade de utilização de ácidos orgânicos (ácidos benzóico, acético, fórmico e lático) como conservantes deste coproduto. O ácido fórmico e benzóico se mostraram eficazes. Outro estudo demonstrou que o uso de sorbato de potássio também foi eficaz na conservação do BSG prensado (Kuntzel e Sonnenberg, 1997). Entretanto, os processos de secagem e/ou estocagem em ambientes de baixa umidade relativa ainda se apresentam como métodos mais eficientes e exequíveis nas diferentes escalas de produção.

Bartolomeé et al. (2002) avaliaram três diferentes métodos de conservação (liofilização, secagem em estufa e congelamento) sobre o conteúdo de pentoses totais (xilose e arabinose) e ácido hidroxicinâmico (ácidos ferúlico e *p* - cumárico) do BSG. Os autores relataram que o congelamento reduziu o teor de arabinose, quando comparado ao conteúdo presente no BSG seco em estufa

e por liofilização. Além disso, dentre estes métodos estudados, a secagem por convecção parece ser o método mais viável para a secagem do BSG, visto que, o congelamento é inadequado porque grandes volumes devem ser armazenados. Além do gasto energético elevado; a liofilização é um processo lento, com alto consumo de energia e equipamentos utilizados.

Recentemente, Thai et al. (2022) compararam o impacto da secagem por infravermelho e secagem por ar quente sobre a composição química e os compostos bioativos do BSG. Os métodos de secagem não apresentaram efeito significativo na composição centesimal, compostos fenólicos e capacidade antioxidante do BSG – fato que reforça o uso de uma secagem convencional de menor custo para estes fins.

De fato, a secagem convectiva (Mallen and Najdanovic-Visak, 2018; M. V. Santos et al., 2024; Stroem et al., 2009; Tang et al., 2005, 2004; Thai et al., 2022) se mostra como alternativa mais viável para a preservação do BSG, reduzindo o seu volume e, consequentemente, os custos de transporte, além de prolongar sua vida útil e facilitar o armazenamento para futuras aplicações industriais. Os parâmetros como a temperatura do ar de secagem, a umidade relativa e a velocidade do ar são os principais parâmetros extrínsecos que influenciam a taxa de secagem (Aghilinategh et al., 2015). Variáveis intrínsecas do material, tais como porosidade, estrutura e propriedades físico-químicas também influenciam as taxas de secagem (Uribe et al., 2014). Dependendo da natureza dos produtos a serem tratados, sejam alimentos ou coprodutos, estes métodos provam ser mais ou menos adaptados.

O estudo de Santos et al. (2024) buscou estabelecer condições seguras de processamento do bagaço de malte para uso como ingrediente funcional. Os autores determinaram que um teor de umidade de 15% (b.s.) ($a_w \leq 0,93$) evita o crescimento de *Bacillus cereus* durante o armazenamento. A secagem em temperaturas de 100°C por 21 min com uma espessura de leito de 1 cm, garantiram uma letalidade de 99% em Bacillus cereus.

Como a secagem é um processo que geralmente apresenta um gasto energético alto, impactando diretamente sobre a viabilidade econômica do projeto de biorrefinaria, é necessário conhecer especificamente a cinética do processo e seus mecanismos envolvidos para promover a secagem e estabilização do BSG, além de minimizar os gastos energéticos. Nesse sentido,

o conhecimento das isotermas e das propriedades termodinâmicas de sorção de água do BSG são necessárias para o projeto adequado dos secadores e das condições de operação. Elas permitem conhecer a umidade de equilíbrio da matriz em uma determinada temperatura de processo, determinar a energia necessária no processo de secagem, avaliar a microestrutura do alimento e o grau de interação entre as moléculas de água e uma dada matriz.

Sanches et al. (2023) avaliaram as propriedades de sorção de água de BSGs de dois diferentes processamentos cervejeiros (estilo “Lager” e “Weiss”) em uma ampla faixa de umidade relativa (5,20-98,5%) e duas faixas de temperaturas: as aplicadas em condições de armazenamento (5-40 ºC) e as mais utilizadas para secagem do subproduto (50-90 ºC). Os autores relataram que a umidade de equilíbrio aumentou com o aumento da umidade relativa e a redução da temperatura. O modelo GAB mostrou-se mais adequado para descrever as isotermas de adsorção dos BSGs, fornecendo dados sobre a umidade da monocamada em uma ampla faixa de temperatura. A análise termodinâmica indicou que o calor isostérico líquido de adsorção, a entropia e a entropia (em módulo), aumentaram com a redução da umidade de equilíbrio do material, indicando que mais energia é necessária para remover as moléculas de água à medida que o material perde umidade. Do ponto de vista energético e de estabilidade, uma atividade de água de 0,4 foi identificada pelos autores como a condição ideal para o armazenamento de BSGs. Portanto, sugere-se que esse subproduto seja armazenado em ambientes com umidade relativa de 40%, o que pode contribuir para uma maior vida útil e para futuras aplicações em biorrefinaria e/ou aplicações alimentícias.

5. PRÉ-TRATAMENTO DO BSG

Partindo de um material estabilizado, o pré-tratamento da biomassa lignocelulósica é a etapa crucial subsequente no processo de biorrefinaria (Wang and Lee, 2021). A lignina, embora não seja composta por carboidratos, é constituída por complexas ligações reticuladas entre cadeias aromáticas de álcoois, que contêm grupos hidroxila e metoxila (Baruah et al., 2018). Esta estrutura complexa reduz significativamente a acessibilidade das proteínas, celulose e hemicelulose às enzimas e aos agentes químicos. Devido à especificidade das ligações da lignina, sua remoção é um desafio, dificultando a

extração de compostos de interesse, assim como a conversão eficiente da celulose e hemicelulose em açúcares fermentescíveis de baixo peso molecular (KUMAR et al., 2020). Portanto, pré-tratamentos eficazes, visando a remoção ou modificação da lignina, tornam-se indispensáveis nesse contexto.

A Figura 2 mostra a estrutura do material lignocelulósico antes e após a realização do pré-tratamento. Para o melhor aproveitamento da composição da biomassa lignocelulósica, a etapa de pré-tratamento faz-se necessária. Ele auxilia na redução da natureza recalcitrante da biomassa, tornando as frações da lignocelulose mais acessíveis às enzimas e agentes químicos (Wang and Lee, 2021).

Figura 2. Estrutura do material lignocelulósico antes e após a realização do pré-tratamento.

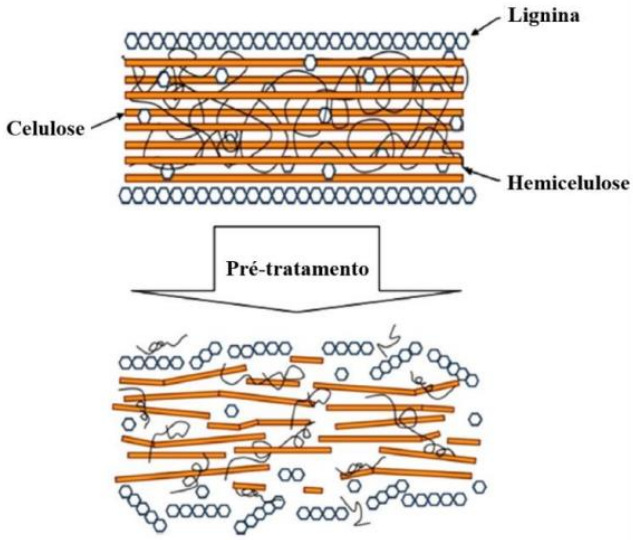

Fonte: Adaptado de Haghighi Mood et al. (2013).

Na literatura, os métodos de pré-tratamento para melhorar a acessibilidade do material lignocelulósico podem ser categorizados em quatro grupos: métodos físicos, químicos, físico-químicos e biológicos (Kumar et al., 2020). Atualmente, estes métodos são combinados de forma a melhorar e intensificar seu rendimento e produtividade (Hassan et al., 2018). Ainda, o uso das chamadas tecnologias emergentes como micro-ondas, irradiação, campos elétricos pulsados, ozônio, alta pressão e ultrassom parecem ser tecnologias promissoras, pois podem aumentar a produtividade dos processos convencionais (Haldar and Purkait, 2021; Hoang et al., 2021; Kumar et al., 2020).

No estudo de Rommi et al., (2018) foi investigado o impacto do pré-tratamento termoquímico e do tratamento enzimático no fracionamento de proteína e lignina do BSG. O estudo revelou que a recuperação de lignina do BSG por extração alcalina pode ser consideravelmente ampliada com pré-tratamentos solubilizadores de carboidratos, como a explosão a vapor e a subsequente hidrólise enzimática da parede celular. Estes pré-tratamentos também demonstraram melhorar a recuperação do hidrolisado proteico após o tratamento com protease. No entanto, em termos de evitar a co-extração de lignina, a BSG não tratada pode ser preferível como matéria-prima para a recuperação enzimática de hidrolisados proteicos. A forte co-extração e co-precipitação parcial de proteína e lignina, juntamente com a remoção incompleta de proteína da lignina mesmo após hidrólise completa, sugerem interações substanciais, possivelmente ligações covalentes, entre proteínas e lignina.

O arabinoxilano (AX) é uma classe de polissacarídeos encontrada em abundância na BSG. O estudo realizado por Reis et al. (2015) demonstrou que o AX pode ser extraído do BSG por meio de um processo de ultrassom em duas etapas. Inicialmente, os resíduos foram pré-lavados usando ultrassom com água e, em seguida, tratados em uma solução de hidróxido de potássio (KOH). As condições ideais para a recuperação de AX incluem uma dispersão de BSG em KOH 2 M, com ultrassom a 750 W, 20 kHz e 100% de amplitude, durante 5 minutos. Este método resultou em um resíduo final com cerca de 47% de polissacarídeos, principalmente compostos por arabinose, xilose, ácido urônico e galactose. Além disso, o processo de ultrassom reduziu significativamente o tempo de extração, de 7 horas para apenas 25 minutos, em comparação com métodos convencionais de extração alcalina, mantendo uma eficiência de recuperação de cerca de 60% para o AX.

O uso de micro-ondas como pré-tratamento tem se destacado por facilitar a extração de compostos fenólicos de baixo peso molecular do BSG. Este método é reconhecido por aumentar a porosidade da parede celular, resultando em uma extração mais eficiente e sustentável, com redução do tempo e do uso de solventes. Recentemente Zago et al. (2022), exploraram o pré-tratamento por micro-ondas para a extração desses compostos a partir de BSG, variando o tempo (5, 15 e 30 minutos) e a potência do micro-ondas (600 e 800 W). Os extratos de BSG pré-tratados por micro-ondas apresentaram uma quantidade

significativamente maior de compostos fenólicos de baixo peso molecular, atingindo até 12,5 e 13,23 mg/g db, e de ácido ferúlico, com valores de 34 e 15 µg/g, em 600 W e 30 minutos. Este método provou ser eficaz ao romper as interações entre os compostos fenólicos e a matriz BSG, destacando o tempo como o fator mais importante no processo de extração, enquanto a potência do micro-ondas não demonstrou uma influência significativa na recuperação desses compostos.

A sacarificação da fração fibrosa do BSG está despertando crescente interesse. Em pesquisas recentes, como o estudo conduzido por Wagner et al. (2021), foram investigados os efeitos de diferentes pré-tratamentos físico-químicos, incluindo auto-hidrólise, H_2O_2 e H_2SO_4, na acessibilidade enzimática do BSG. Os resultados revelaram que as modificações estruturais decorrentes dos pré-tratamentos estavam alinhadas com a remoção de hemicelulose e lignina, resultando em uma maior recuperação da biomassa e produtividade de açúcares. Especificamente, o uso de H_2O_2 (peróxido de hidrogênio) em um pH baixo (5,0) demonstrou ser particularmente eficaz, alcançando uma média de 193,35 mg de açúcares por grama de BSG seco. Os autores concluíram que a combinação deste pré-tratamento com a sacarificação enzimática pode ser uma estratégia promissora para otimizar a utilização dos resíduos de BSG.

6. POTENCIAIS APLICAÇÕES PARA O BAGAÇO DE MALTE (BSG)

6.1. Alimentação animal

Devido ao alto teor de fibras e proteínas, o BSG é geralmente usado como ração animal (por exemplo, para peixes, bovinos, suínos, aves, cães) (Bachmann et al., 2022; Jayant et al., 2018; Mussatto, 2014). No entanto, o nível de sua utilização é insuficiente e grande parte do BSG ainda precisa ser gerenciado.

Gebremedhn et al. (2019) avaliaram os efeitos da inclusão do BSG no desempenho de oviposição e parâmetros de qualidade de galinhas. Os autores avaliaram a inclusão do BSG em níveis de 0, 10, 20, 30 e 40%. Os resultados mostraram que até 40% do BSG adicionado na ração não tem efeito significativo na produção e qualidade (albúmen, gema, casca) dos ovos, porém, o custo da ração diminuiu com a adição de BSG.

He et al. (2020) investigaram os efeitos da substituição da farinha de peixe por um produto rico em proteínas (PP) derivado do BSG na dieta do camarão branco do Pacífico, *Litopenaeus vannamei*. A dieta controle (contendo 35% de farinha de peixe) foi comparada com quatro dietas teste: isonitrogênica (44% proteína bruta), isolipídica (10% gordura bruta) e isocalórica (20 kJ/g), que foram formulados com PP para substituir 10%, 30%, 50% e 70% da proteína da farinha de peixe. Até 50% da farinha de peixe substituída por PP não afetou a sobrevivência dos camarões, o desempenho de crescimento, a eficiência de utilização da ração ou o teor de proteína e o perfil de aminoácidos dos camarões. Entretanto, a substituição de 70% afetou negativamente o ganho percentual de peso e a taxa de crescimento específico dos camarões. Portanto, de acordo com os estudos citados anteriormente, o BSG parece poder ser usado como substituição parcial na alimentação animal para não afetar a produtividade e a qualidade do produto final.

6.2. Inclusão do BSG em alimentos

Outra abordagem é a utilização do BSG em alimentos processados para a alimentação humana. Essa abordagem tem sido amplamente estudada (Cermeño et al., 2021; Czubaszek et al., 2021; Naibaho et al., 2021) principalmente visando a reformulação de produtos com propriedades funcionais. O desenvolvimento de alimentos funcionais e novas fontes de ingredientes são questões de interesse mundial, especialmente para profissionais da área da saúde, cientistas e engenheiros de alimentos. Entretanto, a inserção deste coproduto em matrizes alimentares pode provocar mudanças nas propriedades físico-químicas, tecnológicas, reológicas, texturais e sensoriais (Cermeño et al., 2021), podendo trazer impacto negativo na aceitabilidade dos produtos. Embora pareça desafiador, estudos envolvendo principalmente a inserção de diferentes quantidades do BSG (Czubaszek et al., 2021) e a modificação físico-química e/ou enzimática do BSG (Zeng et al., 2022) para aplicações em alimentos processados é de extrema importância principalmente para alcançar a melhora das propriedades tecnológicas, bioativas, funcionais e sensoriais destes produtos reformulados, viabilizando juntamente o aproveitamento deste coproduto.

Cermeño et al. (2021) estudaram o impacto da adição de BSG não modificado (BSGA) e BSG enzimaticamente modificado (BSGB) sobre as propriedades reológicas, texturais e sensoriais de muffin, quando substituído em diferentes níveis (5, 10 e 15%). A avaliação reológica mostrou uma redução benéfica da viscosidade para a massa contendo BSGB quando comparado ao BSGA. Os muffins contendo BSGB apresentaram dureza reduzida e coloração mais escura quando comparado aos muffins contendo BSGA e sem adição de BSG (controle). Além disso, a avaliação sensorial verificou que o BSGB pode ser adicionado aos muffins em até 10% sem afetar negativamente a aparência geral, textura, odor e cor, aumentando o teor de fibra dos muffins em comparação com o controle, enquanto a substituição do BSGA não teve efeito significativo até 5%. Os autores encerraram concluindo que a modificação enzimática prévia pode melhorar a funcionalidade do BSG para aplicação em produtos de confeitaria, melhorando o conteúdo de proteínas e fibras destes produtos.

Battistini et al. (2021) relataram que o BSG melhorou a recuperação de potenciais cepas probióticas em leite fermentado após exposição a condições gastrointestinais simuladas in vitro. Os autores relataram que o BSG se mostrou como ingrediente rico em fibras que pode ser empregado numa abordagem simbiótica. A adição de BSG em leite fermentado, isoladamente ou em combinação com *L. paracasei* subsp. *paracasei* F-19®, melhorou a resistência do *Strep. thermophilus* TH-4® para condições do trato gastrointestinal simuladas in vitro, sugerindo uma aplicação prospectiva desta cepa tanto como cultura inicial quanto como cultura probiótica. Entretanto, os autores ressaltam que ensaios in vivo e clínicos são necessários para avaliar os possíveis benefícios à saúde conferidos pelo consumo deste produto.

Özvural et al. (2009) avaliaram a utilização do BSG na produção de salsicha. Diferentes níveis de BSG (0%, 1%, 3% e 5 %) foram usadas em substituição do amido + caseinato de sódio. Além disso, 2% de gordura foi removida da formulação para cada 2% de BSG adicionado. O teor de fibra dietética total das salsichas suplementados com BSG aumentaram à medida que o nível de adição foi aumentado. A aceitabilidade geral diminuiu devido ao aumento do BSG e à redução proporcional no nível de gordura. A pontuação gerais de aceitabilidade para a salsicha controle e as salsichas com BSG foram 7,57 e 5,47-7,02 em uma escala de nove pontos, respectivamente,

demonstrando que o BSG tem alto potencial como fonte de fibra alimentar e pode ser usado como substituto de gordura para a produção de produtos cárneos ricos em fibras e com baixo teor de gordura.

Naibaho et al. (2022a) avaliaram o potencial do BSG na fermentação do iogurte e avaliação do seu impacto no comportamento reológico, consistência, propriedades microestruturais e perfil de acidez durante o armazenamento refrigerado. A adição de BSG encurtou o tempo de fermentação, aumentou a viscosidade e a tensão de cisalhamento. O auto conteúdo de fibra dietética no BSG contribuiu para uma menor sinérese, maior tensão de cisalhamento e manutenção da viscosidade em determinados níveis de adição durante o período de armazenamento. O Iogurte adicionado de BSG permitiu o crescimento de bactérias do ácido lático, aumentou a quantidade de ácido lático e aumentou o pH, o que pode ser benéfico para a indústria usar menos adoçante para cobrir a acidez. Além disso, a adição de BSG em certos níveis fortaleceu o nível de sobrevivência de bactérias do ácido lático durante o armazenamento. Sugere-se que uma substituição máxima de 10% de BSG seja mais adequada em produtos de iogurte devido à sua capacidade de preservar o comportamento de fluxo e sinérese, além de outras propriedades físico-químicas.

6.3. Potencial bioativo

Os ácidos fenólicos, naturalmente presentes em muitas plantas, especialmente cereais, frutas e vegetais, são os antioxidantes mais abundantes na dieta humana (Kumar and Goel, 2019). Eles possuem a capacidade de atuar como doadores de hidrogênio/elétrons, agentes redutores e quelantes de metais, sendo relacionado aos benefícios à saúde associados à ingestão alimentar desses compostos (Connolly et al., 2021). Sua presença não está restrita apenas aos alimentos, mas também em muitos resíduos originados da agroindústria.

O potencial antioxidante dos ácidos fenólicos presentes no BSG demonstrou, *in vitro*, um potencial semelhante a alguns polifenóis conhecidos como α-tocoferol e ácido ascórbico (Bonifácio-Lopes et al., 2022). (Martín-García et al., 2020) identificaram um total de 13 compostos fenólicos livres no BSG. Catequina-3-glicose; procianidina B3; catequina; ácido vanílico; quercetina-3-hexosilrutinosídeo; p-hidroxibenzaldeído; vanilina; prodelfinidina B3; ácido p-cumárico; hidroferuloil-glicose; ácido ferúlico; sinapoil hexose e tricina foram os

compostos identificados nos extratos do BSG. Além disso, os vários componentes do BSG (proteínas, aminoácidos, lipídios, ácidos graxos e fibra alimentar) demonstraram ter outras propriedades benéficas, como atividade anti-inflamatória, antimutagênica, antimicrobiana e anti-hipertensiva, entre outras (Bonifácio-Lopes et al., 2022; Chin et al., 2022; Connolly et al., 2021; Steiner et al., 2015; Vieira et al., 2014).

Várias aplicações dos extratos contendo os ácidos fenólicos são frequentemente relatadas na literatura científica. Podem ser usados como aditivos naturais em alimentos para prevenir ou retardar o crescimento microbiano, a oxidação lipídica, proteica e de pigmentos (Bellucci et al., 2022, 2021; Nova-Baza et al., 2022; Tkaczewska et al., 2022), em substituição aos antioxidantes sintéticos utilizados pela indústria de alimentos ou de cosméticos. Além disso, a busca por tais moléculas e extratos é encorajada visando a promoção do sistema imunológico humano (Galanakis, 2018; Galanakis et al., 2021, 2018).

O correto processamento e utilização eficiente de resíduos agroindustriais, considerados matérias-primas de baixo custo, podem atender à crescente demanda por aditivos naturais e alimentos funcionais e nutracêuticos (Kumari et al., 2017). (Naibaho et al., 2022c) avaliaram a influência do tratamento com autoclave (TA) na atividade antioxidante e composição polifenólica do BSG. Os resultados mostraram que o TA aumentou a atividade antioxidante avaliada pelos métodos ORAC, ABTS e FRAP em até 7 vezes em comparação com o BSG não tratado. Nesse contexto, o TA melhorou a liberação dos compostos bioativos da matriz do BSG, oferecendo um processo eficaz para recuperar os compostos bioativos.

Kumari et al. (2019) avaliaram o impacto do pré-tratamento com campo elétrico pulsado sobre a bioatividade e conteúdo de polifenólicos do BSG. O pré-tratamento de campo elétrico pulsado (PEF) melhorou a extração dos fenólicos totais em comparação com extratos do BSG não tratado. Além disso, o BSG tratado com PEF apresentou maior atividade antimicrobiana contra *Salmonella typhimurium* e *Listeria monocytognes* em comparação com os extratos não tratados.

6.4. Proteínas

Atualmente, as proteínas de origem vegetal têm sido consideradas como ingredientes funcionais para formulação e enriquecimento de produtos alimentícios. Além de serem consideradas alternativas versáteis e econômicas em substituição às fontes de origem animal para nutrição humana (López et al., 2018; Sá et al., 2020), sua oferta é menos limitada, com menores impactos ambientais como mudanças climáticas, perda de biodiversidade e esgotamento de água doce (Alemayehu; Bendevis; Jacobsen, 2015; Pojić; mišan; tiwari, 2018).

Várias fontes vegetais têm sido amplamente estudadas como potenciais suplementos proteicos, como os cereais (trigo, milho, cevada, arroz, milheto e sorgo) (Amagliani et al., 2017; Balandrán-Quintana et al., 2015; Phongthai et al., 2016), as leguminosas (feijões, soja, grão de bico, ervilha) (Karaman et al., 2022; Moser et al., 2020; Preece et al., 2017; Yang et al., 2021a), as sementes (linhaça, abóbora, girassol, chia) (Kaur and Ghoshal, 2022; Kumar et al., 2022; Soukoulis et al., 2019), os pseudocereais (amaranto, quinoa) (López et al., 2018), entre outros. Entretanto, a obtenção de extratos proteicos de resíduos agroindustriais vem sendo explorado como fonte alternativa de baixo custo. O aproveitamento dos resíduos para estes fins contribui, não somente para produção de ingredientes de alto valor nutricional e potencial funcional, como também para redução de geração de biomassa e favorecimento da economia circular. Dentre os mais diversos resíduos utilizados para este fim, encontram-se a borra de café (Barrios et al., 2022), resíduo de semente de romã (Guzmán-Lorite et al., 2022), sementes de abóbora (Das et al., 2022), semente de moringa (Kumar et al., 2022), resíduos de nozes (Liu et al., 2022), resíduo de amêndoa (Dias et al., 2022), resíduo do farelo de arroz (Capellini et al., 2017) e o próprio bagaço de malte (Naibaho et al., 2022b; Parchami et al., 2021b).

O BSG removido após a etapa de mosturação é o coproduto cervejeiro mais abundante do processo de produção da cerveja. É frequentemente relatado na literatura que o BSG contém 15-24 g/100 g de proteína em base seca (Mussatto et al., 2006). O estudo recente de Jin et al. (2022) investigou os aminoácidos presentes em quatro amostras de BSG proveniente de quatro cervejarias. Tirosina foi o aminoácido mais abundante nas amostras de BSGs. Todas as quatro amostras de BSGs continham aminoácidos essenciais,

como histidina, isoleucina, leucina, lisina, metionina, fenilalanina, treonina e valina. Os aminoácidos essenciais mais abundantes foram leucina, fenilalanina e metionina.

Embora a BSG tenha um excelente perfil de aminoácidos, é um desafio extrair proteína do BSG com altos rendimentos devido ao fato de que os componentes como lignina e celulose formam uma rede complexa e aprisionam a proteína no interior (LI et al., 2021). Dessa forma, técnicas importantes de extração de proteínas relacionadas a métodos convencionais (à base de água, sal, solvente, detergente, álcalis) (Ibbett et al., 2019a; Silva et al., 2023) e não convencionais (enzimas, micro-ondas, alta pressão, campo de pulso, homogeneização, sonicação) (Arantes da Fonseca et al., 2023; Li et al., 2021), ou a combinação deles podem ser aplicados para melhorar e intensificar a recuperação da proteína do BSG.

Em uma abordagem de fracionamento úmido, He et al. (2021) investigaram a extração de proteínas a partir do BSG. Os resultados indicaram que a condição ideal foi utilizar um carregamento de Alcalase de 5 μL/g com um tempo de hidrólise de 1 hora, resultando em uma alta concentração de proteína (46%) e eficiência de separação de proteínas (80%). Esses achados destacam a eficácia do fracionamento úmido como uma estratégia promissora para extrair proteínas do BSG.

Além disso, o estudo de Silva et al. (2023) examinou a extração alcalina de proteínas do BSG, variando o pH (8-12) e a temperatura da extração (40-80 °C). Condições otimizadas (pH 11, 60 °C) resultaram em alto rendimento de extração (até 87%). A extração suave (pH 8) produziu extratos com maior teor de proteína (>40%) e melhores propriedades funcionais, enquanto condições mais extremas (pH 11 e 12) levaram a concentrados com menor teor de proteína, porém melhorias nas propriedades gelificantes. Este estudo destacou a importância de ajustar pH e temperatura para obter proteínas com funcionalidade desejada.

Por sua vez, o estudo de Farjami et al. (2024) investigou o impacto da precipitação por ácido cítrico (AC) e HCl nas propriedades dos concentrados proteicos de BSG. Os resultados revelaram que a precipitação por ácido cítrico reduziu o teor de proteína e aumentou os teores de lipídios e carboidratos nos concentrados, em comparação com a precipitação por HCl. Além disso, a

formação de ligações cruzadas por ácido cítrico foi confirmada, impactando negativamente a solubilidade proteica e as propriedades emulsificantes, mas melhorando as propriedades de formação de espuma. Esses achados destacam o papel crucial dos precipitantes na modulação das propriedades dos concentrados proteicos BSG.

Particularmente, para proteínas de BSG, até onde sabemos, o procedimento de extração mais bem-sucedido é o método descrito por Qin et al. (2018). No presente estudo, diferentes estratégias de pré-tratamento, incluindo alcalinas, ácidas, enzimáticas e hidrotermais, e suas combinações, foram avaliadas e comparadas com o objetivo de extrair proteína do BSG. Das diferentes opções avaliadas, O pré-tratamento sequencial com ácido alcalino e diluído aumentou a extração proteica para 95%. Entretanto, quantidades significativas de carboidratos e lignina foram solubilizadas juntamente com proteínas, revelando que o uso dessa estratégia não foi seletivo para extração de proteínas. Dessa forma, etapas subsequentes de separação/purificação de proteínas devem ser avaliadas para recuperar separadamente esses componentes não proteicos, como celulose, hemicelulose e lignina e utilizá-los para a produção de produtos de alto valor agregado na perspectiva da biorrefinaria.

6.5. Produção de bioetanol

Os combustíveis fósseis são responsáveis pelo suprimento de aproximadamente 80% da crescente demanda energética mundial, sendo a maior parte atribuída ao setor de transportes (Escobar et al., 2009). Além da exploração incessante e não-sustentável de tais fontes, danos significativos são produzidos ao meio ambiente por parte das emissões de gases de efeito estufa (Beig et al., 2021). Por esta razão, estudos vêm sendo concentrados na busca de fontes alternativas para a produção de biocombustíveis a partir de matéria renovável.

O biocombustível tem se mostrado uma das alternativas mais importantes para atender aos aspectos de sustentabilidade econômica e ambiental (Beig et al., 2021). Além da alta disponibilidade de matéria-prima (biomassa), ele não apresenta emissão líquida de CO_2 quando comparado aos combustíveis fósseis (Wang and Lee, 2021). O biocombustível pode ser

encontrado na forma líquida, gasosa ou sólida quando obtido da biomassa. Alguns exemplos são etanol, metanol, carvão, biodiesel, hidrogênio e metano (Kumar et al., 2020). A Figura 3 mostra a classificação desses produtos como sendo biocombustíveis primários ou secundários.

Figura 3. Classificação dos biocombustíveis.

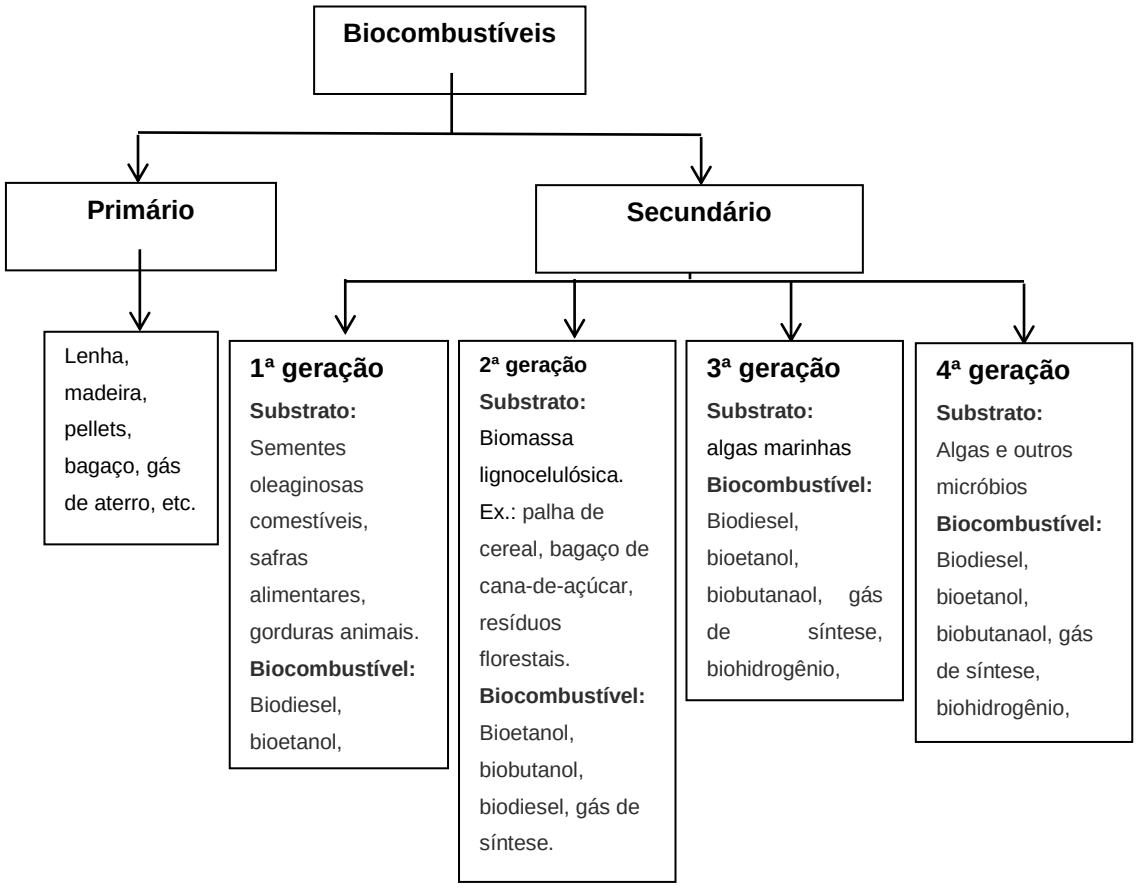

Fonte: Adaptado de Kumar et al. (2020).

Os primários são aqueles incinerados diretamente sem qualquer modificação visando à produção de calor e eletricidade. Por outro lado, os biocombustíveis secundários são obtidos a partir do processamento da biomassa por meio de pré-tratamentos adequados, hidrólise, transesterificação e fermentação para a produção de carvão vegetal, biogás, biodiesel e o próprio bioetanol.

O bioetanol pode ser considerado um dos biocombustíveis mais viáveis para substituir os combustíveis fósseis (Escobar et al., 2009). Ele pode ser produzido por meio da fermentação dos açúcares solúveis contidos em, por exemplo, culturas de cana-de-açúcar, milho, beterraba, batata ou mandioca (Kenney et al., 2014). Embora ricas em carboidratos e de fácil fermentação em

bioetanol, essas culturas são utilizadas principalmente para alimentação humana, limitando seu uso para produção de biocombustível. Dessa forma, o bioetanol de segunda geração (2G) aparece como uma forma de minimizar a competição ao usar outras matérias-primas alternativas ricas em carboidratos, como a biomassa lignocelulósica.

O bioetanol, também chamado de etanol 2G, é obtido a partir do processo de conversão da biomassa de característica lignocelulósica em 4 etapas principais: pré-tratamento adequado, hidrólise, fermentação do açúcar e a destilação do etanol resultante. Visto que as duas últimas etapas já são comumente aplicadas na indústria de etanol de primeira geração, estudos são necessários para compreender e aprimorar as etapas de pré-tratamento e hidrólise.

Wagner et al., (2021) avaliaram as modificações estruturais geradas pelos pré-tratamentos físico-químicos (auto-hidrolítico, H_2O_2 e H_2SO_4) para promover acessibilidade enzimática e assim explorar o BSG. Quando o BSG foi tratado com H_2O_2 a liberação enzimática de açúcar mostrou-se eficiente, obtendo-se 193,35 mg de açúcares/g BSG seco. Assim, a realização desse pré-tratamento com H_2O_2 e sua combinação com sacarificação enzimática representa uma nova estratégia promissora para potencializar o aproveitamento desse resíduo.

Hassan et al. (2020) avaliaram o pré-tratamento por sonicação para aumentar a sacarificação do BSG. Os autores relataram que o pré-tratamento por ultrassom do BSG leva a um rendimento de açúcar redutor 2,1 vezes maior, chegando a um teor de etanol de 17,73 g/100g do BSG pré-tratado obtido após fermentação. Os mesmos concluíram que o pré-tratamento por ultrassom é uma tecnologia potencial para valorização do BSG. Diante disso, pré-tratamentos eficientes da biomassa podem levar a um maior rendimento da hidrólise, resultando em um melhor aproveitamento da biomassa e processos mais eficientes. Nesse sentido, a combinação dos métodos químicos com peróxido de hidrogênio e ultrassom apresentam-se como uma alternativa promissora que demanda estudos específicos para sua avaliação.

6.6. Outras aplicações biotecnológicas

Além das aplicações anteriores, na indústria de biotecnologia, devido à alta porosidade e alta capacidade de sorção, este material pode ser utilizado como suporte para imobilização de levedura e enzimas, ou mesmo como

adsorvente em processos de purificação industrial (de Araújo et al., 2020), processos biotecnológicos (Lech and Labus, 2022), substrato para cultivo de microrganismos, produção de enzimas, produção de ácidos graxos voláteis (Teixeira et al., 2020) biogás (Čater et al., 2015), produção de ácido láctico, ácido carboxílico (Liang and Wan, 2015), produção de xilitol (Dávila et al., 2016) e embalagens biodegradáveis (Shroti and Saini, 2022).

7. CONSIDERAÇÕES FINAIS E PERSPECTIVAS FUTURAS

Esforços crescentes estão sendo direcionados para a reutilização de coprodutos agroindustriais, tanto do ponto de vista ambiental quanto econômico. O bagaço de malte (BSG) é um coproduto gerado em grandes quantidades, podendo ser obtido de cervejarias ao longo de todo o ano e mundialmente. No entanto, seu uso ainda é limitado, sendo utilizado basicamente como ração animal ou simplesmente descartado em aterros. Por apresentar várias frações ricas principalmente em carboidratos, proteínas, lignina e compostos bioativos com atividade antioxidante, o BSG é fonte de uma ampla gama de compostos com propriedades de interesse comercial.

Foram relatados vários estudos abordando as mais diferentes aplicações do BSG para a obtenção de produtos de valor agregado: como ingrediente funcional visando a reformulação de alimentos processados com apelo mais saudável, açúcares fermentescíveis para produção de bioetanol, compostos bioativos para uso como aditivos naturais com aporte antioxidante, produção de enzimas, embalagens biodegradáveis, entre outras.

Embora o BSG seja um material rico em frações valiosas, são necessárias abordagens para gerenciar e estabilizá-lo após a sua geração para posterior processamento. Os principais desafios iniciais para o seu aproveitamento são os custos de transporte do BSG úmido e/ou secagem e as etapas de pré-tratamento. Estudos devem ser basicamente direcionados para otimizar a etapa de secagem e armazenamento. Posteriormente, as condições operacionais de pré-tratamento com custos reduzidos por meio de avaliações tecnoeconômica do processo e maximização de rendimentos dos produtos devem ser almejadas.

8. REFERÊNCIAS

Aghilinategh, N., Rafiee, S., Gholikhani, A., Hosseinpur, S., Omid, M., Mohtasebi, S.S., Maleki, N., 2015. A comparative study of dried apple using hot air,

intermittent and continuous microwave: evaluation of kinetic parameters and physicochemical quality attributes. **Food Sci Nutr** 3, 519–526. https://doi.org/10.1002/FSN3.241

Alemayehu, F.R., Bendevis, M.A., Jacobsen, S.E., 2015. The Potential for Utilizing the Seed Crop Amaranth (Amaranthus spp.) in East Africa as an Alternative Crop to Support Food Security and Climate Change Mitigation. **J Agron Crop Sci** 201, 321–329. https://doi.org/10.1111/JAC.12108

Alonso-Riaño, P., Illera, A.E., Amândio, M.S.T., Xavier, A.M.R.B., Beltrán, S., Teresa Sanz, M., 2023. Valorization of brewer's spent grain by furfural recovery/removal from subcritical water hydrolysates by pervaporation. **Sep Purif Technol** 309, 123008. https://doi.org/10.1016/J.SEPPUR.2022.123008

Amagliani, L., O'Regan, J., Kelly, A.L., O'Mahony, J.A., 2017. The composition, extraction, functionality and applications of rice proteins: A review. **Trends Food Sci Technol** 64, 1–12. https://doi.org/10.1016/J.TIFS.2017.01.008

Arantes da Fonseca, Y., Gurgel, L.V.A., Baêta, B.E.L., Dragone, G., Mussatto, S.I., 2023. Reduced-pressure alkaline pretreatment as an innovative and sustainable technology to extract protein from brewer's spent grain. **J Clean Prod** 416, 137966. https://doi.org/10.1016/J.JCLEPRO.2023.137966

Bachmann, S.A.L., Calvete, T., Féris, L.A., 2022. Potential applications of brewery spent grain: Critical an overview. **J Environ Chem Eng** 10, 106951. https://doi.org/10.1016/J.JECE.2021.106951

Bajwa, D.S., Pourhashem, G., Ullah, A.H., Bajwa, S.G., 2019. A concise review of current lignin production, applications, products and their environmental impact. **Ind Crops Prod** 139, 111526. https://doi.org/10.1016/J.INDCROP.2019.111526

Balandrán-Quintana, R.R., Mercado-Ruiz, J.N., Mendoza-Wilson, A.M., 2015. Wheat Bran Proteins: A Review of Their Uses and Potential. **Food Reviews International** 31, 279–293. https://doi.org/10.1080/87559129.2015.1015137

Barrios, C., Fernández-Delgado, M., López-Linares, J.C., García-Cubero, M.T., Coca, M., Lucas, S., 2022. A techno-economic perspective on a microwave extraction process for efficient protein recovery from agri-food wastes. **Ind Crops Prod** 186, 115166. https://doi.org/10.1016/J.INDCROP.2022.115166

Bartolomeé, B., Santos, M., Jiménez, J.J., Del Nozal, M.J., GÓmez-Cordoveés, C., 2002. Pentoses and Hydroxycinnamic Acids in Brewer's Spent Grain. **J Cereal Sci** 36, 51–58. https://doi.org/10.1006/JCRS.2002.0442

Baruah, J., Nath, B.K., Sharma, R., Kumar, S., Deka, R.C., Baruah, D.C., Kalita, E., 2018. Recent Trends in the Pretreatment of Lignocellulosic Biomass for Value-Added Products. **Front Energy Res** 0, 141. https://doi.org/10.3389/FENRG.2018.00141

Battistini, C., Herkenhoff, M.E., de Souza Leite, M., Vieira, A.D.S., Bedani, R., Saad, S.M.I., 2021. Brewer's Spent Grain Enhanced the Recovery of Potential Probiotic Strains in Fermented Milk After Exposure to In Vitro-Simulated Gastrointestinal Conditions. **Probiotics Antimicrob Proteins** 1, 1–12. https://doi.org/10.1007/S12602-021-09839-8/FIGURES/3

Beig, B., Riaz, M., Raza Naqvi, S., Hassan, M., Zheng, Z., Karimi, K., Pugazhendhi, A., Atabani, A.E., Thuy Lan Chi, N., 2021. Current challenges and innovative developments in pretreatment of lignocellulosic residues for biofuel production: A review. **Fuel** 287, 119670. https://doi.org/10.1016/J.FUEL.2020.119670

Bellucci, E.R.B., dos Santos, J.M., Carvalho, L.T., Borgonovi, T.F., Lorenzo, J.M., Silva-Barretto, A.C. da, 2022. Açaí extract powder as natural antioxidant on pork patties during the refrigerated storage. **Meat Sci** 184, 108667. https://doi.org/10.1016/J.MEATSCI.2021.108667

Bonifácio-Lopes, T., Vilas-Boas, A., Machado, M., Costa, E.M., Silva, S., Pereira, R.N., Campos, D., Teixeira, J.A., Pintado, M., 2022. Exploring the bioactive potential of brewers spent grain ohmic extracts. **Innovative Food Science & Emerging Technologies** 76, 102943. https://doi.org/10.1016/J.IFSET.2022.102943

Borel, L.D.M.S., Lira, T.S., Ribeiro, J.A., Ataíde, C.H., Barrozo, M.A.S., 2018. Pyrolysis of brewer's spent grain: Kinetic study and products identification. **Ind Crops Prod** 121, 388–395. https://doi.org/10.1016/J.INDCROP.2018.05.051

Buffington, J., 2014. The Economic Potential of Brewer's Spent Grain (BSG) as a Biomass Feedstock. **Advances in Chemical Engineering and Science** 2014, 308–318. https://doi.org/10.4236/ACES.2014.43034

Capellini, M.C., Giacomini, V., Cuevas, M.S., Rodrigues, C.E.C., 2017. Rice bran oil extraction using alcoholic solvents: Physicochemical characterization of oil and protein fraction functionality. **Ind Crops Prod** 104, 133–143. https://doi.org/10.1016/J.INDCROP.2017.04.017

Carvalho, G.R. de, Polachini, T.C., Darros-Barbosa, R., Bon, J., Telis-Romero, J., 2018. Effect of intermittent high-intensity sonication and temperature on barley steeping for malt production. **J Cereal Sci** 82, 138–145. https://doi.org/10.1016/J.JCS.2018.06.005

Cassoni, A.C., Costa, P., Mota, I., Vasconcelos, M.W., Pintado, M., 2023. Recovery of lignins with antioxidant activity from Brewer's spent grain and olive tree pruning using deep eutectic solvents. **Chemical Engineering Research and Design** 192, 34–43. https://doi.org/10.1016/J.CHERD.2023.01.053

Čater, M., Fanedl, L., Malovrh, Š., Marinšek Logar, R., 2015. Biogas production from brewery spent grain enhanced by bioaugmentation with hydrolytic anaerobic bacteria. **Bioresour Technol** 186, 261–269. https://doi.org/10.1016/J.BIORTECH.2015.03.029

Cermeño, M., Dermiki, M., Kleekayai, T., Cope, L., McManus, R., Ryan, C., Felix, M., Flynn, C., FitzGerald, R.J., 2021. Effect of enzymatically hydrolysed brewers' spent grain supplementation on the rheological, textural and sensory properties of muffins. **Future Foods** 4, 100085. https://doi.org/10.1016/J.FUFO.2021.100085

Chin, Y.L., Chai, K.F., Chen, W.N., 2022. Upcycling of brewers' spent grains via solid-state fermentation for the production of protein hydrolysates with antioxidant

and techno-functional properties. **Food Chem X** 13, 100184. https://doi.org/10.1016/J.FOCHX.2021.100184

Connolly, A., Cermeño, M., Alashi, A.M., Aluko, R.E., FitzGerald, R.J., 2021. Generation of phenolic-rich extracts from brewers' spent grain and characterisation of their in vitro and in vivo activities. **Innovative Food Science & Emerging Technologies** 68, 102617. https://doi.org/10.1016/J.IFSET.2021.102617

Czubaszek, A., Wojciechowicz-Budzisz, A., Spychaj, R., Kawa-Rygielska, J., 2021. Baking properties of flour and nutritional value of rye bread with brewer's spent grain. **LWT** 150, 111955. https://doi.org/10.1016/J.LWT.2021.111955

Das, M., Devi, L.M., Badwaik, L.S., 2022. Ultrasound-assisted extraction of pumpkin seeds protein and its physicochemical and functional characterization. **Applied Food Research** 2, 100121. https://doi.org/10.1016/J.AFRES.2022.100121

Dávila, J.A., Rosenberg, M., Cardona, C.A., 2016. A biorefinery approach for the production of xylitol, ethanol and polyhydroxybutyrate from brewer's spent grain. **AIMS Agriculture and Food** 1, 52–66. https://doi.org/10.3934/agrfood.2016.1.52

de Araújo, T.P., Quesada, H.B., Bergamasco, R., Vareschini, D.T., de Barros, M.A.S.D., 2020. Activated hydrochar produced from brewer's spent grain and its application in the removal of acetaminophen. **Bioresour Technol** 310, 123399. https://doi.org/10.1016/J.BIORTECH.2020.123399

Dias, F.F.G., Taha, A.Y., Bell, L.N. de M., 2022. Effects of enzymatic extraction on the simultaneous extraction of oil and protein from full-fat almond flour, insoluble microstructure, emulsion stability and functionality. **Future Foods** 5, 100151. https://doi.org/10.1016/J.FUFO.2022.100151

Escobar, J.C., Lora, E.S., Venturini, O.J., Yáñez, E.E., Castillo, E.F., Almazan, O., 2009. Biofuels: Environment, technology and food security. **Renewable and Sustainable Energy Reviews** 13, 1275–1287. https://doi.org/10.1016/J.RSER.2008.08.014

Farjami, T., Sharma, A., Hagen, L., Jensen, I.J., Falch, E., 2024. Comparative study on composition and functional properties of brewer's spent grain proteins precipitated by citric acid and hydrochloric acid. **Food Chem** 446, 138863. https://doi.org/10.1016/J.FOODCHEM.2024.138863

Galanakis, C.M., 2018. Phenols recovered from olive mill wastewater as additives in meat products. **Trends Food Sci Technol** 79, 98–105. https://doi.org/10.1016/J.TIFS.2018.07.010

Galanakis, C.M., Rizou, M., Aldawoud, T.M.S., Ucak, I., Rowan, N.J., 2021. Innovations and technology disruptions in the food sector within the COVID-19 pandemic and post-lockdown era. **Trends Food Sci Technol** 110, 193–200. https://doi.org/10.1016/J.TIFS.2021.02.002

Gasiński, A., Kawa-Rygielska, J., Mikulski, D., Kłosowski, G., Głowacki, A., 2021. Application of white grape pomace in the brewing technology and its impact on the concentration of esters and alcohols, physicochemical parameteres and antioxidative properties of the beer. **Food Chem** 130646. https://doi.org/10.1016/J.FOODCHEM.2021.130646

Gebremedhn, B., Niguse, M., Hagos, B., Tesfamariam, T., Kidane, T., Berhe, A., Gebresilassie, L., Gebreegziabher, L., Gebreegziabher, T., Gebremeskel, Y., 2019. Effects of Dietary Brewery Spent Grain Inclusion on Egg Laying Performance and Quality Parameters of Bovans Brown Chickens. **Brazilian Journal of Poultry Science** 21. https://doi.org/10.1590/1806-9061-2018-0765

Guimarães, B., Polachini, T.C., Augusto, P.E.D., Telis-Romero, J., 2020. Ultrasound-assisted hydration of wheat grains at different temperatures and power applied: Effect on acoustic field, water absorption and germination. **Chemical Engineering and Processing - Process Intensification** 155, 108045. https://doi.org/10.1016/j.cep.2020.108045

Guzmán-Lorite, M., Marina, M.L., García, M.C., 2022. Pressurized liquids vs. high intensity focused ultrasounds for the extraction of proteins from a pomegranate seed waste. **Innovative Food Science & Emerging Technologies** 77, 102958. https://doi.org/10.1016/J.IFSET.2022.102958

Haghighi Mood, S., Hossein Golfeshan, A., Tabatabaei, M., Salehi Jouzani, G., Najafi, G.H., Gholami, M., Ardjmand, M., 2013. Lignocellulosic biomass to bioethanol, a comprehensive review with a focus on pretreatment. **Renewable and Sustainable Energy Reviews** 27, 77–93. https://doi.org/10.1016/J.RSER.2013.06.033

Haldar, D., Purkait, M.K., 2021. A review on the environment-friendly emerging techniques for pretreatment of lignocellulosic biomass: Mechanistic insight and advancements. **Chemosphere** 264, 128523. https://doi.org/10.1016/J.CHEMOSPHERE.2020.128523

Hassan, S.S., Ravindran, R., Jaiswal, S., Tiwari, B.K., Williams, G.A., Jaiswal, A.K., 2020. An evaluation of sonication pretreatment for enhancing saccharification of brewers' spent grain. **Waste Management** 105, 240–247. https://doi.org/10.1016/J.WASMAN.2020.02.012

Hassan, S.S., Williams, G.A., Jaiswal, A.K., 2018. Emerging technologies for the pretreatment of lignocellulosic biomass. **Bioresour Technol** 262, 310–318. https://doi.org/10.1016/J.BIORTECH.2018.04.099

He, Y., Galagarza, O.A., Wang, H., Taylor, Z.W., Ferguson, C.S., Ogejo, J.A., O'Keefe, S.F., Fernández Fraguas, C., Yu, D., Poe, N.E., Wiersema, B.D., Kuhn, D.D., Huang, H., 2020. Protein-rich product recovered from brewer's spent grain can partially replace fishmeal in diets of Pacific white shrimp, Litopenaeus vannamei. **Aquac Res** 51, 3284–3296. https://doi.org/10.1111/ARE.14664

He, Y., Kuhn, D.D., Ogejo, J.A., O'Keefe, S.F., Fraguas, C.F., Wiersema, B.D., Jin, Q., Yu, D., Huang, H., 2019. Wet fractionation process to produce high protein and high fiber products from brewer's spent grain. **Food and Bioproducts Processing** 117, 266–274. https://doi.org/10.1016/J.FBP.2019.07.011

He, Y., Kuhn, D.D., O'Keefe, S.F., Ogejo, J.A., Fraguas, C.F., Wang, H., Huang, H., 2021. Protein production from brewer's spent grain via wet fractionation: process optimization and techno-economic analysis. **Food and Bioproducts**

Processing 126, 234–244.
https://doi.org/10.1016/J.FBP.2021.01.005

Hoang, A.T., Nižetić, S., Ong, H.C., Mofijur, M., Ahmed, S.F., Ashok, B., Bui, V.T.V., Chau, M.Q., 2021. Insight into the recent advances of microwave pretreatment technologies for the conversion of lignocellulosic biomass into sustainable biofuel. **Chemosphere** 281, 130878.
https://doi.org/10.1016/J.CHEMOSPHERE.2021.130878

Ibarruri, J., Cebrián, M., Hernández, I., 2019. Solid State Fermentation of Brewer's Spent Grain Using Rhizopus sp. to Enhance Nutritional Value. **Waste and Biomass Valorization** 2019 10:12 10, 3687–3700.
https://doi.org/10.1007/S12649-019-00654-5

Ibbett, R., White, R., Tucker, G., Foster, T., 2019. Hydro-mechanical processing of brewer's spent grain as a novel route for separation of protein products with differentiated techno-functional properties. **Innovative Food Science & Emerging Technologies** 56, 102184.
https://doi.org/10.1016/J.IFSET.2019.102184

Jaeger, S.R., Worch, T., Phelps, T., Jin, D., Cardello, A. V., 2020. Preference segments among declared craft beer drinkers: Perceptual, attitudinal and behavioral responses underlying craft-style vs. traditional-style flavor preferences. **Food Qual Prefer** 82, 103884.
https://doi.org/10.1016/J.FOODQUAL.2020.103884

Jayant, M., Hassan, M.A., Srivastava, P.P., Meena, D.K., Kumar, P., Kumar, A., Wagde, M.S., 2018. Brewer's spent grains (BSGs) as feedstuff for striped catfish, Pangasianodon hypophthalmus fingerlings: An approach to transform waste into wealth. **J Clean Prod** 199, 716–722.
https://doi.org/10.1016/J.JCLEPRO.2018.07.213

Jin, Z., Lan, Y., Ohm, J.B., Gillespie, J., Schwarz, P., Chen, B., 2022. Physicochemical composition, fermentable sugars, free amino acids, phenolics, and minerals in brewers' spent grains obtained from craft brewing operations. **J Cereal Sci** 104, 103413. https://doi.org/10.1016/J.JCS.2022.103413

Karaman, K., Bekiroglu, H., Kaplan, M., Çiftci, B., Yürürdurmaz, C., Sagdic, O., 2022. A detailed comparative investigation on structural, technofunctional and bioactive characteristics of protein concentrates from different common bean genotypes. **Int J Biol Macromol** 200, 458–469. https://doi.org/10.1016/J.IJBIOMAC.2021.12.170

Kaur, R., Ghoshal, G., 2022. Sunflower protein isolates-composition, extraction and functional properties. **Adv Colloid Interface Sci** 306, 102725. https://doi.org/10.1016/J.CIS.2022.102725

Kenney, K.L., Smith, W.A., Gresham, G.L., Westover, T.L., 2014. Understanding biomass feedstock variability. **Biofuels** 4, 111–127. https://doi.org/10.4155/BFS.12.83

Kumar, B., Bhardwaj, N., Agrawal, K., Chaturvedi, V., Verma, P., 2020. Current perspective on pretreatment technologies using lignocellulosic biomass: An emerging biorefinery concept. **Fuel Processing Technology** 199, 106244. https://doi.org/10.1016/J.FUPROC.2019.106244

Kumar, N., Goel, N., 2019. Phenolic acids: Natural versatile molecules with promising therapeutic applications. **Biotechnology Reports** 24, e00370. https://doi.org/10.1016/J.BTRE.2019.E00370

Kumari, B., Tiwari, B.K., Hossain, M.B., Brunton, N.P., Rai, D.K., 2017. Recent Advances on Application of Ultrasound and Pulsed Electric Field Technologies in the Extraction of Bioactives from Agro-Industrial By-products. **Food and Bioprocess Technology** 2017 11:2 11, 223–241. https://doi.org/10.1007/S11947-017-1961-9

Kumari, B., Tiwari, B.K., Walsh, D., Griffin, T.P., Islam, N., Lyng, J.G., Brunton, N.P., Rai, D.K., 2019. Impact of pulsed electric field pre-treatment on nutritional and polyphenolic contents and bioactivities of light and dark brewer's spent grains. **Innovative Food Science & Emerging Technologies** 54, 200–210. https://doi.org/10.1016/J.IFSET.2019.04.012

Lech, M., Labus, K., 2022. The methods of brewers' spent grain treatment towards the recovery of valuable ingredients contained therein and

comprehensive management of its residues. **Chemical Engineering Research and Design** 183, 494–511. https://doi.org/10.1016/J.CHERD.2022.05.032

Leichtweis, J., Silvestri, S., Stefanello, N., Carissimi, E., 2021. Degradation of ramipril by residues from the brewing industry: A new carbon-based photocatalyst compound. **Chemosphere** 281, 130987. https://doi.org/10.1016/J.CHEMOSPHERE.2021.130987

Li, W., Yang, H., Coldea, T.E., Zhao, H., 2021. Modification of structural and functional characteristics of brewer's spent grain protein by ultrasound assisted extraction. **LWT** 139, 110582. https://doi.org/10.1016/J.LWT.2020.110582

Liang, S., Wan, C., 2015. Carboxylic acid production from brewer's spent grain via mixed culture fermentation. **Bioresour Technol** 182, 179–183. https://doi.org/10.1016/J.BIORTECH.2015.01.082

Liu, D., Di, H., Guo, Y., Betchem, G., Ma, H., 2022. Multi-mode S-type ultrasound-assisted protein extraction from walnut dregs and in situ real-time process monitoring. **Ultrason Sonochem** 89, 106116. https://doi.org/10.1016/J.ULTSONCH.2022.106116

López, D.N., Galante, M., Robson, M., Boeris, V., Spelzini, D., 2018. Amaranth, quinoa and chia protein isolates: Physicochemical and structural properties. **Int J Biol Macromol** 109, 152–159. https://doi.org/10.1016/J.IJBIOMAC.2017.12.080

Lynch, K.M., Steffen, E.J., Arendt, E.K., 2016. Brewers' spent grain: a review with an emphasis on food and health. **Journal of the Institute of Brewing** 122, 553–568. https://doi.org/10.1002/JIB.363

Machado, L.M.M., Lütke, S.F., Perondi, D., Godinho, M., Oliveira, M.L.S., Collazzo, G.C., Dotto, G.L., 2020. Simultaneous production of mesoporous biochar and palmitic acid by pyrolysis of brewing industry wastes. **Waste Management** 113, 96–104. https://doi.org/10.1016/J.WASMAN.2020.05.038

Mallen, E., Najdanovic-Visak, V., 2018. Brewers' spent grains: Drying kinetics and biodiesel production**. Bioresour Technol Rep** 1, 16–23. https://doi.org/10.1016/J.BITEB.2018.01.005

Martín-García, B., Tylewicz, U., Verardo, V., Pasini, F., Gómez-Caravaca, A.M., Caboni, M.F., Dalla Rosa, M., 2020. Pulsed electric field (PEF) as pre-treatment to improve the phenolic compounds recovery from brewers' spent grains. **Innovative Food Science & Emerging Technologies** 64, 102402. https://doi.org/10.1016/J.IFSET.2020.102402

Mello, L.R.P.F., Mali, S., 2014. Use of malt bagasse to produce biodegradable baked foams made from cassava starch. **Ind Crops Prod** 55, 187–193. https://doi.org/10.1016/J.INDCROP.2014.02.015

Moser, P., Nicoletti, V.R., Drusch, S., Brückner-Gühmann, M., 2020. Functional properties of chickpea protein-pectin interfacial complex in buriti oil emulsions and spray dried microcapsules. **Food Hydrocoll** 107, 105929. https://doi.org/10.1016/J.FOODHYD.2020.105929

Mussatto, S.I., 2014. Brewer's spent grain: a valuable feedstock for industrial applications. **J Sci Food Agric** 94, 1264–1275. https://doi.org/10.1002/JSFA.6486

Mussatto, S.I., Dragone, G., Roberto, I.C., 2006. Brewers' spent grain: generation, characteristics and potential applications. **J Cereal Sci** 43, 1–14. https://doi.org/10.1016/J.JCS.2005.06.001

Naibaho, J., Butula, N., Jonuzi, E., Korzeniowska, M., Laaksonen, O., Föste, M., Kütt, M.L., Yang, B., 2022a. Potential of brewers' spent grain in yogurt fermentation and evaluation of its impact in rheological behaviour, consistency, microstructural properties and acidity profile during the refrigerated storage. **Food Hydrocoll** 125, 107412. https://doi.org/10.1016/J.FOODHYD.2021.107412

Naibaho, J., Korzeniowska, M., Wojdyło, A., Figiel, A., Yang, B., Laaksonen, O., Foste, M., Vilu, R., Viiard, E., 2021. Fiber modification of brewers' spent grain by autoclave treatment to improve its properties as a functional food ingredient. **LWT** 149, 111877. https://doi.org/10.1016/J.LWT.2021.111877

Naibaho, J., Korzeniowska, M., Wojdyło, A., Muchdatul Ayunda, H., Foste, M., Yang, B., 2022b. Techno-functional properties of protein from protease-treated

brewers' spent grain (BSG) and investigation of antioxidant activity of extracted proteins and BSG residues. **J Cereal Sci** 107, 103524. https://doi.org/10.1016/J.JCS.2022.103524

Naibaho, J., Wojdyło, A., Korzeniowska, M., Laaksonen, O., Föste, M., Kütt, M.-L., Yang, B., 2022c. Antioxidant activities and polyphenolic identification by UPLC-MS/MS of autoclaved brewers' spent grain. **LWT** 163, 113612. https://doi.org/10.1016/J.LWT.2022.113612

Nova-Baza, D., Olivares-Caro, L., Bustamante, L., Pérez, A.J., Vergara, C., Fuentealba, J., Mardones, C., 2022. Metabolic profile and antioxidant capacity of five Berberis leaves species: A comprehensive study to determine their potential as natural food or ingredient. **Food Research International** 160, 111642. https://doi.org/10.1016/J.FOODRES.2022.111642

Nunes Filho, R.C., Galvan, D., Effting, L., Terhaag, M.M., Yamashita, F., Benassi, M. de T., Spinosa, W.A., 2021. Effects of adding spices with antioxidants compounds in red ale style craft beer: A simplex-centroid mixture design approach. **Food Chem** 365, 130478. https://doi.org/10.1016/J.FOODCHEM.2021.130478

Özvural, E.B., Vural, H., Gökbulut, I., Özboy-Özbaş, Ö., 2009. Utilization of brewer's spent grain in the production of Frankfurters. **Int J Food Sci Technol** 44, 1093–1099. https://doi.org/10.1111/J.1365-2621.2009.01921.X

Parchami, M., Ferreira, J.A., Taherzadeh, M.J., 2021a. Starch and protein recovery from brewer's spent grain using hydrothermal pretreatment and their conversion to edible filamentous fungi – A brewery biorefinery concept. **Bioresour Technol** 337, 125409. https://doi.org/10.1016/J.BIORTECH.2021.125409

Phongthai, S., Lim, S.T., Rawdkuen, S., 2016. Optimization of microwave-assisted extraction of rice bran protein and its hydrolysates properties. **J Cereal Sci** 70, 146–154. https://doi.org/10.1016/J.JCS.2016.06.001

Pojić, M., Mišan, A., Tiwari, B., 2018. Eco-innovative technologies for extraction of proteins for human consumption from renewable protein sources of plant

origin. Trends Food Sci Technol 75, 93–104. https://doi.org/10.1016/J.TIFS.2018.03.010

Preece, K.E., Hooshyar, N., Krijgsman, A.J., Fryer, P.J., Zuidam, N.J., 2017. Intensification of protein extraction from soybean processing materials using hydrodynamic cavitation. **Innovative Food Science & Emerging Technologies** 41, 47–55. https://doi.org/10.1016/J.IFSET.2017.01.002

Qazanfarzadeh, Z., Ganesan, A.R., Mariniello, L., Conterno, L., Kumaravel, V., 2023. Valorization of brewer's spent grain for sustainable food packaging. **J Clean Prod** 385, 135726. https://doi.org/10.1016/J.JCLEPRO.2022.135726

Qin, F., Johansen, A.Z., Mussatto, S.I., 2018. Evaluation of different pretreatment strategies for protein extraction from brewer's spent grains. **Ind Crops Prod** 125, 443–453. https://doi.org/10.1016/J.INDCROP.2018.09.017

Reis, S.F., Coelho, E., Coimbra, M.A., Abu-Ghannam, N., 2015. Improved efficiency of brewer's spent grain arabinoxylans by ultrasound-assisted extraction. **Ultrason Sonochem** 24, 155–164. https://doi.org/10.1016/J.ULTSONCH.2014.10.010

Ribau Teixeira, M., Guarda, E.C., Freitas, E.B., Galinha, C.F., Duque, A.F., Reis, M.A.M., 2020. Valorization of raw brewers' spent grain through the production of volatile fatty acids. **N Biotechnol** 57, 4–10. https://doi.org/10.1016/J.NBT.2020.01.007

Robertson, J.A., I'Anson, K.J.A., Treimo, J., Faulds, C.B., Brocklehurst, T.F., Eijsink, V.G.H., Waldron, K.W., 2010. Profiling brewers' spent grain for composition and microbial ecology at the site of production. **LWT - Food Science and Technology** 43, 890–896. https://doi.org/10.1016/J.LWT.2010.01.019

Rommi, K., Niemi, P., Kemppainen, K., Kruus, K., 2018. Impact of thermochemical pre-treatment and carbohydrate and protein hydrolyzing enzyme treatment on fractionation of protein and lignin from brewer's spent grain. **J Cereal Sci** 79, 168–173. https://doi.org/10.1016/J.JCS.2017.10.005

Roth, M., Jekle, M., Becker, T., 2019. Opportunities for upcycling cereal byproducts with special focus on Distiller's grains. **Trends Food Sci Technol** 91, 282–293. https://doi.org/10.1016/J.TIFS.2019.07.041

Sá, A.G.A., Moreno, Y.M.F., Carciofi, B.A.M., 2020. Plant proteins as high-quality nutritional source for human diet. **Trends Food Sci Technol** 97, 170–184. https://doi.org/10.1016/J.TIFS.2020.01.011

Sanches, M.A.R., Augusto, P.E.D., Polachini, T.C., Telis-Romero, J., 2023. Water sorption properties of brewer's spent grain: A study aimed at its stabilization for further conversion into value-added products. **Biomass Bioenergy** 170, 106718. https://doi.org/10.1016/J.BIOMBIOE.2023.106718

Santos, G.E.D.S. dos, Duarte, C.R., Hori, C.E., Barrozo, M.A.D.S., 2024. Catalytic pyrolysis of brewer's spent grain in spouted bed reactor using calcium oxide for upgrading oil. **Journal of the Energy Institute** 114, 101586. https://doi.org/10.1016/J.JOEI.2024.101586

Santos, M. V., Ranalli, N., Orjuela-Palacio, J., Zaritzky, N., 2024. Brewers spent grain drying: Drying kinetics, moisture sorption isotherms, bioactive compounds stability and *Bacillus cereus* lethality during thermal treatment. **J Food Eng** 364, 111796. https://doi.org/10.1016/J.JFOODENG.2023.111796

Shroti, G.K., Saini, C.S., 2022. Development of edible films from protein of brewer's spent grain: Effect of pH and protein concentration on physical, mechanical and barrier properties of films. **Applied Food Research** 2, 100043. https://doi.org/10.1016/J.AFRES.2022.100043

Sibhatu, H.K., Anuradha Jabasingh, S., Yimam, A., Ahmed, S., 2021. Ferulic acid production from brewery spent grains, an agro-industrial waste. **LWT** 135, 110009. https://doi.org/10.1016/J.LWT.2020.110009

Silva, A.M.M. da, Almeida, F.S., Silva, M.F. da, Goldbeck, R., Sato, A.C.K., 2023. How do pH and temperature influence extraction yield, physicochemical, functional, and rheological characteristics of brewer spent grain protein concentrates? **Food and Bioproducts Processing** 139, 34–45. https://doi.org/10.1016/J.FBP.2023.03.001

Soukoulis, C., Cambier, S., Serchi, T., Tsevdou, M., Gaiani, C., Ferrer, P., Taoukis, P.S., Hoffmann, L., 2019. Rheological and structural characterisation of whey protein acid gels co-structured with chia (Salvia hispanica L.) or flax seed (Linum usitatissimum L.) mucilage. **Food Hydrocoll** 89, 542–553. https://doi.org/10.1016/J.FOODHYD.2018.11.002

Steiner, J., Procopio, S., Becker, T., 2015. Brewer's spent grain: source of value-added polysaccharides for the food industry in reference to the health claims. **European Food Research and Technology** 241, 303–315. https://doi.org/10.1007/S00217-015-2461-7/TABLES/3

Stroem, L.K., Desai, D.K., Hoadley, A.F.A., 2009. Superheated steam drying of Brewer's spent grain in a rotary drum. **Advanced Powder Technology** 20, 240–244. https://doi.org/10.1016/J.APT.2009.03.009

Tang, Z., Cenkowski, S., Izydorczyk, M., 2005. Thin-layer drying of spent grains in superheated steam. **J Food Eng** 67, 457–465. https://doi.org/10.1016/J.JFOODENG.2004.04.040

Tang, Z., Cenkowski, S., Muir, W.E., 2004. Modelling the Superheated-steam Drying of a Fixed Bed of Brewers' Spent Grain. **Biosyst Eng** 87, 67–77. https://doi.org/10.1016/J.BIOSYSTEMSENG.2003.09.008

Thai, S., Avena-Bustillos, R.J., Alves, P., Pan, J., Osorio-Ruiz, A., Miller, J., Tam, C., Rolston, M.R., Teran-Cabanillas, E., Yokoyama, W.H., McHugh, T.H., 2022. Influence of drying methods on health indicators of brewers spent grain for potential upcycling into food products. **Applied Food Research** 2, 100052. https://doi.org/10.1016/J.AFRES.2022.100052

Tkaczewska, J., Zając, M., Jamróz, E., Derbew, H., 2022. Utilising waste from soybean processing as raw materials for the production of preparations with antioxidant properties, serving as natural food preservatives - A pilot study. **LWT** 160, 113282. https://doi.org/10.1016/J.LWT.2022.113282

Uribe, E., Lemus-Mondaca, R., Vega-Gálvez, A., Zamorano, M., Quispe-Fuentes, I., Pasten, A., Di Scala, K., 2014. Influence of process temperature on drying kinetics, physicochemical properties and antioxidant capacity of the olive-

waste cake. **Food Chem** 147, 170–176. https://doi.org/10.1016/J.FOODCHEM.2013.09.121

Vieira, E., Rocha, M.A.M., Coelho, E., Pinho, O., Saraiva, J.A., Ferreira, I.M.P.L.V.O., Coimbra, M.A., 2014. Valuation of brewer's spent grain using a fully recyclable integrated process for extraction of proteins and arabinoxylans. **Ind Crops Prod** 52, 136–143. https://doi.org/10.1016/J.INDCROP.2013.10.012

Wagner, E., Pería, M.E., Ortiz, G.E., Rojas, N.L., Ghiringhelli, P.D., 2021. Valorization of brewer's spent grain by different strategies of structural destabilization and enzymatic saccharification. **Ind Crops Prod** 163, 113329. https://doi.org/10.1016/J.INDCROP.2021.113329

Wang, W., Lee, D.-J., 2021. Lignocellulosic biomass pretreatment by deep eutectic solvents on lignin extraction and saccharification enhancement: A review. **Bioresour Technol** 339, 125587. https://doi.org/10.1016/J.BIORTECH.2021.125587

Yang, D., Gao, X., 2021. Research progress on the antioxidant biological activity of beer and strategy for applications. **Trends Food Sci Technol** 110, 754–764. https://doi.org/10.1016/J.TIFS.2021.02.048

Yang, M., Li, N., Tong, L., Fan, B., Wang, L., Wang, F., Liu, L., 2021a. Comparison of physicochemical properties and volatile flavor compounds of pea protein and mung bean protein-based yogurt. **LWT** 152, 112390. https://doi.org/10.1016/J.LWT.2021.112390

Zago, E., Tillier, C., De Leener, G., Nandasiri, R., Delporte, C., Bernaerts, K. V., Shavandi, A., 2022. Sustainable production of low molecular weight phenolic compounds from Belgian Brewers' spent grain. **Bioresour Technol Rep** 17, 100964. https://doi.org/10.1016/J.BITEB.2022.100964

Zeng, J., Sheng, F., Hu, X., Huang, Z., Tian, X., Wu, Z., 2022. Nutrition promotion of brewer's spent grain by symbiotic fermentation adding Bacillus velezensis and Levilactobacillus brevis. **Food Biosci** 49, 101941. https://doi.org/10.1016/J.FBIO.2022.101941

CAPÍTULO 2

Artigo publicado em "**Biomass and Bioenergy**" ISSN: 1873-2909

Water sorption properties of brewer's spent grain: A study aimed at its stabilization for further conversion into value-added products

Marcio Augusto Ribeiro Sanches[1], Pedro Esteves Duarte Augusto[2], Tiago Carregari Polachini[1], Javier Telis-Romero[1*]

[1]Food Engineering and Technology Department, São Paulo State University, Institute of Biosciences, Humanities and Exact Sciences (Ibilce), Campus São José do Rio Preto, São Paulo, 15.054-000, Brazil.

[2]Université Paris-Saclay, CentraleSupélec, Laboratoire de Génie des Procédés et Matériaux, SFR Condorcet FR CNRS 3417, Centre Européen de Biotechnologie et de Bioéconomie (CEBB), 3 rue des Rouges Terres 51110 Pomacle, France.

*Author to whom correspondence may be addressed. E-mail address: mar.sanches@unesp.br (Javier Telis Romero).

ABSTRACT

Due to its high moisture content and perishability, the water adsorption isotherms, and thermodynamic properties of brewer's spent grain obtained from barley malt (BSGL) and wheat malt based (BSGW) were evaluated under storage and drying conditions. Chemically characterized BSGs were subjected to the static gravimetric method to experimentally obtain the water adsorption isotherms at ten temperatures (5–90 °C). As the best-fitted model (R^2_{adj} > 0.9928 e χ^2 ≤ 0.0001), the GAB parameters were used to determine the adsorption surface

area, spreading pressure, and thermodynamic properties. At temperatures from 5–50 °C, the adsorption isotherms of BSGL and BSGW showed convex curves, typical of type III isotherms. However, at temperatures above 60 °C, the curves started to present typical type II isotherms with sigmoid-shaped sorption behavior. The equilibrium moisture content of BSGs increased with increasing relative humidity and/or decreasing temperature. The spreading pressure increased as the water activity and temperature increased, contrary to that observed for the adsorption surface area. Thermodynamic analysis showed that the net isosteric heat of adsorption, enthalpy, and differential entropy decreased as the equilibrium moisture increased. The compensation theory was confirmed, and its results indicated that the adsorption processes were enthalpy-driven. The positive values for Gibbs free energy indicated that the adsorption processes were not spontaneous, which may be related to the composition of BSGs in terms of lipids and proteins. From an energy and stability point of view, a water activity of 0.4 is the ideal condition for the storage of BSGs.

Keywords: Agro-industrial byproduct; lignocellulosic biomass; Protein; Sorption isotherm; Stabilization; Model fitting.

1. INTRODUCTION

Although there is a growing trend for valorizing agro-industrial by-products as raw materials for different industries, there is a lack of work in the literature on the by-product properties over its processing conditions for stabilization - limiting the adequate and efficient design of the appropriate operations.

Beer is one of the most consumed and appreciated beverages worldwide [1]. On the other hand, brewer's spent grain (BSG) ends by turning into the main solid waste, representing 85% of the total by-products generated in the brewing industry [2]. BSG is made up of the solid part, such as husks and residual starchy endosperm, obtained after filtration of the wort, and the retained water. Representing about 20 kg of wet bagasse for every 100 L of beer produced [3], its composition varies with the beer formulations, in special the amount and type of malted cereal, and whether adjuvants were used during fermentation [4].

Currently, most part of BSG is still used only for animal feed or simply discarded [3], going in the opposite direction to sustainable food production and efforts to zero carbon emissions. In this sense, several studies have studied

different potential applications of BSG, such as an alternative for plant-based protein sources [5] and the use of these proteins to stabilize emulsions [6], recovery of bioactive compounds [7], bioethanol [2] or biogas [8] production, biodegradable packaging [9], xylitol synthesis [3], source of enzymes [10], and even the use of BSG as ingredient in processed foods [11].

However, one of the main challenges in recovering and using agroindustrial by-products is linked to its handling and stabilization [12]. The composition and high moisture content of BSG is one of the challenges for its management and use, as these factors make it susceptible to microbial growth and deterioration, in addition to the increasing transport cost [13]. In this way, BSG needs to go through a drying process to reduce its mass and volume – decreasing transport and storage costs, as well as prolonging its shelf life. Moreover, once the product is dried, adequate stored conditions ensure its availability and integrity for further applications.

For these purposes, some information is necessary for the correct dimensioning of equipment and drying processes, as well as to predict product stability. Water sorption isotherms are curves describing the relation between the food water activity (a_w) and its correspondent equilibrium moisture content (X_{eq}) at a given temperature, providing information on the availability and interactions between water molecules and the components of the solid matrix [14]. In addition to water molecules availability, the binding strength of water to matrix components can also be evaluated through differential enthalpy, while the number of available sorption sites at a specific energy level can be determined through differential entropy [15]. These two thermodynamic properties can still be correlated by the Gibbs free energy. Data about the adsorption surface area also provides important information about the binding properties of water with the solid matrix [16], while the spreading pressure can be understood as the driving force that provides diffusion in porous solids [17].

Despite being the subject of several published reports, research on the water adsorption properties of BSG has not yet been reported, this being the first study to provide and compare data on the water adsorption isotherms and thermodynamic properties of BSGs from two different brewery processing (“Lager” and “Weiss” style). Therefore, this study aimed at determining and comparing the chemical composition, water adsorption isotherms, and

thermodynamic properties of BSG from two different brewery processing, simulating both storage and drying conditions.

2. MATERIAL AND METHODS

2.1. Raw material and sample preparation

Brewer's spent grains (BSGs) were obtained from two different breweries. The present work was focused on studying BSG obtained from predominantly barley or wheat malts as the main malted cereals used in brewing. BSG "Lager" style (BSGL), was supplied by a brewery located in the city of Frutal – MG, Brazil. The beer produced was labeled as “pure malt”, made from a wort whose primitive extract comes exclusively from malted barley or malt extract, according to Brazilian legislation [18]. BSG "Weiss" style (BSGW), was supplied by a brewery located in the city of Blumenau – SC, Brazil. The beer produced was labeled as “wheat beer”, which may have a proportion of wheat malt greater than or equal to fifty-one percent, by weight, on the primitive extract, as a source of sugars, according to Brazilian legislation [18]. The by-products were collected and transported to the UNESP Physical Measurements Laboratory (São José do Rio Preto Campus). Three different batches of BSGL and BSGW were used.

The BSGs were dried in a convective tray dryer at 60 ± 2 °C, until equilibrium moisture was obtained, as performed in previous studies [12,13]. Afterward, the dried BSGs were ground in a rotor mill (model MA340, Marconi, Piracicaba, São Paulo, Brazil) and sieved in a 30 mesh sieve to obtain BSGs with granulometry lower than 595 μm.

2.2. Chemical composition of brewer's spent grains (BSGs)

Firstly, the two BSGs were characterized according to their chemical composition. Protein content was determined using the Kjeldahl method [19], with a conversion factor of 6.25. The mineral components were determined as ashes by incineration in a muffle furnace at 550 °C until white ash was reached [19].

Extractive content was analyzed by the Soxhlet method based on NREL/TP-510-42619 [20]. For this analysis, the biomass had to be subjected to extraction in water for 8 h, followed by extraction in ethanol for 24 h in a Soxhlet extractor.

The extractive-free material obtained after extraction with water and ethanol was subjected to acid hydrolysis to determine structural carbohydrates and lignin, according to the NREL/TP-510-42618 method [21]. The Klason lignin content was determined gravimetrically as an insoluble residue, according to Gomide and Demuner [22]. Acid-soluble lignin was measured by UV spectroscopy (Cary 50 Probe, Varian) at wavelengths 215 and 280 nm according to Goldschimid [23].

The determination of cellulose and hemicellulose contents followed the methodology adapted from NREL/TP-510-42618 [21]. These methods were carried out by the analysis in high-performance liquid chromatography (HPLC), in the Shimadzu Prominence chromatograph, using the filtered hydrolyzate obtained previously to the determination of insoluble lignin content of the sample (Klason method). Glucose, xylose, and arabinose monomers were quantified. The analysis conditions were: Phenomenex Rezex RPM-Monosaccharide column, lead stationary phase, mobile phase composed of 85% water and 15% acetonitrile, temperature controlled at 80 °C, the flow rate at 0.85 $mL \cdot min^{-1}$, for 18 min, with quantification by detector evaporative with light scattering (ELSD). When calculating the content of these constituents, the dilution made in the process of quantification of insoluble lignin was considered. To convert the contents of monomers into the contents of cellulose, xylan, and arabinose, it was considered the contents of glucose, xylose, and arabinose, respectively. For cellulose content, the considered factor was 0.9, while for xylan and arabinan it was 0.88. Furthermore, the hemicellulose content was considered as the sum of the xylan and arabinan contents, as they represent the main constituents of this polymer [24]. Compositing results were expressed as mean ± standard deviation of five replicates.

2.3. Determination of the sorption isotherms

The water adsorption isotherms were analyzed using the static gravimetric method [25] at ten different temperatures, simulating storage (5, 10, 20, 30 e 40 °C) and drying (50, 60, 70, 80, and 90°C) conditions. For this, glass desiccators containing saturated solutions of LiBr, LiCl, $MgCl_2$, Nai, K_2CO_3, $Mg(NO_3)_2$, NaBr, KI, NaCl, $(NH_4)_2SO_4$, KCl, KNO_3 e K_2SO_4 were used to simulate environments with different relative humidities (RHs), which in equilibrium, are known as a_w ·

100. Temperatures that simulate storage conditions were provided by a BOD-type chamber (MA 830/A, Marconi, Brazil), and those that simulate drying conditions were controlled in an oven (MA035/2, Marconi, Brazil). The a_w values for each saline solution at different temperatures were obtained according to Labuza [26].

Approximately 3 grams of the BSGs were weighed (in triplicate) and placed in containers. After that, they were inserted into desiccators containing the different saturated saline solutions. The mass of the samples was weighed on an analytical balance (AUW220D, Shimadzu, Japan) until reaching constant mass, which took approximately 3 weeks. The X_{eq} of samples at each condition was calculated using the initial sample weight difference.

For prediction purposes, the mathematical models (Table 1) used in this study were chosen based on the study by Polachini et al. [12], for describing the sorption behavior of cassava bagasse. In addition, these models are commonly used to describe the experimental data and the mechanisms of sorption behavior agri-food products [13,27,28].

Table 1. Mathematical models fitted to the water adsorption isotherms data of the BSGs samples.

Model name	Model	Reference	Equation
GAB	$Xeq = \frac{X_m \times C \times k \times aw}{(1 - k \times aw)(1 + (C - 1)k \times aw)}$	Lomauro et al. (1985)	(1)
Halsey	$Xeq = (-h_1 \times ln(aw))^{-\frac{1}{h_2}}$	Halsey (1948)	(2)
Henderson	$Xeq = \left(-\frac{1}{H_1} \times ln(1 - aw)\right)^{\frac{1}{H_2}}$	Boquet et al. (1978)	(3)
Oswin	$Xeq = M \times \left(\frac{aw}{1 - aw}\right)^N$	Oswin (1946)	(4)
Peleg	$Xeq = k_1 \times aw^{n_1} + k_2 \times aw^{n_2}$	Peleg (1993)	(5)

C, k, k_1, n_1, k_2, n_2, M, N, h_1, h_2 H_1 e *H_2* are constants of the models, X_m represents the monolayer moisture content (dry basis), X_{eq} is the equilibrium moisture content and a_w is the water activity.

These models were tested to describe the water adsorption isotherms of the BSGs. Fitting models to experimental data was performed by nonlinear regression using OriginPro 8.0 software (OriginLab Corporation, Northampton, MA). Fitting accuracy was analyzed through the determination coefficient (R^2_{Adj}), and chi-square (χ^2). Adjusted determination coefficients (R^2_{Adj}) close to 1, and χ^2 close to 0 indicate a great accuracy of the model to the experimental data.

$$R^2_{Adj} = 1 - \frac{n-1}{n-(k+1)}(1 - R^2) \quad (6)$$

$$\chi 2 = \frac{\sum_{i=1}^{N}(exp-pred)^2}{N-z} \quad (7)$$

n is the number of observations, *k* is the number of parameters in the model (excluding the constant), R^2 is the determination coefficient; exp are the experimental results; pred are the predicted results and N is the number of data values and z is the number of constants.

2.4. Adsorption surface area (ASA), Spreading pressure (Φ), and Thermodynamic properties

The adsorption surface area provides important information about the binding properties of water with the solid matrix. The adsorption surface area of BSG's was determined through Equation (8), as reported by [16].

$$ASA = X_m \frac{1}{M_{H2O}} A_{H2O} N_A = 3.53 \cdot 10^3 X_m \quad (8)$$

where ASA is the adsorption surface area ($m^2 \cdot g^{-1}$); N_A is the Avogadro's number ($6 \cdot 10^{23}$ moléculas$\cdot mol^{-1}$); M_{H2O} is the molecular weight of water (18 g$\cdot mol^{-1}$); A_{H2O} is the area of a water molecule ($1.06 \cdot 10^{-19}$ m^2); X_m is the moisture content of the monolayer (kg$\cdot kg^{-1}$ dry base).

Spreading pressure is the driving force that provides diffusion in porous solids. The spreading pressure was calculated from the equation (9) reported by [29]:

$$\Phi = \frac{K_B \cdot T}{A_m} \cdot \ln\left[\frac{1 + c \cdot k \cdot a_w - k \cdot a_w}{1 - k \cdot a_w}\right] \quad (9)$$

where Φ is the spreading pressure (J·m^2); T is the temperature (K); A_m is the surface area of a water molecule (1.06·10^{-19} m^2); K_B is the Boltzmann constant (1.38·10^{-23} J·K^{-1}); c and k are the parameters of the GAB model.

The net isosteric heat of adsorption is a thermodynamic property that describes the binding energy between the matrix and the water molecules as a function of the water content. It can be determined through the slope of the Clausius-Clapeyron equation (Eq. (10)), according to [30], as performed in previous studies [13,28].

$$\frac{\partial(ln\ a_w)}{\partial\left(\frac{1}{T}\right)}|_{Xeq} = -\frac{q_{st}}{R} \quad (10)$$

where q_{st} is the net isosteric heat of adsorption; T is the absolute temperature (K); R is the universal gas constant (8.314 J·mol^{-1}·K^{-1}). The water activity corresponding to certain equilibrium humidity was obtained through the model chosen to represent the adsorption isotherms of BSGs. As seen as the behavior of water adsorption can be represented through thermodynamic properties, the values of entropy (ΔS, J·mol^{-1}·K^{-1}) and differential enthalpy (ΔH, J·mol^{-1}) were obtained through Equation (11) using the same procedure used to determine q_{st}.

$$ln\ (a_w) = -\frac{\Delta H}{RT} + \frac{\Delta S}{R} \quad (11)$$

The Gibbs free energy (ΔG, J·mol^{-1}), which represents the free energy available to perform useful work and to assess the spontaneity of the process [16], was calculated using Equation (12) [30]:

$$\Delta G = RT \cdot ln\ a_w \quad (12)$$

Confirmation of a linear relationship between entropy and enthalpy variations is frequently used in the literature [12,13,28] to prove the theory of thermodynamical compensation, according to Equation (13):

$$\Delta H = T_B \cdot (\Delta S) + \Delta G \quad (13)$$

where, T_B is the isokinetic temperature (K), which represents the temperature at which all sorption phenomena occur at the same rate.

Another requirement to validate the theory of compensation is to compare the isokinetic temperature with the harmonic mean temperature T_{Hm} [31,32] given by Equation (14), where n is the number of isotherms.

$$T_{hm} = \frac{n}{\sum_{i-1}^{n}\left(\frac{1}{T}\right)} \quad (14)$$

To assess whether there is a statistically significant difference between the isokinetic temperature and the harmonic mean temperature, a confidence interval of $(1-\alpha)\cdot 100\%$ was calculated using Equation (15):

$$T_B = T_B \pm t_{m-2,\alpha/2}\sqrt{Var(T_B)} \quad (15)$$

In which,

$$T_B = \frac{\sum(\Delta H - \overline{\Delta H})\cdot(\Delta S - \overline{\Delta S})}{\sum(\Delta S - \overline{\Delta S})^2} \quad (16)$$

$$Var(T_B) = \frac{\sum(\Delta H - \overline{\Delta G_B} - T_B \Delta S)^2}{(m-2)\cdot\sum(\Delta S - \overline{\Delta S})^2} \quad (17)$$

m represents the number of data pairs (ΔH, ΔS), $\overline{\Delta H}$ the average enthalpy, and $\overline{\Delta S}$ the average entropy. A statistical significance α of 0.05 was used to calculate the confidence interval of 95%.

3. RESULTS AND DISCUSSION

3.1. Chemical composition

Table 2 presents the chemical composition obtained for BSGL and BSGW samples. Both BSGs had a high protein content (>21% on a dry basis (db)), with the highest (P<0.05) content found in the BSGW. The protein contents were higher or in the same order of other vegetables sources, such as pea that contains 20-25% of proteins (db) [33]; quinoa (*Chenopodium quinoa*) with approximately 13% of proteins (db) [34] or beans that contain 17.7-27.9% proteins (db) [35].

Table 2. Chemical composition of BSGL and BSGW (in g/100 g dry basis).

Component	BSGL*	BSGW*	P value
Proteins	21.489 ± 0.647 [b]	24.196 ± 0.215 [a]	0.0023
Extractives	8.368 ± 0.066 [a]	8.333 ± 0.101 [a]	0.6469
Ashes	3.674 ± 0.388 [a]	3.874 ± 0.317 [a]	0.5267
Cellulose	15.870 ± 0.784 [a]	15.416 ± 0.212 [a]	0.3868
Hemicellulose (Xylan)	23.629 ± 0.375 [a]	23.485 ± 0.091 [a]	0.5537
Hemicellulose (Arabinan)	4.851 ± 0.147 [a]	4.634 ± 0.079 [a]	0.0876
Insoluble Lignin	17.702 ± 0.284 [a]	16.757 ± 0.321 [b]	0.0187
Soluble Lignin	2.968 ± 0.049 [a]	2.934 ± 0.149 [a]	0.7288

In fact, because of that, the extraction and evaluation of the technological properties of BSG proteins have been studied [5,36] as an alternative plant-based protein source, although the industrial processing of BSG still needs a previous evaluation of physical and thermodynamical properties for an appropriate process design. In addition, the reuse of BSG proteins is in line with global trends toward the use of vegetable proteins for the human diet [37,38], as well as towards the integral use of renewable resources (transforming by products into co-products and, thus, products, within the principle of circular economy). A small part of extractives (approximately 8.3%) and ashes (approximately 3%) also makes up the structure of these biomasses.

Another important part of the composition of BSGs is the content of cellulose, hemicellulose, and lignin, with potential application in biorefinery. BSGL and BSGW had the same content ($P>0.05$) of cellulose (approximately 15%), hemicellulose (Xylan approximately 23%; Arabinan; approximately 4%) and soluble lignin (approximately 2.9%). However, BSGL showed a higher ($P<0.05$) insoluble lignin content (17.7%) when compared to BSGW (16.7%). The complex matrix of lignocellulose is mainly formed by a thick structure of hemicellulose and lignin, which surrounds the cellulose molecules. The observed slightly higher content of insoluble lignin in BSGL may present an indicative about its lower reactivity and its slightly higher difficulty of removal from the complex. The high crystalline structure of cellulose, which is grouped into a matrix of polymers-lignin and hemicellulose, is the main difficulty regarding biomass recalcitrance. The fraction of crystalline cellulose directly impacts the efficiency of the hydrolysis

process [10], requiring it to undergo pre-treatment steps. After undergoing hydrolysis, BSG proved to be an important source of sugar that can be used to produce bioethanol [10,39].

Moreover, the recovery of agro-industrial waste for the development of innovative bio-based polymeric materials [40,41] is a topic of growing importance. Moreirinha et al. [9] developed antioxidant and antimicrobial films based on BSG arabinoxylans, nanocellulose, and feruloylated compounds aiming at producing active packaging. These authors obtained films with antioxidant properties, antimicrobial activity against bacteria such as *Staphylococcus aureus* and *Escherichia coli*, and antifungal activity against *Candida albicans* – showing the potential application of BSGs in active food packaging systems. Edible films could be successfully developed by adding BSG proteins [42]. The study of [43] demonstrated that the use of BSG as a functional filler in polypropylene matrix improved the degradability of the polypropylene matrix, resulting in more eco-friendly materials.

Other recent studies have shown interesting applications such as the use of BSG as carbon source for itaconate production with engineered *Ustilago maydis* after hydrothermal and enzymatic pre-treatments [44]; BSG liquor as a feedstock for lactate production with *Lactobacillus delbrueckii* subsp. *lactis* [45]; microwave pre-treated BSG for biobutanol production [46], among other value-added products [4]. These studies reinforce the potential of this by-product, generally considered waste, to be used as raw material in biorefinery processes with a wide range of industrial applications.

3.2. Water sorption isotherms

Figure 1 shows the changes in equilibrium moisture contents (X_{eq}) of BSGL and BSGW as a function of water activity (a_w) under storage and drying conditions. The values of X_{eq} and a_w (Supplementary Material - Table S1) ranged from 0.0236-0.7648 g of water·g^{-1} of dry matter and 0.0520-0.9848, respectively. Analyzing the data of X_{eq} and a_w at the same temperature, it is noted that X_{eq} increased because of the increase in a_w. On the other hand, it is possible to observe that in the same a_w, the X_{eq} decreased with increasing temperature.

Figure 1. Water adsorption isotherms of BSGs with the fitted GAB model at temperatures that simulate storage and drying conditions (points are experimental data; vertical bars are the standard deviation).

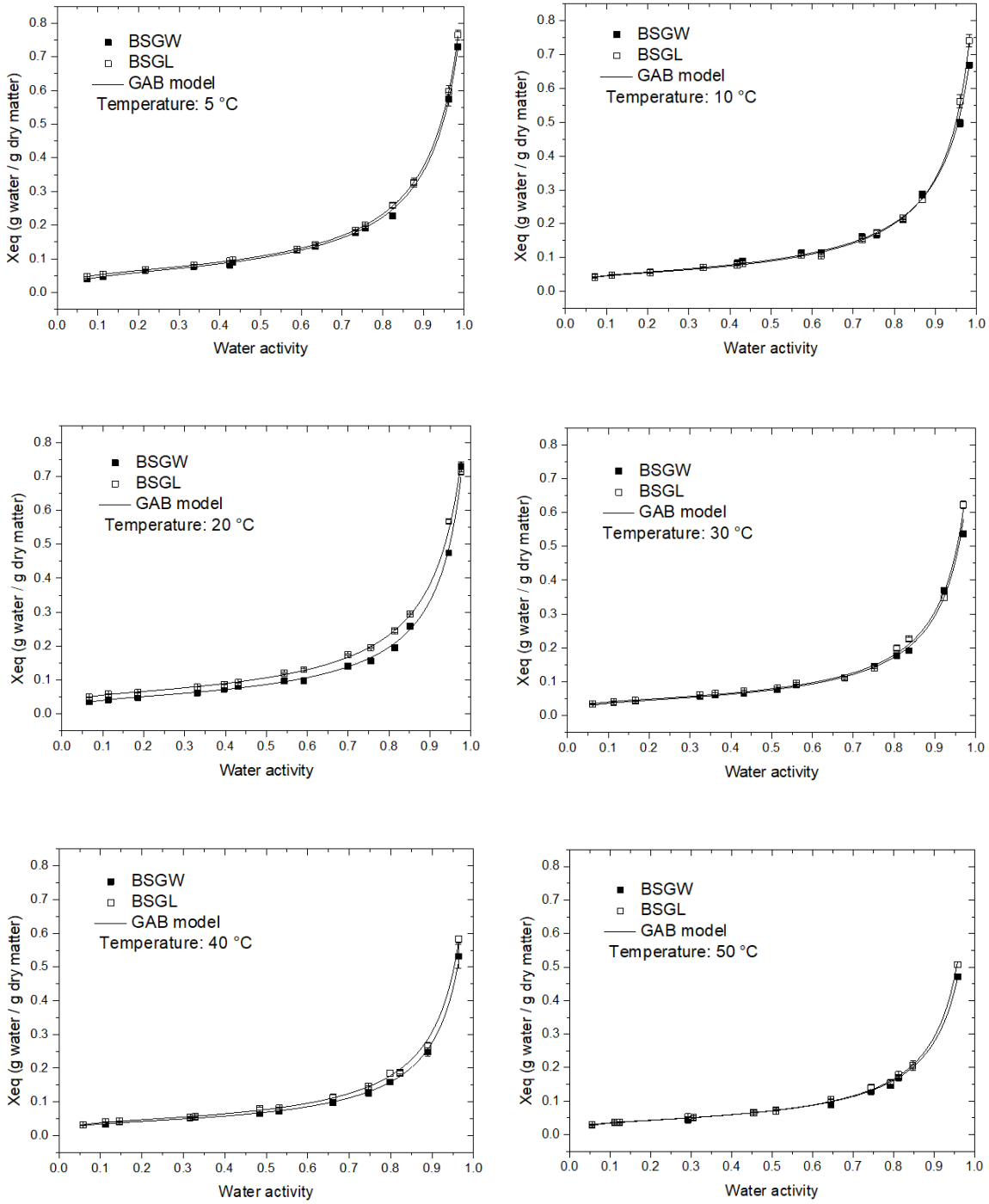

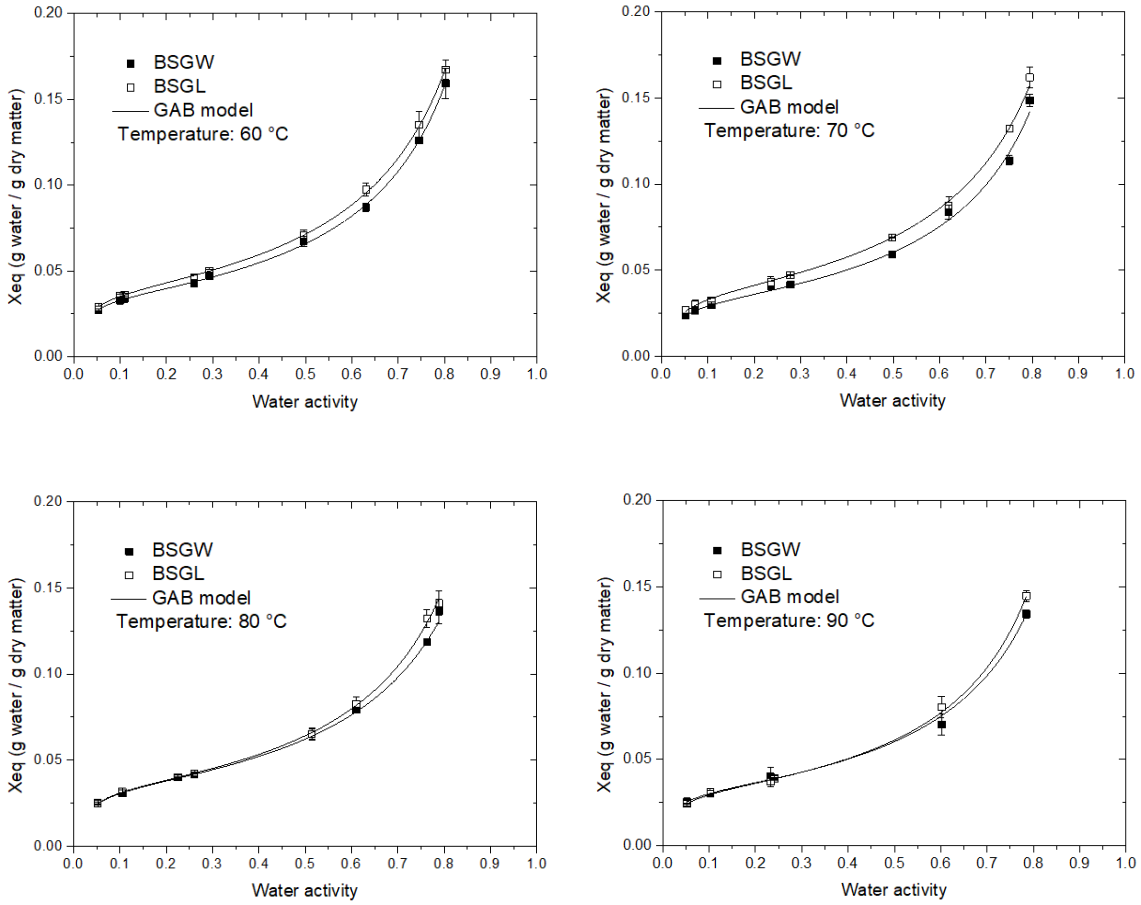

BSGL = Brewer's spent grain "Lager" style; BSGW = Brewer's spent grain "Weiss" style.

This behavior is probably related to the increase in the kinetic energy and the excitation state of the water molecules due to the increase in temperature, which probably reduced the attractive forces between the water molecules and the binding sites of the solid matrix. It makes easier their separation from the binding sites [25], thus promoting a reduction in the moisture content.

Figure 1 also shows higher X_{eq} values in the BSGL isotherms compared to BSGW ones, at almost all temperatures studied, mainly in regions of water activity close to 1. This demonstrates that the BSGL presented a greater water uptake capacity when compared to the BSGW. It can be a consequence of the higher protein content observed for BSGW when compared to BSGL. BSG proteins have a high content of hydrophobic amino acids (barley hordein and glutelins such as phenylalanine, valine, leucine, isoleucine, and methionine), as reported by [36]. In this sense, the greater amount of these nonpolar components may have hindered the water adsorption phenomena in the BSGW, reflecting in lower X_{eq} values.

The shape of the adsorption curves of BSGL and BSGW (Figure 1) were similar at each temperature studied. At temperatures from 5 to 50 °C, the adsorption isotherms of BSGL and BSGW showed convex curves, typical from type III isotherms from Brunauer classification [47]. These types of isotherms are commonly found for starchy and/or high-sugar products [25]. However, at temperatures above 60 °C, there was a slight change in the behavior of the sorption curves of BSGs. The curves started to present a typical behavior of type II isotherms [47], with sigmoid-shaped sorption. According to Mathlouthi [47], water sorption isotherms are generally described by three different regions: (1) the region with $a_w < 0.3$ is composed of the monolayer moisture, which is strongly bound to the non-aqueous constituents of the matrix, through ionic bonds, and is not available for the growth of microorganisms nor enzymatic reactions; (2) the region with a_w between 0.3 and 0.7 is composed of the vicinal water, which presents an almost linear behavior and represents the next layer of water adjacent to the water of the monolayer; (3) the region with $a_w \geq 0.7$ presents water molecules that are less strongly bound to the non-aqueous components of the matrix, and that are available for chemical, enzymatic and microbiological reactions.

This changing behavior in the isotherms shape may be related to the gelatinization temperature of the residual starch present in BSGs. The adsorbed moisture in the matrix penetrated the amorphous regions of the granules, and above 60 °C in the presence of water, the intermolecular hydrogen bonds are broken down, releasing amylose and amylopectin chains, and resulting in the loss of crystalline zones [49]. The dispersion of such polysaccharides may have decreased the steric hindrance for water binding in comparison with non-gelatinized starch granules, making the transition from the second region of multi-layered moisture content towards the free water molecules zone slightly easier.

However, regardless of the isotherms type, the adsorption curves of BSGs showed an abrupt adsorption of water from the range of $a_w \geq 0.7$, which is probably related to the chemical composition of these materials, such as lignin, cellulose, hemicellulose, which have hydrophilic structures capable of water absorption [50]. In fact, similar adsorption curves have been reported for other lignocellulosic materials, such as cassava bagasse, papaya seed, and different types of wood [12,13,51].

Together with the composition, the water relations reinforce BSGs are easily degradable materials, whose processing (as drying or refrigeration) is needed for stabilization before any other step of valorisation. The sorption isotherms were then evaluated through different models (Table 1), to provide ready-to-use information for further processing developments and thermodynamic analysis. Among the evaluated models, the GAB and Peleg models presented lower values of χ^2 and R^2_{adj} closer to 1 at all the evaluated temperatures (Supplementary Material - Table S2).

The GAB model was chosen to describe the water adsorption isotherms for the BSGs at all studied temperatures due to the advantage of having parameters with physical meaning. Figure 2 shows residual plot distributions for the GAB equation in all temperatures.

Figure 2. Residual plot distributions for GAB equation in all temperatures.

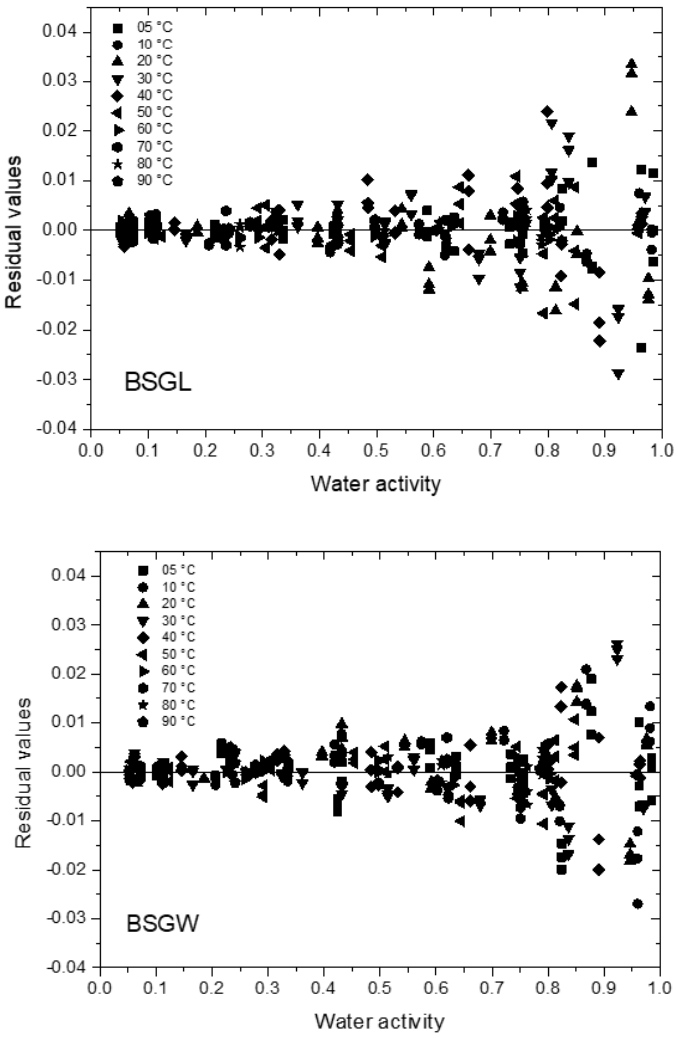

BSGL = Brewer's spent grain "Lager" style; BSGW = Brewer's spent grain "Weiss" style.

A standard distribution in the residue's plots of the BSGs was verified. Residual values tend to increase with increasing water activity. Al-muhtaseb; Mcminn; Magee [25] considered GAB model as the most versatile model for predicting water adsorption isotherms of food-based products over a wide range of a_w.

In fact, several studies concluded that GAB was the most suitable model to predict the isotherms of both food [52,53] and lignocellulosic-based materials [12,29,51]. The theoretical basis of the GAB model is the assumption of localized physical adsorption in multilayers with no lateral interactions: subsequent layers of water have less interaction with the sorbent surface and the first shell of water evenly covers the sorbent surface and is very tightly bound in a monolayer [54].

In the GAB model, the water content of the monolayer (X_m) corresponds to the amount of water strongly adsorbed to the primary adsorption sites. It is considered as the limit value of stability in foods because in this moisture range the rates of deterioration reactions due to the presence of water are negligible [14]. After the formation of the monolayer, water molecules occupy the adsorption sites to create the multilayers successively through relatively weak bonds [55].

Figure 3 shows the values of X_m as a function of temperature. The X_m values for BSGL and BSGW decreased because of the increase in temperature.

Figure 3. X_m values for BSGL and BSGW as a function of temperature.

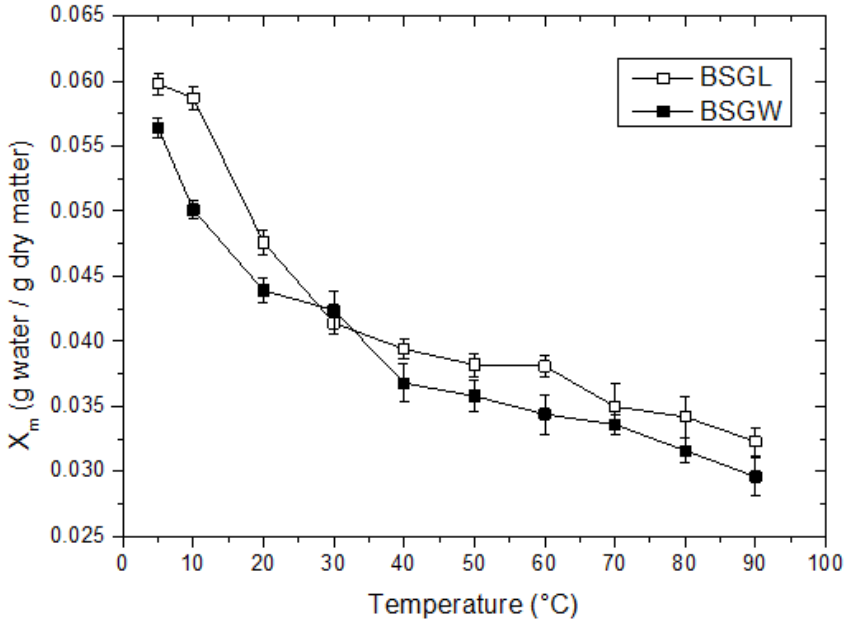

The lowest values of X_m were found for the isotherms at 90 °C and the highest values were found for the isotherms at 5 °C, corroborating the effects of temperature on the X_{eq} of the BSGs. When analyzing the decay of the X_m values with increasing temperature, it could be seen that, above 40 ºC, such values had less significant decrease compared to lower temperatures. Together with the drying kinetics and energy consumption, this value can be considered when designing drying processes of BSGs to avoid spending energy without significant reduction in the monolayer moisture content.

The constant C is related to the binding strength of the monolayer's water to the matrix's active sites [56]. The increase in temperature caused a reduction in the values of C. This trend agrees with the decrease in X_m with increasing temperature, indicating that, above 40 ºC, there were not significant changes in the binding strength represented by C values. This decreasing behavior with increasing temperature has also been reported for other matrices such as non-conventional exudate gum (from *Prosopis alba*) [53] and tamarind seed mucilage [57]. Adsorbent-adsorbate interactions are likely exothermic, resulting in lower C values with increasing temperature [53,58].

The K values are related to the interactions between the adsorbent and the molecules in the multilayers. When K is equal to 1, the water in the multilayers has the properties of liquid water [59]. In this study, the K values were very close to the unit, ranging from 0.9372 to 0.9933 for all the samples and temperatures. Because the water molecules in the multilayers are weakly bound, behaving as liquid water, the need by subjecting the BSGs through adequate stabilization processes to limit the availability of free water for chemical reactions is reinforced. For this, the reported results become essential. Furthermore, the K values showed a tendency to increase as the temperature increased probably because of an increased agitation degree of the molecules by the temperature effect.

3.4. Adsorption surface area (ASA)

The ASA provides important information on the binding properties of water with the solid matrix [57]. This property was calculated using the parameter X_m obtained by the GAB model, through Equation (4) for the 10 temperatures evaluated in this study.

According to Figure 4, the results ranged from 114.01 to 211.09 $m^2 \cdot g^{-1}$ dry solids for BSGL and from 104.48 to 199.09 $m^2 \cdot g^{-1}$ dry solids for BSGW.

Figure 4. Adsorption surface area (ASA) of BSGs as a function of temperature (points are experimental data; vertical bars are the standard deviation).

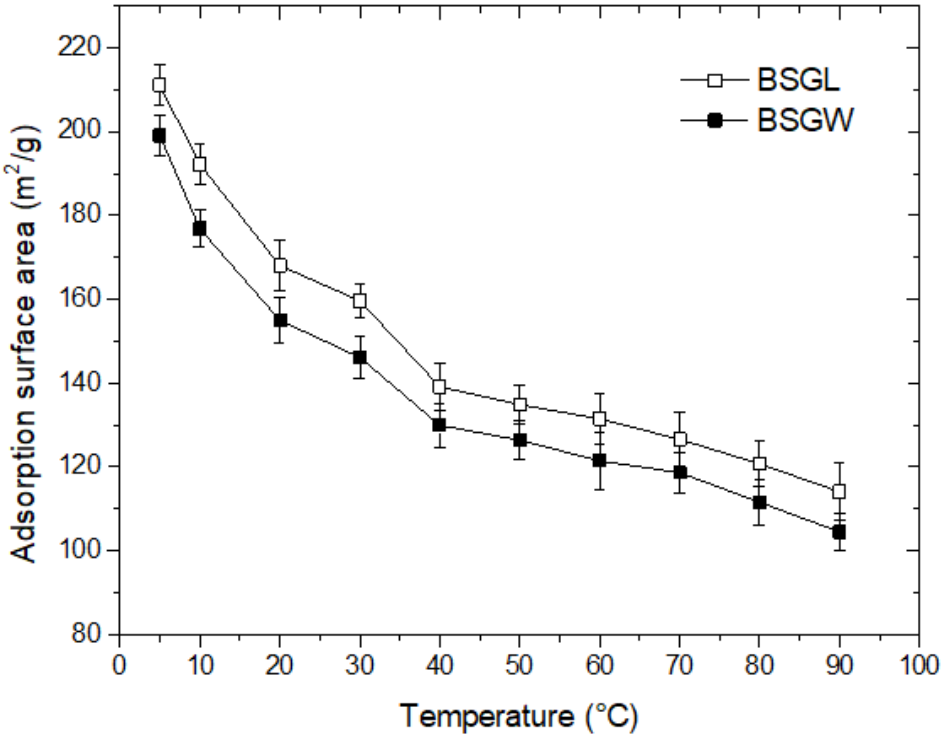

The increase in temperature reduced the ASA for both BSGs, confirming that the availability of active sites and the binding energies associated with water sorption decreased, which probably caused the reduction in the total sorption capacity [60] of BSGs, corroborating the effects of temperature on water sorption isotherms (Figure 1). This reduction in the number of active sites is probably related to temperature-induced physical and chemical changes [16].

At low temperatures (up to 30 °C), BSGL showed a slightly higher ASA when compared to BSGW. The higher ASA in the BSGL may be related to the higher equilibrium moisture (X_{eq}) found in the isotherms of the BSGL (Figure 1), mainly in regions of water activity close to 1. The ASA of several agro-industrial by-products is due to the existence of an intrinsic microporous structure of these materials [13,57]. The number and size of pores, chemical composition, and the interaction of structure and surface in the matrix determine the total sorption area, while the surface pore properties influence the rate and extent of the sorption process [16,60] of the BSGs.

3.5. Spreading pressure (Φ)

The spreading pressure (Φ) can be understood as the driving force responsible for diffusion in porous solids [61], representing the excess free energy on the surface, showing the increase in surface tension at sorption sites due to absorbed molecules [62].

Figure 5 shows the spreading pressure as a function of water activity at different temperatures for the BSGL and for the BSGW.

Figure 5. Spreading pressure as a function of water activity at different temperatures for a) BSGL and b) BSGW (points are experimental data; vertical bars are the standard deviation).

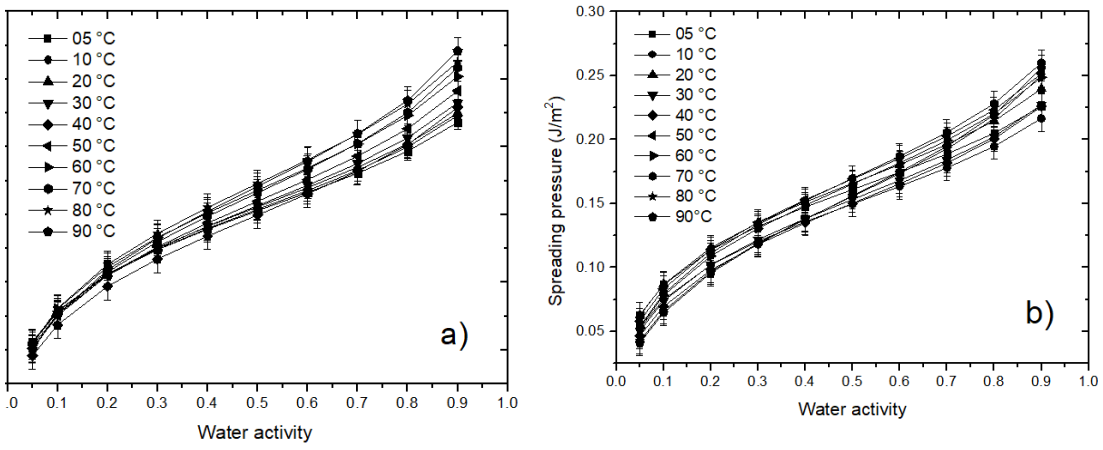

The results indicate that the Φ reduced mainly because of the reduction in the water activity of the BSGs. This shows that the reduction in water activity caused a reduction in the surface potential of the BSGs, reducing the free energy at the surface, which is the driving force responsible for diffusion. Higher spreading pressure values indicate a high affinity between active sites and water molecules. Thus, the higher the value of Φ, the more hygroscopic the product [61]. In contrast, there was a small effect of temperature on the values of Φ when compared to the effects of a_w. The Φ values decreased as the temperature decreased. This same behavior regarding temperature was reported in chestnut wood [29], potato and sweet potato flakes [62], and chironji kernels [63].

3.6. Thermodynamic properties

3.6.1. Net isosteric heat of adsorption (q_{st})

The net isosteric heat of adsorption (q_{st}) provides information on the state of water in foods and can also be used to estimate the amount of energy required during the drying process [16] of BSGs. Given the satisfactory prediction of the water adsorption isotherms of the BSGs using the GAB model, the a_w predicted by this model at a constant equilibrium moisture content (X_{eq}), ranging from 0.1 to 0.45 g of water·g^{-1} dry matter, was used to determine the q_{st}.

According to Figure 6, the energy required for the water adsorption to occur varied from 140.88 to 12356.26 J·mol^{-1} for BSGL and from 156.71 to 14412,31 J·mol^{-1} for BSGW, in a range of X_{eq} between 0.05 and 0.45 (g water / g dry matter).

For cassava bagasse, Polachini et al. [12] reported q_{st} ranging between 850 and 21550 J/mol in a X_{eq} range from 0.05 up to 0.30 g water / g dry matter. Such values are similar in magnitude to the ones found in the present work. Rosa et al. [13] presented relatively lower q_{st} values for papaya seed, which ranged from 560 to 8710 J/mol in a X_{eq} interval between 0.30 and 0.48 g water / g dry matter. It is valid to highlight that such values depends on the equilibrium moisture content range investigated, but also on the studied material – reinforcing the need by studying each product specifically.

Figure 6. Net isosteric heat of sorption of BSGs as a function of equilibrium moisture content (points are experimental data; vertical bars are the standard deviation).

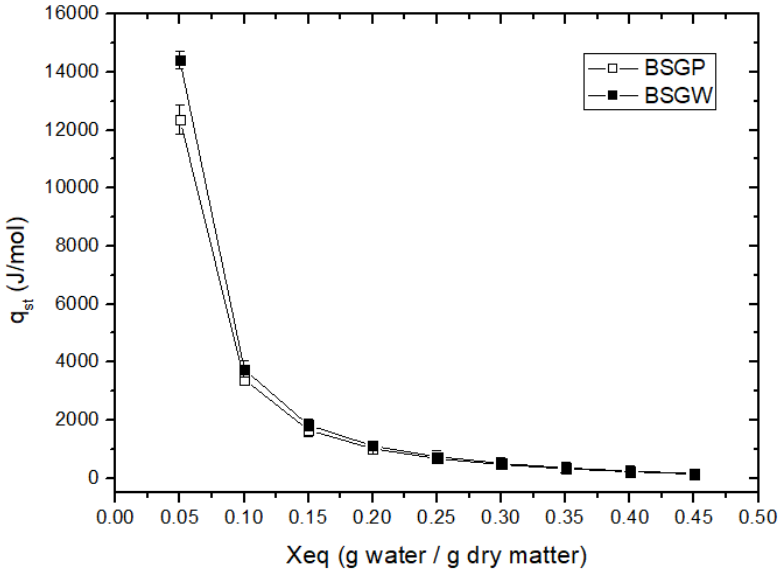

BSGL = Brewer's spent grain "Lager" style; BSGW = Brewer's spent grain "Weiss" style.

In both BSGs, an increase in q_{st} was observed due to the reduction of X_{eq}, showing that more heat is needed as the material's moisture decreases during drying. It can be related to the fact that, in regions of low moisture content, water molecules are strongly bound to macromolecules such as cellulose, hemicellulose, lignin, and proteins present in the structure of the material, when compared to water from adjacent multilayers. This trend was also observed in other lignocellulosic-based materials such as cassava bagasse [12], different types of wood [29] papaya seeds [13], and wheat malt [28].

As initially reported, the stability of this by-product is strongly dependent on a_w and X_{eq} conditions, which are key parameters for its management and use. In addition to the high a_w providing highly favorable conditions for the growth of microorganisms, non-enzymatic browning, and enzymatic reactions, it can also cause changes in the technological and sensory properties of this by-product when considering it as an ingredient in food products [64]. Thus, designing the ideal conditions for the water activity of the BSGs aiming at lower energy consumption during the drying process and maximum stability during storage can contribute to the management and reuse of BSGs with preserved quality.

Considering that microbial growth and enzymatic activity are the main responsible for drastically affecting the quality of BSGs, it is advisable to store such by-products under suitable conditions. According to Bonazzi; Dumoulin [61], these reactions have a high reaction rate above a water activity of 0.4. Another factor that can cause undesirable reactions is lipid oxidation, which has a lower reaction rate in water activity between 0.2 to 0.4. From an energy point of view, the lower the X_{eq}, the higher the enthalpy and heat of adsorption values, indicating that more energy is needed to remove water molecules under these conditions. Therefore, from an energy and stability point of view, the ideal long-term storage condition for BSGs was considered when the water activity reached 0.4. Thus, BSGs must be stored in environments with a relative humidity of 40%, which can contribute to longer shelf life.

3.6.2. Differential enthalpy and entropy

Differential enthalpy and entropy are thermodynamic properties that can be used to evaluate the water adsorption behavior of BSGs. These properties

were calculated using Equation (13), over a range of X_{eq} from 0.1 to 0.45 (dry basis).

Figure 7. Change in enthalpy and entropy of BSGs as a function of equilibrium moisture contents (points are experimental data; vertical bars are the standard deviation).

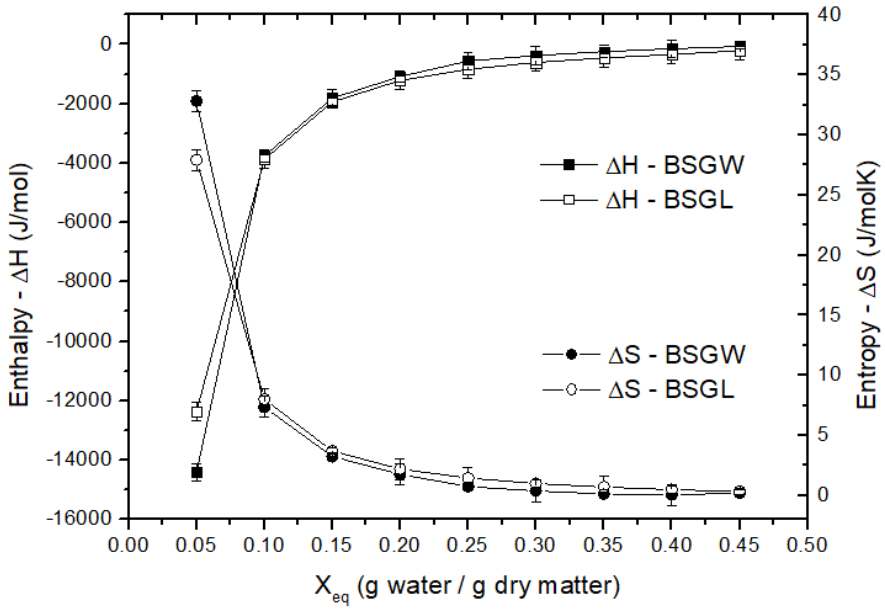

BSGL = Brewer's spent grain "Lager" style; BSGW = Brewer's spent grain "Weiss" style.

Enthalpy is a property that informs the variations of thermal energy involved between the water molecules with the matrix (sorbent) during the adsorption processes [66,67]. This property ranged from -3757.01 to -156.71 J·mol^{-1} for BSGL and from -3303.56 to -140.88 J·mol^{-1} for BSGW (Figure 7).

The negative enthalpy values indicates that there are binding forces involved in the adsorption process, in addition to characterizing the process as exothermic [66,68]. Furthermore, this property is like the isosteric heat of adsorption, meaning it represents the energy required to do useful work [30].

Entropy is a measure of the degree of disorder in a water sorption system, being a measure of the unavailability of energy to carry out a given process [66], as in drying. In this study, the differential entropy ranged from 0.01 to 7.59 J·mol^{-1}·K^{-1} for BSGL and from 0.003 to 6.60 J·mol^{-1}·K^{-1} for BSGW (Figure 7). In modulus, both enthalpy and entropy increased as the moisture content of the BSGs is reduced. This is probably associated with reductions in adsorption surface area and spreading pressure (driving force responsible for diffusion in porous solids) as the material loses moisture, being this more expressive in

regions with moisture below 0.2 g of water·g^{-1} of dry matter, indicating that more energy is needed to remove water molecules under these conditions. Furthermore, it is noteworthy that the moisture at which the maximum enthalpy and entropy values, in modulus, were reached are very close to the monolayer moisture values obtained from the GAB model. It is due to the presence of highly active polar sites that bind water to incorporate moisture in the food matrix monolayer [69]. On the other hand, the formation of multiple layers of adsorbed water is probably the main reason for the decrease in enthalpy and entropy with increasing moisture content [25]. The same behavior was reported in lignocellulosic materials such as cassava bagasse [12], papaya seeds [13],and different types of wood [29].

3.6.3. Enthalpy-entropy compensation theory

Compensation theory is used to evaluate physical and chemical phenomena [68], such as the water sorption reactions that occur during BSGs processing. Moreover, it provides information about the reaction mechanism and whether the reaction is controlled by enthalpy, where there will be greater molecular interaction due to the reduction of freedom or the binding of molecules in the system, generating greater organization or order; or entropy, where there will be disorganization and greater freedom of molecules in the system [70].

Figure 8 presents the linear relationships between differential enthalpy and entropy for BSGs. These linear relationships are considered strong when the adjusted coefficients of determination (R^2_{adj}) were greater than 0.99, being the first important requirement to validate the existence of the theory of enthalpy-entropy compensation. In this work, it was found a R^2_{adj} higher than 0.999 for both samples, confirming that changes in entropy are linearly accompanied by changes in enthalpy.

The second requirement to confirm the existence of the compensation theory is to compare the isokinetic temperature (T_b) with the harmonic mean temperature (T_{hm}). If these temperatures are statistically different, the second requirement to confirm a linear chemical compensation pattern is confirmed [31,32]. Therefore, the parameters T_b and ΔG_b were calculated using Equation (11).

Figure 8. Linear relationship between differential enthalpy and differential entropy values for BSGL and BSGW.

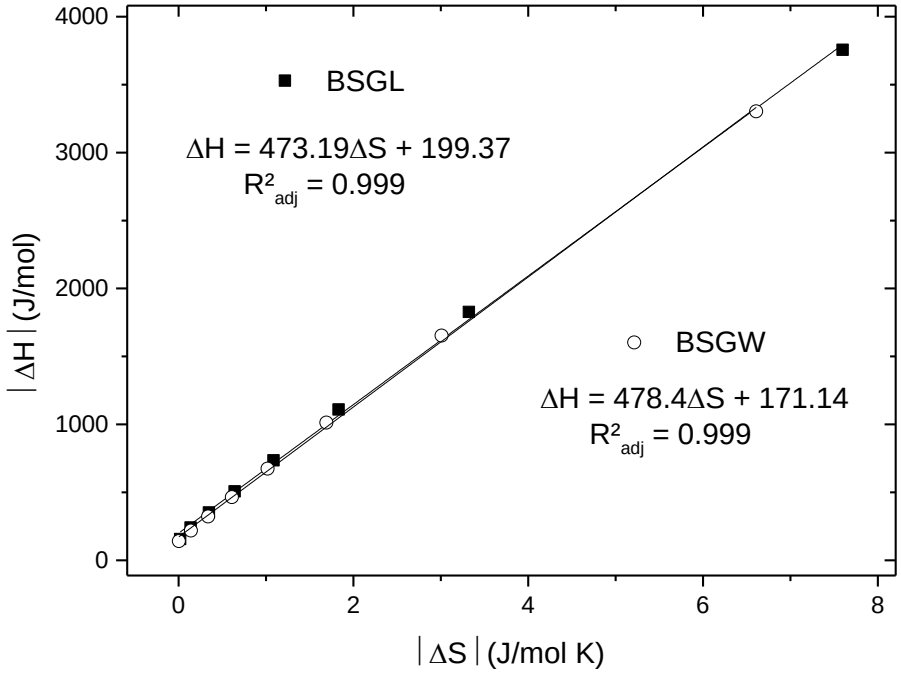

BSGL = Brewer's spent grain "Lager" style; BSGW = Brewer's spent grain "Weiss" style.

The isokinetic temperature (T_b) for BSGL and BSGW were 473.19 ± 13.82 K and 478.4 ± 11.88 K, respectively. The harmonic mean temperature (T_{hm}) resulted in a value of 316.20 K for both BSGs. Thus, the harmonic mean temperature (T_{hm}) is significantly lower than the isokinetic temperature (T_b) with 95% confidence. This means that the adsorption process is enthalpy controlled [70]. In fact, the sorption of most products appears to be controlled by enthalpy [12,13,17]. Gabas; Menegalli; Telis-Romero [67] state that, when the water sorption process is controlled by enthalpy, the microstructure of the material is stable (within the studied temperature range) and does not significantly change during the water sorption phenomenon. The values of Gibbs free energy at the T_b (ΔG_b) obtained in the present study were 199.37 J·mol^{-1} for BSGL and 171.14 J·mol^{-1} for BSGW. Both assumed positive values, indicating that the adsorption process of BSGs is not spontaneous ($+\Delta G_b$). This fact may be related to the composition of BSGs in terms of lipids and proteins. Recently, Abeynayake et al. [36] studied BSG proteins and identified a high content of hydrophobic amino acid content of barley hordein and glutelins such as phenylalanine, valine, leucine, isoleucine, and methionine. These nonpolar components make the water adsorption phenomena difficult, corroborating the fact that the adsorption process

is not spontaneous. This indicates that the product does not spontaneously absorb moisture from the environment, which is desirable for the stability of the by-product.

4. CONCLUSIONS

In this study, the water adsorption properties of brewer's spent grain (BSG) obtained from barley- and wheat-malt based brewery process (“Lager” – BSGL and “Weiss” – BSGW) were evaluated in a wide temperature range (5 - 90°C) to cover conditions for stabilization – from storage to drying processes. At temperatures from 5 to 50 °C, the adsorption isotherms of BSGL and BSGW showed convex curves, typical of type III isotherms. However, at temperatures above 60 °C, the curves started to present a typical behavior of type II isotherms with sigmoid-shaped sorption. The equilibrium moisture increased as a result of the increase in relative humidity and reduction in temperature. Water binding properties seemed to be slightly hampered by the higher protein contents observed in BSGW samples. The GAB model was the most suitable model to describe the adsorption isotherms of BSGs, providing data on the monolayer moisture in this wide temperature range. Thermodynamic analysis showed that the net isosteric heat of adsorption and the differential entropy decreased as the equilibrium moisture increased. The spreading pressure increased mainly as the water activity increased. The linear relationship between enthalpy and entropy confirmed the theory of compensation and showed that the adsorption processes of BSGs were driven by enthalpy. The Gibbs free energy indicated that the adsorption processes were not spontaneous. From an energy and stability point of view, a water activity of 0.4 is the ideal condition for the storage of BSGs. Thus, this by-product must be stored in environments with a relative humidity of 40% to stabilize the BSGs, generating humidity levels between 0.05-0.09 (g of water·g^{-1} dry matter), depending on the temperature, which can contribute to longer shelf life for future applications in biorefinery and/or food applications.

Declaration of competing interest

The authors declare no conflict of interest.

Acknowledgments

This study was financed in part by the São Paulo Research Foundation (FAPESP) – Grant n°2022/05272-8 and by the Coordenação de Aperfeiçoamento de Pessoal de Nível Superior - Brasil (CAPES) - Finance Code 001.

This study was in part carried out in the Centre Européen de Biotechnologie et de Bioéconomie (CEBB), supported by the Région Grand Est, Département de la Marne, Greater Reims (France) and the European Union. In particular, the authors would like to thank the Département de la Marne, Greater Reims, Région Grand Est and the European Union along with the European Regional Development Fund (ERDF Champagne Ardenne 2014-2020) for their financial support of the Chair of Biotechnology of CentraleSupélec.

5. SUPPLEMENTARY MATERIAL

Table S1 Experimental data on equilibrium moisture content of BSGs versus water activity at the temperatures studied (average ± standard deviation).

5 °C			10 °C			20 °C			30 °C		
a_w*	X_{eq}		a_w*	X_{eq}		a_w*	X_{eq}		a_w*	X_{eq}	
	BSGL	BSGW		BSGL	BSGW		BSGL	BSGW		BSGL	BSGW
0.0743	0.0473 ± 0.0008	0.0400 ± 0.0019	0.0714	0.0407 ± 0.0005	0.0430 ± 0.0003	0.0661	0.0487 ± 0.0009	0.0348 ± 0.0008	0.0616	0.0343 ± 0.0006	0.0323 ± 0.0015
0.1126	0.0544 ± 0.0008	0.0462 ± 0.0019	0.1129	0.0481 ± 0.0003	0.0482 ± 0.0011	0.1131	0.0577 ± 0.0014	0.0410 ± 0.0006	0.1128	0.0411 ± 0.0006	0.0385 ± 0.0014
0.2168	0.0668 ± 0.0018	0.0662 ± 0.0030	0.2061	0.0554 ± 0.0006	0.0568 ± 0.0012	0.1856	0.0622 ± 0.0016	0.0477 ± 0.0006	0.1657	0.0445 ± 0.0011	0.0419 ± 0.0011
0.3360	0.0814 ± 0.0012	0.0775 ± 0.0027	0.3347	0.0710 ± 0.0005	0.0700 ± 0.0003	0.3307	0.0785 ± 0.0016	0.0615 ± 0.0009	0.3244	0.0608 ± 0.0013	0.0564 ± 0.0004
0.4242	0.0938 ± 0.0018	0.0818 ± 0.0020	0.4183	0.0780 ± 0.0010	0.0843 ± 0.0017	0.3965	0.0860 ± 0.0018	0.0724 ± 0.0009	0.3615	0.0645 ± 0.0029	0.0599 ± 0.0017
0.4313	0.0958 ± 0.0022	0.0911 ± 0.0014	0.4314	0.0829 ± 0.0011	0.0899 ± 0.0016	0.4316	0.0925 ± 0.0025	0.0803 ± 0.0022	0.4317	0.0721 ± 0.0028	0.0650 ± 0.0002
0.5886	0.1293 ± 0.0011	0.1259 ± 0.0018	0.5736	0.1065 ± 0.0022	0.1134 ± 0.0020	0.5438	0.1201 ± 0.0017	0.0963 ± 0.0006	0.5140	0.0808 ± 0.0019	0.0757 ± 0.0012
0.6351	0.1426 ± 0.0030	0.1372 ± 0.0058	0.6215	0.1058 ± 0.0037	0.1149 ± 0.0035	0.5914	0.1301 ± 0.0026	0.0975 ± 0.0013	0.5603	0.0947 ± 0.0017	0.0901 ± 0.0005
0.7330	0.1854 ± 0.0017	0.1783 ± 0.0038	0.7211	0.1520 ± 0.0022	0.1618 ± 0.0034	0.6990	0.1746 ± 0.0037	0.1402 ± 0.0009	0.6789	0.1119 ± 0.0028	0.1114 ± 0.0019
0.7565	0.1995 ± 0.0029	0.1910 ± 0.0077	0.7567	0.1738 ± 0.0029	0.1671 ± 0.0035	0.7547	0.1949 ± 0.0066	0.1552 ± 0.0027	0.7509	0.1399 ± 0.0019	0.1442 ± 0.0026
0.8242	0.2590 ± 0.0070	0.2279 ± 0.0070	0.8206	0.2161 ± 0.0047	0.2110 ± 0.0025	0.8134	0.2447 ± 0.0043	0.1953 ± 0.0029	0.8063	0.1984 ± 0.0070	0.1772 ± 0.0061
0.8767	0.3273 ± 0.0132	0.3268 ± 0.0062	0.8677	0.2703 ± 0.0017	0.2884 ± 0.0024	0.8511	0.2951 ± 0.0069	0.2582 ± 0.0043	0.8362	0.2260 ± 0.0057	0.1912 ± 0.0026
0.9627	0.5972 ± 0.0186	0.5749 ± 0.0205	0.9596	0.5613 ± 0.0054	0.4971 ± 0.0107	0.9462	0.5675 ± 0.0192	0.4747 ± 0.0084	0.9231	0.3486 ± 0.0094	0.3698 ± 0.0030
0.9848	0.7648 ± 0.0155	0.7294 ± 0.0098	0.9818	0.7403 ± 0.0073	0.6677 ± 0.0039	0.9759	0.7143 ± 0.0187	0.7295 ± 0.0149	0.9700	0.6236 ± 0.0109	0.5370 ± 0.0091

40 °C			50 °C			60 °C			70 °C		
a_w*	X_{eq}		a_w*	X_{eq}		a_w*	X_{eq}		a_w*	X_{eq}	
	BSGL	BSGW		BSGL	BSGW		BSGL	BSGW		BSGL	BSGW
0.0580	0.0315 ± 0.0006	0.0305 ± 0.0004	0.0553	0.0307 ± 0.0016	0.0281 ± 0.0019	0.0533	0.0289 ± 0.0009	0.0275 ± 0.0019	0.0523	0.0269 ± 0.0020	0.0236 ± 0.0011
0.1121	0.0400 ± 0.0006	0.0343 ± 0.0003	0.1110	0.0374 ± 0.0029	0.0350 ± 0.0018	0.1095	0.0362 ± 0.0006	0.0339 ± 0.0014	0.1075	0.0325 ± 0.0012	0.0297 ± 0.0002
0.1455	0.0431 ± 0.0008	0.0402 ± 0.0012	0.1238	0.0372 ± 0.0011	0.0354 ± 0.0025	0.0998	0.0358 ± 0.0009	0.0328 ± 0.0017	0.0723	0.0304 ± 0.0015	0.0263 ± 0.0011
0.3160	0.0554 ± 0.0021	0.0531 ± 0.0009	0.3054	0.0527 ± 0.0031	0.0509 ± 0.0004	0.2926	0.0500 ± 0.0010	0.0472 ± 0.0021	0.2777	0.0470 ± 0.0003	0.0415 ± 0.0005
0.3288	0.0565 ± 0.0043	0.0547 ± 0.0009	0.2921	0.0532 ± 0.0012	0.0441 ± 0.0019	0.2595	0.0463 ± 0.0015	0.0429 ± 0.0018	0.2357	0.0429 ± 0.0036	0.0410 ± 0.0025
0.4842	0.0798 ± 0.0036	0.0668 ± 0.0019	0.4544	0.0643 ± 0.0032	0.0663 ± 0.0008	0.4966	0.0709 ± 0.0032	0.0672 ± 0.0027	0.4970	0.0689 ± 0.0002	0.0590 ± 0.0008
0.5317	0.0811 ± 0.0032	0.0720 ± 0.0046	0.5093	0.0705 ± 0.0005	0.0732 ± 0.0019	0.6311	0.0974 ± 0.0036	0.0871 ± 0.0023	0.6193	0.0874 ± 0.0051	0.0837 ± 0.0041
0.6609	0.1134 ± 0.0070	0.0973 ± 0.0042	0.6449	0.1053 ± 0.0018	0.0883 ± 0.0030	0.7450	0.1352 ± 0.0080	0.1261 ± 0.0009	0.7506	0.1321 ± 0.0018	0.1137 ± 0.0028
0.7468	0.1462 ± 0.0032	0.1263 ± 0.0031	0.7443	0.1408 ± 0.0069	0.1287 ± 0.0060	0.8025	0.1672 ± 0.0057	0.1593 ± 0.0088	0.7949	0.1619 ± 0.0059	0.1486 ± 0.0036
0.7991	0.1852 ± 0.0091	0.1588 ± 0.0033	0.7920	0.1550 ± 0.0073	0.1472 ± 0.0041						
0.8232	0.1877 ± 0.0052	0.1845 ± 0.0086	0.8120	0.1788 ± 0.0013	0.1700 ± 0.0037						
0.8903	0.2660 ± 0.0104	0.2481 ± 0.0125	0.8478	0.2060 ± 0.0140	0.2054 ± 0.0035						
0.9641	0.5823 ± 0.0108	0.5317 ± 0.0353	0.9582	0.5074 ± 0.0081	0.4712 ± 0.0056						

80 °C			90 °C		
a_w*	X_{eq}		a_w*	X_{eq}	
	BSGL	BSGW		BSGL	BSGW
0.0520	0.0248 ± 0.0008	0.0250 ± 0.0004	0.0526	0.0243 ± 0.0003	0.0253 ± 0.0023
0.1051	0.0317 ± 0.0008	0.0307 ± 0.0003	0.1023	0.0311 ± 0.0011	0.0301 ± 0.0018
0.2605	0.0421 ± 0.0012	0.0416 ± 0.0008	0.2412	0.0386 ± 0.0006	0.0390 ± 0.0005
0.2252	0.0400 ± 0.0015	0.0399 ± 0.0006	0.2325	0.0372 ± 0.0020	0.0400 ± 0.0056
0.5143	0.0652 ± 0.0037	0.0651 ± 0.0032	0.6021	0.0804 ± 0.0061	0.0703 ± 0.0062
0.6097	0.0825 ± 0.0044	0.0793 ± 0.0016	0.7850	0.1448 ± 0.0033	0.1344 ± 0.0023
0.7629	0.1321 ± 0.0052	0.1186 ± 0.0014			
0.7890	0.1411 ± 0.0071	0.1365 ± 0.0071			

Table S2 Fitting parameters of the proposed models fitted to the adsorption data.

T (°C)	Model						Fitting parameters			
	GAB									
	X_m		C		k		R_{Adj}^2		χ^2	
	BSGL	BSGW	BSGL	BSGW	BSGL	BSGW	BSGL	BSGW	BSGL	BSGW
5	0.0598	0.0564	76.1689	95.6266	0.9375	0.9372	0.9999	0.9988	<0.0001	0.0001
10	0.0587	0.0501	70.2431	64.1169	0.9532	0.9411	0.9996	0.9973	<0.0001	0.0001
20	0.0476	0.0439	65.5893	82.0667	0.9405	0.9626	0.9976	0.9981	0.0001	0.0001
30	0.0414	0.0424	56.0584	52.2692	0.9620	0.9527	0.9963	0.9959	0.0001	0.0001
40	0.0394	0.0368	41.0072	42.8096	0.9668	0.9508	0.9975	0.9989	0.0001	<0.0001
50	0.0382	0.0358	46.8779	58.4730	0.9650	0.9674	0.9991	0.9987	<0.0001	<0.0001
60	0.0381	0.0344	50.4859	47.5695	0.9647	0.9623	0.9996	0.9994	<0.0001	<0.0001
70	0.0350	0.0336	41.3370	45.5037	0.9856	0.9784	0.9992	0.9928	<0.0001	<0.0001
80	0.0342	0.0316	44.8590	29.3419	0.9671	0.9857	0.9986	0.9980	<0.0001	<0.0001
90	0.0323	0.0296	36.5881	26.5033	0.9924	0.9933	0.9988	0.9963	<0.0001	<0.0001
T (°C)	Peleg									
	k1		n1		k2		n2		R_{Adj}^2		χ^2	
	BSGL	BSGW	BSGL	BSGW	BSGL	BSGW	BSGL	BSGW	BSGL	BSGW	BSGL	BSGW
5	0.6603	0.6319	10.9333	10.8331	0.1908	0.1821	0.6871	0.7137	0.9956	0.9961	0.0002	0.0002
10	0.1710	0.1639	0.6108	0.6535	0.6418	0.5899	10.3297	11.0209	0.9953	0.9914	0.0002	0.0003
20	0.1486	0.7750	0.5833	15.8932	0.7629	0.1936	10.6053	0.9662	0.9983	0.9904	0.0001	0.0004
30	0.1627	0.1158	0.8188	0.5604	0.6884	0.5681	13.7159	9.7746	0.9859	0.9973	0.0004	0.0001
40	0.1592	0.6340	0.7993	11.9789	0.7112	0.1208	14.1113	0.6330	0.9909	0.9924	0.0002	0.0001
50	0.1129	0.0984	0.5548	0.5028	0.6092	0.5578	10.1155	9.3525	0.9951	0.9982	0.0001	<0.0001
60	0.2593	0.0714	4.3434	0.3384	0.0711	0.2870	0.3059	5.1615	0.9992	0.9981	<0.0001	<0.0001
70	0.3154	0.0728	5.4712	0.3969	0.0767	0.3052	0.3700	5.9231	0.9977	0.9891	<0.0001	<0.0001
80	0.0620	0.0671	0.3043	0.3449	0.2222	0.2094	4.0817	4.5285	0.9996	0.9957	<0.0001	<0.0001
90	0.2451	0.0605	3.9826	0.3000	0.0548	0.2935	0.2658	5.4684	0.9994	0.9996	<0.0001	<0.0001
T (°C)	Halsey									
	h1				h2				R_{Adj}^2		χ^2	

	BSGL	BSGW	BSGL	BSGW	BSGL	BSGW	BSGL	BSGW
5	100.7093	109.9107	2.0704	2.0602	0.9766	0.9724	0.0011	0.0012
10	94.9177	111.0451	1.9808	1.9582	0.9813	0.9865	0.0008	0.0005
20	62.4824	66.0896	1.6912	1.6178	0.9814	0.9954	0.0008	0.0002
30	68.0977	86.4013	1.5781	1.6655	0.9960	0.9827	0.0001	0.0004
40	61.4193	69.5778	1.4964	1.4860	0.9991	0.9986	<0.0001	0.0001
50	63.4499	71.3083	1.4731	1.4916	0.9990	0.9973	<0.0001	0.0001
60	61.2584	63.9645	1.4459	1.4227	0.9977	0.9952	<0.0001	0.0001
70	57.0334	65.6116	1.3921	1.3897	0.9955	0.9898	<0.0001	0.0001
80	67.6192	84.8914	1.4207	1.4875	0.9973	0.9970	<0.0001	0.0001
90	58.0276	76.9061	1.3612	1.4399	0.9970	0.9862	<0.0001	0.0001

Henderson

T (°C)	H1		H2		R_{Adj}^2		χ^2	
	BSGL	BSGW	BSGL	BSGW	BSGL	BSGW	BSGL	BSGW
5	5.3037	5.4941	0.8711	0.8658	0.9855	0.9856	0.0007	0.0006
10	5.3729	5.7600	0.8575	0.8481	0.9822	0.9811	0.0007	0.0006
20	4.6470	4.7557	0.7352	0.6975	0.9785	0.9789	0.0009	0.0008
30	5.0705	5.7017	0.7128	0.7655	0.9691	0.9738	0.0008	0.0006
40	4.9355	5.1898	0.6764	0.6663	0.9608	0.9637	0.0009	0.0007
50	5.1865	5.5003	0.6890	0.7019	0.9596	0.9622	0.0007	0.0005
60	25.8697	27.0504	1.4737	1.4497	0.9390	0.9289	0.0001	0.0002
70	25.5715	29.7569	1.4449	1.4452	0.9330	0.9286	0.0002	0.0001
80	27.1755	36.5055	1.4227	1.5188	0.9468	0.9462	0.0001	0.0001
90	26.8241	40.6830	1.4320	1.5638	0.9382	0.9049	0.0001	0.0002

Oswin

T (°C)	M		N		R_{Adj}^2		χ^2	
	BSGL	BSGW	BSGL	BSGW	BSGL	BSGW	BSGL	BSGW
5	0.1262	0.1197	0.4434	0.4456	0.9857	0.9826	0.0007	0.0007
10	0.1184	0.1066	0.4616	0.4670	0.9879	0.9921	0.0005	0.0003
20	0.1040	0.0902	0.5412	0.5672	0.9852	0.9965	0.0006	0.0001
30	0.0838	0.0834	0.5767	0.5438	0.9949	0.9864	0.0001	0.0003
40	0.0780	0.0702	0.6074	0.6128	0.9945	0.9940	0.0001	0.0001
50	0.0738	0.0707	0.6122	0.6035	0.9933	0.9931	0.0001	0.0001

60	0.0807	0.0751	0.4864	0.4946	0.9759	0.9694	0.0001	0.0001
70	0.0773	0.0696	0.4998	0.5003	0.9710	0.9662	0.0001	0.0001
80	0.0716	0.0694	0.4986	0.4722	0.9789	0.9788	<0.0001	0.0001
90	0.0725	0.0690	0.5085	0.4739	0.9740	0.9520	0.0001	0.0001

Iglesias & Chirife

T (°C)	A		B		R_{Adj}^2		χ^2	
	BSGL	**BSGW**	**BSGL**	**BSGW**	**BSGL**	**BSGW**	**BSGL**	**BSGW**
5	0.1257	0.1187	0.0113	0.0108	0.8451	0.8382	0.0071	0.0069
10	0.1139	0.1027	0.0127	0.0118	0.8705	0.8859	0.0052	0.0039
20	0.0918	0.0799	0.0181	0.0174	0.9086	0.9441	0.0040	0.0022
30	0.0702	0.0695	0.0183	0.0161	0.9496	0.9088	0.0013	0.0019
40	0.0627	0.0564	0.0203	0.0186	0.9664	0.9659	0.0008	0.0006
50	0.0556	0.0531	0.0206	0.0192	0.9669	0.9594	0.0005	0.0006
60	0.0336	0.0309	0.0341	0.0322	0.9925	0.9954	<0.0001	0.0001
70	0.0302	0.0271	0.0343	0.0309	0.9950	0.9888	<0.0001	0.0001
80	0.0295	0.0299	0.0311	0.0287	0.9915	0.9893	<0.0001	0.0001
90	0.0269	0.0275	0.0328	0.0292	0.9953	0.9948	<0.0001	0.0001

6. REFERENCES

[1] M. Yang, X. Zhai, X. Huang, Z. Li, J. Shi, Q. Li, X. Zou, M. Battino, Rapid discrimination of beer based on quantitative aroma determination using colorimetric sensor array, **Food Chem**. 363 (2021) 130297. https://doi.org/10.1016/J.FOODCHEM.2021.130297.

[2] M. Kavalopoulos, V. Stoumpou, A. Christofi, S. Mai, E.M. Barampouti, K. Moustakas, D. Malamis, M. Loizidou, Sustainable valorisation pathways mitigating environmental pollution from brewers' spent grains, **Environmental Pollution**. 270 (2021) 116069. https://doi.org/10.1016/J.ENVPOL.2020.116069.

[3] N.P.P. Pabbathi, A. Velidandi, S. Pogula, P.K. Gandam, R.R. Baadhe, M. Sharma, R. Sirohi, V.K. Thakur, V.K. Gupta, Brewer's spent grains-based biorefineries: A critical review, **Fuel.** 317 (2022) 123435. https://doi.org/10.1016/J.FUEL.2022.123435.

[4] S.A.L. Bachmann, T. Calvete, L.A. Féris, Potential applications of brewery spent grain: Critical an overview, **J Environ Chem Eng.** 10 (2022) 106951. https://doi.org/10.1016/J.JECE.2021.106951.

[5] W. Li, H. Yang, T.E. Coldea, H. Zhao, Modification of structural and functional characteristics of brewer's spent grain protein by ultrasound assisted extraction, **LWT.** 139 (2021) 110582. https://doi.org/10.1016/J.LWT.2020.110582.

[6] R. Ibbett, R. White, G. Tucker, T. Foster, Hydro-mechanical processing of brewer's spent grain as a novel route for separation of protein products with differentiated techno-functional properties, **Innovative Food Science & Emerging Technologies.** 56 (2019) 102184. https://doi.org/10.1016/J.IFSET.2019.102184.

[7] T. Bonifácio-Lopes, A. Vilas-Boas, M. Machado, E.M. Costa, S. Silva, R.N. Pereira, D. Campos, J.A. Teixeira, M. Pintado, Exploring the bioactive potential of brewers spent grain ohmic extracts, **Innovative Food Science &**

Emerging Technologies. 76 (2022) 102943. https://doi.org/10.1016/J.IFSET.2022.102943.

[8] M. Panjičko, G.D. Zupančič, L. Fanedl, R.M. Logar, M. Tišma, B. Zelić, Biogas production from brewery spent grain as a mono-substrate in a two-stage process composed of solid-state anaerobic digestion and granular biomass reactors, **J Clean Prod.** 166 (2017) 519–529. https://doi.org/10.1016/J.JCLEPRO.2017.07.197.

[9] C. Moreirinha, C. Vilela, N.H.C.S. Silva, R.J.B. Pinto, A. Almeida, M.A.M. Rocha, E. Coelho, M.A. Coimbra, A.J.D. Silvestre, C.S.R. Freire, Antioxidant and antimicrobial films based on brewers spent grain arabinoxylans, nanocellulose and feruloylated compounds for active packaging, **Food Hydrocoll.** 108 (2020) 105836. https://doi.org/10.1016/J.FOODHYD.2020.105836.

[10] E. Wagner, M.E. Pería, G.E. Ortiz, N.L. Rojas, P.D. Ghiringhelli, Valorization of brewer's spent grain by different strategies of structural destabilization and enzymatic saccharification, **Ind Crops Prod.** 163 (2021) 113329. https://doi.org/10.1016/J.INDCROP.2021.113329.

[11] J. Naibaho, M. Korzeniowska, Brewers' spent grain in food systems: Processing and final products quality as a function of fiber modification treatment, **J Food Sci.** 86 (2021) 1532–1551. https://doi.org/10.1111/1750-3841.15714.

[12] T.C. Polachini, L.F.L. Betiol, J.F. Lopes-Filho, J. Telis-Romero, Water adsorption isotherms and thermodynamic properties of cassava bagasse, **Thermochim Acta.** 632 (2016) 79–85. https://doi.org/10.1016/j.tca.2016.03.032.

[13] D.P. Rosa, R.R. Evangelista, A.L. Borges Machado, M.A.R. Sanches, J. Telis-Romero, Water sorption properties of papaya seeds (Carica papaya L.) formosa variety: An assessment under storage and drying conditions, **LWT.** 138 (2021) 110458. https://doi.org/10.1016/j.lwt.2020.110458.

[14] M.L.F. Freitas, T.C. Polachini, A.C. de Souza, J. Telis-Romero, Sorption isotherms and thermodynamic properties of grated Parmesan cheese, **Int J Food Sci Technol.** 51 (2016) 250–259. https://doi.org/10.1111/ijfs.12969.

[15] R. Moreira, F. Chenlo, M.D. Torres, N. Vallejo, Thermodynamic analysis of experimental sorption isotherms of loquat and quince fruits, **J Food Eng.** 88 (2008) 514–521. https://doi.org/10.1016/J.JFOODENG.2008.03.011.

[16] B.K. Koua, P.M.E. Koffi, P. Gbaha, S. Toure, Thermodynamic analysis of sorption isotherms of cassava (Manihot esculenta), **J Food Sci Technol.** 51 (2014) 1711–1723. https://doi.org/10.1007/s13197-012-0687-y.

[17] C. Carvalho Lago, C.P.Z. Noreña, Thermodynamic analysis of sorption isotherms of dehydrated yacon (Smallanthus sonchifolius) bagasse, **Food Biosci.** 12 (2015) 26–33. https://doi.org/10.1016/J.FBIO.2015.07.001.

[18] MAPA. **Ministério da Agricultura, Pecuária e Abastecimento.** Instrução normativa nº 65, de 10 de dezembro de 2019. Estabelece os padrões de identidade e qualidade para os produtos de cervejaria. Diário Oficial da União: seção 1, Brasília, DF, ed. 239, p. 31.

[19] AOAC, **Association of Official Analytical Chemistry**, 18th ed., Gaithersburg, 2007.

[20] A. Sluiter, R. Ruiz, C. Scarlata, J. Sluiter & D. J. Templeton, Determination of extractives in biomass. **Laboratory analytical procedure (LAP)** 1617.4 (2008) 1- 16.

[21] A. Sluiter, R. Ruiz, C. Scarlata, J. Sluiter & D. J. Determination of structural carbohydrates and lignin in biomass. **Laboratory analytical procedure (LAP)** 1617.1 (2008): 1-16.

[22] J. L. Gomide and J. D. Braz. Determinação do teor de lignina em material lenhoso: método Klason modificado. **O papel** 47 (1986) 36-38.

[23] Goldschimid, O. **Ultraviolet spectra. Lignins: occurrence, formation, structure and reactions** 1 (1971) 241-266.

[24] K. Filippi, H. Papapostolou, M. Alexandri, A. Vlysidis, E.D. Myrtsi, D. Ladakis, C. Pateraki, S.A. Haroutounian, A. Koutinas, Integrated biorefinery development using winery waste streams for the production of bacterial cellulose,

succinic acid and value-added fractions, **Bioresour Technol**. 343 (2022) 125989. https://doi.org/10.1016/J.BIORTECH.2021.125989.

[25] A.H. Al-Muhtaseb, W.A.M. McMinn, T.R.A. Magee, Moisture Sorption Isotherm Characteristics of Food Products: A Review, **Food and Bioproducts Processing.** 80 (2002) 118–128. https://doi.org/10.1205/09603080252938753.

[26] T. Labuza, Creation of moisture sorption isotherms for hygroscopic materials. Sorption isotherm methods. **In International Symposium on Humidity and Moisture. (1963).** Washington: American Society of Heating, Refrigerating and Air Conditioning Engineers.

[27] R. Martínez-Las Heras, A. Heredia, M.L. Castelló, A. Andrés, Moisture sorption isotherms and isosteric heat of sorption of dry persimmon leaves, **Food Biosci.** 7 (2014) 88–94. https://doi.org/10.1016/J.FBIO.2014.06.002.

[28] K.S. Silva, T.C. Polachini, M. Luna-Flores, G. Luna-Solano, O. Resende, J. Telis-Romero, Sorption isotherms and thermodynamic properties of wheat malt under storage conditions, **J Food Process Eng.** (2021) e13784. https://doi.org/10.1111/jfpe.13784.

[29] C. Simón, L.G. Esteban, P. de Palacios, F.G. Fernández, A. García-Iruela, Thermodynamic properties of the water sorption isotherms of wood of limba (Terminalia superba Engl. & Diels), obeche (Triplochiton scleroxylon K. Schum.), radiata pine (Pinus radiata D. Don) and chestnut (Castanea sativa Mill.), **Ind Crops Prod.** 94 (2016) 122–131. https://doi.org/10.1016/J.INDCROP.2016.08.008.

[30] S.S.H. Rizvi, Thermodynamic Properties of Foods in Dehydration, in: M.A. Rao, S.S.H. Rizvi, A.K. Datta (Eds.), **Engineering Properties of Foods,** 3rd ed., Taylor & Francis Group, Boca Raton, FL, 2005.

[31] R.R. Krug, W.G. Hunter, R.A. Grieger, Enthalpy-entropy compensation. 1. Some fundamental statistical problems associated with the

analysis of van't hoff and arrhenius data**, Journal of Physical Chemistry**. 80 (1976) 2335–2341. https://doi.org/10.1021/j100562a006.

[32] R.R. Krug, W.G. Hunter, R.A. Grieger, Enthalpy-entropy compensation. 2. Separation of the chemical from the statistical effect, **Journal of Physical Chemistry**. 80 (1976) 2341–2351. https://doi.org/10.1021/j100562a007.

[33] Z.X. Lu, J.F. He, Y.C. Zhang, D.J. Bing, Composition, physicochemical properties of pea protein and its application in functional foods. **Critical reviews in food science and nutrition**, 60 (2019) 2593–2605. https://doi.org/10.1080/10408398.2019.1651248.

[34] P. Mattila, S. Mäkinen, M. Eurola, T. Jalava, J.M. Pihlava, J. Hellström, A. Pihlanto, Nutritional Value of Commercial Protein-Rich Plant Products, **Plant Foods for Human Nutrition**. 73 (2018) 108–115. https://doi.org/10.1007/S11130-018-0660-7/TABLES/4.

[35] F.G.B. Los, A.A.F. Zielinski, J.P. Wojeicchowski, A. Nogueira, I.M. Demiate, Beans (Phaseolus vulgaris L.): whole seeds with complex chemical composition, **Curr Opin Food Sci.** 19 (2018) 63–71. https://doi.org/10.1016/J.COFS.2018.01.010.

[36] R. Abeynayake, S. Zhang, W. Yang, L. Chen, Development of antioxidant peptides from brewers' spent grain proteins, **LWT.** 158 (2022) 113162. https://doi.org/10.1016/J.LWT.2022.113162.

[37] M. Tan, M.A. Nawaz, R. Buckow, Functional and food application of plant proteins – a review, **Food Reviews International**, (2021). https://doi.org/10.1080/87559129.2021.1955918.

[38] A.G.A. Sá, Y.M.F. Moreno, B.A.M. Carciofi, Plant proteins as high-quality nutritional source for human diet, **Trends Food Sci Technol**. 97 (2020) 170–184. https://doi.org/10.1016/J.TIFS.2020.01.011.

[39] W.G. Sganzerla, G.L. Zabot, P.C. Torres-Mayanga, L.S. Buller, S.I. Mussatto, T. Forster-Carneiro, Techno-economic assessment of subcritical water

hydrolysis process for sugars production from brewer's spent grains, **Ind Crops Prod.** 171 (2021) 113836. https://doi.org/10.1016/J.INDCROP.2021.113836.

[40] M.A. Ribeiro Sanches, C. Camelo-Silva, L. Tussolini, M. Tussolini, R.C. Zambiazi, P. Becker Pertuzatti, Development, characterization and optimization of biopolymers films based on starch and flour from jabuticaba (Myrciaria cauliflora) peel, **Food Chem**. 343 (2021) 128430. https://doi.org/10.1016/j.foodchem.2020.128430.

[41] M.A. Ribeiro Sanches, C. Camelo-Silva, C. da Silva Carvalho, J. Rafael de Mello, N.G. Barroso, E. Lopes da Silva Barros, P.P. Silva, P.B. Pertuzatti, Active packaging with starch, red cabbage extract and sweet whey: Characterization and application in meat, **LWT**. 135 (2021) 110275. https://doi.org/10.1016/j.lwt.2020.110275.

[42] G.K. Shroti, C.S. Saini, Development of edible films from protein of brewer's spent grain: Effect of pH and protein concentration on physical, mechanical and barrier properties of films, **Applied Food Research**. 2 (2022) 100043. https://doi.org/10.1016/J.AFRES.2022.100043.

[43] A. Revert, M. Reig, V.J. Seguí, T. Boronat, V. Fombuena, R. Balart, Upgrading brewer's spent grain as functional filler in polypropylene matrix, **Polym Compos**. 38 (2017) 40–47. https://doi.org/10.1002/PC.23558.

[44] J. Weiermüller, A. Akermann, W. Laudensack, J. Chodorski, L.M. Blank, R. Ulber, Brewers' spent grain as carbon source for itaconate production with engineered Ustilago maydis, **Bioresour Technol**. 336 (2021) 125262. https://doi.org/10.1016/J.BIORTECH.2021.125262.

[45] A. Akermann, J. Weiermüller, J. Christmann, L. Guirande, G. Glaser, A. Knaus, R. Ulber, Brewers' spent grain liquor as a feedstock for lactate production with Lactobacillus delbrueckii subsp. lactis, **Eng Life Sci**. 20 (2020) 168–180. https://doi.org/10.1002/ELSC.201900143.

[46] J.C. López-Linares, M.T. García-Cubero, S. Lucas, M. Coca, Integral valorization of cellulosic and hemicellulosic sugars for biobutanol production: ABE fermentation of the whole slurry from microwave pretreated

brewer's spent grain, **Biomass Bioenergy**. 135 (2020) 105524. https://doi.org/10.1016/J.BIOMBIOE.2020.105524.

[47] S. Brunauer, L.S. Deming, W.E. Deming, E. Teller, On the theory of the van der Waals adsorption of gases, **J Am Chem Soc**. 62 (1940) 1723–1732.

[48] M. Mathlouthi, Water content, water activity, water structure and the stability of foodstuffs, **Food Control.** 12 (2001) 409–417. https://doi.org/10.1016/S0956-7135(01)00032-9.

[49] N. Singh, J. Singh, L. Kaur, N.S. Sodhi, B.S. Gill, Morphological, thermal and rheological properties of starches from different botanical sources, **Food Chem.** 81 (2003) 219–231. https://doi.org/10.1016/S0308-8146(02)00416-8.

[50] M.A. Lazouk, R. Savoire, A. Kaddour, J. Castello, J.L. Lanoisellé, E. Van Hecke, B. Thomasset, Oilseeds sorption isoterms, mechanical properties and pressing: Global view of water impact, **J Food Eng.** 153 (2015) 73–80. https://doi.org/10.1016/j.jfoodeng.2014.12.008.

[51] Q. Chen, G. Wang, X.X. Ma, M.L. Chen, C.H. Fang, B.H. Fei, The effect of graded fibrous structure of bamboo (Phyllostachys edulis) on its water vapor sorption isotherms**, Ind Crops Prod.** 151 (2020) 112467. https://doi.org/10.1016/J.INDCROP.2020.112467.

[52] L.F.L. Betiol, R.R. Evangelista, M.A.R. Sanches, R.C. Basso, B. Gullón, J.M. Lorenzo, A.C. da S. Barretto, J. Telis-Romero, Influence of temperature and chemical composition on water sorption isotherms for dry-cured ham, **Lwt.** 123 (2020) 109112. https://doi.org/10.1016/j.lwt.2020.109112.

[53] F.E. Vasile, M.A. Judis, M.F. Mazzobre, Moisture sorption properties and glass transition temperature of a non-conventional exudate gum (Prosopis alba) from northeast Argentine, **Food Research International.** 131 (2020) 109033. https://doi.org/10.1016/J.FOODRES.2020.109033.

[54] E.J. Quirijns, A.J.B. van Boxtel, W.K.P. van Loon, G. van Straten, Sorption isotherms, GAB parameters and isosteric heat of sorption, **J Sci Food Agric.** 85 (2005) 1805–1814. https://doi.org/10.1002/JSFA.2140.

[55] S. Kaya, T. Kahyaoglu, Thermodynamic properties and sorption equilibrium of pestil (grape leather), **J Food Eng.** 71 (2005) 200–207. https://doi.org/10.1016/J.JFOODENG.2004.10.034.

[56] K. Muzaffar, P. Kumar, Moisture sorption isotherms and storage study of spray dried tamarind pulp powder, **Powder Technol.** 291 (2016) 322–327. https://doi.org/10.1016/J.POWTEC.2015.12.046.

[57] E. Alpizar-Reyes, H. Carrillo-Navas, R. Romero-Romero, V. Varela-Guerrero, J. Alvarez-Ramírez, C. Pérez-Alonso, Thermodynamic sorption properties and glass transition temperature of tamarind seed mucilage (Tamarindus indica L.), **Food and Bioproducts Processing**. 101 (2017) 166–176. https://doi.org/10.1016/J.FBP.2016.11.006.

[58] L.L. Diosady, S.S.H. Rizvi, W. Cai, D.J. Jagdeo, Moisture Sorption Isotherms of Canola Meals, and Applications to Packaging, **J Food Sci**. 61 (1996) 204–208. https://doi.org/10.1111/J.1365-2621.1996.TB14760.X.

[59] C. Pérez-Alonso, C.I. Beristain, C. Lobato-Calleros, M.E. Rodríguez-Huezo, E.J. Vernon-Carter, Thermodynamic analysis of the sorption isotherms of pure and blended carbohydrate polymers, **J Food Eng.** 77 (2006) 753–760. https://doi.org/10.1016/J.JFOODENG.2005.08.002.

[60] S.K. Velázquez-Gutiérrez, A.C. Figueira, M.E. Rodríguez-Huezo, A. Román-Guerrero, H. Carrillo-Navas, C. Pérez-Alonso, Sorption isotherms, thermodynamic properties and glass transition temperature of mucilage extracted from chia seeds (Salvia hispanica L.), **Carbohydr Polym.** 121 (2015) 411–419. https://doi.org/10.1016/j.carbpol.2014.11.068.

[61] M.D. Torres, R. Moreira, F. Chenlo, M.J. Vázquez, Water adsorption isotherms of carboxymethyl cellulose, guar, locust bean, tragacanth and xanthan gums, **Carbohydr Polym.** 89 (2012) 592–598. https://doi.org/10.1016/J.CARBPOL.2012.03.055.

[62] C.C. Lago, M. Liendo-Cárdenas, C.P.Z. Noreña, Thermodynamic sorption properties of potato and sweet potato flakes, **Food and Bioproducts Processing**. 91 (2013) 389–395. https://doi.org/10.1016/J.FBP.2013.02.005.

[63] S.N. Sahu, A. Tiwari, J.K. Sahu, S.N. Naik, I. Baitharu, E. Kariali, Moisture sorption isotherms and thermodynamic properties of sorbed water of chironji (Buchanania lanzan Spreng.) kernels at different storage conditions, **Journal of Food Measurement and Characterization**. 12 (2018) 2626–2635. https://doi.org/10.1007/S11694-018-9880-7/TABLES/3.

[64] J. Naibaho, N. Butula, E. Jonuzi, M. Korzeniowska, O. Laaksonen, M. Föste, M.L. Kütt, B. Yang, Potential of brewers' spent grain in yogurt fermentation and evaluation of its impact in rheological behaviour, consistency, microstructural properties and acidity profile during the refrigerated storage, **Food Hydrocoll**. 125 (2022) 107412. https://doi.org/10.1016/J.FOODHYD.2021.107412.

[65] C. Bonazzi, E. Dumoulin, Quality Changes in Food Materials as Influenced by Drying Processes, **Modern Drying Technology**. (2014) 1–20. https://doi.org/10.1002/9783527631728.CH14.

[66] W.A.M. McMinn, A.H. Al-Muhtaseb, T.R.A. Magee, Enthalpy–entropy compensation in sorption phenomena of starch materials, **Food Research International**. 38 (2005) 505–510. https://doi.org/10.1016/J.FOODRES.2004.11.004.

[67] A. Garvín, P.E.D. Augusto, R. Ibarz, A. Ibarz, Kinetic and thermodynamic compensation study of the hydration of faba beans (Vicia faba L.), **Food Research International**. 119 (2019) 390–397. https://doi.org/10.1016/J.FOODRES.2019.02.002.

[68] A. Garvín, R. Ibarz, A. Ibarz, Kinetic and thermodynamic compensation. A current and practical review for foods, **Food Research International**. 96 (2017) 132–153. https://doi.org/10.1016/J.FOODRES.2017.03.004.

[69] M.A. Al-Mahasneh, M.M. Bani Amer, T.M. Rababah, Modeling moisture sorption isotherms in roasted green wheat using least square regression and neural-fuzzy techniques, **Food and Bioproducts Processing**. 90 (2012) 165–170. https://doi.org/10.1016/J.FBP.2011.02.007.

[70] J.C. Spada, C.P.Z. Noreña, L.D.F. Marczak, I.C. Tessaro, Water adsorption isotherms of microcapsules with hydrolyzed pinhão (Araucaria angustifolia seeds) starch as wall material, **J Food Eng**. 114 (2013) 64–69. https://doi.org/10.1016/j.jfoodeng.2012.07.019.

[71] A.L. Gabas, F.C. Menegalli, J. Telis-Romero, Water Sorption Enthalpy-Entropy Compensation Based on Isotherms of Plum Skin and Pulp, **J Food Sci**. 65 (2000) 680–680. https://doi.org/10.1111/J.1365-2621.2000.TB16072.X.

CAPÍTULO 3

Manuscrito submetido em “**Food and Bioproducts Processing**”
ISSN: 0960-3085

Valorization of brewer's spent grains (BSG) through alkaline hydrogen peroxide processing: effect on composition, structure and rheological properties

Marcio Augusto Ribeiro Sanches[1], Vitor Augusto Lopes Stochi[1], André Luiz Borges-Machado[1], Pedro Esteves Duarte Augusto[2], Tiago Carregari Polachini[1], Javier Telis-Romero[1]

[1]Food Engineering and Technology Department, São Paulo State University, Institute of Biosciences, Humanities and Exact Sciences (Ibilce), Campus São José do Rio Preto, São Paulo, 15.054-000, Brazil.

[2]Université Paris-Saclay, CentraleSupélec, Laboratoire de Génie des Procédés et Matériaux, Centre Européen de Biotechnologie et de Bioéconomie (CEBB), 3 rue des Rouges Terres 51110 Pomacle, France.

*Author to whom correspondence may be addressed. E-mail address: mar.sanches@unesp.br (Marcio Augusto Ribeiro Sanches).

ABSTRACT

This study investigated the impact of alkaline processing with hydrogen peroxide (AHP) on the chemical composition, structure, and rheological properties of brewer's spent grains (BSG). Suspensions with different concentrations of BSG (2–8%) and AHP (1–8%) were subjected to different processing times (0–12 h). The BSG chemical composition, morphology, crystallinity, modifications of functional groups, and rheological behavior were evaluated over processing. Increasing the concentration of AHP in the suspension and the processing time

improved the removal of proteins, lignin, and extractives from BSG into the suspension and, consequently, increased the cellulose and hemicellulose content in the processed BSG. On the other hand, higher concentrations of BSG in the suspension slightly reduced the removal efficiency of these components. AHP processing also induced thinning of the cell wall and changes in particle shape. These changes together with the increase in crystallinity of the processed BSG indicated the material destructuring. FTIR spectra showed reduced intensity of lignin and protein post-processing, indicating their removal, while peaks related to cellulose and hemicellulose increased in processed BSG. The flow curves of the suspensions were adjusted to the Herschel-Bulkley model, exhibiting non-Newtonian behavior with flow yield stress ($1.529\ Pa < \tau_0 < 4.646\ Pa$) and pseudoplasticity ($0.830 < n < 0.969$) in all conditions. Flow resistance increased with increasing concentration of AHP, BSG, and processing time. Notably, the increase in processing time resulted in greater removal of BSG components, especially proteins, lignin, and extractives, which significantly contributed to the increase in both the flow yield stress and the consistency index of the suspensions. All this information is useful and will support the design of equipment and processes, especially those involving the extraction of proteins and the conversion of the BSG lignocellulose fraction into biofuels.

Keywords: Agro-industrial by-product; Waste valorization; Lignocellulosic biomass; Delignification; Pseudoplastic.

1. INTRODUCTION

The valorization of agro-industrial by-products is a necessary approach in the context of global sustainability, bioeconomy and circular economy. However, a notable gap in the literature concerns the engineering properties of both by-products, intermediate and final products, limiting their process design. Notably, the rheological properties are needed to design different unit operations for processing, such as pumping, mixing, flow through heat exchangers, bioreactors, filtrations, centrifugation, among others. However, although literature presents much information about the rheological properties of agro-industrial products, it fails in characterizing their by-products. This compromises the effective scaling

up and implementation of operations required to transform the by-products into value-added products.

Brewer's spent grains (BSG) constitutes 85% (w/w) of the total by-products of brewing industry, comprising hulls, residual starchy endosperm, and retained water (Borel et al., 2018; Fernández-Delgado et al., 2019; Pabbathi et al., 2022; Sanches et al., 2023). About 38 million tons of BSG are globally produced (Statista, 2023), demonstrating the abundance of this valuable by-product as a renewable resource.

BSG consists predominantly of lignocellulosic material, rich in cellulose (15–25%; dry basis), hemicellulose (20–40%; dry basis), lignin (10–20%; dry basis), and proteins (15-30%; dry basis) (Agrawal et al., 2023; Sanches et al., 2023). Therefore, its use as an energy source by producing biofuels stands out, as well as being an important source of vegetable proteins, further expanding its potential for use. However, the recalcitrant nature of this biomass represents a challenge, making access to reagents and/or enzymes difficult and preventing the efficient use of its components (Alonso-Riaño et al., 2023; Qin et al., 2018; Sganzerla et al., 2021). Overcoming this issue requires treatment steps to weaken bonds within cell wall components, increasing accessibility to reagents and/or enzymes.

Alkaline hydrogen peroxide (AHP) emerges as a promising treatment method, generating radical species under alkaline conditions that selectively react with lignin, resulting in the delignification of biomass (Ho et al., 2019; Huang et al., 2021; Xia et al., 2022b, 2022a; Zhang et al., 2022). This step is crucial for the subsequent enzymatic hydrolysis of BSG, aiming to obtain sugars to produce bioethanol through fermentation (Agrawal et al., 2023; Li et al., 2019; Wagner et al., 2021). Furthermore, the structural modifications caused by AHP processing can enhance the efficiency of protein extraction from BSG.

However, this treatment was not evaluated so far in BSG, nor its effect on BSG structure and properties. In order to fill this knowledge gap, this study investigated how the AHP process affects the BSG composition, structure and rheological properties, correlating them. Those results will facilitate decision-making involved in the design and optimization of processes to valorize this by-product.

2. MATERIAL AND METHODS

2.1. Raw material and sample preparation

The wet BSG was supplied by a local brewery (Frutal, MG, Brazil), coming from a “pure malt” beer (i.e., produced from a wort whose primitive extract comes exclusively from malted barley or malt extract). BSG was immediately dried in a convective tray dryer at 60 ± 2 °C until equilibrium moisture, as in our previous study (Sanches et al., 2023b). Subsequently, the dry BSG was ground in a rotor mill (model MA340, Marconi, Piracicaba, São Paulo, Brazil) and sieved through a 30-mesh sieve to obtain BSG with a particle size of less than 595 μm.

2.2. Alkaline hydrogen peroxide (AHP) processing

Diluted alkaline solutions were prepared by varying the hydrogen peroxide content (50% solution; purity>99.95%), (Perfyl Tech, São Bernardo do Campo, São Paulo), in distilled water at the following concentrations: 1, 2, 4, 6, and 8% (g of hydrogen peroxide per 100 g of dispersant). Afterward, the solutions were adjusted to pH 11.5 ± 0.1 using 1 M NaOH. These solutions were added to BSG to obtain suspensions with final solid concentrations of 2, 4, 6, and 8% (g of BSG per 100 g of suspension). The combination of different concentrations of BSG and AHP was processed for 0, 1, 4, 6, 8, and 12 hours in a shaking incubator chamber at 40 rpm (MARCONI MA 830/A). All suspensions were processed at 20 °C.

2.3. Characterization of BSG before, during and after processing

To investigate the impact of AHP processing on BSG composition and structure, some trials were selected (Table 1) covering the minimum and maximum values of the variables studied. Those conditions were subjected to detailed analyses to evaluate chemical composition and structural changes.

Table 1. Pretreatment conditions selected to evaluate the effects of alkaline hydrogen peroxide concentration (X_{AHP}, %), BSG concentration (X_{BSG}, %), and pretreatment time (h) on the chemical composition of pretreated BSG.

Conditions	Variable		
	Processing time (h)	X_{AHP} (%)	X_{BSG} (%)
Effect of alkaline hydrogen peroxide concentration (XAHP, %)			
T1	1	1	2
T2	1	8	2
Effect of BSG concentration (X_{BSG}, %)			
T1	1	1	2
T3	1	1	8
Effect of pretreatment time (h)			
T2	1	8	2
T4	12	8	2

2.3.1. Chemical composition

Protein content was determined using the Kjeldahl method with a correction factor of 6.25 (AOAC, 2007). The NREL/TP-510-42619 method (Sluiter et al., 2005) was used to determine extractive content. The extractive-free material was subjected to acid hydrolysis according to the NREL/TP-510-42618 method (Sluiter et al., 2008) for the structural determination of carbohydrates and lignin. The Klason lignin (insoluble) was determined gravimetrically as an insoluble residue, according to Gomide and Demuner (1986). On the other hand, acid-soluble lignin was determined by UV spectroscopy, according to Goldschimid (1971), at wavelengths 215 and 280 nm. Cellulose and hemicellulose contents were determined following the methodology adapted from NREL/TP-510-42618 (Sluiter et al., 2008), using high-performance liquid chromatography (HPLC). For this, the filtered hydrolysate obtained before determining the insoluble lignin content (Klason method) was used. The conditions of the chromatographic analyses and the factors used in the calculation to obtain the levels of these constituents were the same as those used in our previous study (Sanches et al., 2023b). All results were expressed as mean ± standard deviation.

2.3.2. BSG structure: particle morphology

The CX31 optical microscope (produced by Olympus, Tokyo, Japan) with a camera attached to 4x and 10x magnitudes was used to evaluate the BSG particles morphology. To prepare the glass slides, samples were dispersed in distilled water and images were obtained from various areas of the microscope slides. The biomass was marked with a Nile red solution to identify and highlight the presence of proteins. The particles were characterized using the aspect ratio (a_r), which is determined by the relationship between length (L) and width (w). CellSens software version 1.18 (Olympus, Tokyo, Japan) was used to measure these characteristic dimensions for 100 particles in different fields of view.

2.3.3. Particle crystallinity: X-ray diffraction

X-ray diffraction measurements were performed on a diffractometer (Rigaku, RINT 2000, Japan) operating at a voltage of 30 kV and a current of 10 mA using Kα radiation and L = 1542 Å. The diffractograms were obtained at angles (2θ) ranging from 5° to 60° at a scan rate of 5°/min. The crystallinity index (CrI) was determined by the Segal method (Segal et al., 1959).

2.3.4. Functional groups: Fourier transform infrared spectroscopy (FTIR)

The attenuated reflectance technique (ATR) was used to determine the absorption spectra in the 4.000-400 cm^{-1} infrared region by Fourier transform using a Spectrum Two spectrophotometer (PerkinElmer, Waltham, USA). FTIR spectra were recorded in 10 scans per spectrum with a resolution of 4 cm^{-1}.

2.4. Rheology of BSG particle suspensions

Rheological measurements were performed using an AR-G2 rotational rheometer (TA Instruments, New Castle, USA). This rheometer used a reed-type SPC (Starch Pasting Cell) geometry to avoid particle sedimentation and sliding effects, as performed in previous studies (Polachini et al., 2019; Polachini et al., 2016). Samples of approximately 28 mL, from the different analyzed conditions, were subjected to shear rate descending ramp adjusted from 263.341 to 1.011 s^{-1}. All different combinations between AHP concentrations (1, 2, 4, 6, 8 g of hydrogen peroxide per 100 g of dispersant), BSG concentrations (2, 4, 6, 8 g of BSG per 100 g of suspension), and processing time (0, 1, 4, 6, 8 and 12 hours)

were evaluated at five different temperatures (20, 30, 40, 50 and 60 °C) using a temperature-controlled bath and a new sample for each test. Shear stress data were obtained from the Universal Analysis 2000 version 4.7 data acquisition system (TA Instruments, New Castle, USA).

The rheological behavior was evaluated using the Herschel-Bulkley model (Eq. (1)), which includes Newton, Ostwald-de-Waele and Bingham models.

$$\sigma = \sigma_0 + \kappa \cdot \gamma^n \quad (1)$$

where, σ (Pa) is the shear stress; γ (s^{-1}) is the shear rate; σ_0 (Pa) is the flow yield stress; κ ($Pa \cdot s^n$) is the consistency index and n (dimensionless) is the fluid behavior index.

The accuracy of the adjustment of the mathematical models were evaluated by analyzing the adjusted coefficient of determination (R_{adj}^2) and through the root mean square error (RMSE). OriginPro 8.0 software (OriginLab Corporation, Northampton, USA) was used to plot the graphs and perform non-linear regressions to adjust the models to the experimental data. The experiments were carried out in three independent replicates. The significant difference between the mean parameters of the best model was assessed using analysis of variance (ANOVA), and the difference between the mean results was assessed using the Tukey test, at a confidence level of 95%, with the aid of the software Statistica 7.0 (Statsoft Inc., USA).

3. RESULTS AND DISCUSSION

3.1. Characterization of unprocessed and processed BSG

3.1.1. Chemical composition

In an attempt to identify and describe the main variables, the effects of AHP concentrations (1-8%), BSG concentrations (2-8%), and processing time (1-12 h) on the chemical composition of BSG were evaluated before and after processing. The initial composition of BSG was ~30% hemicellulose (~25% xylan and ~5% arabinan) and ~17% cellulose which adds up to a total carbohydrate content of ~47%. The cellulose and hemicellulose contents make BSG a promising by-product for ethanol production. However, BSG also presented ~19% of lignin (~16% of insoluble lignin and ~3% of soluble lignin). For BSG be hydrolyzed by enzymes, it is necessary to pretreat this material to remove mainly

the lignin, as the high crystalline structure of cellulose, which is grouped in a matrix of polymers-lignin and hemicellulose, is the main difficulty in relation to the recalcitrance of the biomass (Wagner et al., 2021). Although lignin removal is the main objective of the processing steps, it is a polyphenolic macromolecule and can be isolated to obtain phenolic acids, especially ferulic and p-coumaric acids, compounds of interest in the food, cosmetic, and pharmaceutical industries (Mussatto et al., 2007).

In addition to the carbohydrate fraction, BSG presented 21.26% ± 0.12 of proteins and a small fraction of extractives (7.99% ± 0.06) and ash (3.75% ± 0.35). The large amount of proteins in BSG demonstrates its potential as an alternative source of vegetable protein. However, it is challenging to extract protein in BSG with high yields due to the complex network formed between lignin and cellulose that traps the protein inside (Li et al., 2021), demonstrating the need for the processing step.

3.1.1.1. Effect of AHP concentration

Table 2 presents the chemical composition of the BSG solid residue after the different processing conditions. By increasing the AHP concentration in the dispersant from 1% (T1) up to 8% (T2), keeping the solids concentration constant, the proportions of lignin removal were about ~15% and ~22%, respectively, in relation to the unprocessed BSG. The increase in the concentration of AHP used in processing probably made more radical species available (e.g., HO· and HOO·) that reacted selectively with lignin, providing greater delignification of the biomass (Cabrera et al., 2014; Ho et al., 2019). Furthermore, this delignification with increasing AHP is probably also responsible for improving the contact of the alkaline solution with the BSG matrix, which improved the removal of BSG proteins by ~59% (T1) and ~73% (T2) in relation to unprocessed BSG. The alkalization of the medium (pH>10) is commonly applied for solubilizing and extracting plant-based proteins from solid matrix (Silva et al., 2023), which is in agreement to the results shown in Table 2. After processing with AHP, proteins can also be recovered through isoelectric precipitation, as performed in previous studies using AHP (Aider et al., 2023a; El-Kadiri et al., 2013).

Table 2. Chemical composition of untreated BSG and after pretreatments (g / 100g db).

Conditions	Proteín	Cellulose	Hemicellulose (Xylan)	Hemicellulose (Arabinan)	Insoluble Lignin	Soluble Lignin	Extractives	Aches
BSG	21.26 ± 0.12	17.50 ± 0.05	24.82 ± 0.29	4.81 ± 0.01	16.81 ± 0.14	2.77 ± 0.19	7.99 ± 0.06	3.75 ± 0.35
Effect of alkaline hydrogen peroxide concentration (X_{AHP}, %)								
T1	8.59 ± 0.21 [a]	27.91 ± 0.19 [b]	34.33 ± 0.17 [b]	5.57 ± 0.11 [b]	13.14 ± 0.07 [a]	3.35 ± 0.02 [a]	3.93 ± 0.09 [a]	2.92 ± 0.02 [a]
T2	5.69 ± 0.23 [b]	29.45 ± 0.34 [a]	35.68 ± 0.29 [a]	6.01 ± 0.12 [a]	12.97 ± 0.06 [b]	3.23 ± 0.06 [b]	3.79 ± 0.08 [b]	2.86 ± 0.12 [a]
Effect of BSG concentration (X_{BSG}, %)								
T1	8.59 ± 0.21 [b]	27.91 ± 0.19 [a]	34.33 ± 0.17 [a]	5.57 ± 0.11 [a]	13.14 ± 0.07 [a]	3.35 ± 0.02 [b]	3.93 ± 0.09 [a]	2.92 ± 0.02 [a]
T3	8.91 ± 0.11 [a]	27.35 ± 0.08 [b]	34.18 ± 0.08 [a]	5.16 ± 0.02 [b]	13.35 ± 0.13 [a]	3.55 ± 0.10 [a]	4.02 ± 0.13 [a]	3.10 ± 0.22 [a]
Effect of pretreatment time (h)								
T2	5.69 ± 0.23 [a]	29.45 ± 0.34 [b]	35.68 ± 0.29 [b]	6.01 ± 0.12 [b]	12.97 ± 0.26 [a]	3.23 ± 0.06 [a]	3.79 ± 0.08 [a]	2.86 ± 0.12 [a]
T4	4.30 ± 0.20 [b]	34.34 ± 0.23 [a]	36.71 ± 0.26 [a]	6.23 ± 0.04 [a]	9.19 ± 0.17 [b]	3.16 ± 0.27 [b]	3.47 ± 0.11 [b]	2.18 ± 0.08 [b]

After partial delignification and protein removal, there was a significant consequent increase in the fraction of carbohydrates (cellulose and hemicellulose) in the processed solid matrix, when compared to the unprocessed BSG. By increasing from 1% (T1) to 8% (T2) AHP in the dispersant, cellulose content increased ~59% (T1) and ~68% (T2) compared to unprocessed BSG. Similarly, hemicellulose increased by ~34% (T1) and ~40% (T2), compared to unprocessed BSG. The increased concentration of cellulose and hemicellulose in the processed solid matrix suggests a more accessible and conducive substrate for efficient bioethanol production, highlighting the promising potential of the processing in improving the conversion of BSG into biofuels.

3.1.1.2. Effect of BSG concentration

Table 2 also shows the effect of BSG concentration in the suspension, treated with the same concentration of AHP (1%) in the dispersing medium. The increase from 2% (T1) to 8% (T3) of BSG resulted in lignin removal of ~15% (T1) and ~13% (T3), respectively, compared to unprocessed BSG. On the other hand, the protein content of these treatments was statistically equal, achieving a removal of ~59% of proteins, compared to unprocessed BSG. The reduction in lignin removal demonstrates that the increase in biomass loading slightly reduced the processing efficiency, most likely due to the reduction in contact solvent-matrix and, consequently, AHP effectiveness. During processing, AHP dissociates in water, forming derivative radicals that depolymerize lignin (Cabrera et al., 2014; Ho et al., 2019). However, during processing, the particles swell, reducing the solvent/biomass ratio (Polachini et al., 2016). Therefore, the greater the biomass loading, the greater this effect. It results in the reduction of radicals production and, consequently, in the loss of effectiveness.

When analyzing the solid fraction, a slight decrease in the proportion of cellulose and hemicellulose was observed in the solid processed with 8% BSG (T3), compared to the solid processed with 2% BSG (T1). This behavior was expected due to the small reduction in delignification efficiency, resulting in a solid fraction characterized by a relatively greater presence of lignin, and a slight reduction in the proportion of cellulose and hemicellulose.

It is worth mentioning that the increase from 2% to 8% of BSG in the suspension caused only a small loss of processing efficiency. This reinforces the ability of AHP to delignify BSG, maintaining an almost similar processing efficiency even when the amount of BSG in the suspension was greatly increased. On the other hand, this is useful because higher solid loadings are preferable in industrial-scale processing, increasing the economic viability of the BSG conversion process into value-added products.

3.1.1.3. Influence of processing time

The effect of AHP processing duration on the composition of the processed BSG is also shown in Table 2. By increasing the processing time from 1 h to 12 h, the lignin removals in the processed residue were increased from ~17% for (T2 – 1 h of processing) up to ~36% (T4 – 12 h of processing) in relation to unprocessed BSG.

Similarly to the previous treatments, the protein was also removed by ~73% (T2) and ~79% (T4), in relation to unprocessed BSG. After 12 h of processing, the cellulose content in the processed residue increased by 68.29% (T2) and 96.23% (T4) while hemicellulose increased slightly by 40.70% (T2) and 44.92% (T4) compared to unprocessed BSG. The effects of increasing processing time can be justified by the longer contact time between BSG and radical species (for example, HO· and HOO·) generated by AHP which react selectively with lignin, providing intense delignification of the biomass (Cabrera et al., 2014; Ho et al., 2019) ending up by improving the removal of lignin and proteins into the liquid phase. However, it is worth mentioning that a long exposure time of the proteins solubilized in the suspension in contact with the radical species generated by AHP can cause denaturation of the proteins and/or adverse effects on their techno-functional properties. Therefore, studies in this scope should be investigated.

3.1.2. Structural characterization

3.1.2.1. BSG structure: particle morphology

Figure 1 shows micrographs of the particles from the different processing conditions. The particles presented varied morphologies such as rounded, rectangular, and elongated shapes, with different particle sizes, which is typical

of lignocellulosic byproducts. Peanut shells (Polachini et al., 2016), sugarcane bagasse (Kane et al., 2023), and even cassava bagasse (Polachini et al., 2019) showed similar shapes.

Microscopies also revealed crucial information about the efficiency and severity of structural modifications in BSG in response to different processing. Initially, the presence of intensely stained particles in unprocessed BSG confirms its protein-rich nature. These particles became distinctly red-stained due to absorption of the dye, likely associated with the internal aleurone tissue-containing protein of BSG. However, after all processing, a drastic reduction in the color of the particles was observed, indicating that the different processes were effective in solubilizing the BSG proteins in the suspension, which corroborates the results of the chemical composition, in which there was a reduction in the protein content in the processed BSG's.

The less rigorous processing (T1 and T3), using the lowest concentration of AHP (1%) and different biomass loading, presented darker particles with few notable differences among them. These results corroborate with the conclusions of the chemical composition analysis – indicating that increasing biomass concentration from 1% (T1) to 8% (T3) resulted in minimal changes in the chemical composition of the processed matrix. On the other hand, it reinforces the AHP processing capacity even at high solids concentrations. However, T2 processing (AHP concentration - 8%) showed lighter particles, indicating that the higher concentration of AHP in the processing may have caused the thinning of the cell wall, which plays a crucial role in the structural integrity of BSG, very probably due to its delignification. These findings are probably related to the greater removal of proteins and lignin into the suspension, combined with the increased concentration of cellulose and hemicellulose in the solid.

When increasing the processing time (differences between T3 and T4), a significant change in the shape of the particles was noticed, which appeared finer with a needle shape, demonstrating a great disruption of the BSG. This is probably related to the longer contact time between BSG, and radical species generated by AHP, providing intense delignification of the biomass (Cabrera et al., 2014; Ho et al., 2019).

Figure 1. Optical microscopy images at 4× and 10× magnification for untreated BSG (a and b), T1 (c and d), T2 (e and f), T3 (g and h), T4 (i and j).

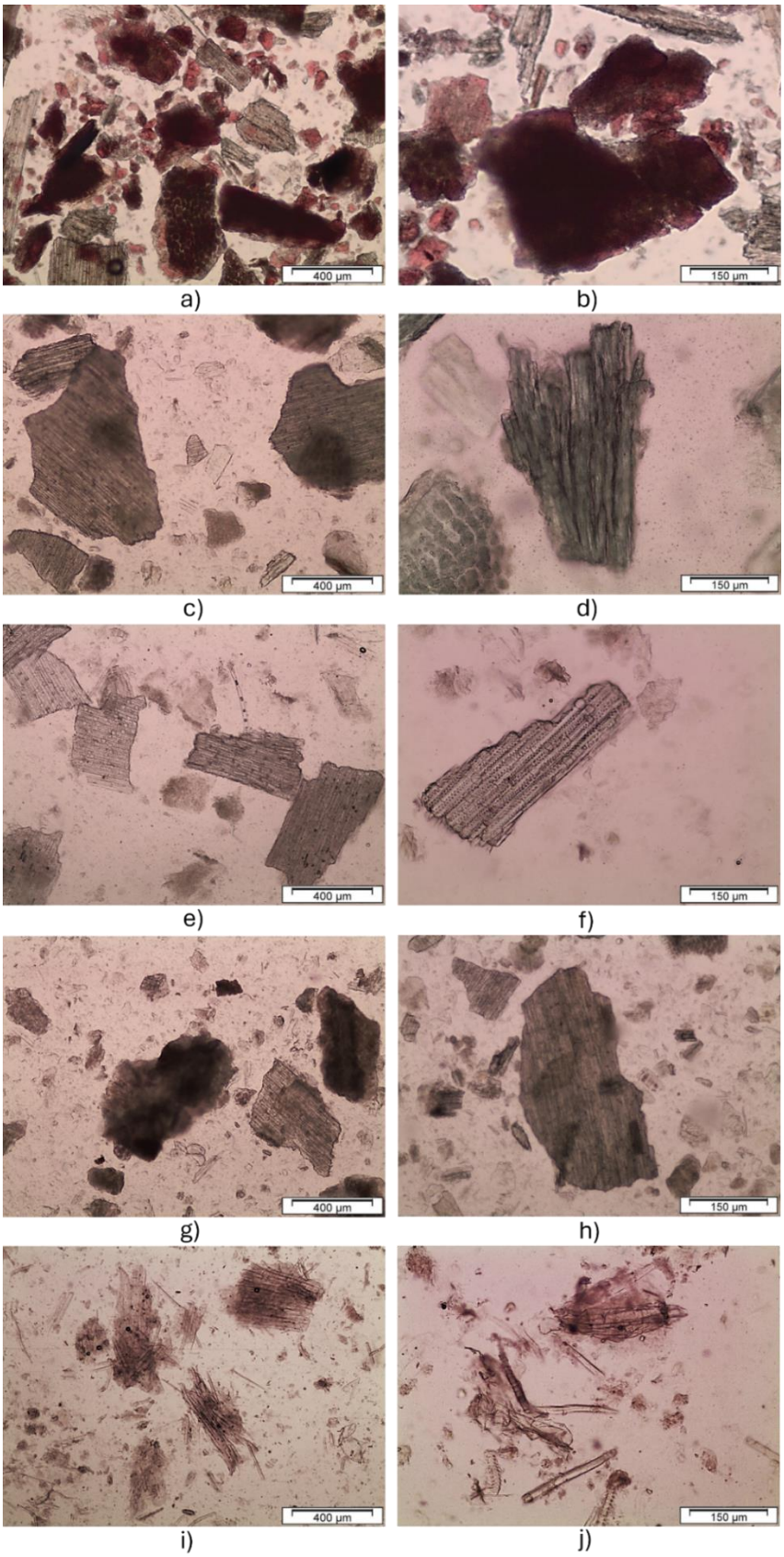

These findings are also in agreement with the results of the chemical composition, which showed that the processing time was the factor that caused the greatest delignification of the matrix and, consequently, greater removal of proteins for the suspension.

Due to the structural changes caused by the different processing, the aspect ratio (a_r) of the samples was also evaluated from the microscopic images - Figure 1. More than 75% of the particles analyzed (except for T4) presented proportions < 1.5 and 1.5 – 2, like other agro-industrial waste (EL-Sayed and Mostafa, 2014; Polachini et al., 2019). However, T4 presents only ~50% of the particles analyzed in this same category. The other 50% had proportions distributed above 2, highlighting the fact that ~ 20% have a_r above 3, which reinforces the significant change in the shape of the particles, which appeared finer with a needle shape, as reported previously. These microstructural changes, together with changes in chemical composition mainly due to the removal of lignin and proteins into the suspension, can impact the rheological properties of these suspensions, which demonstrates a complex relationship between the microstructure and the macroscopic properties of the suspension.

3.1.2.2. Particle crystallinity: X-ray diffraction

The crystallinity index (*CrI*) is the ratio between the crystalline fraction of cellulose and the amorphous fraction of the biomass (Moodley and Kana, 2017), being one of the main factors that influence the efficiency of BSG hydrolysis. To further illustrate the role of AHP processing conditions, the change in *CrI* of unprocessed BSG and after processing were investigated by XRD analysis. The XRD spectra (Figure 2-a) of unprocessed BSG and processing conditions T1 and T3 showed a typical type I structure with a diffraction peak around 22°, representing the cellulose peak (Pereira et al., 2021).

The similarity between these profiles indicates that processing conditions with 1% AHP (T3 and T4) did not cause major changes in the crystalline form of cellulose (Zhang et al., 2022), most likely due to the complex lignocellulose matrix, formed mainly by a thick structure of hemicellulose and lignin that surrounds cellulose molecules (Saravanan et al., 2022).

Another interesting aspect is related to the extended profile of this peak, which indicates amorphous regions since this material can be considered

semicrystalline. Unprocessed BSG had a low *CrI* value (31%), probably due to the high content of amorphous substances such as hemicellulose and lignin (Yan et al., 2020).

Figure 2. XRD diffraction a) and FTIR b) profiles of unprocessed BSG and after processing.

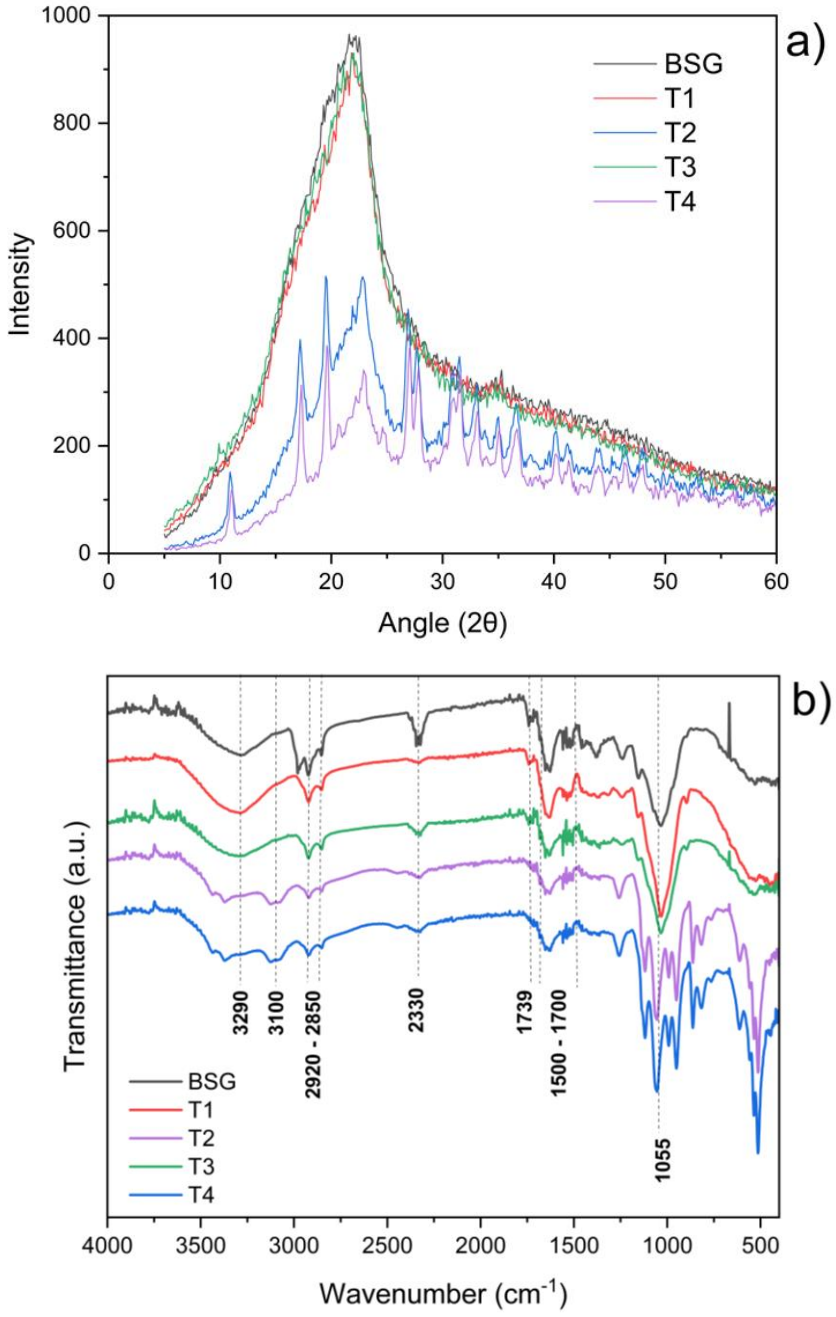

Similar XRD profiles of unprocessed BSG have been reported in the literature (Pereira et al., 2021; Sibhatu et al., 2021b; Sun et al., 2024). After T1 and T3 processing conditions, the *CrI* increased to 33%. This small change in *CrI* is in

agreement with the results of the chemical composition and microscopy, as T1 and T3 were the processing conditions with the lowest capacity to remove lignin and proteins, in addition to low structural changes.

More aggressive conditions such as T2 (8% AHP) and T4 (12h processing) drastically altered the XRD spectra and *CrI* of the processed BSG. This is evidenced by the appearance of several peaks with diffraction angles of 11°, 17°, 20°, and 23°, more defined and with lower intensity, being related to the crystallinity induced by processing with AHP, indicating structural disorganization of the BSG. This behavior is also reported in the literature as the conversion of type I cellulose into type II cellulose (Owolabi et al., 2017; Sibhatu et al., 2021b). After the treatments, crystallinity increased to 49% (T2) and 63% (T4), which can be attributed to the relative increase in the cellulose content in the solid residue (Zhang et al., 2022), due to the removal of proteins, extractives, and lignin from solid BSG to the suspension, which is also consistent with the chemical composition results. A similar increase in *CrI* after AHP processing was reported in different lignocellulosic materials such as corncob (Su et al., 2015), corn stover (Li et al., 2018), bamboo (Zhan et al., 2022), and sugar cane bagasse (Zhang et al., 2022). Furthermore, the literature reports that this effect can lead to a high conversion rate of cellulose into fermentable sugars because a large part of the lignin was partially solubilized during processing. These results highlight the potential of AHP processing to modify the structure of BSG, making it more suitable for industrial applications, especially in the production of biofuels and value-added products.

3.1.2.3. Functional groups: Fourier transform infrared spectroscopy (FTIR)

Fourier transform infrared spectroscopy (FTIR) is commonly used to indicate changes in composition according to the evaluation of the functional groups belonging to each component. Figure 2-b shows the FTIR of unprocessed and processed BSG. The processed BSGs showed significant changes in band intensities in the characteristic peaks for cellulose (3290 cm^{-1}), proteins (1500–1700 cm^{-1}), lignin (1240 cm^{-1}), and hemicellulose (1030 cm^{-1}), compared to unprocessed BSG. These modifications indicate that the processing altered the lignocellulosic structure of BSG, mainly due to the breaking of chemical bonds induced by the processing conditions.

The band stretching signal at 3310 cm^{-1} represents the presence of hydroxyl and amine groups, indicating cellulose and hemicellulose (Naibaho et al., 2021). In this band, the intensity was more evident after processing T2 (higher concentration of AHP) and T4 (longer processing time), which may be related to the significant increase in cellulose and hemicellulose. The peak at ~2900 cm^{-1} is related to the asymmetric stretching of CH_2 functional groups, which is the typical structure of polysaccharides present in BSG. Furthermore, the band at 1739 cm^{-1} indicates the breaking of the ester and carboxylic bonds in hemicellulose (Dos Santos et al., 2015). This band was reduced after processing conditions T1 and T3, with a marked decrease observed after processing conditions T2 and T4. The reduction of the amorphous region of the hemicellulose might be associated with the results present in the observed increase in the CrI of the samples.

The region between 1700 and 1600 cm^{-1} can be attributed to the presence of proteins (amide I) (Naibaho et al., 2021) present in BSG. The drastic reduction of these peaks indicates that the alkaline processing solubilized part of the proteins into the liquid. On the other hand, the presence of peaks after the most severe processing conditions (T2 and T4) reinforces the difficulty of delignifying this matrix and extracting BSG proteins in high yields, due to the complex network formed between lignin and cellulose that entraps the protein.

The spectra also revealed characteristic bands of lignin, corresponding to its aromatic structure, at approximately 1514 cm^{-1} and 1450 cm^{-1}, as reported by (Cassoni et al., 2023b). Furthermore, there was a marked reduction in the peak at 1526 cm^{-1} which represents C=C bonds in the aromatic ring of lignin for the processed BSGs (Ravindran et al., 2019a).

The peaks at 1055 cm^{-1} and 895 cm^{-1} are associated with the C—O stretching and C—H vibrations of cellulose (Alemdar and Sain, 2008) present in all spectra. Furthermore, the most severe processing conditions (T2 and T4) caused the appearance of several peaks around the main peak (1055 cm^{-1}), different from the spectra of unprocessed BSG and less severe treatments (T1 and T3). This corroborates the results found in the XRD spectra where these more severe processing conditions drastically altered the crystallinity of the cellulose present in BSG, evidenced by the appearance of several peaks with different diffraction angles, being related to the crystallinity induced by the

processing with AHP, indicating intense structural disorganization of BSG after these processing.

In general, peaks related to lignin and proteins showed greater intensity in unprocessed BSG and were reduced after processing conditions with a more significant reduction observed in T2 and T4. On the other hand, peaks related to cellulose and hemicellulose seem to undergo increases/modifications, being directly related to the increase in the percentages of cellulosic components. In this way, the observation of the modified patterns in the FTIR spectra, notably the variations in the peaks related to cellulose, hemicellulose, lignin, and proteins, is in direct agreement with the results obtained in the chemical composition, morphological, and structural (XRD) analyses of the BSG subjected to different processing conditions. This convergence of evidence consistently reinforces the specific and differentiated impacts of processing conditions on the composition and structure of BSG, which in turn can directly impact the rheological behavior of processed suspensions.

3.2. Flow behavior

The Herschel-Bulkley model could be fitted with high accuracy ($R_{adj}^2 \geq 0.999$) to the rheograms obtained for BSG suspension. The results of the fitting procedures are presented in Figure 3. Complete data was provided in the Supplementary Material.

Figure 3 presents some fitting results of the Herschel-Bulkley model to the experimental rheograms in order to show the effect of different concentrations of AHP and BSG in suspensions processed at 20°C at different processing times.
In general, shear stresses increased with increasing AHP, BSG, and processing time. Suspensions with up to 4% BSG and 4% AHP (*n* from 0.955-0.966), showed an almost linear relationship between shear stress versus shear rate, which may suggest behavior close to that of Newtonian fluids. As expected, and considering the non-sphericity of the suspended particles, the flow behavior begins to suggest a shear thinning behavior when increasing the concentrations of BSG and AHP above 4%. This behavior is intensified in suspensions with 8% BSG regardless of the concentration of AHP used.

Figure 3. Rheograms of alkaline BSG suspensions as a function of processing time.

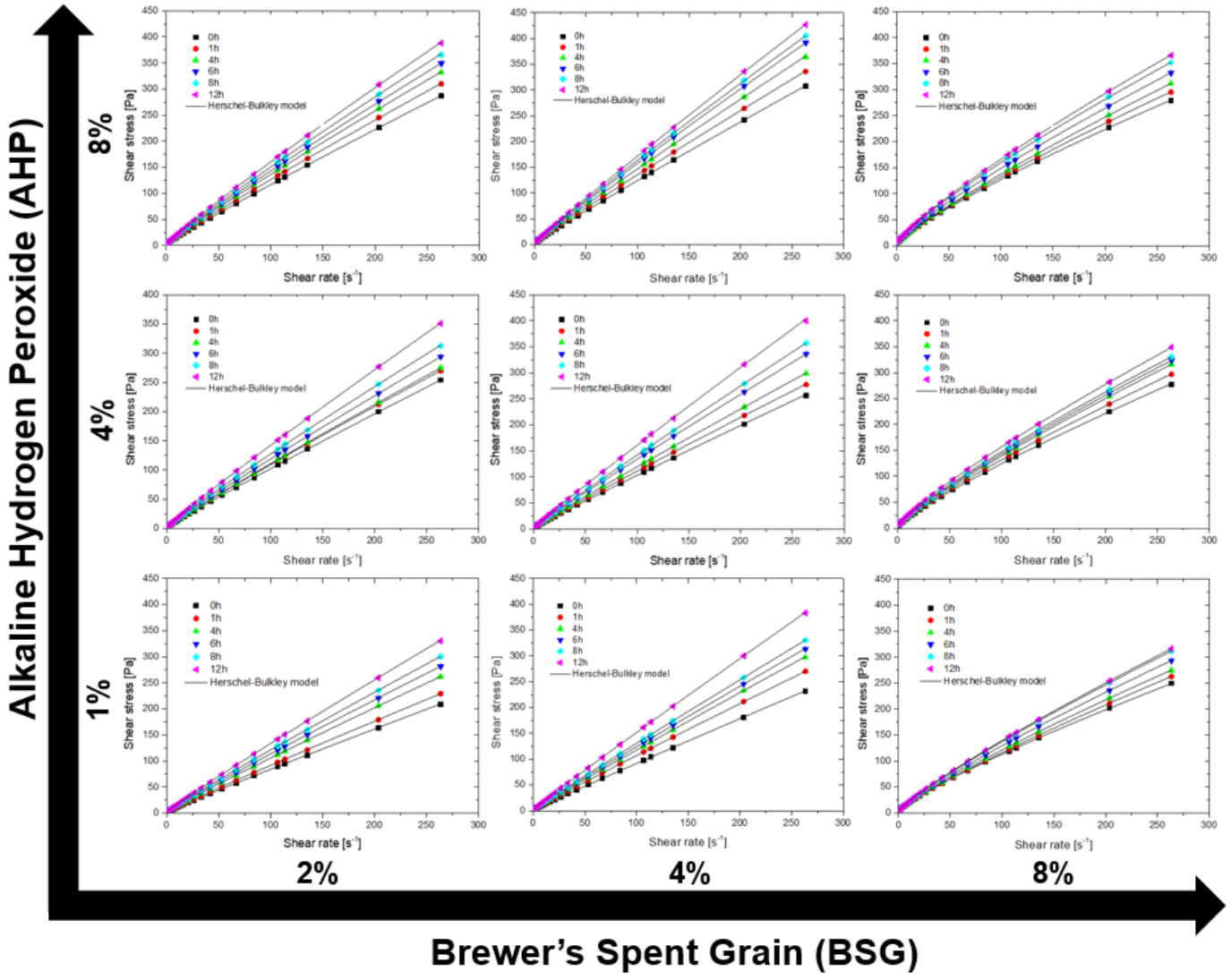

Although relatively small, the suspensions presented flow yield stresses, demonstrating the attractive interactions among particles.

Figure 4 shows that the suspensions with minimum concentrations of AHP (1%), and BSG (2%), immediately prepared (time 0) started to show significant flow yield stresses (τ_0 = 1.632 ± 0.037 Pa) and flow behavior index (n) less than 1 (0.968 ± 0.001), suggesting pseudoplastic behavior.

Figure 4. Rheological parameters of alkaline BSG suspensions as a function of processing time.

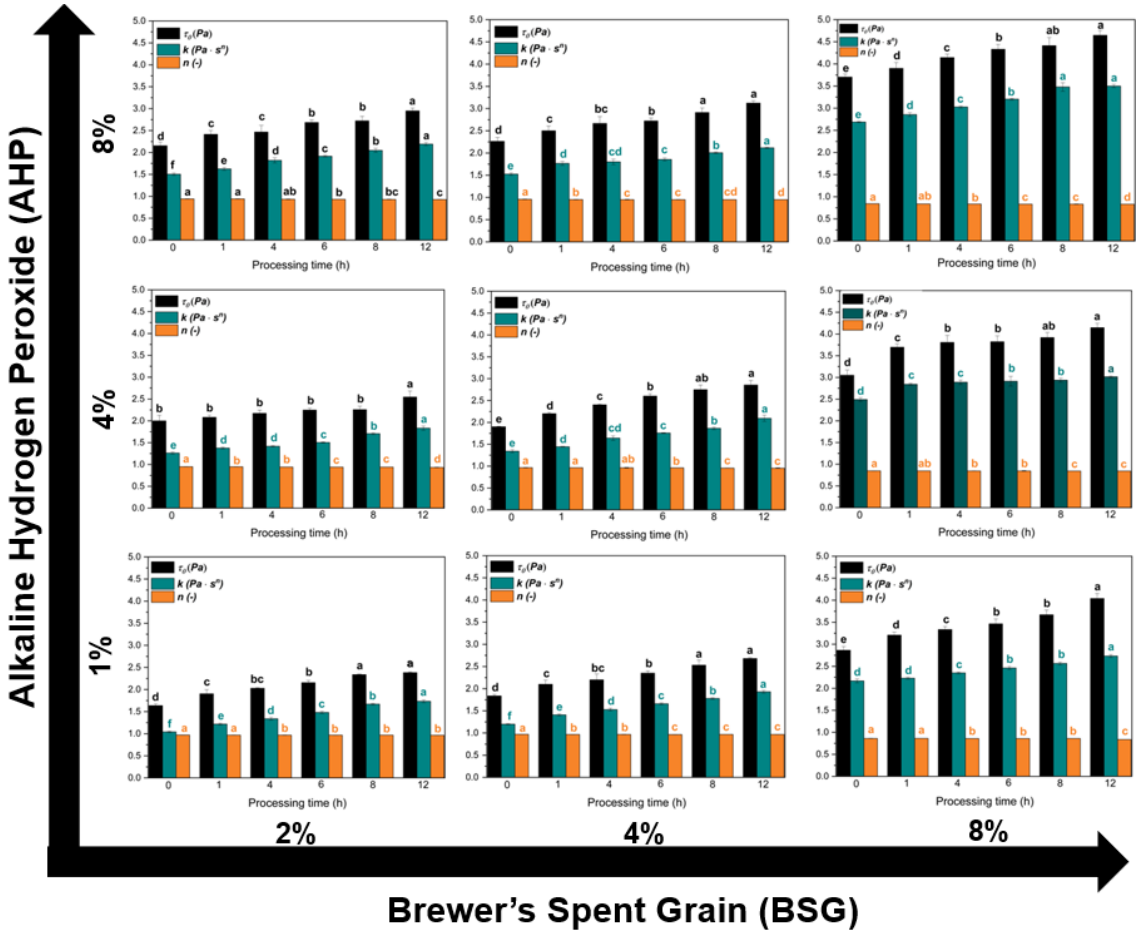

These results lead to an interesting comparison with previous studies on the rheology of acid suspensions of cassava bagasse (Polachini et al., 2019) and peanut shells (Polachini et al., 2016). These studies reported a transition from Newtonian to pseudoplastic behavior only when the solids concentration was 6% (cassava bagasse) and 10% (peanut shells). It is worth mentioning that these studies also evaluated immediately prepared suspensions (time 0).

The observed differences can be attributed to the different processing agents, chemical composition, and particle size of the biomasses. In this study, in addition to the suspension being alkaline (pH 11.5), AHP under these conditions quickly dissociates in water and begins to react with the BSG components.

Furthermore, BSG is a lignocellulosic and protein-rich material, while cassava bagasse contains large amounts of starch, and peanut shells are predominantly lignocellulosic. This shows that different processing agents, variations in chemical composition, and particle structure play a fundamental role in rheological responses - reinforcing the need to study each product specifically.

To simplify calculations in unit operations designs, especially in dilute conditions, it is possible to consider that suspensions behave like Newtonian fluids. This assumption becomes viable in suspensions containing up to 4% BSG and up to 4% AHP, where τ_0 are relatively low, and the n approaches 1. This condition converts the Herschel-Bulkley model into the Newton model. Interestingly, Coussot, (2005) argued that, in suspensions with a solids concentration of less than 4%, interactions between biomass particles can be considered insignificant, resulting in the prevalence of Newtonian behavior. It is worth mentioning that this behavior is a function of biomass composition and structuring, which dictates the interaction of particle-particle and particle-dispersant.

3.2.1. Effect of AHP and BSG concentrations

The AHP concentration had a significant impact on the rheological properties of the suspensions at different processing times. In general, when comparing suspensions with fixed concentrations of BSG at 2% at the same processing times, increasing the AHP concentration in the dispersant increased the values of τ_0 (Pa) and k (Pa·s^n) and decreased the values of n (-). In other words, the increase of AHP concentration promotes enough interaction among the components in suspension to cause a deviation of Newtonian behavior.

For suspensions with low concentrations of BSG (2%), immediately prepared (time 0), it was observed that increasing the AHP concentration in the dispersant from 1% to 8% significantly increased τ_0 (Pa) from 1.636 ± 0.037 to

2.15442 ± 0.080; and k (Pa·s^n) from 1.040 ± 0.017 to 1.504 ± 0.030. In contrast, n (-) decreased from 0.968 ± 0.003 to 0.940 ± 0.004.

Analyzing the more concentrated BSG suspensions (8%), after a longer processing time (12 h), a similar pattern was observed. The value of τ_0 (Pa) increased from 4.040 ± 0.115 to 4.645 ± 0.159, while k (Pa·s^n) increased from 2.733 ± 0.034 to 3.500 ± 0.034, and n (-) decreased from 0.837 ± 0.002 to 0.830 ± 0.002. These observations indicate that increasing AHP concentration consistently influences the rheological properties of suspensions, regardless of BSG concentration and processing time.

The results discussed in the previous sections revealed that increasing the concentration of AHP promoted the thinning of the BSG cell wall layers, which resulted in the release of components previously retained in the disperse phase (e.g. proteins, lignin, and extractives) towards the dispersant. The presence of these high molecular weight components in the dispersing phase probably increased the viscosity and the initial stress needed by the suspensions to start flowing. Furthermore, the alkaline pH of the suspensions (11.5) together with the oxidizing effect of the AHP generally increases the protein solubility and causes their unfolding. It is linked to the breaking of hydrogen bonds and hydrophobic interactions that maintain the three-dimensional structure of proteins (Li et al., 2022). As a result, functional groups are exposed that can interact with water and/or AHP molecules in the suspension through hydrogen bonds and other interactions. Additionally, proteins can also interact with each other through protein-protein interactions, forming protein aggregates or complexes (Sow et al., 2018a). It causes particles o shear among each other, which contributes to the flow resistance.

The BSG concentration also significantly impacted the rheological properties of the suspensions. In a scenario where the AHP concentration remains at 1%, it is observed that an increase in the BSG concentration from 2% to 8%, had a significant impact on the rheological properties. The values of τ_0 (Pa) underwent a notable increase, going from 1.636 ± 0.037 up to 2.864 ± 0.084. Simultaneously, the value of k (Pa·s^n) increased from 1.040 ± 0.017 to 2.168 ± 0.045. In contrast, the value of n (-) decreased from 0.968 ± 0.003 to 0.860 ± 0.004.

Similarly, this response pattern in rheological properties is not restricted only to the evaluated AHP concentration of 1%. By extending the analysis to higher concentrations of AHP, such as 4% and 8%, as well as exploring different processing times, there was a remarkable consistency in this behavior. This observation highlights the sensitivity of the rheological responses of suspensions to the studied changes in the experimental conditions.

As previously observed, the chemical composition and structural characteristics had minor impact when processing suspensions when BSG concentration in the suspensions was increased. Unsurprisingly, the impacts on rheological parameters can be attributed mainly to frictional interactions and/or formation of agglomerates in addition to possible particle swelling. All these phenomena may reduce the role of the dispersant in the suspension, prevailing the particle-particle interactions as the driving mechanisms to govern the rheological properties (Polachini et al., 2016; Volynets et al., 2017). The increase of particles concentration will contribute to the intensification of these mechanisms, thus resulting in in higher pseudoplasticity of BSG suspensions.

3.2.2. Effect of processing time

Figure 4 also shows how the rheological parameters of the suspensions with different concentrations of AHP and BSG were affected by the processing time. As the processing time was prolonged, there was an increase in the τ_0 and k of the suspensions, with decreasing n values.

In addition to the release of components previously retained in the dispersed phase (e.g. proteins, lignin, and extractives) towards the dispersing phase, structural changes were also observed as a consequence of the processing time. It could be seen the presence of smaller and finer particles (Figure 1) as the processing time increased, which may also have a specific contribution to the changes in the rheological parameters of the suspensions.

The increase in the concentration of small and fine particles in BSG suspensions may have triggered a series of effects that directly impacted the rheological characteristics of these suspensions. Firstly, the increase in the specific surface area of the BSG particles may have promoted a more intense interaction with the dispersing phase. Furthermore, when attractive forces

between particles prevail, collisions between them will lead to the formation of clusters, which further restrict the relative movement between them. These structures, in turn, can retain the dispersing phase, further increasing viscosity and shear strength (Olhero and Ferreira, 2004). In fact, the suspension flow behavior index tends to decrease with increasing sample treatment time. This indicates that the greater quantity of flakes resulting from the treatment undergoes destructuring when the suspension is subjected to high deformation. Furthermore, the isolated particles begin to align with the flow, resulting in a drop in apparent viscosity under these conditions. Together, these effects contribute to the manifestation of a more viscous rheological behavior in biomass suspensions as structural modifications occur with increasing processing time.

3.2.3. Temperature dependence

Temperature also had a significant influence on the rheological parameters. The results of τ_0, k and n for all processing conditions at different temperatures are presented in the supplementary material. Unlike the effects observed when changing the concentration of BSG and AHP, the increase in temperature from 20 °C up to 50 °C caused a significant reduction in both τ_0 and k of the suspensions without significant changes in n. This phenomenon is attributed to the greater molecular mobility resulting from the separation of particles due to the increase in the agitation degree. It reduces the viscosity and specific mass of liquid materials (Burlawar et al., 2022; Polachini et al., 2016).

In a practical point of view, the increase in temperature made the suspensions to flow more easily – thus, requiring less energy to start flowing and shearing. Increasing temperature tend to result in suspensions with lower apparent viscosity, indicating a more efficient response to the applied forces. Although this technique makes easier their processing with a potential reduction in energy consumption, it is worth of investigating the technological impact of increasing temperature in the suspensions and the process itself. It is interesting to note that the fluid behavior index remained relatively constant, indicating that temperature variations did not have a significant impact in the pseudoplastic nature of the suspensions.

Figure 5. Rheograms of alkaline BSG suspensions as a function of temperature.

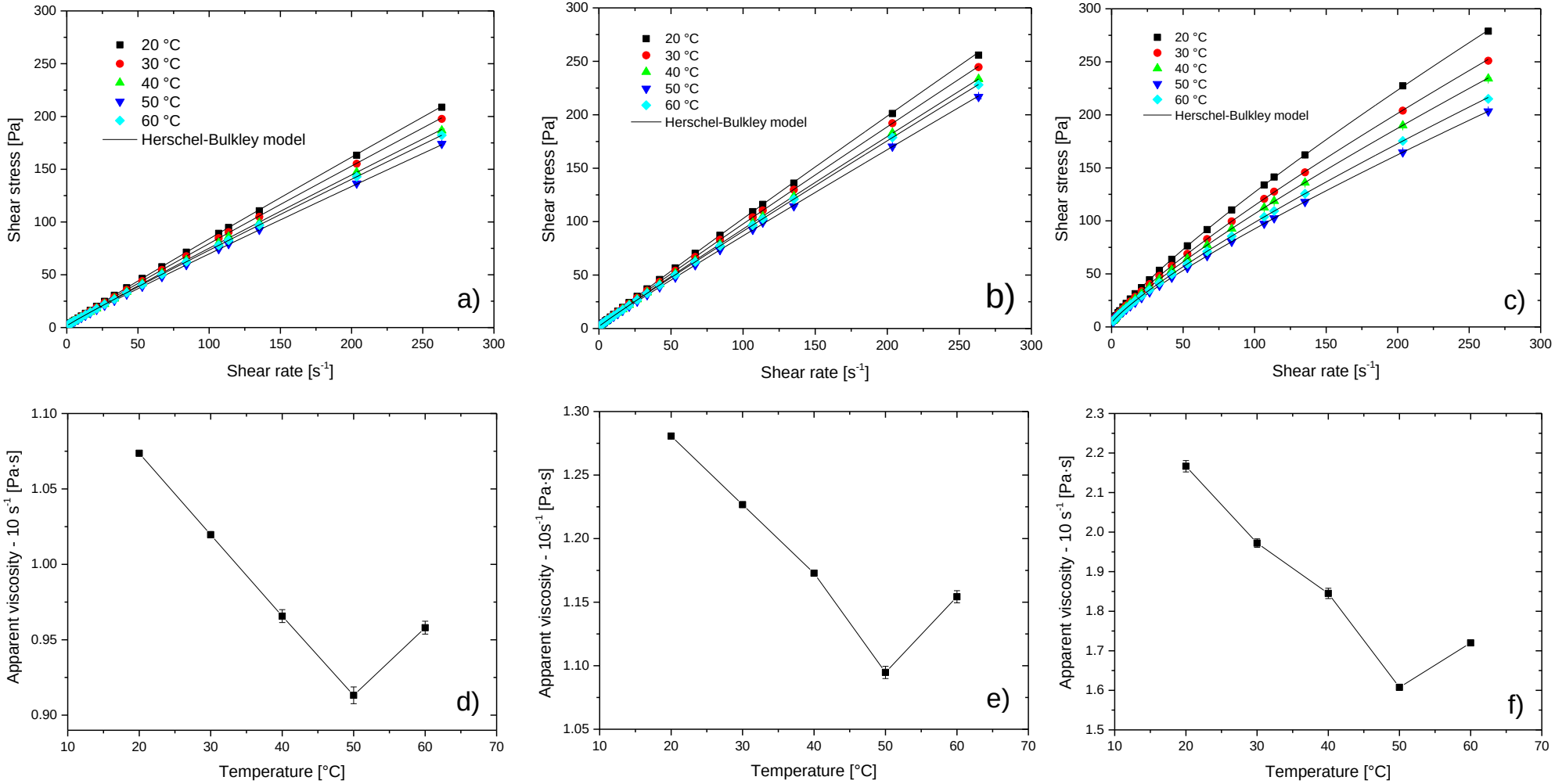

Where a) and d) 1% AHP and 2% BSG; b) and e) 4% AHP and 4% BSG; c) and f) 8% AHP and 8% BSG.

Figure 5 displays selected rheograms illustrating a significant behavior at 60°C, emphasizing a distinctive response observed in the suspensions. Increasing the temperature from 50 °C to 60 °C resulted in a more prominent increase in both τ_0 and k of the suspensions (Supplementary material). It results in a significant increase in the apparent viscosity and in the amount of energy required by the suspension to flow. This atypical variation can be attributed to the presence of residual starch in BSG, which may underwent a gelatinization process.

Several previous studies (Lima Moraes dos Santos et al., 2023; López-Linares et al., 2020b; Parchami et al., 2021a; Qazanfarzadeh et al., 2023; Rojas-Pérez et al., 2022) identified BSG as a matrix that contains substantial levels of starch. The increase in the apparent viscosity of the suspensions at 60 °C may be associated with the gelatinization temperature of the residual starch present in BSG. According to the literature, the gelatinization of barley starch is expected to occur approximately between 53 ºC and 63 ºC (Gebre et al., 2024; Langenaeken et al., 2019).

In the presence of water, the moisture adsorbed by the BSG matrix tended to penetrated the amorphous regions of the starch granules, breaking the intermolecular hydrogen bonds and releasing amylose and amylopectin chains, resulting in the loss of crystalline zones (Singh et al., 2003). This phenomenon is known to increase the viscosity of starch-containing suspensions, explaining the observation of greater flow resistance at this specific point in the temperature range.

This behavior also highlights the need by avoiding working with BSG above 50 °C for BSG. This substantial increase in the viscosity of the suspensions due to starch gelatinization would imply in unnecessary energy expenditure. Additionally, suspensions with high viscosity also offer resistance to the contact between H_2O_2-biomass – raising difficulties for mass transfer mechanisms and process efficiency. This correlation between the rheological behavior and starch gelatinization in BSG highlights the complexity of the factors that influence the rheological properties of this particular suspension, providing important information for an efficient control of the industrial process.

4. CONCLUSIONS

The high content of proteins (~21%), cellulose, and hemicellulose (total ~47%) in dry brewer's spent grains (BSG) highlighted the need for a properly designed conversion process. It concerns not only the extraction of proteins but also the conversion of the lignocellulose fraction of BSG into biofuels. Therefore, this study investigated the impact of alkaline processing with hydrogen peroxide (AHP) on the chemical composition, structure, and rheological properties of BSG.

AHP processing had a notable impact on the structure and properties of BSG suspensions. Increasing the concentration of AHP in the suspension and the processing time improved the removal of proteins, lignin, and extractives from BSG towards the suspension. It increased, consequently, relative content of cellulose and hemicellulose in the processed BSG. However, increasing the concentration of BSG in the suspension slightly reduced the removal efficiency of these components due to the difficulties associated to mass transfer.

Processing BSG with AHP also caused morphological changes to the particles. A higher concentration of AHP in the suspension caused the thinning of the cell walls, while longer processing time caused changes in the particle shape. These changes, together with the increase in the crystallinity of the processed BSG, indicated the material had its structure affected. Furthermore, FTIR spectra confirmed reductions in lignin and protein intensity, providing information about their removal, while new peaks around the main one, related to cellulose and hemicellulose, appeared in the processed BSG.

Regarding the rheological properties, the Herschel-Bulkley model fitted the flow curves fitted with high accuracy, demonstrating non-Newtonian behavior with flow yield stress (1.529 Pa < τ_0 < 4.646 Pa) and pseudoplasticity (0.830 < n < 0.969) in all of the tested conditions. The flow resistance (τ_0, k) was increased, and the flow index behavior (n) decreased with increasing AHP concentration, BSG loading and processing time. The increasing temperature had an expected decreasing effect when in the range of 20 to 50 °C. Specifically, at 60 °C, gelatinization of residual starch in BSG may have taken place, and a more significant contribution to the increase in the resistance to flow appeared. All the reported information is useful and will support the design of processes and

equipment, especially those involving the extraction of proteins and the conversion of the lignocellulose fraction of BSG into biofuels.

Declaration of competing interest

The authors declare no conflict of interest.

Acknowledgments

This study was financed in part by the São Paulo Research Foundation (FAPESP) – Grant n°2022/05272-8 and by the Coordenação de Aperfeiçoamento de Pessoal de Nível Superior - Brasil (CAPES) - Finance Code 001.

Communauté Urbaine du Grand Reims, Département de la Marne, Région Grand Est and European Union (FEDER Champagne-Ardenne 2014-2020, FEDER Grand Est 2021-2027) are acknowledged for their financial support to the Chair of Biotechnology of CentraleSupélec and the Centre Européen de Biotechnologie et de Bioéconomie (CEBB).

5. References

Agrawal, D., Gopaliya, D., Willoughby, N., Khare, S.K., Kumar, V., 2023. Recycling potential of brewer's spent grains for circular biorefineries. **Curr Opin Green Sustain Chem** 40, 100748. https://doi.org/10.1016/J.COGSC.2022.100748

Aider, M., Ndiaye, M., & Karim, A. (2023). Optimization of canola meal bleaching by hydrogen peroxide, protein extraction and characterization of their functional properties. **Future Foods**, *8*, 100282. https://doi.org/10.1016/j.fufo.2023.100282

Alemdar, A., Sain, M., 2008. Isolation and characterization of nanofibers from agricultural residues – Wheat straw and soy hulls. **Bioresour Technol** 99, 1664–1671. https://doi.org/10.1016/J.BIORTECH.2007.04.029

Alonso-Riaño, P., Ramos, C., Trigueros, E., Beltrán, S., Sanz, M.T., 2023. Study of subcritical water scale-up from laboratory to pilot system for brewer's spent grain valorization. **Ind Crops Prod** 191, 115927. https://doi.org/10.1016/J.INDCROP.2022.115927

AOAC, 2007. Association of Official Analytical Chemistry, 18th ed, **In: Official methods of analysis to AOAC International**. Gaithersburg.

Borel, L.D.M.S., Lira, T.S., Ribeiro, J.A., Ataíde, C.H., Barrozo, M.A.S., 2018. Pyrolysis of brewer's spent grain: Kinetic study and products identification. **Ind Crops Prod** 121, 388–395. https://doi.org/10.1016/J.INDCROP.2018.05.051

Burlawar, S., Klingenberg, D.J., Root, T.W., Scott, C.T., Houtman, C.J., Bourne, K.J., Gleisner, R., Subramaniam, V., 2022. Effect of temperature on the rheology of concentrated suspensions containing lignocellulosic biomass particles. **Biomass Bioenergy** 156, 106298. https://doi.org/10.1016/J.BIOMBIOE.2021.106298

Cabrera, E., Muñoz, M.J., Martín, R., Caro, I., Curbelo, C., Díaz, A.B., 2014. Alkaline and alkaline peroxide pretreatments at mild temperature to enhance enzymatic hydrolysis of rice hulls and straw. **Bioresour Technol** 167, 1–7. https://doi.org/10.1016/J.BIORTECH.2014.05.103

Cassoni, A.C., Costa, P., Mota, I., Vasconcelos, M.W., Pintado, M., 2023. Recovery of lignins with antioxidant activity from Brewer's spent grain and olive tree pruning using deep eutectic solvents. **Chemical Engineering Research and Design** 192, 34–43. https://doi.org/10.1016/J.CHERD.2023.01.053

Dos Santos, D.M., De Lacerda Bukzem, A., Ascheri, D.P.R., Signini, R., De Aquino, G.L.B., 2015. Microwave-assisted carboxymethylation of cellulose extracted from brewer's spent grain. **Carbohydr Polym** 131, 125–133. https://doi.org/10.1016/J.CARBPOL.2015.05.051

EL-Sayed, S.A., Mostafa, M.E., 2014. Analysis of Grain Size Statistic and Particle Size Distribution of Biomass Powders. **Waste Biomass Valorization** 5, 1005–1018. https://doi.org/10.1007/S12649-014-9308-5/TABLES/9

El-Kadiri, I., Khelifi, M., & Aider, M. (2013). The effect of hydrogen peroxide bleaching of canola meal on product colour, dry matter and protein extractability and molecular weight profile. **International journal of food science & technology**, *48*(5), 1071-1085. https://doi.org/10.1111/ijfs.12065

Fernández-Delgado, M., Plaza, P.E., Coca, M., García-Cubero, M.T., González-Benito, G., Lucas, S., 2019. Comparison of mild alkaline and oxidative pretreatment methods for biobutanol production from brewer's spent grains. **Ind Crops Prod** 130, 409–419. https://doi.org/10.1016/J.INDCROP.2018.12.087

Gebre, B.A., Xu, Z., Ma, M., Lakew, B., Sui, Z., Corke, H., 2024. Starch molecular structure, physicochemical properties and in vitro digestibility of Ethiopian malt barley varieties. **Int J Biol Macromol** 256, 128407. https://doi.org/10.1016/J.IJBIOMAC.2023.128407

Goldschimid, O. (1971). Ultraviolet spectra. Lignins. New York: **Wiley Interscience**, 241-266.

Gomide, J. L., & Demuner, B. J. (1986). Determinação do teor de lignina em material lenhoso: método Klason modificado. **O papel**, 47(8), 36-38.

Ho, M.C., Ong, V.Z., Wu, T.Y., 2019. Potential use of alkaline hydrogen peroxide in lignocellulosic biomass pretreatment and valorization – A review. **Renewable and Sustainable Energy Reviews** 112, 75–86. https://doi.org/10.1016/J.RSER.2019.04.082

Huang, Y., Chu, Q., Tong, W., Wu, S., Jin, Y., Hu, J., Song, K., 2021. Carbocation scavenger assisted acid pretreatment followed by mild alkaline hydrogen peroxide (AHP) treatment for efficient production of fermentable sugars and lignin adsorbents from hardwood biomass. **Ind Crops Prod** 170, 113737. https://doi.org/10.1016/J.INDCROP.2021.113737

Kane, A.O., Cortez, A.A., Pellegrini, V.O.A., Ngom, B.D., Filgueiras, J.G., de Azevedo, E.R., Polikarpov, I., 2023. Combined liquid hot water and sulfonation pretreatment of sugarcane bagasse to maximize fermentable sugars production.

Ind Crops Prod 201, 116849. https://doi.org/10.1016/J.INDCROP.2023.116849

Langenaeken, N.A., De Schepper, C.F., De Schutter, D.P., Courtin, C.M., 2019. Different gelatinization characteristics of small and large barley starch granules impact their enzymatic hydrolysis and sugar production during mashing. **Food Chem** 295, 138–146. https://doi.org/10.1016/J.FOODCHEM.2019.05.045

Li, H., Xiong, L., Chen, Xindong, Luo, M., Chen, Xuefang, Wang, C., Huang, C., Chen, Xinde, 2019. Enhanced enzymatic hydrolysis of wheat straw via a combination of alkaline hydrogen peroxide and lithium chloride/N,N-dimethylacetamide pretreatment. **Ind Crops Prod** 137, 332–338. https://doi.org/10.1016/J.INDCROP.2019.05.027

Li, J., Lu, M., Guo, X., Zhang, H., Li, Y., Han, L., 2018. Insights into the improvement of alkaline hydrogen peroxide (AHP) pretreatment on the enzymatic hydrolysis of corn stover: Chemical and microstructural analyses. **Bioresour Technol** 265, 1–7. https://doi.org/10.1016/J.BIORTECH.2018.05.082

Li, Q., Yang, H., Coldea, T.E., Andersen, M.L., Li, W., Zhao, H., 2022. Enzymolysis kinetics, thermodynamics and structural property of brewer's spent grain protein pretreated with ultrasound. **Food and Bioproducts Processing** 132, 130–140. https://doi.org/10.1016/J.FBP.2022.01.001

Li, W., Yang, H., Coldea, T.E., Zhao, H., 2021. Modification of structural and functional characteristics of brewer's spent grain protein by ultrasound assisted extraction. **LWT** 139, 110582. https://doi.org/10.1016/J.LWT.2020.110582

Lima Moraes dos Santos, A., de Sousa e Silva, A., Sales Morais, N.W., Bezerra dos Santos, A., 2023. Brewery Spent Grain as sustainable source for value-added bioproducts: Opportunities and new insights in the integrated lignocellulosic biorefinery concept. **Ind Crops Prod** 206, 117685. https://doi.org/10.1016/J.INDCROP.2023.117685

López-Linares, J.C., García-Cubero, M.T., Lucas, S., Coca, M., 2020. Integral valorization of cellulosic and hemicellulosic sugars for biobutanol production: ABE fermentation of the whole slurry from microwave pretreated brewer's spent

grain. **Biomass Bioenergy** 135, 105524. https://doi.org/10.1016/J.BIOMBIOE.2020.105524

Moodley, P., Kana, E.B.G., 2017. Microwave-assisted inorganic salt pretreatment of sugarcane leaf waste: Effect on physiochemical structure and enzymatic saccharification. **Bioresour Technol** 235, 35–42. https://doi.org/10.1016/J.BIORTECH.2017.03.031

Mussatto, S.I., Dragone, G., Roberto, I.C., 2007. Ferulic and p-coumaric acids extraction by alkaline hydrolysis of brewer's spent grain. **Ind Crops Prod** 25, 231–237. https://doi.org/10.1016/J.INDCROP.2006.11.001

Naibaho, J., Korzeniowska, M., Wojdyło, A., Figiel, A., Yang, B., Laaksonen, O., Foste, M., Vilu, R., Viiard, E., 2021. Fiber modification of brewers' spent grain by autoclave treatment to improve its properties as a functional food ingredient. **LWT** 149, 111877. https://doi.org/10.1016/J.LWT.2021.111877

Olhero, S.M., Ferreira, J.M.F., 2004. Influence of particle size distribution on rheology and particle packing of silica-based suspensions. **Powder Technol** 139, 69–75. https://doi.org/10.1016/J.POWTEC.2003.10.004

Owolabi, A.F., Haafiz, M.K.M., Hossain, M.S., Hussin, M.H., Fazita, M.R.N., 2017. Influence of alkaline hydrogen peroxide pre-hydrolysis on the isolation of microcrystalline cellulose from oil palm fronds. **Int J Biol Macromol** 95, 1228–1234. https://doi.org/10.1016/J.IJBIOMAC.2016.11.016

Pabbathi, N.P.P., Velidandi, A., Pogula, S., Gandam, P.K., Baadhe, R.R., Sharma, M., Sirohi, R., Thakur, V.K., Gupta, V.K., 2022. Brewer's spent grains-based biorefineries: A critical review. **Fuel** 317, 123435. https://doi.org/10.1016/J.FUEL.2022.123435

Parchami, M., Ferreira, J.A., Taherzadeh, M.J., 2021. Starch and protein recovery from brewer's spent grain using hydrothermal pretreatment and their conversion to edible filamentous fungi – A brewery biorefinery concept. **Bioresour Technol** 337, 125409. https://doi.org/10.1016/J.BIORTECH.2021.125409

Pereira, G.N., Cesca, K., Cubas, A.L.V., Bianchet, R.T., Junior, S.E.B., Zanella, E., Stambuk, B.U., Poletto, P., de Oliveira, D., 2021. Non-thermal plasma as an innovative pretreatment technology in delignification of brewery by-product. **Innovative Food Science & Emerging Technologies** 74, 102827. https://doi.org/10.1016/J.IFSET.2021.102827

Coussot, P. 2005. Rheometry of Pastes, **Suspensions, and Granular Materials: Applications in Industry and Environment**, John Wiley & Sons. ed. Hoboken, New Jersey.

Polachini, T.C., Mulet, A., Cárcel, J.A., Telis-Romero, J., 2019. Rheology of acid suspensions containing cassava bagasse: Effect of biomass loading, acid content and temperature**. Powder Technol** 354, 271–280. https://doi.org/10.1016/J.POWTEC.2019.05.086

Polachini, T.C., Sato, A.C.K., Cunha, R.L., Telis-Romero, J., 2016. Density and rheology of acid suspensions of peanut waste in different conditions: An engineering basis for bioethanol production. **Powder Technol** 294, 168–176. https://doi.org/10.1016/J.POWTEC.2016.02.022

Qazanfarzadeh, Z., Ganesan, A.R., Mariniello, L., Conterno, L., Kumaravel, V., 2023. Valorization of brewer's spent grain for sustainable food packaging. **J Clean Prod** 385, 135726. https://doi.org/10.1016/J.JCLEPRO.2022.135726

Qin, F., Johansen, A.Z., Mussatto, S.I., 2018. Evaluation of different pretreatment strategies for protein extraction from brewer's spent grains. **Ind Crops Prod** 125, 443–453. https://doi.org/10.1016/J.INDCROP.2018.09.017

Ravindran, R., Sarangapani, C., Jaiswal, S., Lu, P., Cullen, P.J., Bourke, P., Jaiswal, A.K., 2019. Improving enzymatic hydrolysis of brewer spent grain with nonthermal plasma. **Bioresour Technol** 282, 520–524. https://doi.org/10.1016/J.BIORTECH.2019.03.071

Rojas-Pérez, L.C., Narváez-Rincón, P.C., Ballesteros, I., 2022. Improving sugar extraction from brewers' spent grain using sequential deproteinization and acid-catalyzed steam explosion in a biorefinery context. **Biomass Bioenergy** 159, 106389. https://doi.org/10.1016/J.BIOMBIOE.2022.106389

Sanches, M.A.R., Augusto, P.E.D., Polachini, T.C., Telis-Romero, J., 2023. Water sorption properties of brewer's spent grain: A study aimed at its stabilization for further conversion into value-added products. **Biomass Bioenergy** 170, 106718. https://doi.org/10.1016/J.BIOMBIOE.2023.106718

Saravanan, A., Senthil Kumar, P., Jeevanantham, S., Karishma, S., Vo, D.V.N., 2022. Recent advances and sustainable development of biofuels production from lignocellulosic biomass. **Bioresour Technol** 344, 126203. https://doi.org/10.1016/J.BIORTECH.2021.126203

Segal, L., Creely, J.J., A.E. Martin, J., Conrad, C.M., 2016. An Empirical Method for Estimating the Degree of Crystallinity of Native Cellulose Using the X-Ray Diffractometer. **Textile research journal** 29, 786–794. https://doi.org/10.1177/004051755902901003

Sganzerla, W.G., Zabot, G.L., Torres-Mayanga, P.C., Buller, L.S., Mussatto, S.I., Forster-Carneiro, T., 2021. Techno-economic assessment of subcritical water hydrolysis process for sugars production from brewer's spent grains. **Ind Crops Prod** 171, 113836. https://doi.org/10.1016/J.INDCROP.2021.113836

Sibhatu, H.K., Anuradha Jabasingh, S., Yimam, A., Ahmed, S., 2021. Ferulic acid production from brewery spent grains, an agro-industrial waste. **LWT** 135, 110009. https://doi.org/10.1016/J.LWT.2020.110009

Silva, A.M.M. da, Almeida, F.S., Silva, M.F. da, Goldbeck, R., Sato, A.C.K., 2023. How do pH and temperature influence extraction yield, physicochemical, functional, and rheological characteristics of brewer spent grain protein concentrates? **Food and Bioproducts Processing** 139, 34–45. https://doi.org/10.1016/J.FBP.2023.03.001

Singh, N., Singh, J., Kaur, L., Sodhi, N.S., Gill, B.S., 2003. Morphological, thermal and rheological properties of starches from different botanical sources. **Food Chem** 81, 219–231. https://doi.org/10.1016/S0308-8146(02)00416-8

Sluiter, A., Hames, B., Ruiz, R., Scarlata, C., Sluiter, J., Templeton, D., & Crocker, D. L. A. P. (2008). Determination of structural carbohydrates and lignin in biomass. **Laboratory analytical procedure**, 1617(1), 1-16.

Sluiter, A., Ruiz, R., Scarlata, C., Sluiter, J., & Templeton, D. J. L. A. P. (2005). Determination of extractives in biomass. **Laboratory analytical procedure (LAP)**, 1617(4), 1-16.

Sow, L.C., Nicole Chong, J.M., Liao, Q.X., Yang, H., 2018. Effects of κ-carrageenan on the structure and rheological properties of fish gelatin. **J Food Eng** 239, 92–103. https://doi.org/10.1016/J.JFOODENG.2018.05.035

Su, Y., Du, R., Guo, H., Cao, M., Wu, Q., Su, R., Qi, W., He, Z., 2015. Fractional pretreatment of lignocellulose by alkaline hydrogen peroxide: Characterization of its major components. **Food and Bioproducts Processing** 94, 322–330. https://doi.org/10.1016/J.FBP.2014.04.001

Sun, W., Zhang, Z., Li, X., Lu, X., Liu, G., Qin, Y., Zhao, J., Qu, Y., 2024. Production of single cell protein from brewer's spent grain through enzymatic saccharification and fermentation enhanced by ammoniation pretreatment. **Bioresour Technol** 394, 130242. https://doi.org/10.1016/J.BIORTECH.2023.130242

Volynets, B., Ein-Mozaffari, F., Dahman, Y., 2017. Biomass processing into ethanol: Pretreatment, enzymatic hydrolysis, fermentation, rheology, and mixing. **Green Processing and Synthesis** 6, 1–22. https://doi.org/10.1515/gps-2016-0017

Wagner, E., Pería, M.E., Ortiz, G.E., Rojas, N.L., Ghiringhelli, P.D., 2021. Valorization of brewer's spent grain by different strategies of structural destabilization and enzymatic saccharification. **Ind Crops Prod** 163, 113329. https://doi.org/10.1016/J.INDCROP.2021.113329

Statista (2023). **Beer production worldwide from 1998 to 2022**. Available online at:https://www.statista.com/statistics/270275/worldwide-beer-production/ (accessed on February 7, 2024).

Xia, Y., Liu, Q., Hu, X., Li, X., Huang, Y., Li, W., Ma, L., 2022a. Structural evolution during corn stalk acidic and alkaline hydrogen peroxide pretreatment. **Ind Crops Prod** 176, 114386. https://doi.org/10.1016/J.INDCROP.2021.114386

Xia, Y., Liu, Q., Wang, H., Hu, X., Li, X., Li, W., Ma, L., 2022b. Chemical and ultrastructural evolutions of corn stalk during sequential acid and alkaline hydrogen peroxide pretreatment. **Biomass Bioenergy** 160, 106443. https://doi.org/10.1016/J.BIOMBIOE.2022.106443

Yan, X., Cheng, J.R., Wang, Y.T., Zhu, M.J., 2020. Enhanced lignin removal and enzymolysis efficiency of grass waste by hydrogen peroxide synergized dilute alkali pretreatment. **Bioresour Technol** 301, 122756.

Zhan, Y., Cheng, J., Liu, X., Huang, C., Wang, J., Han, S., Fang, G., Meng, X., Ragauskas, A.J., 2022. Assessing the availability of two bamboo species for fermentable sugars by alkaline hydrogen peroxide pretreatment. **Bioresour Technol** 349, 126854. https://doi.org/10.1016/J.BIORTECH.2022.126854

Zhang, J., Li, K., Liu, S., Huang, S., Xu, C., 2022. Alkaline hydrogen peroxide pretreatment combined with bio-additives to boost high-solids enzymatic hydrolysis of sugarcane bagasse for succinic acid processing. **Bioresour Technol** 345, 126550.

6. Supplementary Material

Table S1. Suspensions processed for 0 hours.

Temp. (°C)	Parameters	BSG concentration (2%)					BSG concentration (4%)				
		AHP concentration (X_{AHP})					AHP concentration (X_{AHP})				
		1	2	4	6	8	1	2	4	6	8
20	$\tau 0$ (Pa)	1.671 ± 0.048	1.767 ± 0.043	2.000 ± 0.126	2.186 ± 0.034	2.154 ± 0.081	1.636 ± 0.037	1.691 ± 0.054	1.701 ± 0.152	2.016 ± 0.033	2.263 ± 0.084
	k (Pa·s^n)	1.017 ± 0.012	1.095 ± 0.011	1.263 ± 0.025	1.307 ± 0.012	1.504 ± 0.031	1.041 ± 0.017	1.110 ± 0.013	1.244 ± 0.037	1.353 ± 0.012	1.525 ± 0.031
	n (−)	0.954 ± 0.003	0.953 ± 0.003	0.951 ± 0.003	0.946 ± 0.002	0.941 ± 0.005	0.969 ± 0.004	0.965 ± 0.003	0.955 ± 0.006	0.959 ± 0.002	0.951 ± 0.005
	R^2_{adj}	> 0.999	> 0.999	> 0.999	> 0.999	> 0.999	> 0.999	> 0.999	> 0.999	> 0.999	> 0.999
	RMSE	< 0.257	< 0.525	< 0.367	< 0.360	< 0.379	< 0.231	< 0.296	< 0.491	< 0.394	< 0.405
30	$\tau 0$ (Pa)	1.529 ± 0.070	1.730 ± 0.061	1.930 ± 0.108	2.047 ± 0.068	2.178 ± 0.069	1.500 ± 0.074	1.720 ± 0.062	1.860 ± 0.112	2.041 ± 0.074	2.265 ± 0.071
	k (Pa·s^n)	0.921 ± 0.024	0.989 ± 0.015	1.077 ± 0.022	1.179 ± 0.019	1.365 ± 0.017	0.945 ± 0.025	0.975 ± 0.014	1.078 ± 0.022	1.219 ± 0.020	1.356 ± 0.017
	n (−)	0.952 ± 0.006	0.955 ± 0.003	0.951 ± 0.003	0.948 ± 0.003	0.944 ± 0.003	0.964 ± 0.006	0.968 ± 0.003	0.964 ± 0.003	0.961 ± 0.003	0.958 ± 0.003
	R^2_{adj}	> 0.999	> 0.999	> 0.999	> 0.999	> 0.999	> 0.999	> 0.999	> 0.999	> 0.999	> 0.999
	RMSE	< 0.439	< 0.251	< 0.314	< 0.322	< 0.365	< 0.476	< 0.264	< 0.331	< 0.356	< 0.390
40	$\tau 0$ (Pa)	1.610 ± 0.014	1.751 ± 0.052	1.839 ± 0.087	1.942 ± 0.080	2.242 ± 0.054	1.596 ± 0.083	1.611 ± 0.048	1.753 ± 0.154	1.935 ± 0.083	2.317 ± 0.057
	k (Pa·s^n)	0.838 ± 0.007	0.911 ± 0.015	1.027 ± 0.018	1.181 ± 0.033	1.303 ± 0.017	0.863 ± 0.018	0.844 ± 0.014	1.050 ± 0.039	1.186 ± 0.033	1.384 ± 0.017
	n (−)	0.956 ± 0.002	0.954 ± 0.003	0.950 ± 0.003	0.943 ± 0.006	0.945 ± 0.003	0.967 ± 0.004	0.967 ± 0.003	0.957 ± 0.007	0.956 ± 0.006	0.959 ± 0.003
	R^2_{adj}	> 0.999	> 0.999	> 0.999	> 0.999	> 0.999	> 0.999	> 0.999	> 0.999	> 0.999	> 0.999
	RMSE	< 0.242	< 0.094	< 0.265	< 0.301	< 0.315	< 0.162	< 0.092	< 0.512	< 0.323	< 0.359
50	$\tau 0$ (Pa)	1.575 ± 0.079	1.760 ± 0.083	1.889 ± 0.086	1.882 ± 0.093	2.152 ± 0.135	1.614 ± 0.043	1.651 ± 0.080	1.708 ± 0.105	1.927 ± 0.104	2.218 ± 0.143
	k (Pa·s^n)	0.839 ± 0.018	0.924 ± 0.015	1.015 ± 0.018	1.123 ± 0.024	1.333 ± 0.038	0.811 ± 0.005	0.848 ± 0.014	1.031 ± 0.033	1.183 ± 0.026	1.373 ± 0.040
	n (−)	0.955 ± 0.004	0.951 ± 0.003	0.947 ± 0.003	0.939 ± 0.005	0.939 ± 0.006	0.968 ± 0.001	0.964 ± 0.003	0.959 ± 0.007	0.952 ± 0.005	0.948 ± 0.006
	R^2_{adj}	> 0.999	> 0.999	> 0.999	> 0.999	> 0.999	> 0.999	> 0.999	> 0.999	> 0.999	> 0.999
	RMSE	< 0.149	< 0.270	< 0.258	< 0.429	< 0.507	< 0.227	< 0.262	< 0.507	< 0.479	< 0.544
60	$\tau 0$ (Pa)	1.684 ± 0.083	1.723 ± 0.116	1.970 ± 0.129	2.044 ± 0.123	2.332 ± 0.078	1.779 ± 0.077	1.731 ± 0.028	1.902 ± 0.135	2.105 ± 0.133	2.264 ± 0.079
	k (Pa·s^n)	0.882 ± 0.019	0.993 ± 0.035	1.054 ± 0.035	1.151 ± 0.037	1.382 ± 0.030	0.843 ± 0.011	0.967 ± 0.006	1.059 ± 0.035	1.203 ± 0.039	1.362 ± 0.029
	n (−)	0.955 ± 0.004	0.947 ± 0.007	0.948 ± 0.006	0.944 ± 0.006	0.939 ± 0.005	0.971 ± 0.002	0.966 ± 0.001	0.963 ± 0.006	0.957 ± 0.006	0.950 ± 0.005
	R^2_{adj}	> 0.999	> 0.999	> 0.999	> 0.999	> 0.999	> 0.999	> 0.999	> 0.999	> 0.999	> 0.999
	RMSE	< 0.156	< 0.462	< 0.225	< 0.242	< 0.366	< 0.268	< 0.075	< 0.244	< 0.270	< 0.380

Table S1. Suspensions pretreated for 0 hours (continuation).

Temp. (°C)	Parameters	BSG concentration (6%)					BSG concentration (8%)				
		AHP concentration (X_{AHP})					AHP concentration (X_{AHP})				
		1	2	4	6	8	1	2	4	6	8
20	*τ0 (Pa)*	2.398 ± 0.112	2.255 ± 0.043	2.660 ± 0.073	2.644 ± 0.289	3.091 ± 0.133	2.864 ± 0.184	2.866 ± 0.139	3.050 ± 0.119	3.561 ± 0.128	3.703 ± 0.072
	k (Pa·s^n)	1.602 ± 0.025	1.714 ± 0.024	1.733 ± 0.012	1.973 ± 0.091	2.161 ± 0.025	2.168 ± 0.046	2.300 ± 0.045	2.491 ± 0.042	2.523 ± 0.022	2.688 ± 0.016
	n (−)	0.913 ± 0.003	0.905 ± 0.003	0.900 ± 0.001	0.891 ± 0.009	0.889 ± 0.002	0.859 ± 0.004	0.852 ± 0.003	0.844 ± 0.003	0.843 ± 0.001	0.831 ± 0.001
	R^2_{adj}	> 0.999	> 0.999	> 0.999	> 0.999	> 0.999	> 0.999	> 0.999	> 0.999	> 0.999	> 0.999
	RMSE	< 0.399	< 0.357	< 0.354	< 0.563	< 0.489	< 0.432	< 0.386	< 0.353	< 0.724	< 0.408
30	*τ0 (Pa)*	2.171 ± 0.062	2.385 ± 0.120	2.597 ± 0.065	2.607 ± 0.073	2.784 ± 0.171	2.672 ± 0.160	2.615 ± 0.079	2.891 ± 0.232	3.280 ± 0.063	3.458 ± 0.030
	k (Pa·s^n)	1.423 ± 0.015	1.491 ± 0.025	1.554 ± 0.011	1.737 ± 0.021	1.988 ± 0.059	1.878 ± 0.040	2.011 ± 0.026	2.193 ± 0.080	2.272 ± 0.034	2.440 ± 0.024
	n (−)	0.911 ± 0.002	0.909 ± 0.003	0.900 ± 0.001	0.896 ± 0.002	0.887 ± 0.006	0.859 ± 0.004	0.854 ± 0.003	0.845 ± 0.007	0.841 ± 0.003	0.829 ± 0.002
	R^2_{adj}	> 0.999	> 0.999	> 0.999	> 0.999	> 0.999	> 0.999	> 0.999	> 0.999	> 0.999	> 0.999
	RMSE	< 0.323	< 0.581	< 0.318	< 0.167	< 0.314	< 0.375	< 0.174	< 0.493	< 0.151	< 0.361
40	*τ0 (Pa)*	2.103 ± 0.095	2.160 ± 0.015	2.390 ± 0.042	2.547 ± 0.067	2.908 ± 0.115	2.543 ± 0.141	2.630 ± 0.078	2.933 ± 0.124	3.020 ± 0.104	3.379 ± 0.057
	k (Pa·s^n)	1.271 ± 0.033	1.248 ± 0.005	1.511 ± 0.017	1.597 ± 0.019	1.811 ± 0.028	1.638 ± 0.035	1.758 ± 0.023	1.792 ± 0.031	2.081 ± 0.035	2.245 ± 0.007
	n (−)	0.911 ± 0.005	0.908 ± 0.001	0.896 ± 0.003	0.896 ± 0.002	0.891 ± 0.003	0.859 ± 0.004	0.855 ± 0.002	0.849 ± 0.003	0.837 ± 0.003	0.831 ± 0.001
	R^2_{adj}	> 0.999	> 0.999	> 0.999	> 0.999	> 0.999	> 0.999	> 0.999	> 0.999	> 0.999	> 0.999
	RMSE	< 0.146	< 0.061	< 0.203	< 0.154	< 0.415	< 0.329	< 0.155	< 0.201	< 0.320	< 0.336
50	*τ0 (Pa)*	2.028 ± 0.109	2.156 ± 0.096	2.323 ± 0.038	2.463 ± 0.156	2.835 ± 0.070	2.376 ± 0.082	2.455 ± 0.068	2.812 ± 0.090	2.916 ± 0.075	3.117 ± 0.066
	k (Pa·s^n)	1.200 ± 0.033	1.155 ± 0.026	1.330 ± 0.013	1.478 ± 0.051	1.704 ± 0.018	1.328 ± 0.026	1.395 ± 0.024	1.535 ± 0.032	1.793 ± 0.020	1.926 ± 0.017
	n (−)	0.907 ± 0.006	0.906 ± 0.005	0.900 ± 0.002	0.896 ± 0.007	0.888 ± 0.002	0.855 ± 0.004	0.852 ± 0.003	0.849 ± 0.004	0.835 ± 0.002	0.833 ± 0.002
	R^2_{adj}	> 0.999	> 0.999	> 0.999	> 0.999	> 0.999	> 0.999	> 0.999	> 0.999	> 0.999	> 0.999
	RMSE	< 0.254	< 0.446	< 0.133	< 0.245	< 0.345	< 0.229	< 0.207	< 0.106	< 0.221	< 0.111
60	*τ0 (Pa)*	2.024 ± 0.044	2.283 ± 0.053	2.124 ± 0.122	2.664 ± 0.059	2.647 ± 0.044	2.370 ± 0.055	2.551 ± 0.066	2.848 ± 0.113	2.947 ± 0.095	3.205 ± 0.183
	k (Pa·s^n)	1.739 ± 0.024	1.169 ± 0.008	1.409 ± 0.042	1.494 ± 0.009	1.797 ± 0.013	1.470 ± 0.021	1.493 ± 0.020	1.625 ± 0.028	1.902 ± 0.032	2.105 ± 0.063
	n (−)	0.907 ± 0.003	0.905 ± 0.002	0.894 ± 0.006	0.897 ± 0.001	0.882 ± 0.002	0.855 ± 0.003	0.855 ± 0.002	0.849 ± 0.003	0.836 ± 0.003	0.828 ± 0.006
	R^2_{adj}	> 0.999	> 0.999	> 0.999	> 0.999	> 0.999	> 0.999	> 0.999	> 0.999	> 0.999	> 0.999
	RMSE	< 0.365	< 0.246	< 0.407	< 0.352	< 0.335	< 0.245	< 0.132	< 0.183	< 0.292	< 0.436

Table S2. Suspensions pretreated for 1 hour.

Temp. (°C)	Parameters	BSG concentration (2%)					BSG concentration (4%)				
		AHP concentration (X_{AHP})					AHP concentration (X_{AHP})				
		1	2	4	6	8	1	2	4	6	8
20	***τ0 (Pa)***	1.898 ± 0.055	1.784 ± 0.141	2.081 ± 0.046	2.258 ± 0.171	2.414 ± 0.088	1.905 ± 0.092	1.891 ± 0.115	2.200 ± 0.028	2.363 ± 0.191	2.601 ± 0.168
	k (Pa·s^n)	1.083 ± 0.012	1.219 ± 0.039	1.376 ± 0.022	1.415 ± 0.047	1.627 ± 0.034	1.219 ± 0.022	1.318 ± 0.035	1.417 ± 0.008	1.618 ± 0.051	1.800 ± 0.044
	n (−)	0.959 ± 0.002	0.950 ± 0.006	0.949 ± 0.004	0.946 ± 0.006	0.941 ± 0.005	0.968 ± 0.003	0.961 ± 0.006	0.965 ± 0.001	0.955 ± 0.007	0.952 ± 0.005
	R^2_{adj}	> 0.999	> 0.999	> 0.999	> 0.999	> 0.999	> 0.999	> 0.999	> 0.999	> 0.999	> 0.999
	RMSE	< 0.281	< 0.468	< 0.171	< 0.299	< 0.429	< 0.191	< 0.554	< 0.426	< 0.661	< 0.435
30	***τ0 (Pa)***	1.782 ± 0.036	1.753 ± 0.140	2.067 ± 0.117	2.242 ± 0.074	2.509 ± 0.057	1.858 ± 0.038	1.851 ± 0.067	2.146 ± 0.026	2.294 ± 0.061	2.599 ± 0.101
	k (Pa·s^n)	0.983 ± 0.017	1.100 ± 0.039	1.165 ± 0.023	1.276 ± 0.021	1.417 ± 0.015	1.085 ± 0.016	1.152 ± 0.024	1.284 ± 0.007	1.472 ± 0.004	1.608 ± 0.027
	n (−)	0.954 ± 0.004	0.950 ± 0.007	0.951 ± 0.003	0.948 ± 0.003	0.945 ± 0.002	0.968 ± 0.003	0.969 ± 0.004	0.966 ± 0.001	0.954 ± 0.001	0.952 ± 0.004
	R^2_{adj}	> 0.999	> 0.999	> 0.999	> 0.999	> 0.999	> 0.999	> 0.999	> 0.999	> 0.999	> 0.999
	RMSE	< 0.205	< 0.520	< 0.340	< 0.349	< 0.365	< 0.311	< 0.352	< 0.389	< 0.385	< 0.449
40	***τ0 (Pa)***	1.703 ± 0.070	1.743 ± 0.047	1.959 ± 0.115	2.129 ± 0.087	2.509 ± 0.057	1.824 ± 0.160	2.012 ± 0.039	2.146 ± 0.026	2.290 ± 0.058	2.555 ± 0.051
	k (Pa·s^n)	0.925 ± 0.025	1.001 ± 0.009	1.118 ± 0.030	1.278 ± 0.036	1.417 ± 0.015	1.018 ± 0.031	0.993 ± 0.016	1.284 ± 0.007	1.395 ± 0.004	1.652 ± 0.024
	n (−)	0.951 ± 0.006	0.952 ± 0.002	0.948 ± 0.005	0.943 ± 0.006	0.945 ± 0.002	0.963 ± 0.006	0.969 ± 0.003	0.966 ± 0.001	0.955 ± 0.001	0.954 ± 0.003
	R^2_{adj}	> 0.999	> 0.999	> 0.999	> 0.999	> 0.999	> 0.999	> 0.999	> 0.999	> 0.999	> 0.999
	RMSE	< 0.440	< 0.105	< 0.239	< 0.326	< 0.365	< 0.312	< 0.272	< 0.389	< 0.367	< 0.469
50	***τ0 (Pa)***	1.755 ± 0.015	1.807 ± 0.084	1.958 ± 0.164	2.268 ± 0.108	2.342 ± 0.171	1.897 ± 0.016	1.960 ± 0.048	2.149 ± 0.108	2.374 ± 0.051	2.567 ± 0.052
	k (Pa·s^n)	0.904 ± 0.008	1.001 ± 0.027	1.116 ± 0.049	1.174 ± 0.017	1.416 ± 0.049	0.947 ± 0.008	1.009 ± 0.022	1.211 ± 0.031	1.369 ± 0.020	1.536 ± 0.023
	n (−)	0.958 ± 0.002	0.952 ± 0.005	0.944 ± 0.009	0.947 ± 0.003	0.953 ± 0.007	0.969 ± 0.002	0.961 ± 0.005	0.958 ± 0.005	0.956 ± 0.003	0.954 ± 0.004
	R^2_{adj}	> 0.999	> 0.999	> 0.999	> 0.999	> 0.999	> 0.999	> 0.999	> 0.999	> 0.999	> 0.999
	RMSE	< 0.264	< 0.175	< 0.418	< 0.338	< 0.346	< 0.289	< 0.283	< 0.353	< 0.394	< 0.739
60	***τ0 (Pa)***	1.876 ± 0.091	1.854 ± 0.168	2.193 ± 0.123	2.295 ± 0.137	2.454 ± 0.085	1.996 ± 0.017	2.017 ± 0.087	2.368 ± 0.107	2.494 ± 0.053	2.532 ± 0.147
	k (Pa·s^n)	0.954 ± 0.021	1.071 ± 0.045	1.140 ± 0.024	1.245 ± 0.040	1.484 ± 0.032	1.000 ± 0.008	1.018 ± 0.028	1.248 ± 0.028	1.424 ± 0.021	1.601 ± 0.038
	n (−)	0.957 ± 0.004	0.949 ± 0.008	0.948 ± 0.004	0.954 ± 0.006	0.943 ± 0.005	0.968 ± 0.002	0.959 ± 0.006	0.961 ± 0.005	0.953 ± 0.003	0.952 ± 0.005
	R^2_{adj}	> 0.999	> 0.999	> 0.999	> 0.999	> 0.999	> 0.999	> 0.999	> 0.999	> 0.999	> 0.999
	RMSE	< 0.171	< 0.411	< 0.329	< 0.275	< 0.401	< 0.304	< 0.505	< 0.227	< 0.404	< 0.388

Table S2. Suspensions pretreated for 1 hour (continuation).

Temp. (°C)	Parameters	BSG concentration (6%)					BSG concentration (8%)				
		AHP concentration (X_{AHP})					AHP concentration (X_{AHP})				
		1	2	4	6	8	1	2	4	6	8
20	$\tau 0$ (Pa)	2.843 ± 0.202	2.926 ± 0.135	3.014 ± 0.131	3.331 ± 0.137	3.274 ± 0.076	3.207 ± 0.068	3.744 ± 0.097	3.919 ± 0.079	3.923 ± 0.231	4.376 ± 0.131
	k (Pa·s^n)	1.868 ± 0.043	1.956 ± 0.039	2.185 ± 0.040	2.322 ± 0.021	2.486 ± 0.015	2.573 ± 0.024	2.588 ± 0.018	2.842 ± 0.023	3.014 ± 0.063	3.156 ± 0.041
	n (−)	0.908 ± 0.005	0.904 ± 0.004	0.903 ± 0.004	0.896 ± 0.001	0.889 ± 0.001	0.859 ± 0.002	0.864 ± 0.001	0.846 ± 0.001	0.839 ± 0.004	0.842 ± 0.002
	R^2_{adj}	> 0.999	> 0.999	> 0.999	> 0.999	> 0.999	> 0.999	> 0.999	> 0.999	> 0.999	> 0.999
	RMSE	< 0.465	< 0.427	< 0.414	< 0.851	< 0.502	< 0.353	< 0.303	< 0.239	< 0.554	< 0.246
30	$\tau 0$ (Pa)	2.530 ± 0.179	2.631 ± 0.082	2.607 ± 0.245	3.015 ± 0.058	3.119 ± 0.040	2.205 ± 1.796	3.268 ± 0.177	3.323 ± 0.214	3.404 ± 0.164	4.000 ± 0.394
	k (Pa·s^n)	1.657 ± 0.038	1.778 ± 0.024	1.948 ± 0.073	2.105 ± 0.030	2.486 ± 0.022	1.447 ± 1.233	3.045 ± 0.052	2.555 ± 0.078	2.759 ± 0.070	2.899 ± 0.148
	n (−)	0.907 ± 0.005	0.902 ± 0.003	0.903 ± 0.007	0.896 ± 0.003	0.886 ± 0.002	0.574 ± 0.496	0.853 ± 0.003	0.840 ± 0.006	0.833 ± 0.005	0.843 ± 0.010
	R^2_{adj}	> 0.999	> 0.999	> 0.999	> 0.999	> 0.999	> 0.999	> 0.999	> 0.999	> 0.999	> 0.999
	RMSE	< 0.411	< 0.195	< 0.598	< 0.172	< 0.474	< 0.379	< 0.450	< 0.562	< 0.586	< 0.645
40	$\tau 0$ (Pa)	2.530 ± 0.179	2.623 ± 0.078	2.804 ± 0.133	2.798 ± 0.117	3.177 ± 0.074	3.075 ± 0.122	3.151 ± 0.120	3.411 ± 0.100	3.660 ± 0.052	3.965 ± 0.214
	k (Pa·s^n)	1.657 ± 0.038	1.495 ± 0.021	1.731 ± 0.030	1.970 ± 0.034	2.148 ± 0.009	1.882 ± 0.047	2.053 ± 0.035	2.202 ± 0.035	2.395 ± 0.023	2.688 ± 0.071
	n (−)	0.907 ± 0.005	0.906 ± 0.003	0.899 ± 0.003	0.892 ± 0.003	0.887 ± 0.001	0.860 ± 0.005	0.853 ± 0.003	0.846 ± 0.003	0.841 ± 0.002	0.841 ± 0.006
	R^2_{adj}	> 0.999	> 0.999	> 0.999	> 0.999	> 0.999	> 0.999	> 0.999	> 0.999	> 0.999	> 0.999
	RMSE	< 0.411	< 0.171	< 0.230	< 0.387	< 0.414	< 0.170	< 0.305	< 0.643	< 0.383	< 0.502
50	$\tau 0$ (Pa)	2.535 ± 0.105	2.602 ± 0.083	2.817 ± 0.097	2.747 ± 0.088	3.058 ± 0.209	2.929 ± 0.077	3.120 ± 0.047	3.259 ± 0.146	3.423 ± 0.085	3.844 ± 0.11
	k (Pa·s^n)	1.339 ± 0.028	1.397 ± 0.025	1.571 ± 0.031	1.820 ± 0.021	2.073 ± 0.063	1.466 ± 0.033	1.626 ± 0.013	1.821 ± 0.039	1.962 ± 0.026	2.329 ± 0.033
	n (−)	0.903 ± 0.004	0.903 ± 0.004	0.899 ± 0.004	0.888 ± 0.002	0.884 ± 0.006	0.859 ± 0.005	0.853 ± 0.001	0.846 ± 0.004	0.842 ± 0.002	0.834 ± 0.003
	R^2_{adj}	> 0.999	> 0.999	> 0.999	> 0.999	> 0.999	> 0.999	> 0.999	> 0.999	> 0.999	> 0.999
	RMSE	< 0.301	< 0.266	< 0.127	< 0.290	< 0.570	< 0.244	< 0.143	< 0.350	< 0.156	< 0.361
60	$\tau 0$ (Pa)	2.443 ± 0.070	2.605 ± 0.073	2.781 ± 0.125	2.870 ± 0.110	3.260 ± 0.081	2.961 ± 0.084	3.169 ± 0.054	3.286 ± 0.078	3.418 ± 0.090	3.790 ± 0.22
	k (Pa·s^n)	1.398 ± 0.021	1.392 ± 0.019	1.622 ± 0.028	1.856 ± 0.032	2.086 ± 0.019	1.600 ± 0.036	1.763 ± 0.015	1.993 ± 0.032	2.102 ± 0.028	2.476 ± 0.078
	n (−)	0.906 ± 0.003	0.906 ± 0.003	0.899 ± 0.003	0.889 ± 0.003	0.889 ± 0.002	0.859 ± 0.005	0.857 ± 0.002	0.846 ± 0.003	0.842 ± 0.002	0.831 ± 0.006
	R^2_{adj}	> 0.999	> 0.999	> 0.999	> 0.999	> 0.999	> 0.999	> 0.999	> 0.999	> 0.999	> 0.999
	RMSE	< 0.300	< 0.159	< 0.216	< 0.361	< 0.159	< 0.265	< 0.542	< 0.137	< 0.166	< 0.298

Table S3. Suspensions processed for 4 hours.

Temp. (°C)	Parameters	BSG concentration (2%)					BSG concentration (4%)				
		AHP concentration (X_{AHP})					AHP concentration (X_{AHP})				
		1	2	4	6	8	1	2	4	6	8
20	***τ0 (Pa)***	1.933 ± 0.065	2.054 ± 0.015	2.173 ± 0.074	2.361 ± 0.057	2.467 ± 0.203	2.030 ± 0.130	2.059 ± 0.194	2.114 ± 0.197	2.427 ± 0.254	2.666 ± 0.229
	k (Pa·s^n)	1.316 ± 0.009	1.423 ± 0.012	1.417 ± 0.017	1.596 ± 0.016	1.820 ± 0.058	1.339 ± 0.032	1.484 ± 0.052	1.213 ± 0.051	1.701 ± 0.075	1.856 ± 0.062
	n (−)	0.948 ± 0.001	0.947 ± 0.002	0.940 ± 0.002	0.935 ±0.003	0.933 ± 0.006	0.968 ± 0.005	0.962 ± 0.007	0.963 ± 0.008	0.952 ± 0.009	0.953 ± 0.006
	R^2_{adj}	> 0.999	> 0.999	> 0.999	> 0.999	> 0.999	> 0.999	> 0.999	> 0.999	> 0.999	> 0.999
	RMSE	< 0.323	< 0.368	< 0.348	< 0.702	< 0.360	< 0.351	< 0.740	< 0.500	< 0.661	< 0.405
30	***τ0 (Pa)***	1.894 ± 0.020	1.889 ± 0.099	2.061 ± 0.177	2.323 ± 0.102	2.497 ± 0.080	2.071 ± 0.016	2.136 ± 0.060	2.366 ± 0.140	2.367 ± 0.235	2.678 ± 0.107
	k (Pa·s^n)	1.102 ± 0.010	1.232 ± 0.034	1.319 ± 0.035	1.394 ± 0.027	1.602 ± 0.020	1.200 ± 0.007	1.229 ± 0.012	1.339 ± 0.027	1.565 ± 0.069	1.812 ± 0.029
	n (−)	0.950 ± 0.002	0.945 ± 0.006	0.938 ± 0.006	0.937 ± 0.004	0.935 ± 0.003	0.971 ± 0.002	0.966 ± 0.002	0.964 ± 0.003	0.953 ± 0.009	0.955 ± 0.003
	R^2_{adj}	> 0.999	> 0.999	> 0.999	> 0.999	> 0.999	> 0.999	> 0.999	> 0.999	> 0.999	> 0.999
	RMSE	< 0.290	< 0.567	< 0.590	< 0.135	< 0.409	< 0.164	< 0.139	< 0.412	< 0.612	< 0.512
40	***τ0 (Pa)***	1.759 ± 0.070	1.967 ± 0.041	2.125 ± 0.036	2.286 ± 0.095	2.382 ± 0.23 1	2.068 ± 0.108	2.012 ± 0.098	2.235 ± 0.140	2.364 ± 0.224	2.679 ± 0.141
	k (Pa·s^n)	1.065 ± 0.024	1.218 ± 0.022	1.263 ± 0.100	1.408 ± 0.031	1.711 ± 0.072	1.123 ± 0.024	1.153 ± 0.031	1.329 ± 0.036	1.491 ± 0.066	1.670 ± 0.045
	n (−)	0.944 ± 0.005	0.946 ± 0.004	0.942 ± 0.002	0.934 ± 0.005	0.931 ± 0.008	0.970 ± 0.004	0.967 ± 0.005	0.962 ± 0.005	0.954 ± 0.009	0.956 ± 0.005
	R^2_{adj}	> 0.999	> 0.999	> 0.999	> 0.999	> 0.999	> 0.999	> 0.999	> 0.999	> 0.999	> 0.999
	RMSE	< 0.414	< 0.335	< 0.342	< 0.226	< 0.597	< 0.213	< 0.216	< 0.305	< 0.586	< 0.239
50	***τ0 (Pa)***	1.824 ± 0.047	1.982 ± 0.036	2.119 ± 0.143	2.143 ± 0.190	2.706 ± 0.085	2.025 ± 0.059	1.953 ± 0.189	2.297 ± 0.131	2.399 ± 0.223	2.772 ± 0.189
	k (Pa·s^n)	1.084 ± 0.021	1.070 ± 0.019	1.279 ± 0.040	1.408 ± 0.060	1.662 ± 0.009	1.126 ± 0.007	1.164 ± 0.049	1.243 ± 0.034	1.478 ± 0.065	1.675 ± 0.048
	n (−)	0.945 ± 0.004	0.943 ± 0.004	0.939 ± 0.006	0.931 ± 0.008	0.938 ± 0.001	0.966 ± 0.001	0.963 ± 0.008	0.958 ± 0.005	0.955 ± 0.009	0.953 ± 0.006
	R^2_{adj}	> 0.999	> 0.999	> 0.999	> 0.999	> 0.999	> 0.999	> 0.999	> 0.999	> 0.999	> 0.999
	RMSE	< 0.296	< 0.291	< 0.465	< 0.493	< 0.459	< 0.312	< 0.479	< 0.280	< 0.584	< 0.491
60	***τ0 (Pa)***	1.987 ± 0.096	2.145 ± 0.095	2.216 ± 0.101	2.455 ± 0.106	2.753 ± 0.217	2.033 ± 0.157	2.114 ± 0.197	2.418 ± 0.137	2.697 ± 0.167	2.773 ± 0.190
	k (Pa·s^n)	1.131 ± 0.019	1.136 ± 0.024	1.187 ± 0.025	1.424 ± 0.022	1.723 ± 0.064	1.200 ± 0.043	1.213 ± 0.051	1.305 ± 0.036	1.499 ± 0.032	1.736 ± 0.056
	n (−)	0.946 ± 0.003	0.944 ± 0.004	0.941 ± 0.004	0.936 ± 0.003	0.936 ± 0.007	0.961 ± 0.007	0.963 ± 0.008	0.958 ± 0.005	0.958 ± 0.004	0.953 ± 0.006
	R^2_{adj}	> 0.999	> 0.999	> 0.999	> 0.999	> 0.999	> 0.999	> 0.999	> 0.999	> 0.999	> 0.999
	RMSE	< 0.275	< 0.275	< 0.197	< 0.391	< 0.348	< 0.597	< 0.500	< 0.293	< 0.450	< 0.381

Table S3. Suspensions processed for 4 hours (continuation).

Temp. (°C)	Parameters	BSG concentration (6%)					BSG concentration (8%)				
		AHP concentration (X_{AHP})					AHP concentration (X_{AHP})				
		1	2	4	6	8	1	2	4	6	8
20	*τ0 (Pa)*	2.676 ± 0.310	2.917 ± 0.137	3.281 ± 0.166	3.169 ± 0.067	3.372 ± 0.320	3.336 ± 0.068	3.682 ± 0.026	3.808 ± 0.159	3.979 ± 0.111	4.404 ± 0.076
	k (Pa·s^n)	2.003 ± 0.094	2.016 ± 0.025	2.078 ± 0.035	2.374 ± 0.034	2.691 ± 0.099	2.562 ± 0.024	2.565 ± 0.023	2.890 ± 0.052	3.062 ± 0.027	3.328 ± 0.023
	n (−)	0.908 ± 0.009	0.911 ± 0.003	0.904 ± 0.003	0.893 ± 0.004	0.885 ± 0.007	0.860 ± 0.002	0.860 ± 0.002	0.845 ± 0.004	0.840 ± 0.002	0.837 ± 0.001
	R^2_{adj}	> 0.999	> 0.999	> 0.999	> 0.999	> 0.999	> 0.999	> 0.999	> 0.999	> 0.999	> 0.999
	RMSE	< 0.620	< 0.499	< 0.790	< 0.856	< 0.742	< 0.228	< 0.292	< 0.379	< 0.595	< 384
30	*τ0 (Pa)*	2.557 ± 0.274	2.611 ± 0.034	3.200 ± 0.150	3.008 ± 0.091	3.444 ± 0.124	2.718 ± 0.809	3.357 ± 0.022	3.556 ± 0.136	3.604 ± 0.094	4.065 ± 0.217
	k (Pa·s^n)	1.758 ± 0.080	1.523 ± 0.010	1.870 ± 0.032	2.135 ± 0.016	2.374 ± 0.040	1.835 ± 0.653	2.679 ± 0.011	2.541 ± 0.049	2.775 ± 0.040	3.013 ± 0.079
	n (−)	0.910 ± 0.009	0.910 ± 0.001	0.904 ± 0.003	0.893 ± 0.002	0.891 ± 0.003	0.717 ± 0.245	0.854 ± 0.001	0.845 ± 0.004	0.837 ± 0.003	0.837 ± 0.005
	R^2_{adj}	> 0.999	> 0.999	> 0.999	> 0.999	> 0.999	> 0.999	> 0.999	> 0.999	> 0.999	> 0.999
	RMSE	< 0.551	< 0.075	< 0.713	< 0.423	< 0.184	< 0.460	< 0.454	< 0.341	< 0.340	< 0.411
40	*τ0 (Pa)*	2.631 ± 0.049	2.611 ± 0.034	2.935 ± 0.145	2.923 ± 0.049	3.438 ± 0.116	3.153 ± 0.082	3.209 ± 0.065	3.347 ± 0.148	3.732 ± 0.094	3.976 ± 0.143
	k (Pa·s^n)	1.528 ± 0.016	1.523 ± 0.010	1.812 ± 0.030	1.984 ± 0.018	2.201 ± 0.037	1.889 ± 0.034	2.048 ± 0.019	2.255 ± 0.056	2.453 ± 0.038	2.745 ± 0.051
	n (−)	0.915 ± 0.002	0.910 ± 0.001	0.904 ± 0.003	0.892 ± 0.002	0.889 ± 0.003	0.862 ± 0.003	0.853 ± 0.002	0.846 ± 0.005	0.840 ± 0.003	0.837 ± 0.004
	R^2_{adj}	> 0.999	> 0.999	> 0.999	> 0.999	> 0.999	> 0.999	> 0.999	> 0.999	> 0.999	> 0.999
	RMSE	< 0.135	< 0.075	< 0.690	< 0.261	< 0.170	< 0.133	< 0.327	< 0.499	< 0.409	< 0.355
50	*τ0 (Pa)*	2.661 ± 0.036	2.599 ± 0.115	2.697 ± 0.058	2.981 ± 0.059	3.311 ± 0.346	3.011 ± 0.110	3.172 ± 0.048	3.230 ± 0.103	3.427 ± 0.082	3.766 ± 0.024
	k (Pa·s^n)	1.414 ± 0.008	1.412 ± 0.024	1.638 ± 0.022	1.971 ± 0.008	2.126 ± 0.109	1.657 ± 0.048	1.798 ± 0.014	2.044 ± 0.024	2.207 ± 0.020	2.548 ± 0.014
	n (−)	0.911 ± 0.001	0.906 ± 0.003	0.898 ± 0.003	0.892 ± 0.001	0.886 ± 0.010	0.860 ± 0.006	0.856 ± 0.002	0.846 ± 0.002	0.840 ± 0.002	0.829 ± 0.001
	R^2_{adj}	> 0.999	> 0.999	> 0.999	> 0.999	> 0.999	> 0.999	> 0.999	> 0.999	> 0.999	> 0.999
	RMSE	< 0.354	< 0.544	< 0.222	< 0.387	< 0.591	< 0.275	< 0.295	< 0.219	< 0.216	< 0.349
60	*τ0 (Pa)*	2.617 ± 0.094	2.797 ± 0.117	2.699 ± 0.048	2.801 ± 0.205	3.442 ± 0.038	2.995 ± 0.107	3.091 ± 0.032	3.229 ± 0.093	3.428 ± 0.025	3.894 ± 0.084
	k (Pa·s^n)	1.368 ± 0.017	1.424 ± 0.024	1.640 ± 0.023	1.855 ± 0.060	2.033 ± 0.015	1.590 ± 0.046	1.666 ± 0.011	1.873 ± 0.026	2.069 ± 0.017	2.369 ± 0.028
	n (−)	0.911 ± 0.003	0.907 ± 0.003	0.899 ± 0.004	0.893 ± 0.006	0.892 ± 0.001	0.860 ± 0.006	0.853 ± 0.001	0.847 ± 0.003	0.841 ± 0.002	0.833 ± 0.003
	R^2_{adj}	> 0.999	> 0.999	> 0.999	> 0.999	> 0.999	> 0.999	> 0.999	> 0.999	> 0.999	> 0.999
	RMSE	< 0.342	< 0.552	< 0.611	< 0.535	< 0.194	< 0.264	< 0.146	< 0.200	< 0.360	< 0.221

Table S4. Suspensions processed for 6 hours.

Temp. (°C)	Parameters	BSG concentration (2%)					BSG concentration (4%)				
		AHP concentration (X_{AHP})					AHP concentration (X_{AHP})				
		1	2	4	6	8	1	2	4	4	6	1
20	*τ0 (Pa)*	1.992 ± 0.103	2.005 ± 0.023	2.257 ± 0.040	2.426 ± 0.061	2.723 ± 0.060	2.055 ± 0.050	2.140 ± 0.072	2.404 ± 0.053	2.593 ± 0.035	2.913 ± 0.065
	k (Pa·s^n)	1.349 ± 0.035	1.407 ± 0.009	1.505 ± 0.015	1.690 ± 0.022	1.916 ± 0.018	1.482 ± 0.025	1.605 ± 0.016	1.577 ± 0.010	1.781 ± 0.010	2.007 ± 0.034
	n (−)	0.945 ± 0.006	0.941 ± 0.001	0.940 ± 0.002	0.937 ± 0.002	0.931 ± 0.002	0.965 ± 0.004	0.963 ± 0.002	0.961 ± 0.001	0.958 ± 0.001	0.951 ± 0.004
	R^2_{adj}	> 0.999	> 0.999	> 0.999	> 0.999	> 0.999	> 0.999	> 0.999	> 0.999	> 0.999	> 0.999
	RMSE	< 0.362	< 0.192	< 0.377	< 0.749	< 0.359	< 0.441	< 0.246	< 0.173	< 0.870	< 0.250
30	*τ0 (Pa)*	1.908 ± 0.073	1.896 ± 0.049	2.090 ± 0.105	2.402 ± 0.023	2.514 ± 0.150	1.934 ± 0.077	1.992 ± 0.063	2.309 ± 0.062	2.621 ± 0.029	2.562 ± 0.177
	k (Pa·s^n)	1.217 ± 0.026	1.315 ± 0.012	1.419 ± 0.035	1.563 ± 0.009	1.836 ± 0.042	1.267 ± 0.021	1.371 ± 0.013	1.469 ± 0.021	1.630 ± 0.007	1.859 ± 0.051
	n (−)	0.947 ± 0.004	0.944 ± 0.002	0.937 ± 0.005	0.938 ± 0.001	0.931 ± 0.005	0.965 ± 0.003	0.967 ± 0.002	0.961 ± 0.003	0.960 ± 0.001	0.946 ± 0.006
	R^2_{adj}	> 0.999	> 0.999	> 0.999	> 0.999	> 0.999	> 0.999	> 0.999	> 0.999	> 0.999	> 0.999
	RMSE	< 0.166	< 0.336	< 0.533	< 0.413	< 0.670	< 0.327	< 0.215	< 0.268	< 0.124	< 0.700
40	*τ0 (Pa)*	1.997 ± 0.095	1.961 ± 0.116	2.169 ± 0.028	2.393 ± 0.137	2.457 ± 0.189	2.072 ± 0.050	2.155 ± 0.105	2.284 ± 0.066	2.548 ± 0.134	2.829 ± 0.092
	k (Pa·s^n)	1.134 ± 0.015	1.153 ± 0.031	1.377 ± 0.023	1.502 ± 0.032	1.786 ± 0.064	1.155 ± 0.011	1.208 ± 0.026	1.432 ± 0.015	1.566 ± 0.027	1.859 ± 0.019
	n (−)	0.949 ± 0.002	0.941 ± 0.005	0.940 ± 0.003	0.936 ± 0.004	0.929 ± 0.007	0.969 ± 0.002	0.969 ± 0.004	0.963 ± 0.003	0.959 ± 0.003	0.954 ± 0.002
	R^2_{adj}	> 0.999	> 0.999	> 0.999	> 0.999	> 0.999	> 0.999	> 0.999	> 0.999	> 0.999	> 0.999
	RMSE	< 0.328	< 0.265	< 0.533	< 0.243	< 0.616	< 0.114	< 0.350	< 0.391	< 0.420	< 0.196
50	*τ0 (Pa)*	1.908 ± 0.149	2.090 ± 0.081	2.258 ± 0.166	2.371 ± 0.058	2.715 ± 0.054	2.073 ± 0.155	2.122 ± 0.055	2.418 ± 0.140	2.605 ± 0.132	2.761 ± 0.081
	k (Pa·s^n)	1.151 ± 0.044	1.125 ± 0.032	1.287 ± 0.038	1.508 ± 0.016	1.736 ± 0.018	1.222 ± 0.043	1.206 ± 0.006	1.328 ± 0.024	1.540 ± 0.026	1.897 ± 0.013
	n (−)	0.945 ± 0.007	0.944 ± 0.005	0.939 ± 0.006	0.934 ± 0.002	0.933 ± 0.003	0.966 ± 0.007	0.968 ± 0.001	0.965 ± 0.004	0.958 ± 0.003	0.950 ± 0.001
	R^2_{adj}	> 0.999	> 0.999	> 0.999	> 0.999	> 0.999	> 0.999	> 0.999	> 0.999	> 0.999	> 0.999
	RMSE	< 0.270	< 0.306	< 0.303	< 0.391	< 0.200	< 0.348	< 0.338	< 0.368	< 0.411	< 0.486
60	*τ0 (Pa)*	2.062 ± 0.065	2.130 ± 0.069	2.338 ± 0.049	2.550 ± 0.043	2.686 ± 0.123	2.204 ± 0.065	2.263 ± 0.027	2.505 ± 0.030	2.817 ± 0.096	2.659 ± 0.258
	k (Pa·s^n)	1.181 ± 0.025	1.194 ± 0.018	1.334 ± 0.017	1.541 ± 0.010	1.682 ± 0.033	1.278 ± 0.025	1.287 ± 0.018	1.401 ± 0.004	1.582 ± 0.028	1.983 ± 0.066
	n (−)	0.946 ± 0.005	0.941 ± 0.003	0.941 ± 0.002	0.936 ± 0.002	0.938 ± 0.004	0.969 ± 0.004	0.963 ± 0.003	0.959 ± 0.001	0.958 ± 0.004	0.946 ± 0.006
	R^2_{adj}	> 0.999	> 0.999	> 0.999	> 0.999	> 0.999	> 0.999	> 0.999	> 0.999	> 0.999	> 0.999
	RMSE	< 0.320	< 0.301	< 0.605	< 0.683	< 0.164	< 0.389	< 0.646	< 0.182	< 0.259	< 0.747

Table S4. Suspensions processed for 6 hours (continuation).

Temp. (°C)	Parameters	BSG concentration (6%)					BSG concentration (8%)				
		AHP concentration (X_{AHP})					AHP concentration (X_{AHP})				
		1	2	4	6	8	1	2	4	6	8
20	$\tau 0$ (Pa)	3.124 ± 0.078	2.957 ± 0.058	2.642 ± 0.023	2.672 ± 0.064	2.689 ± 0.088	3.465 ± 0.111	3.620 ± 0.128	3.696 ± 0.333	4.035 ± 0.210	4.432 ± 0.108
	k (Pa·s^n)	1.911 ± 0.011	2.142 ± 0.023	1.491 ± 0.010	1.481 ± 0.024	1.485 ± 0.026	2.550 ± 0.036	2.541 ± 0.061	2.937 ± 0.111	3.110 ± 0.052	3.500 ± 0.021
	n (−)	0.913 ± 0.001	0.906 ± 0.003	0.907 ± 0.001	0.908 ± 0.003	0.907 ± 0.004	0.860 ± 0.003	0.855 ± 0.005	0.844 ± 0.008	0.841 ± 0.003	0.832 ± 0.001
	R^2_{adj}	> 0.999	> 0.999	> 0.999	> 0.999	> 0.999	> 0.999	> 0.999	> 0.999	> 0.999	> 0.999
	RMSE	< 0.479	< 0.300	< 0.576	< 0.128	< 0.154	< 0.228	< 0.281	< 0.657	< 0.881	< 0.522
30	$\tau 0$ (Pa)	2.888 ± 0.217	2.693 ± 0.051	2.642 ± 0.023	2.689 ± 0.088	2.672 ± 0.064	3.232 ± 0.324	3.445 ± 0.193	3.789 ± 0.145	3.804 ± 0.033	4.131 ± 0.097
	k (Pa·s^n)	1.742 ± 0.054	1.894 ± 0.020	1.491 ± 0.010	1.485 ± 0.026	1.481 ± 0.024	2.223 ± 0.108	2.313 ± 0.033	2.528 ± 0.045	2.792 ± 0.011	3.128 ± 0.019
	n (−)	0.908 ± 0.006	0.906 ± 0.003	0.907 ± 0.001	0.907 ± 0.004	0.908 ± 0.003	0.860 ± 0.009	0.856 ± 0.003	0.850 ± 0.003	0.841 ± 0.001	0.831 ± 0.001
	R^2_{adj}	> 0.999	> 0.999	> 0.999	> 0.999	> 0.999	> 0.999	> 0.999	> 0.999	> 0.999	> 0.999
	RMSE	< 0.427	< 0.265	< 0.576	< 0.154	< 0.128	< 0.540	< 0.458	< 0.260	< 0.098	< 0.465
40	$\tau 0$ (Pa)	2.688 ± 0.129	2.624 ± 0.043	2.667 ± 0.022	2.689 ± 0.088	2.627 ± 0.251	3.231 ± 0.043	3.266 ± 0.061	3.284 ± 0.196	3.803 ± 0.183	3.987 ± 0.075
	k (Pa·s^n)	1.583 ± 0.041	1.611 ± 0.017	1.484 ± 0.005	1.485 ± 0.026	1.510 ± 0.064	1.896 ± 0.021	2.042 ± 0.016	2.308 ± 0.081	2.511 ± 0.058	2.802 ± 0.031
	n (−)	0.906 ± 0.005	0.906 ± 0.003	0.907 ± 0.001	0.907 ± 0.004	0.904 ± 0.008	0.864 ± 0.002	0.854 ± 0.002	0.846 ± 0.007	0.839 ± 0.005	0.832 ± 0.003
	R^2_{adj}	> 0.999	> 0.999	> 0.999	> 0.999	> 0.999	> 0.999	> 0.999	> 0.999	> 0.999	> 0.999
	RMSE	< 0.005	< 0.226	< 0.576	< 0.154	< 0.460	< 0.163	< 0.349	< 0.397	< 0.709	< 0.279
50	$\tau 0$ (Pa)	2.688 ± 0.129	2.683 ± 0.132	2.547 ± 0.169	2.689 ± 0.088	2.536 ± 0.189	3.061 ± 0.137	3.175 ± 0.056	3.173 ± 0.209	3.436 ± 0.075	3.741 ± 0.191
	k (Pa·s^n)	1.583 ± 0.041	1.484 ± 0.024	1.529 ± 0.049	1.485 ± 0.026	1.529 ± 0.055	1.714 ± 0.060	1.833 ± 0.014	2.095 ± 0.059	2.311 ± 0.013	2.619 ± 0.078
	n (−)	0.906 ± 0.005	0.907 ± 0.003	0.901 ± 0.006	0.907 ± 0.004	0.902 ± 0.007	0.860 ± 0.007	0.854 ± 0.002	0.846 ± 0.005	0.838 ± 0.001	0.827 ± 0.006
	R^2_{adj}	> 0.999	> 0.999	> 0.999	> 0.999	> 0.999	> 0.999	> 0.999	> 0.999	> 0.999	> 0.999
	RMSE	< 0.608	< 0.315	< 0.460	< 0.154	< 0.460	< 0.285	< 0.314	< 0.302	< 0.356	< 0.540
60	$\tau 0$ (Pa)	2.524 ± 0.064	2.716 ± 0.094	2.629 ± 0.094	2.689 ± 0.088	2.536 ± 0.189	3.061 ± 0.137	3.063 ± 0.035	3.198 ± 0.041	3.434 ± 0.062	3.944 ± 0.060
	k (Pa·s^n)	1.422 ± 0.016	1.484 ± 0.023	1.499 ± 0.026	1.485 ± 0.026	1.529 ± 0.055	1.714 ± 0.060	1.706 ± 0.013	1.925 ± 0.014	2.176 ± 0.034	2.408 ± 0.023
	n (−)	0.909 ± 0.002	0.907 ± 0.003	0.905 ± 0.004	0.907 ± 0.004	0.902 ± 0.007	0.860 ± 0.007	0.853 ± 0.002	0.848 ± 0.001	0.839 ± 0.004	0.832 ± 0.002
	R^2_{adj}	> 0.999	> 0.999	> 0.999	> 0.999	> 0.999	> 0.999	> 0.999	> 0.999	> 0.999	> 0.999
	RMSE	< 0.165	< 0.204	< 0.315	< 0.154	< 0.460	< 0.285	< 0.149	< 0.070	< 0.615	< 0.179

Table S5. Suspensions processed for 8 hours.

Temp. (°C)	Parameters	BSG concentration (2%)					BSG concentration (4%)				
		AHP concentration (X_{AHP})					AHP concentration (X_{AHP})				
		1	2	4	6	8	1	2	4	6	8
20	***τ0 (Pa)***	2.107 ± 0.125	1.974 ± 0.233	2.247 ± 0.075	2.577 ± 0.154	2.684 ± 0.174	2.338 ± 0.117	2.361 ± 0.152	2.554 ± 0.207	2.580 ± 0.291	2.722 ± 0.103
	k (Pa·s^n)	1.513 ± 0.040	1.603 ± 0.070	1.706 ± 0.023	1.736 ± 0.044	2.048 ± 0.047	1.470 ± 0.021	1.533 ± 0.031	1.643 ± 0.030	1.892 ± 0.077	2.117 ± 0.017
	n (−)	0.948 ± 0.005	0.942 ± 0.009	0.934 ± 0.003	0.934 ± 0.005	0.929 ± 0.005	0.970 ± 0.002	0.966 ± 0.004	0.964 ± 0.004	0.954 ± 0.008	0.951 ± 0.002
	R^2_{adj}	> 0.999	> 0.999	> 0.999	> 0.999	> 0.999	> 0.999	> 0.999	> 0.999	> 0.999	> 0.999
	RMSE	< 0.258	< 0.592	< 0.440	< 0.424	< 0.742	< 0.250	< 0.256	< 0.504	< 0.740	< 0.999
30	***τ0 (Pa)***	1.909 ± 0.218	2.013 ± 0.215	2.307 ± 0.044	2.444 ± 0.032	2.722 ± 0.037	2.284 ± 0.088	2.317 ± 0.056	2.491 ± 0.192	2.520 ± 0.271	2.714 ± 0.061
	k (Pa·s^n)	1.426 ± 0.060	1.471 ± 0.065	1.551 ± 0.003	1.611 ± 0.002	1.858 ± 0.016	1.331 ± 0.025	1.432 ± 0.015	1.521 ± 0.028	1.753 ± 0.071	1.976 ± 0.012
	n (−)	0.944 ± 0.008	0.943 ± 0.009	0.9373 ± 0.001	0.935 ± 0.003	0.933 ± 0.002	0.970 ± 0.003	0.969 ± 0.002	0.965 ± 0.004	0.955 ± 0.008	0.951 ± 0.002
	R^2_{adj}	> 0.999	> 0.999	> 0.999	> 0.999	> 0.999	> 0.999	> 0.999	> 0.999	> 0.999	> 0.999
	RMSE	< 0.532	< 0.546	< 0.401	< 0.225	< 0.482	< 0.135	< 0.141	< 0.469	< 0.690	< 0.294
40	***τ0 (Pa)***	2.057 ± 0.043	2.204 ± 0.106	2.204 ± 0.117	2.371 ± 0.097	2.700 ± 0.159	2.143 ± 0.227	2.071 ± 0.221	2.397 ± 0.168	2.544 ± 0.168	2.702 ± 0.015
	k (Pa·s^n)	1.314 ± 0.021	1.277 ± 0.020	1.502 ± 0.037	1.571 ± 0.034	1.821 ± 0.041	1.360 ± 0.060	1.273 ± 0.062	1.512 ± 0.049	1.679 ± 0.043	1.954 ± 0.018
	n (−)	0.949 ± 0.004	0.945 ± 0.003	0.938 ± 0.005	0.936 ± 0.005	0.933 ± 0.004	0.966 ± 0.009	0.966 ± 0.009	0.959 ± 0.006	0.956 ± 0.005	0.950 ± 0.002
	R^2_{adj}	> 0.999	> 0.999	> 0.999	> 0.999	> 0.999	> 0.999	> 0.999	> 0.999	> 0.999	> 0.999
	RMSE	< 0.163	< 0.364	< 0.339	< 0.693	< 0.469	< 0.692	< 0.647	< 0.341	< 0.480	< 0.545
50	***τ0 (Pa)***	2.143 ± 0.092	2.107 ± 0.131	2.312 ± 0.184	2.576 ± 0.016	2.755 ± 0.039	2.230 ± 0.025	2.218 ± 0.099	2.459 ± 0.157	2.751 ± 0.083	2.819 ± 0.116
	k (Pa·s^n)	1.173 ± 0.018	1.280 ± 0.036	1.483 ± 0.051	1.532 ± 0.007	1.804 ± 0.003	1.239 ± 0.012	1.252 ± 0.033	1.414 ± 0.046	1.619 ± 0.014	1.911 ± 0.017
	n (−)	0.949 ± 0.003	0.940 ± 0.005	0.938 ± 0.007	0.936 ± 0.001	0.933 ± 0.003	0.972 ± 0.002	0.965 ± 0.006	0.959 ± 0.006	0.961 ± 0.002	0.954 ± 0.002
	R^2_{adj}	> 0.999	> 0.999	> 0.999	> 0.999	> 0.999	> 0.999	> 0.999	> 0.999	> 0.999	> 0.999
	RMSE	< 0.340	< 0.263	< 0.561	< 0.356	< 0.411	< 0.137	< 0.358	< 0.320	< 0.267	< 0.500
60	***τ0 (Pa)***	2.254 ± 0.123	2.301 ± 0.053	2.467 ± 0.121	2.594 ± 0.067	2.712 ± 0.243	2.293 ± 0.011	2.360 ± 0.073	2.533 ± 0.044	2.720 ± 0.053	2.932 ± 0.055
	k (Pa·s^n)	1.222 ± 0.025	1.328 ± 0.015	1.587 ± 0.036	1.603 ± 0.028	1.901 ± 0.077	1.299 ± 0.006	1.302 ± 0.029	1.489 ± 0.024	1.714 ± 0.016	1.885 ± 0.020
	n (−)	0.951 ± 0.003	0.946 ± 0.003	0.942 ± 0.004	0.934 ± 0.004	0.931 ± 0.008	0.968 ± 0.001	0.964 ± 0.005	0.958 ± 0.004	0.955 ± 0.002	0.951 ± 0.003
	R^2_{adj}	> 0.999	> 0.999	> 0.999	> 0.999	> 0.999	> 0.999	> 0.999	> 0.999	> 0.999	> 0.999
	RMSE	< 0.357	< 0.360	< 0.428	< 0.305	< 0.819	< 0.394	< 0.241	< 0.429	< 0.303	< 0.327

Table S5. Suspensions processed for 8 hours (continuation).

Temp. (°C)	Parameters	BSG concentration (6%)					BSG concentration (8%)				
		AHP concentration (X_{AHP})					AHP concentration (X_{AHP})				
		1	2	4	6	8	1	2	4	6	8
20	***τ0 (Pa)***	2.739 ± 0.079	2.646 ± 0.187	2.715 ± 0.095	2.638 ± 0.067	2.588 ± 0.214	3.671 ± 0.106	3.795 ± 0.190	4.147 ± 0.214	4.167 ± 0.145	4.413 ± 0.285
	k (Pa·s^n)	1.467 ± 0.023	1.509 ± 0.045	1.481 ± 0.020	1.492 ± 0.010	1.512 ± 0.064	2.565 ± 0.032	2.716 ± 0.062	2.912 ± 0.042	3.194 ± 0.033	3.480 ± 0.097
	n (−)	0.909 ± 0.003	0.904 ± 0.006	0.908 ± 0.002	0.906 ± 0.002	0.904 ± 0.008	0.862 ± 0.002	0.855 ± 0.005	0.847 ± 0.003	0.839 ± 0.002	0.832 ± 0.005
	R^2_{adj}	> 0.999	> 0.999	> 0.999	> 0.999	> 0.999	> 0.999	> 0.999	> 0.999	> 0.999	> 0.999
	RMSE	< 0.331	< 0.363	< 0.204	< 0.315	< 0.460	< 0.216	< 0.407	< 0.851	< 0.851	< 0.418
30	***τ0 (Pa)***	2.739 ± 0.079	2.646 ± 0.187	2.726 ± 0.087	2.537 ± 0.158	2.713 ± 0.046	3.315 ± 0.331	3.628 ± 0.159	3.898 ± 0.027	4.086 ± 0.158	4.314 ± 0.135
	k (Pa·s^n)	1.467 ± 0.023	1.509 ± 0.045	1.478 ± 0.019	1.535 ± 0.042	1.472 ± 0.019	2.259 ± 0.116	2.282 ± 0.052	2.620 ± 0.015	2.830 ± 0.061	3.077 ± 0.047
	n (−)	0.909 ± 0.003	0.904 ± 0.006	0.908 ± 0.002	0.900 ± 0.005	0.909 ± 0.003	0.861 ± 0.010	0.853 ± 0.005	0.845 ± 0.001	0.840 ± 0.004	0.838 ± 0.003
	R^2_{adj}	> 0.999	> 0.999	> 0.999	> 0.999	> 0.999	> 0.999	> 0.999	> 0.999	> 0.999	> 0.999
	RMSE	< 0.331	< 0.363	< 0.204	< 0.460	< 0.128	< 0.551	< 0.340	< 0.206	< 0.206	< 0.484
40	***τ0 (Pa)***	2.730 ± 0.127	2.598 ± 0.119	2.726 ± 0.087	2.638 ± 0.089	2.713 ± 0.046	3.157 ± 0.292	3.534 ± 0.044	3.452 ± 0.056	3.748 ± 0.314	4.130 ± 0.214
	k (Pa·s^n)	1.471 ± 0.039	1.509 ± 0.035	1.478 ± 0.019	1.491 ± 0.017	1.472 ± 0.019	1.988 ± 0.102	2.077 ± 0.012	2.364 ± 0.037	2.611 ± 0.109	2.825 ± 0.063
	n (−)	0.909 ± 0.005	0.904 ± 0.005	0.908 ± 0.002	0.906 ± 0.003	0.909 ± 0.003	0.861 ± 0.010	0.857 ± 0.001	0.845 ± 0.004	0.834 ± 0.008	0.834 ± 0.004
	R^2_{adj}	> 0.999	> 0.999	> 0.999	> 0.999	> 0.999	> 0.999	> 0.999	> 0.999	> 0.999	> 0.999
	RMSE	< 0.168	< 0.289	< 0.204	< 0.315	< 0.128	< 0.485	< 0.638	< 0.686	< 0.686	< 0.513
50	***τ0 (Pa)***	2.799 ± 0.059	2.692 ± 0.119	2.617 ± 0.030	2.714 ± 0.091	3.333 ± 0.109	2.942 ± 0.156	3.049 ± 0.045	3.274 ± 0.176	3.958 ± 0.341	4.040 ± 0.115
	k (Pa·s^n)	1.451 ± 0.009	1.485 ± 0.025	1.500 ± 0.021	1.478 ± 0.031	2.139 ± 0.033	1.597 ± 0.055	1.746 ± 0.021	2.043 ± 0.053	2.222 ± 0.110	2.305 ± 0.034
	n (−)	0.911 ± 0.001	0.907 ± 0.003	0.905 ± 0.004	0.908 ± 0.004	0.890 ± 0.003	0.861 ± 0.007	0.853 ± 0.003	0.839 ± 0.005	0.837 ± 0.009	0.838 ± 0.003
	R^2_{adj}	> 0.999	> 0.999	> 0.999	> 0.999	> 0.999	> 0.999	> 0.999	> 0.999	> 0.999	> 0.999
	RMSE	< 0.363	< 0.204	< 0.576	< 0.154	< 0.437	< 0.224	< 0.192	< 0.450	< 0.450	< 429
60	***τ0 (Pa)***	2.758 ± 0.024	2.657 ± 0.063	2.632 ± 0.039	2.714 ± 0.091	3.174 ± 0.207	3.056 ± 0.060	3.124 ± 0.131	3.337 ± 0.071	3.830 ± 0.071	3.921 ± 0.196
	k (Pa·s^n)	1.458 ± 0.007	1.491 ± 0.017	1.499 ± 0.022	1.478 ± 0.031	2.205 ± 0.063	1.742 ± 0.011	1.869 ± 0.031	2.137 ± 0.012	2.335 ± 0.032	2.625 ± 0.077
	n (−)	0.911 ± 0.001	0.907 ± 0.002	0.905 ± 0.004	0.908 ± 0.004	0.888 ± 0.006	0.864 ± 0.001	0.856 ± 0.003	0.844 ± 0.001	0.841 ± 0.003	0.834 ± 0.006
	R^2_{adj}	> 0.999	> 0.999	> 0.999	> 0.999	> 0.999	> 0.999	> 0.999	> 0.999	> 0.999	> 0.999
	RMSE	< 0.151	< 0.171	< 0.576	< 0.154	< 0.349	> 0.359	< 0.214	< 0.339	< 0.339	< 0.319

Table S6. Suspensions processed for 12 hours.

Temp. (°C)	Parameters	BSG concentration (2%)					BSG concentration (4%)				
		AHP concentration (X_{AHP})					AHP concentration (X_{AHP})				
		1	2	4	6	8	1	2	4	6	8
20	*τ0 (Pa)*	2.207 ± 0.201	2.168 ± 0.121	2.546 ± 0.138	2.790 ± 0.091	2.950 ± 0.066	2.382 ± 0.186	2.381 ± 0.217	2.490 ± 0.243	2.817 ± 0.122	3.124 ± 0.051
	k (Pa·s^n)	1.680 ± 0.054	1.748 ± 0.032	1.833 ± 0.048	1.976 ± 0.023	2.191 ± 0.036	1.734 ± 0.030	1.854 ± 0.062	1.937 ± 0.072	1.966 ± 0.053	1.767 ± 0.014
	n (−)	0.946 ± 0.007	0.946 ± 0.004	0.942 ± 0.006	0.937 ± 0.002	0.928 ± 0.004	0.968 ± 0.003	0.961 ± 0.007	0.956 ± 0.007	0.954 ± 0.006	0.959 ± 0.001
	R^2_{adj}	> 0.999	> 0.999	> 0.999	> 0.999	> 0.999	> 0.999	> 0.999	> 0.999	> 0.999	> 0.999
	RMSE	< 0.658	< 0.370	< 0.464	< 0.510	< 0.540	< 0.482	< 0.919	< 0.936	< 0.531	< 0.291
30	*τ0 (Pa)*	2.152 ± 0.186	2.196 ± 0.095	2.367 ± 0.245	2.629 ± 0.117	2.884 ± 0.059	2.357 ± 0.005	2.494 ± 0.155	2.490 ± 0.227	2.819 ± 0.198	3.134 ± 0.111
	k (Pa·s^n)	1.568 ± 0.050	1.626 ± 0.026	1.731 ± 0.075	1.876 ± 0.047	2.011 ± 0.018	1.617 ± 0.007	1.652 ± 0.029	1.803 ± 0.067	1.816 ± 0.030	2.064 ± 0.037
	n (−)	0.943 ± 0.007	0.941 ± 0.003	0.940 ± 0.009	0.933 ± 0.005	0.930 ± 0.002	0.963 ± 0.001	0.968 ± 0.004	0.957 ± 0.007	0.955 ± 0.003	0.956 ± 0.003
	R^2_{adj}	> 0.999	> 0.999	> 0.999	> 0.999	> 0.999	> 0.999	> 0.999	> 0.999	> 0.999	> 0.999
	RMSE	< 0.607	< 0.335	< 0.632	< 0.299	< 0.253	< 0.212	< 0.461	< 0.876	< 0.537	< 0.252
40	*τ0 (Pa)*	2.251 ± 0.154	2.101 ± 0.131	2.578 ± 0.132	2.735 ± 0.200	2.749 ± 0.298	2.198 ± 0.189	2.522 ± 0.047	2.650 ± 0.107	2.691 ± 0.119	2.927 ± 0.129
	k (Pa·s^n)	1.464 ± 0.028	1.478 ± 0.040	1.619 ± 0.020	1.779 ± 0.031	2.096 ± 0.084	1.562 ± 0.056	1.488 ± 0.024	1.692 ± 0.027	1.775 ± 0.032	2.057 ± 0.056
	n (−)	0.947 ± 0.004	0.939 ± 0.005	0.943 ± 0.002	0.936 ± 0.003	0.930 ± 0.008	0.962 ± 0.007	0.967 ± 0.004	0.961 ± 0.003	0.954 ± 0.004	0.953 ± 0.006
	R^2_{adj}	> 0.999	> 0.999	> 0.999	> 0.999	> 0.999	> 0.999	> 0.999	> 0.999	> 0.999	> 0.999
	RMSE	< 0.372	< 0.540	< 0.455	< 0.487	< 0.726	< 0.776	< 0.200	< 0.248	< 0.391	< 0.985
50	*τ0 (Pa)*	2.299 ± 0.148	2.384 ± 0.051	2.627 ± 0.131	2.785 ± 0.198	2.927 ± 0.234	2.301 ± 0.170	2.581 ± 0.046	2.592 ± 0.174	2.650 ± 0.208	3.104 ± 0.193
	k (Pa·s^n)	1.382 ± 0.026	1.419 ± 0.018	1.610 ± 0.020	1.754 ± 0.031	1.925 ± 0.069	1.395 ± 0.050	1.451 ± 0.024	1.660 ± 0.038	1.795 ± 0.059	2.029 ± 0.029
	n (−)	0.950 ± 0.004	0.947 ± 0.003	0.942 ± 0.002	0.937 ± 0.003	0.933 ± 0.007	0.965 ± 0.007	0.968 ± 0.004	0.965 ± 0.004	0.950 ± 0.006	0.953 ± 0.002
	R^2_{adj}	> 0.999	> 0.999	> 0.999	> 0.999	> 0.999	> 0.999	> 0.999	> 0.999	> 0.999	> 0.999
	RMSE	< 0.356	< 0.174	< 0.451	< 0.483	< 0.425	< 0.704	< 0.196	< 0.458	< 0.690	< 0.594
60	*τ0 (Pa)*	2.406 ± 0.135	2.521 ± 0.122	2.770 ± 0.142	2.809 ± 0.189	3.085 ± 0.174	2.586 ± 0.070	2.674 ± 0.162	2.719 ± 0.189	2.943 ± 0.109	3.056 ± 0.239
	k (Pa·s^n)	1.437 ± 0.022	1.478 ± 0.033	1.647 ± 0.029	1.826 ± 0.059	1.967 ± 0.062	1.425 ± 0.013	1.527 ± 0.025	1.804 ± 0.041	1.811 ± 0.028	2.125 ± 0.047
	n (−)	0.950 ± 0.003	0.950 ± 0.004	0.945 ± 0.003	0.933 ± 0.006	0.933 ± 0.007	0.966 ± 0.002	0.967 ± 0.003	0.965 ± 0.004	0.954 ± 0.003	0.953 ± 0.005
	R^2_{adj}	> 0.999	> 0.999	> 0.999	> 0.999	> 0.999	> 0.999	> 0.999	> 0.999	> 0.999	> 0.999
	RMSE	< 0.679	< 0.154	< 0.468	< 0.362	< 0.476	< 0.161	< 0.475	< 0.497	< 0.256	< 0.621

Table S6. Suspensions processed for 12 hours (continuation).

Temp. (°C)	Parameters	BSG concentration (6%)					BSG concentration (8%)				
		% Peróxido					% Peróxido				
		1	2	4	6	8	1	2	4	6	8
20	$\tau 0$ (Pa)	3.065 ± 0.200	3.010 ± 0.062	3.306 ± 0.036	3.467 ± 0.070	3.781 ± 0.105	4.040 ± 0.115	3.578 ± 0.066	3.822 ± 0.099	4.088 ± 0.422	4.646 ± 0.160
	k (Pa·s^n)	2.083 ± 0.048	2.237 ± 0.016	2.297 ± 0.013	2.509 ± 0.025	2.775 ± 0.017	2.305 ± 0.034	2.910 ± 0.041	3.015 ± 0.019	3.292 ± 0.150	3.305 ± 0.035
	n (−)	0.911 ± 0.004	0.904 ± 0.002	0.900 ± 0.002	0.895 ± 0.002	0.890 ± 0.001	0.838 ± 0.003	0.856 ± 0.003	0.845 ± 0.001	0.837 ± 0.009	0.835 ± 0.002
	R^2_{adj}	> 0.999	> 0.999	> 0.999	> 0.999	> 0.999	> 0.999	> 0.999	> 0.999	> 0.999	> 0.999
	RMSE	< 0.515	< 0.252	< 0.229	< 0.244	< 0.629	< 0.429	< 0.470	< 0.477	< 0.710	< 0.602
30	$\tau 0$ (Pa)	2.819 ± 0.170	3.010 ± 0.069	3.092 ± 0.043	3.334 ± 0.064	3.473 ± 0.263	3.326 ± 0.091	3.569 ± 0.177	3.779 ± 0.089	4.100 ± 0.120	4.240 ± 0.225
	k (Pa·s^n)	1.858 ± 0.055	1.914 ± 0.015	2.079 ± 0.030	2.280 ± 0.022	2.543 ± 0.088	2.449 ± 0.025	2.507 ± 0.042	2.689 ± 0.017	2.885 ± 0.037	3.032 ± 0.088
	n (−)	0.909 ± 0.006	0.908 ± 0.002	0.899 ± 0.004	0.895 ± 0.002	0.888 ± 0.007	0.859 ± 0.002	0.857 ± 0.003	0.845 ± 0.001	0.842 ± 0.002	0.832 ± 0.006
	R^2_{adj}	> 0.999	> 0.999	> 0.999	> 0.999	> 0.999	> 0.999	> 0.999	> 0.999	> 0.999	> 0.999
	RMSE	< 0.327	< 0.743	< 0.774	< 0.222	< 0.403	< 0.427	< 0.766	< 0.477	< 0.225	< 0.364
40	$\tau 0$ (Pa)	2.860 ± 0.116	3.025 ± 0.082	2.857 ± 0.084	3.133 ± 0.313	3.584 ± 0.149	3.175 ± 0.142	3.375 ± 0.025	3.412 ± 0.065	4.100 ± 0.120	4.247 ± 0.139
	k (Pa·s^n)	1.655 ± 0.026	1.719 ± 0.025	1.955 ± 0.013	2.139 ± 0.099	2.405 ± 0.027	2.162 ± 0.055	2.108 ± 0.008	2.432 ± 0.027	2.885 ± 0.037	2.790 ± 0.041
	n (−)	0.912 ± 0.003	0.910 ± 0.003	0.898 ± 0.002	0.890 ± 0.009	0.890 ± 0.002	0.854 ± 0.005	0.854 ± 0.001	0.845 ± 0.003	0.842 ± 0.002	0.838 ± 0.003
	R^2_{adj}	> 0.999	> 0.999	> 0.999	> 0.999	> 0.999	> 0.999	> 0.999	> 0.999	> 0.999	> 0.999
	RMSE	< 0.413	< 0.239	< 0.395	< 0.607	< 0.547	< 0.189	< 0.079	< 0.427	< 0.225	< 0.517
50	$\tau 0$ (Pa)	2.825 ± 0.085	2.741 ± 0.044	2.852 ± 0.177	3.226 ± 0.313	3.578 ± 0.139	2.968 ± 0.039	3.242 ± 0.064	3.446 ± 0.052	3.770 ± 0.210	3.995 ± 0.088
	k (Pa·s^n)	1.509 ± 0.015	1.531 ± 0.013	1.757 ± 0.047	1.963 ± 0.101	2.255 ± 0.021	1.738 ± 0.024	1.811 ± 0.011	2.050 ± 0.020	2.250 ± 0.078	2.478 ± 0.025
	n (−)	0.910 ± 0.002	0.903 ± 0.002	0.893 ± 0.005	0.894 ± 0.010	0.891 ± 0.002	0.859 ± 0.003	0.854 ± 0.001	0.846 ± 0.002	0.840 ± 0.007	0.836 ± 0.002
	R^2_{adj}	> 0.999	> 0.999	> 0.999	> 0.999	> 0.999	> 0.999	> 0.999	> 0.999	> 0.999	> 0.999
	RMSE	< 0.341	< 0.583	< 0.508	< 0.569	< 0.515	< 0.287	< 0.302	< 0.162	< 0.284	< 0.388
60	$\tau 0$ (Pa)	2.607 ± 0.043	2.677 ± 0.053	2.739 ± 0.179	3.288 ± 0.084	3.329 ± 0.177	2.979 ± 0.167	3.342 ± 0.144	3.197 ± 0.169	3.925 ± 0.075	3.834 ± 0.055
	k (Pa·s^n)	1.616 ± 0.012	1.672 ± 0.023	1.788 ± 0.048	1.981 ± 0.024	2.347 ± 0.067	2.209 ± 0.060	1.905 ± 0.044	2.251 ± 0.067	2.367 ± 0.016	2.704 ± 0.021
	n (−)	0.907 ± 0.002	0.902 ± 0.003	0.892 ± 0.005	0.896 ± 0.002	0.885 ± 0.006	0.850 ± 0.006	0.854 ± 0.005	0.840 ± 0.006	0.842 ± 0.001	0.830 ± 0.002
	R^2_{adj}	> 0.999	> 0.999	> 0.999	> 0.999	> 0.999	> 0.999	> 0.999	> 0.999	> 0.999	> 0.999
	RMSE	< 0.343	< 0.346	< 0.514	< 0.191	< 0.367	< 0.348	< 0.579	< 0.495	< 0.446	< 0.385

CAPÍTULO 4

Manuscrito a ser submetido em “**Food and Bioproducts Processing**” ISSN: 0960-3085

Extraction of proteins from brewer's spent grain using ultrasound and alkaline hydrogen peroxide: impact on extraction yield, structural and techno-functional properties

Marcio Augusto Ribeiro-Sanches1*, Pedro Esteves Duarte Augusto[2], Tiago Carregari Polachini[1], Javier Telis-Romero[1]

[1]Food Engineering and Technology Department, São Paulo State University, Institute of Biosciences, Humanities and Exact Sciences (Ibilce), Campus São José do Rio Preto, São Paulo, 15.054-000, Brazil.

[2]Université Paris-Saclay, CentraleSupélec, Laboratoire de Génie des Procédés et Matériaux, Centre Européen de Biotechnologie et de Bioéconomie (CEBB), 3 rue des Rouges Terres 51110 Pomacle, France.

*Author to whom correspondence may be addressed. E-mail address: mar.sanches@unesp.br (Marcio Augusto Ribeiro Sanches).

ABSTRACT

Brewer's spent grain (BSG) is an abundant agro-industrial by-product and a low-cost sustainable source of proteins. This study evaluated the use of high-intensity ultrasound (US) and/or alkaline hydrogen peroxide (AHP) in the extraction process and the structural and technical-functional properties of proteins extracted from BSG. Four extraction processes were evaluated: EC - extraction using the conventional method; EAHP - extraction using alkaline hydrogen peroxide – AHP (3%); EUS: ultrasound extraction – US (1200 W); EAHPUS: extraction using AHP (3%) and US (1200 W). EAHP and EUS caused structural

changes in the BSG matrix, resulting in higher protein extraction yield compared to EC. EAHPUS was even more effective, leading to greater matrix disintegration and higher protein extraction. Structural analyses (SEM, FTIR, and X-ray diffraction) showed that the EAHP, EUS, and EAHPUS concentrate presented fragmentation and disordered arrangement, changes in the secondary structures of proteins, characterized by the reduction of more ordered structures, such as the α-helix and β-sheet. Also, there was an increase in partially (β-turn) and totally disordered structures (random coil), in addition to a reduction in the size of protein crystals, suggesting greater flexibility and unfolding of proteins, especially in the EAHP and EAHPUS concentrate. Techno-functional properties were influenced by different extraction methods. EUS improved the water holding capacity and did not affect the color of the extracted proteins, while EAHP and EAHPUS reduced the water-holding capacity and caused a noticeable change in color. All treatments improved the foaming capacity and stability and the emulsion capacity and stability compared to EC, while no effect was observed on the oil holding capacity. Therefore, the results highlight the potential of using ultrasound and/or alkaline hydrogen peroxide to improve the extraction of BSG proteins, although the effects on techno-functional properties must be considered for different applications.

Keywords: Agro-industrial byproduct; Alkaline extraction; BSG protein concentrate; Foam; Emulsion.

1. INTRODUCTION

The growing increase in demand for alternative sources of proteins highlights the urgent need to find alternative and sustainable sources of proteins to ensure global food security (Fonseca et al., 2023; Fasolin et al., 2019). Moreover, the food industry generates enormous amounts of biomass waste comprising containing cellulose, hemicellulose, lignin, and proteins.

Obtaining proteins from agro-industrial by-products is, therefore, a promising solution (Bayomie and Romdhana, 2023) that not only meets this demand but also currently contributes to achieving the UN Sustainable Development Goals, including SDG 2 (Zero Hunger), SDG 12 (Sustainable Consumption and Production) and SDG 15 (Life on Land). This approach not only

reduces pressure on natural resources but also promotes more sustainable agricultural and food practices, aligned with the vision of a responsible future.

Brewer's spent grain (BSG) is an abundant resource in the brewing industry, representing around 85% of the solid by-products generated (Kavalopoulos et al., 2021; Sanches et al., 2023). Rich in proteins, with contents varying between 15-30% w/w, in addition to containing cellulose (15–25%; dry basis), hemicellulose (20–40%; dry basis) and lignin (10–20%; dry basis) (Agrawal et al., 2023), BSG has been underutilized, generally destined for animal feed (Pabbathi et al., 2022), composting (Assandri et al., 2020) or simply discarded, going in the opposite direction to sustainability. Therefore, studies aimed at converting them into value-added products are necessary.

Although BSG is rich in proteins, it is challenging to extract them in high yields, due to the complex network formed between lignin and cellulose that traps the proteins inside. Therefore, different strategies using ultrasound-assisted alkaline extraction (Li et al., 2021), reduced pressure alkaline treatment (Fonseca et al., 2023), high-temperature alkaline extraction (Silva et al., 2023), hydromechanical processing (Ibbett et al., 2019), enzymatic (Paz et al., 2019), pressurized liquids (González-García et al., 2021) and subcritical water (Alonso-Riaño et al., 2021) have been studied to extract proteins from BSG. The method described by Qin et al. (2018), which involves a sequential three-step pretreatment followed by autoclaving, demonstrated high protein recovery (94%). However, this method consumes a lot of time and energy, making it difficult to apply on a large scale. In this sense, adequate and efficient processing steps are required to improve the accessibility of BSG.

Alkaline hydrogen peroxide (AHP) is a promising processing method, generating radical species under alkaline conditions that selectively react with lignin, resulting in delignification of biomass (Ho et al., 2019; Zhang et al., 2022). However, the performance of AHP can be further intensified through the use of combined technologies. Ultrasound-assisted processing (US) may be an affordable, easy, and effective approach to assist in the extraction of proteins from BSG (Li et al., 2021). Perturbation in microporous particles, high-speed interparticle collisions, cavitation bubble implosion, microjet formation, and microturbulence can increase extraction yield in the biological matrix (Kadam et al., 2015). However, it is important to highlight that, although the combined

techniques can increase the extraction yield, there are still uncertainties regarding the effects on the structural and techno-functional properties of the extracted proteins.

Taking all these aspects into consideration, this study aims to evaluate the use of high-intensity ultrasound and/or alkaline hydrogen peroxide in the protein extraction from BSG, also characterizing the obtained proteins in relation to both structural and techno-functional properties.

2. MATERIAL AND METHODS

2.1. Raw material and sample preparation

The wet BSG was supplied by a brewery located in the city of Frutal – MG, Brazil. After collection, the BSG was dried in a convective tray dryer at 60 ± 2 °C, until equilibrium moisture, as performed in a previous study (Sanches et al., 2023). Subsequently, the dry BSG was ground in a rotor mill (model MA340, Marconi, Piracicaba, São Paulo, Brazil) and sieved through a 30-mesh sieve to obtain BSG with a particle size of less than 595 μm.

2.2. Chemical composition and amino acid profile of BSG

Protein content was analyzed using the Kjeldahl method with a correction factor of 6.25 (AOAC, 2007). The extractive content was determined by the NREL/TP-510-42619 method (Sluiter et al., 2005). The extractive-free material was subjected to acid hydrolysis according to the NREL/TP-510-42618 method (Sluiter et al., 2008) to evaluate the carbohydrate and lignin composition. Klason lignin was determined gravimetrically as an insoluble residue, following the protocol of Gomide and Demuner (1986). Acid-soluble lignin was analyzed by UV spectroscopy at wavelengths of 215 and 280 nm, as described by Goldschimid (1971).

Cellulose and hemicellulose contents were determined by an adaptation of the NREL/TP-510-42618 method (Sluiter et al., 2008), using high-performance liquid chromatography (HPLC). For this, the filtered hydrolysate, obtained before determining the insoluble lignin content (Klason method), was used. The calculation conditions and factors were the same as those used in a previous study (Sanches et al., 2023).

Quantification of total amino acids was performed by high-performance liquid chromatography (Hagen et al., 1989; White et al., 1986), except tryptophan, determined spectrophotometrically (Spies, 1949). Amino acid contents were expressed as g of amino acids/100 g of dry BSG.

2.3. Extraction of proteins from BSG

Protein extraction using the isoelectric precipitation method were carried out according to the following treatments: EC: extraction using conventional method; EAHP: extraction using alkaline hydrogen peroxide - AHP (3%); EUS: extraction using ultrasound (1200 W); EAHPUS: extraction using AHP (3%) and US (1200 W). These experimental conditions were established based on pre-tests and refined through prior evaluation. BSG was dispersed in distilled water at a ratio of 1:20 (m/v) and the pH was adjusted to 12 (using 2 M NaOH) to promote protein solubilization as performed by Silva et al. (2023). In assay with AHP, it was added together with distilled water.

For the application of ultrasound, the VCX 1500 HV ultrasonic equipment (Sonics and Materials, USA) was used to produce sound waves at 20 kHz of frequency, capable of varying from 20 to 100%, with a maximum nominal power of 1500 W. The processor was equipped with a model CV294 titanium probe, 2.5 cm in diameter (Sonics & Materials Inc., Newtown, USA). The container containing the suspension was immersed in a thermostatic bath with a controlled temperature of 25 ± 2 °C. The ultrasound nominal power was set at 1200 W. Ultrasound was applied using the pulsed system (1 second on; 1 second off) to avoid overheating the system. The ultrasound treatment time was set at 30 minutes, based on this study of Li et al. (2021). After the ultrasound application time, the suspensions were stirred in a mechanical shaker (MA261, Marconi, Brazil) at 2000 rpm for 30 minutes. The experiments without ultrasound application were shaken for 60 minutes at a temperature of 25 °C. For all trials, treatment time was 60 minutes.

After the treatments, the suspensions were centrifuged (9500 g, 30 min at 10 °C) to obtain the protein-rich supernatant. Afterward, the pH of the protein-rich supernatant was adjusted to 3.8 using 2 M HCl, as carried out in other studies (Li et al., 2021), resulting in isoelectric precipitation of the proteins. This material was centrifuged again (9500 g, 30 min at 10 °C), and the precipitated material was

collected. The precipitate was dissolved in deionized water and the pH was adjusted to 7.0 using 2 M HCl. The protein solutions obtained were freeze-dried for 72 h and stored in airtight containers for further analysis.

2.4. Characterization of protein concentrate

2.4.1. Protein content and extraction yield

The protein content of the protein concentrate was determined using the Kjeldahl method (AOAC, 2007), with a conversion factor of 6.25. The protein extraction yield (PEY (%)) was calculated using the protein mass in the protein concentrate and dry BSG, using equation 1.

$$PEY(\%) = \left[\frac{Mass\ of\ protein\ in\ dry\ protein\ fraction\ (g)}{Mass\ of\ protein\ in\ dry\ BSG\ raw\ material\ (g)}\right] \times 100 \quad (1)$$

2.4.2. Fourier-transform infrared spectroscopy (FTIR) and protein secondary structure

The infrared spectra of the protein concentrate were recorded using a Fourier transform infrared spectrometer (PerkinElmer, Waltham, USA) at 400-4000 cm^{-1}, placing the samples directly on the ATR crystal. The spectra were subjected to Fourier autodeconvolution, second derivative analysis, and curve fitting to identify peaks in the amide I band region (1700 and 1600 cm^{-1}), using OriginPro 2016 software (OriginLab, Northampton, USA). The resulting peaks were classified into secondary structures, including β-sheet (1600-1640 cm^{-1}), random coil (1640-1650 cm^{-1}), α-helix (1650-1660 cm^{-1}) e β-turn (1660–1700 cm^{-1}) (Li et al., 2022; Ling et al., 2019). The percentages of peak areas were used to quantify the secondary structures of the proteins.

2.4.3. X-ray diffraction pattern (XRD)

The XRD pattern of the protein concentrate was measured using an X-ray diffraction meter (Rigaku, RINT 2000, Japan). The equipment operated at a voltage of 30 kV and a current of 10 mA using Kα radiation and L = 1542 Å. The diffractograms were obtained at angles (2θ) ranging from 5° to 60° at a scan rate of 5°/min.

2.4.4. Microstructure by scanning electron microscopy (SEM)

To verify the effect of the extraction process on the BSG plant cell matrix and its protein concentrates, microstructural analysis was carried out on BSG raw material, on the BSG residue after protein extraction (dried in a forced air convection oven at 40 °C for 12 h), as performed by Silva et al. (2023) and in protein concentrates (dried in a freeze dryer for 72 h) using a scanning electron microscope (EVO-LS15-ZEIS). The samples were placed on conductive adhesive, adhered to the sample table, coated with gold, and viewed under the following conditions: vacuum = 10.0 kV, DP = 11.5 mm, and magnitude of 250, 500x, 1000x, and 2500x.

2.4.5. Techno-functional Properties

2.4.5.1. Water holding capacity (WHC) and oil holding capacity (OHC)

The water/oil holding capacity was determined according to Stone et al. (2015). Protein concentrate (0.5 g) was mixed with water or soybean oil (5.0 g) in microtubes and vortexed for 10 s every 5 min for 30 min. After centrifugation at 10,000 g for 15 min, the supernatants were discarded, and the precipitates were weighed again to calculate WHC and OHC according to equation (2).

$$WHC\ ou\ OHC = \frac{WG}{W_0} \cdot 100 \quad (2)$$

In Eq. (2), WG is the mass gained by the material (difference between the final and initial mass) and W_0 is the initial mass.

2.4.5.2. Foaming Properties

The foaming properties of the protein concentrate were determined according to Stone et al. (2015). For this, fifteen mL (v_{li}) of 1.00% (w/w) protein solution (based on the protein content by weight within the dry powder) was prepared and stirred at 7200 rpm (T-25 Ultra-Turrax®, IKA, Germany) for 5 min. The foam obtained was added to a graduated cylinder and the volume of foam formed was measured. The foam volume was recorded at time zero (V_{fi}) and after 120 min (V_{ft}). Foaming capacity (FC) was calculated using Equation 3, while foam stability (FS) was evaluated using Equation 4.

$$FC\ (\%) = \frac{V_{fi}}{V_{li}} \cdot 100 \quad (3)$$

$$FS\ (\%) = \frac{V_{ft}}{V_{fi}} \cdot 100 \quad (4)$$

2.4.5.3. Emulsion Properties

Emulsification capacity (EC) and stability (ES) were analyzed as described by Stone et al. (2015). For EC, different amounts of soybean oil (by weight) were added to 2.00 g of 1% protein solution (based on the protein content in the dry powder). The mixture was homogenized (7200 rpm, for 5 min) and its conductivity was measured using a conductivity meter. EC was determined by the point at which the transition from oil-in-water emulsion to water-in-oil emulsion occurred, indicated by a significant drop in conductivity. Emulsification capacity was expressed as g of homogenized oil per g of protein before inversion.

For ES, a 50:50 oil-in-water emulsion (5.00 ml of protein solution (V_B) and 5.00 ml of soybean oil) was prepared with a 1.00% protein solution (based on the content of protein in dry powder). After homogenization (7200 rpm, for 5 min), the emulsion was left to rest for 120 min. Stability was calculated by measuring the volume of the aqueous layer (V_A) separated after this time (equation 5).

$$ES\ (\%) = \frac{V_B - V_A}{V_B} \times 100 \quad (5)$$

2.4.5.4. Instrumental color

The color of protein concentrate was evaluated using Konica Minolta equipment (CR-S, Konica Minolta, Japan). The parameters were determined: L* (lightness), a* (+a* = red, -a* = green) and b* (+b* = yellow, –b* = blue), chroma (C*), angle of Hue (h*). From these parameters, the total color difference (ΔE) was calculated according to equation 6.

$$\Delta E = \sqrt{\left(L^*_{sample} - L^*_{standard}\right)^2 + \left(a^*_{sample} - a^*_{standard}\right)^2 + \left(b^*_{sample} - b^*_{standard}\right)^2} \quad (6)$$

were, $L^*_{standard}, a^*_{standard}, b^*_{standard}$ are the color parameters of the sample obtained through extraction using the conventional method (EC).

2.5. Statistical analysis

The experiments were carried out in three independent replicates. Data were analyzed using OriginPro 9.0 software (OriginLab Corporation, Northampton, MA) and STATISTICA software version 7.0 (Statsoft Inc., USA). Variance analysis (ANOVA) followed by Tukey post hoc test was applied to

determine the difference between samples at a 5% significance level. Data were expressed as mean ± standard deviation.

3. RESULTS AND DISCUSSION

3.1. Chemical composition and amino acid profile of BSG

The raw BSG used in this work is mainly composed of 29.89% hemicellulose (25.19 ± 0.16% xylan and 4.70 ± 0.05% arabinan) and 16.09 ± 0.07% cellulose, which is in line with studies reporting that BSG is a promising by-product for ethanol production (Alonso-Riaño et al., 2022; Ravindran et al., 2019; Sun et al., 2024; Wagner et al., 2021). It also contains 20.97% lignin (17.95 ± 0.11% insoluble and 3.02 ± 0.03% soluble), extractives (8.30 ± 0.07%) and ash (3.75 ± 0.05%). Lignin is identified as the main molecule that hinders the extraction of proteins from BSG. In addition to the carbohydrate fraction, BSG presented 21.18 ± 0.12 % proteins. These values are within the range reported for this raw material (Santos et al., 2023; Rodriguez et al., 2023). The crude protein content in BSG is higher than in other agro-industrial by-products, such as defatted avocado meal which contains ~15% (Wang et al., 2019), banana peel flour which contains ~10% (Deb et al., 2022) and orange seed flour which contains ~17% (Ulloa et al., 2023). Although lower than soybean, which typically contains 35-45% protein (db) (Huang et al., 2023; Singh and Krishnaswamy, 2022), BSG's protein content is comparable to certain beans, ranging from 17–28% proteins (db) (Locali-Pereira et al., 2024; Telles et al., 2017) and peas with 20–25% of proteins (db) (Hadidi et al., 2022; Lu et al., 2019), which are “established” sources of vegetable protein, indicating that BSG is a very attractive low-cost source to obtain protein for future industrial applications.

Regarding the amino acid profile of these proteins, the results show that BSG contains a variety of essential and non-essential amino acids, which are fundamental components in human nutrition. The essential amino acids found in BSG (g of amino acids/100 g of dry BSG) were histidine (0.50 ± 0.01), threonine (0.67 ± 0.03), valine (1.23 ± 0.02), methionine (0.48 ± 0.01), isoleucine (0.93 ± 0.02), leucine (1.74 ± 0.01), tryptophan (0.14 ± 0.02) phenylalanine (1.39 ± 0.01) and lysine (0.91 ± 0.01). On the other hand, the non-essential amino acids found in BSG were aspartic acid (1.69 ± 0.04), glutamic acid (4.99 ± 0.06), proline (2.24 ± 0.01), serine (0.99 ± 0.01), glycine (0.90 ± 0.01), arginine (1.20 ± 0.01), alanine

(1.02 ± 0.01), tyrosine (0.85 ± 0.01) and cystine (0.63 ± 0.02). The presence of these essential and non-essential amino acids in BSG demonstrates that it can be a valuable nutritional source, especially if used in the formulation of foods, animal feed or protein supplements.

3.2. Influence of processing on protein extraction

3.2.1. Protein content and yield

Figure 1 shows the protein content (Fig. 1-a) and extraction yield (Fig. 1-b) for the different treatments.

Figure 1. Protein content (a) and extraction yield (b) of protein fractions as a function of the extraction method.

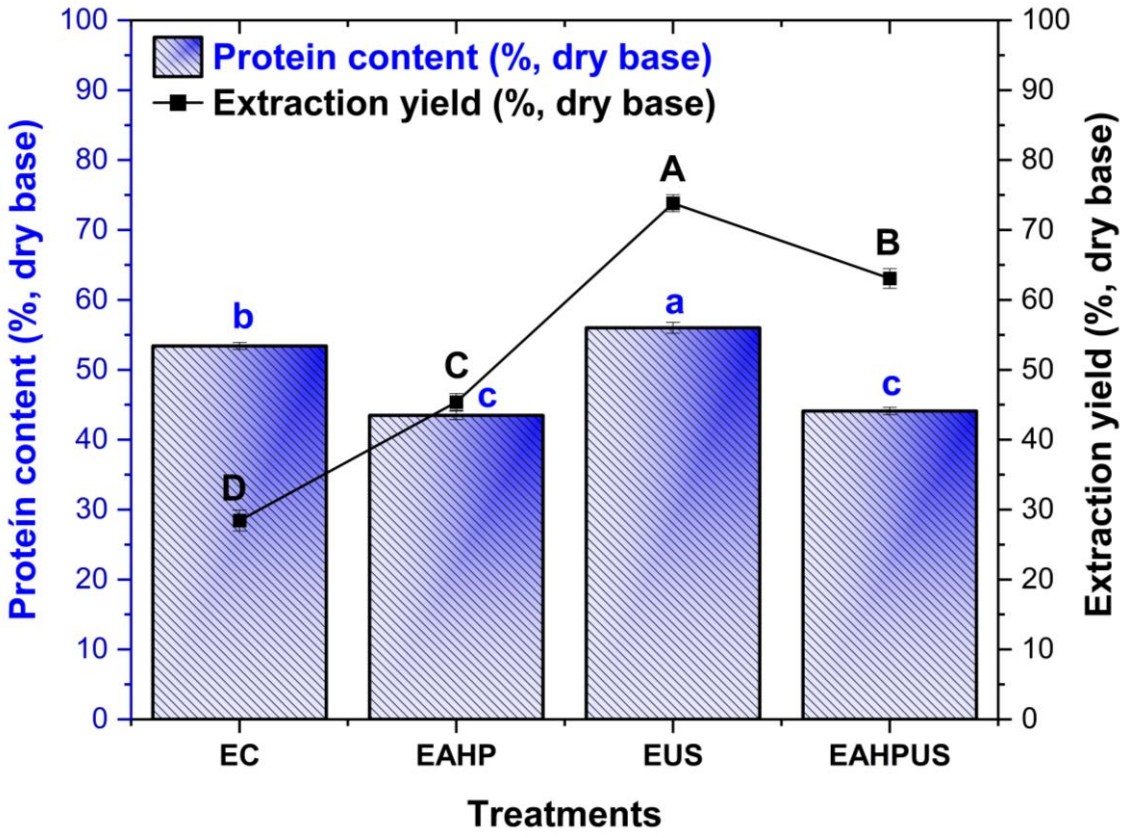

It is noted that EAHP increased the extraction yield, although its protein content decreased, when compared to EC. This demonstrates that AHP probably reacted selectively with lignin, providing delignification of the biomass, and facilitating the penetration of reagents into the matrix, also improving protein extraction (Ho et al., 2019). However, other non-protein compounds may have been carried into

the protein concentrate – resulting in an overall reduction in the protein content in the concentrate obtained.

On the other hand, extraction using only ultrasound (EUS) not only increased protein content, but also resulted in the highest extraction yield among treatments. Unlike AHP, the effects of ultrasound are likely related to other mechanisms. Transient cavitation near the surface of BSG particles results in the formation of microjets on their surface, inducing ruptures and microchannels in the tissue, in addition to increasing the permeability of the BSG cell wall (Li et al., 2021). On the other hand, the "sponge effect" is another mechanism that may contribute to the benefits of ultrasound. When ultrasonic waves pass through the BSG, they cause compressions and expansions in the matrix, similar to a sponge being repeatedly squeezed and released (Miano et al., 2017). This phenomenon facilitates direct mass flow and opens pathways for mass transfer through the microchannels and pores of the BSG. Together, those effects contributed to increasing protein extraction from BSG.

The combination of AHP and US (EAHPUS) was also effective, as it improved the extraction yield when compared to EC and EAHP. This result indicates synergy between the two extraction strategies, where the effects of AHP on biomass delignification and the effects of US on the formation of microjets and microchannels in the BSG structures acted synergistically and increased the overall protein extraction efficiency. However, it is important to note that even in this combined treatment, a reduction in the protein content in the extracts was observed, again indicating the possibility of transport of other non-protein compounds such as extractives, cellulose, hemicellulose, and lignin, which are initially present in BSG, into the protein concentrate, probably due to the use of AHP. It is essential to highlight that these beneficial modifications to the extraction yield, resulting from the different strategies used, must not negatively compromise the techno-functional properties of the protein concentrate.

3.2.2. BSG matrix disruption

Most cereal grains have a protein concentrate in their endosperm, which is surrounded by three distinct anatomical layers: the aleurone layer, the seed coat, and the pericarp (Bacic and Stone, 1981; Silva et al., 2023). SEM images were obtained to evaluate the degradation of BSG structures by different

extraction strategies. As shown in Figure 2, the BSG raw material exhibited a rigid and rough surface with small cavities (indicated by the white arrow), which is the common characteristic of most biomasses. Furthermore, regular channels that make up the plant's vascular system can be seen in Figure 2-F (indicated by a white rectangle). These da channels were also reported by Fontana et al. (2018) at BSG. This structure is responsible for trapping proteins inside (Lynch et al., 2016; Silva et al., 2023), the main difficulty in obtaining proteins from cereals, when compared to legume matrix.

After EC, EAHP or EUS, the residues showed a significantly smoother surface when compared to BSG raw material, indicating the possible elimination of soluble elements such as lignin, extractives and a part of the more accessible proteins contained in BSG. Pereira et al. (2021) also observed that, after pretreating BSG with non-thermal plasma, the samples exhibited a more uniform surface due to the removal of more soluble components.

No significant differences were observed between EC, EAHP and EUS in the microscopic analysis, except for some loose and dispersed fragments (Fig. 2-K, indicated by white circles) on the surface of EAHP, possibly due to the action of ·OH free radicals attacking the lignin. Furthermore, some areas with a rougher and more irregular surface were identified in EUS, as evidenced by figures 2-M, N, and O (indicated by white circles), which can be attributed to ultrasound-induced cavitation. These few structural modifications observed in EAHP and EUS may have facilitated the contact between the matrix and the alkaline solution, resulting in an increase in the protein extraction yield of these treatments. However, the matrix structure was still considerably rigid and compact, which is in line with the previously discussed difficulties in obtaining high protein extraction yields from BSG.

Figure 2. Scanning electron microscopy images of the BSG raw material and residues after the different extraction processes.

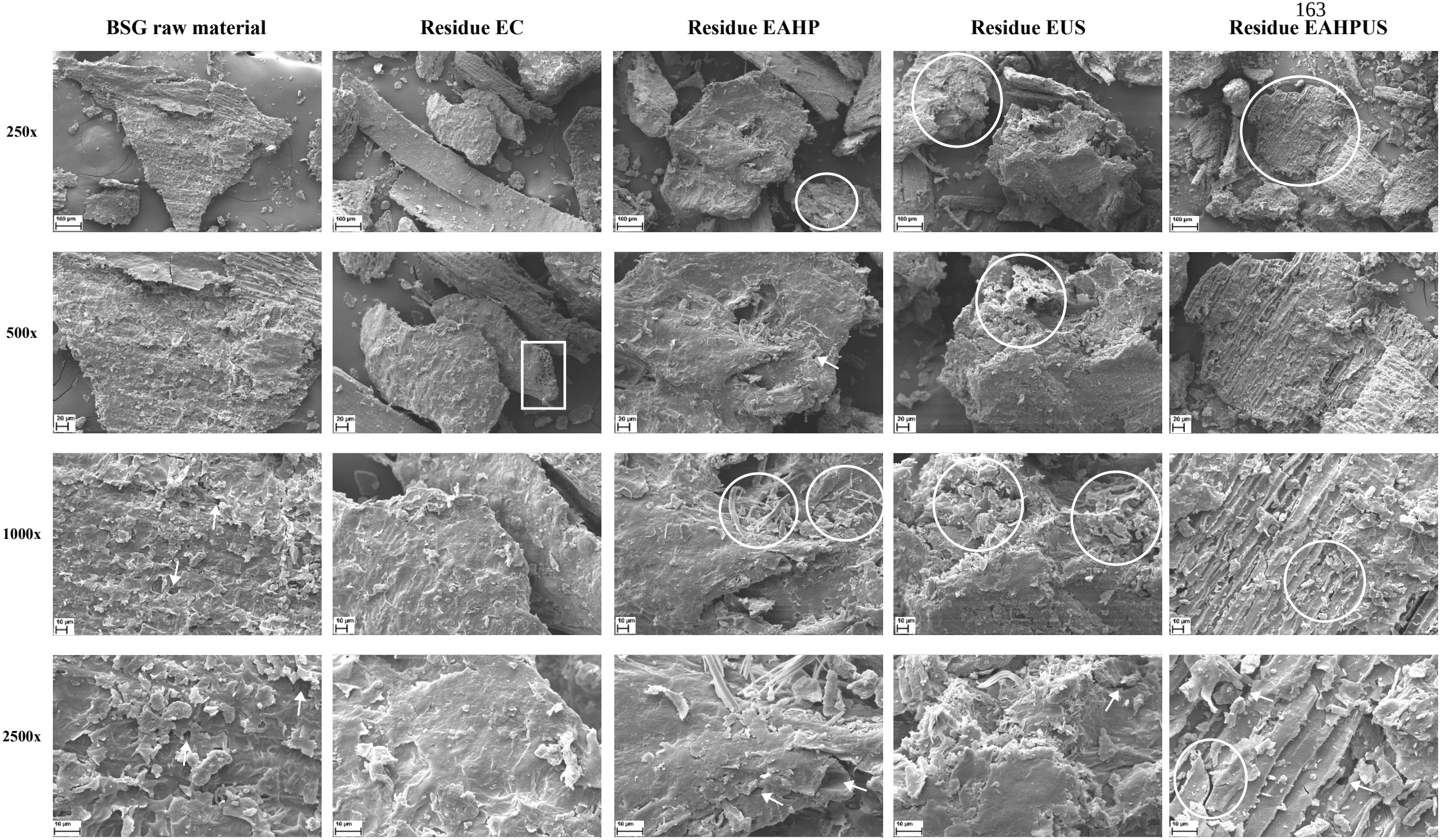
BSG raw material
Residue EC
Residue EAHP
Residue EUS
Residue EAHPUS
250x
500x
1000x
2500x

The combination of AHP and US (EAHPUS) proved to be more effective, resulting in a synergistic effect of the oxidizing properties of AHP and the cavitation effects generated by US. The surface of BSG after EAHPUS exhibited the appearance of striations, some cracks, and cavities on the surface of BSG. The mechanical action generated by ultrasound may have helped in the uniform dispersion of ·HO and ·HOO radical species generated by AHP in the BSG matrix, a fact that justifies the higher extraction yield obtained in EAHPUS.

3.3. Characterization of BSG protein concentrate

3.3.1. Microstructure by scanning electron microscopy (SEM)

Scanning electron microscopy is a commonly employed and reliable method for analyzing microstructures of protein concentrates (Li et al., 2022; Yeasmin et al., 2024) and can help understand possible differences in the structural and techno-functional properties of BSG protein concentrates. Notably, the microstructure of protein concentrate (Figure 3) extracted under different conditions showed some differences.

The EC protein concentrate exhibited large particles, with a compact microstructure, presenting relatively flat surfaces. The microstructure of the EUS protein concentrate is quite similar to the microstructure of EC, however, the EUS images at 250X apparently show a greater quantity of smaller and/or more fragmented particles, when compared to EC. Shear forces, microflow, shock waves and free radicals produced by ultrasonic cavitation bubbles may have caused particle thinning/size reduction. However, it is worth highlighting that the impact of AHP treatments surpassed the changes induced by ultrasound alone.

The microstructure of EAHP and EAHPUS protein concentrates exhibited a higher proportion of smaller particles when compared to EC and EUS. These particles were also quite heterogeneous and fragmented, indicating a large increase in the surface area of the particles of these protein concentrates.

Figure 3. Scanning electron microscopy images of protein fractions.

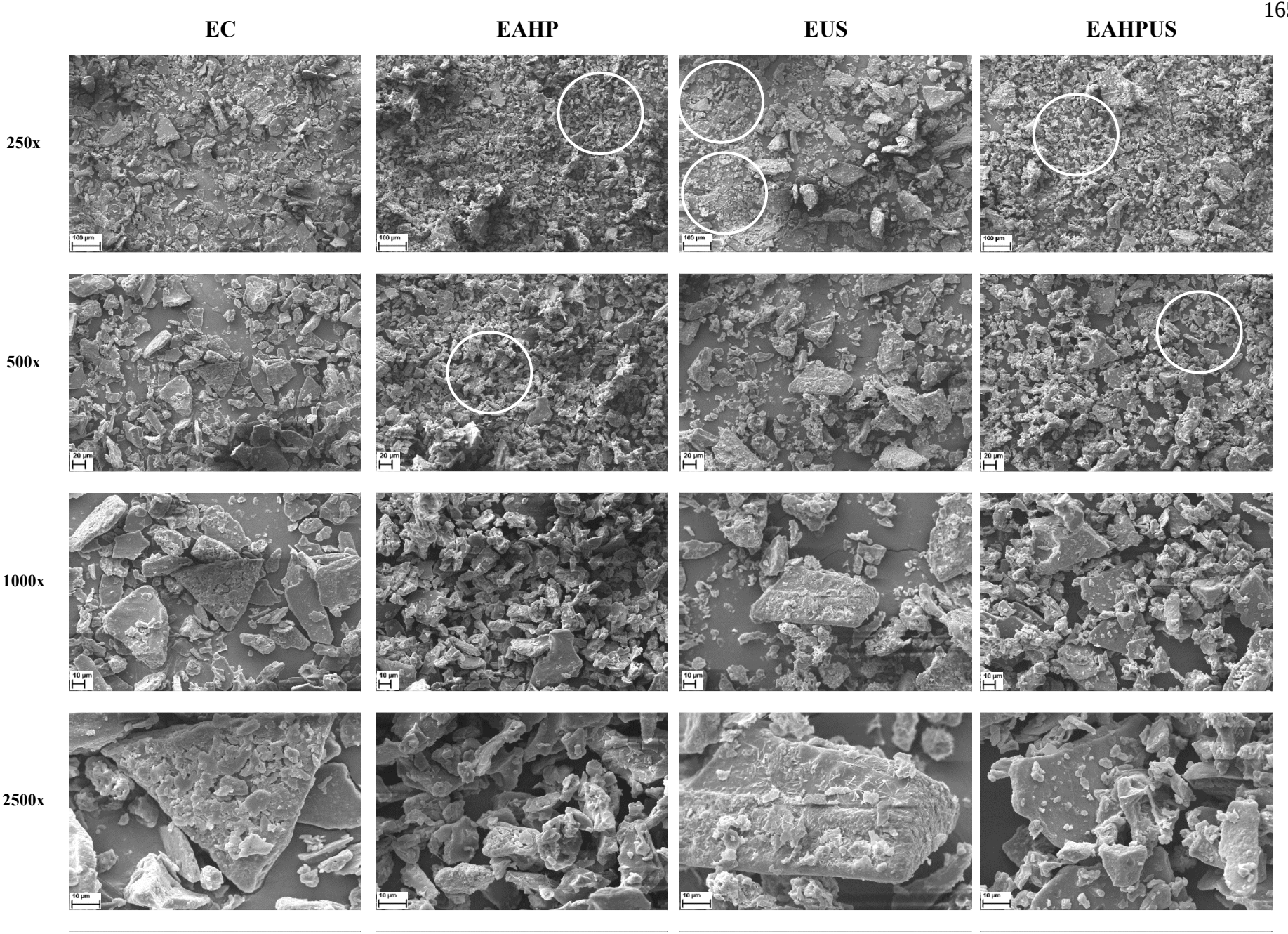
EC
EAHP
EUS
EAHPUS
250x
500x
1000x
2500x
100 µm
20 µm
10 µm

These changes indicated that the oxidizing properties of AHP alone or combined with ultrasonic waves may have caused protein depolymerization, the process by which high molecular weight proteins are broken down into lower molecular weight fragments. This usually occurs due to the breaking of covalent bonds, such as peptide bonds, that hold the amino acid chains of proteins together in their three-dimensional structure. In fact, El-Kadiri et al. (2013) demonstrated through sodium dodecyl sulfate polyacrylamide gel electrophoresis (SDS-PAGE) the depolymerization effect of AHP on high molecular weight proteins from canola bran. As a result of depolymerization, proteins can become fragmented into smaller units, which can have significant effects on their structural and techno-functional properties.

3.3.2. Fourier-transform infrared spectroscopy (FTIR) and protein secondary structure

The Fourier transform infrared spectroscopy (FTIR) spectra (Figure 4-a) revealed characteristic bands of Amide A and B, which absorb close to 3300 and 3070 cm^{-1}, respectively (Farjami et al., 2024). They also revealed characteristic bands of Amide I (1600–1700 cm^{-1}), Amide II (1500–1550 cm^{-1}) and Amide III (1200–1300 cm^{-1}) (Li et al., 2022; Sanches et al., 2021a, 2021b). In addition to proteins, FTIR spectra also detected bands characteristic of other macronutrients such as lipids (3000-2800 cm^{-1}) and carbohydrates (1200-900 cm^{-1}) (Andrade et al., 2019; Gholizadeh et al., 2014).

Regarding protein conformation, the Amide I region (1700-1600 cm^{-1}) is the region most susceptible to variations in the secondary structure of proteins, which is influenced by the peptide bonds of the α-helix, β-sheet, β-turn and random coil conformations along the protein chain (Sun et al., 2020). The deconvolution of the amide I region in the FTIR spectrum (1600–1700 cm^{-1}) showed differences in the composition of the secondary structures of the BSG protein concentrate (Figure 4-b). The results showed that all samples contained high β-turn content (42-50%), β-sheet (24-36%), intermediate α-helix content (13-17%), and low random coil content (4-11%).

Among these four secondary structural conformations, the α-helix and the β-sheet are the most ordered structures. EC showed the highest α-helix content, followed by EUS.

Figure 4. Fourier transform infrared spectroscopy (FTIR) (a), secondary structure (b), and XRD diffraction of protein fractions (c).

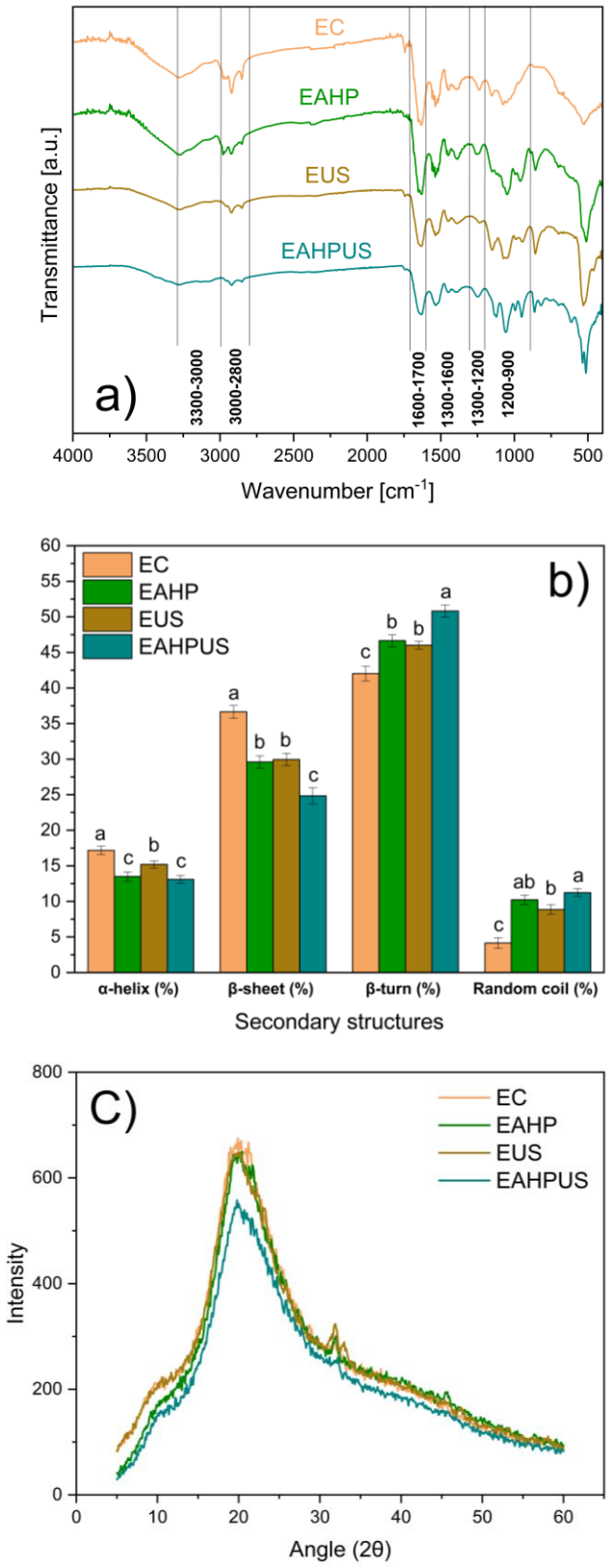

The EAHP and EAHPUS treatments presented the lowest α-helix contents, with no significant difference between them. For β-sheet, EC also showed the highest content among treatments. EUS and EAHP had similar β-sheet contents to each other, while EAHPUS had the lowest content.

On the other hand, β-turn structures are relatively loose and partially ordered. EC presented the lowest β-turn content among the treatments. Furthermore, EAHP and EUS treatments showed similar β-turn content to each other. However, EAHPUS showed the highest β-turn content. Although less ordered, the β-turn still contributes to the three-dimensional stability of proteins.

The random coil is the loosest and most disordered secondary structure. Among the treatments, EAHP and EAHPUS presented the highest random coil contents, with no difference between them. The EUS treatment has a lower random coil content when compared to EAHPUS, but similar to the random coil content of EAHP. Furthermore, all other treatments showed more random coil structures than EC.

These results demonstrate that the initial rigid structure of BSG proteins, extracted by EC, underwent changes in structural conformation when using ultrasound and/or hydrogen peroxide, with these modifications being more intense, especially in treatments that used AHP. Probably, the species of HO and HOO radicals generated by AHP and/or the shear forces, shock waves, micro streaming and free radicals induced by ultrasound probably caused the unfolding or even depolymerization of the proteins (Cui et al., 2021; El-Kadiri et al., 2013). Breaking the covalent bonds (including peptide bonds) and hydrogen bonds that maintain the three-dimensional structure of proteins can lead to a reorganization of secondary structures (Li et al., 2022), resulting in a decrease in more ordered structures, such as α-helices and β-sheets, and an increase in the proportion of more disordered structures, such as β-turns and random coil structures. It is worth noting that these modifications, to a certain extent, can be beneficial, as they result in increased structural flexibility (Sow et al., 2018), and can directly impact the techno-functional properties of proteins.

3.3.3. X-ray diffraction pattern (XRD)

X-ray diffraction (XRD) is currently the predominant method for investigating the existence of amorphous or crystalline regions in the molecular structure of protein concentrates (Mir et al., 2021; Yeasmin et al., 2024; Yu et al.,

2015). Figure 4-c shows the XRD spectra of the protein concentrate obtained after the different extraction processes. The presence of two main peaks is observed: one around 2θ = 10° (crystalline regions I), with low intensity, and the other around 2θ = 20° (crystalline regions II) (Yu et al., 2015), with high intensity. The absence of sharp peaks suggests that the protein concentrate has amorphous characteristics (Malik and Saini, 2018). While crystalline structures exhibit a rigid and well-defined arrangement, amorphous structures are characterized by a more flexible and disorganized structure. Qadir and Wani (2023) reported that the presence of amorphous behavior of protein concentrates indicates that they can be easily combined with macro- and micronutrients for the development of protein-based supplements.

Both peaks in the diffractogram were found at similar angles, but with different intensities. The diffraction intensity and diffraction angle (2θ) are related to the crystal size: the smaller the crystal size, the lower the diffraction intensity and the larger the diffraction angles (Yu et al., 2015). When comparing the EC and EUS diffractograms, a similarity in the peak around 2θ = 10° is observed for both treatments. However, this same peak was reduced in the EAHP and EAHPUS diffractograms. As for the peak around 2θ = 20°, a similarity was noted between the diffractograms for EC, EAHP and EUS, with only a notable reduction in the case of EAHPUS. The reduction in diffraction intensity, mainly for EAHP and EAHPUS, can be attributed to a possible smaller size of the crystals of these protein concentrates. Protein concentrates with smaller structures tend to be more flexible and dynamic, which can also influence their techno-functional properties.

3.3.4. Techno-functional properties of protein concentrate

3.3.4.1. Water holding capacity (WHC) and oil holding capacity (OHC)

WHC and OHC are important technological properties of proteins, which not only direct their possible applications, but also have a significant impact on technological and sensory properties when applied to products (Dakhili et al., 2019; Dnyaneshwar Patil et al., 2024). WHC of BSG protein concentrate ranged from 3.24 – 5.17 (g/g). Different protein concentrates plant-based (pigeon peas, faba beans, peas, chickpeas) presented WHC of 0.58 – 4.5 (g/g) (Dnyaneshwar Patil et al., 2024; Locali-Pereira et al., 2024; do Carmo et al., 2020). These results

indicate that the protein concentrate of BSG have a water holding capacity similar to that of other plant-based proteins, highlighting their potential for various applications in the food industry. High WHC values of proteins are desirable in gel-like foods, such as mayonnaise, creams, and meat products such as sausage, mortadella, cooked ham as proteins retain water and provide a desirable texture to the products (Barretto et al., 2022).

As shown in Figure 5-a, WHC was increased in EUS when compared to EC. On the other hand, EAHP and EAHPUS presented lower WHC when compared to EC. Deconvolution of FTIR spectra revealed that EUS, EAHP and EAHPUS underwent modifications in their secondary structures, including a reduction in more ordered structures and an increase in the proportion of more disordered structures, which are related to the unfolding of the protein structure. However, these modifications to protein structures can have different effects depending on the treatment. The modifications caused in EUS seem to have improved the interactions of proteins with water molecules, which may be related to the exposure of peptide bonds and polar side chains of proteins (Li et al., 2021). On the other hand, AHP-induced modifications appear to negatively affect the ability to interact with water molecules, either due to the exposure of hydrophobic groups buried within the molecular protein or to a reduction in the availability of binding sites (Li et al., 2021), even in the case where ultrasound was applied in combination with AHP (EAHPUS). Furthermore, such differences could also be due to the other non-protein compounds that were extracted in EAHP and EAHPUS, as these treatments have the lowest protein contents.

On the other hand, OHC (Figure 5-a) was the only techno-functional properties evaluated that was not affected by any of the treatments. In the present study, the OHC of protein concentrate varied between 3.16 and 3.36 (g/g), with no significant difference between treatments. Silva et al. (2023) evaluated the influence of pH (8-12) and extraction temperature (40-60 °C) and did not observe effects on the OHC (3,2 – 5,1 g/g) of BSG protein concentrate. OHC is influenced by the interaction of the aliphatic chains of lipids with the nonpolar side chains of the amino acids of proteins (Withana-Gamage et al., 2011).

Figure 5. Techno-functional properties of protein fractions.

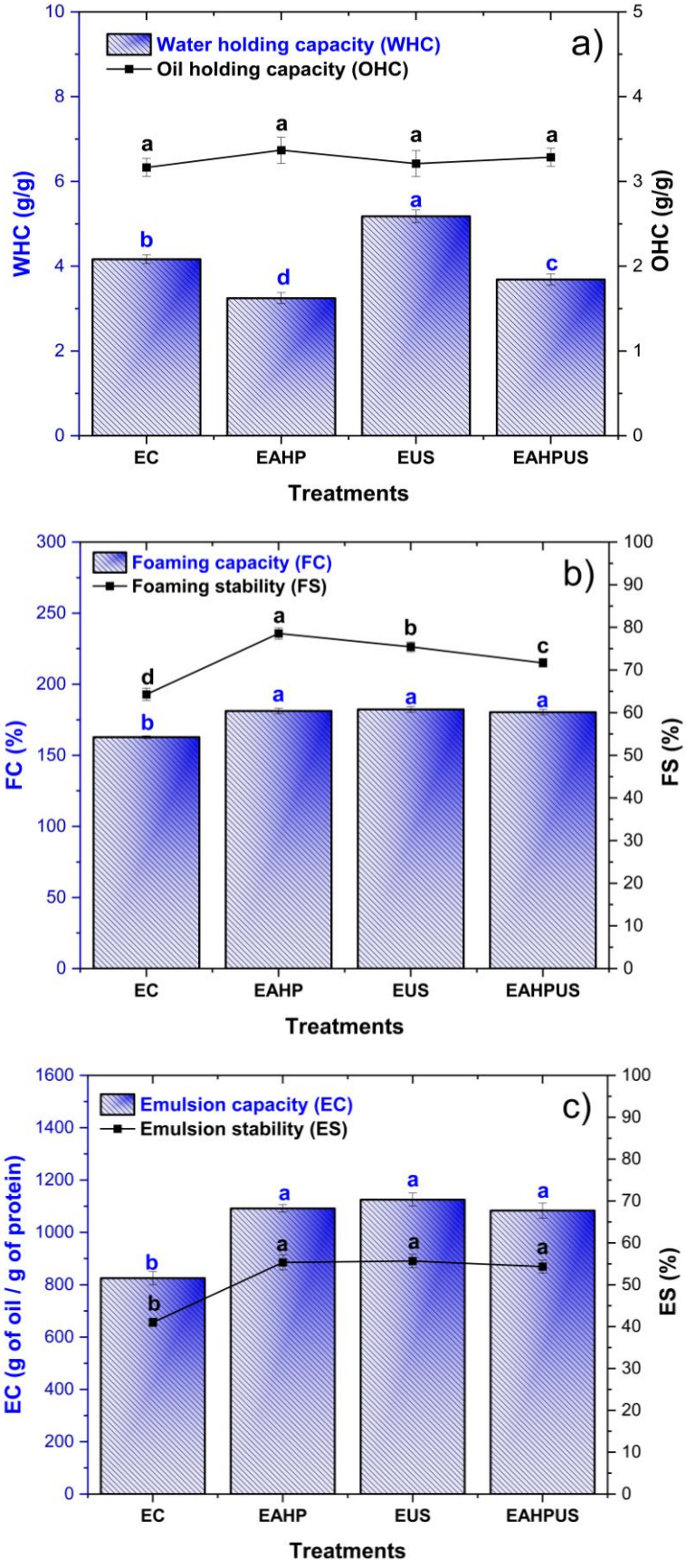

However, although the different protein concentrates in this study have different protein contents, these results suggest that OHC does not depend solely on the total amount of proteins in the different concentrates. Although the affinity of hydrophilic or lipophilic groups can influence OHC, it is important to highlight that this property is mainly attributed to the physical entrapment of the oil (Kinsella, 1979).

The results of this study highlight the high OHC of BSG protein concentrate, especially when compared to other established sources of vegetable proteins. While previous studies found an OHC between 1.5 and 2.8 g/g for pea protein (Kapoor et al., 2024), less than 2 g/g for soy protein concentrate and isolate (Gouvêa et al., 2023), and quinoa protein concentrate (2.4 – 2.8 g/g) (Wang et al., 2021), our results showed higher values. This can be attributed to the rich profile of hydrophobic amino acids found in BSG, including phenylalanine, valine, leucine, isoleucine, and methionine, originating from barley hordein and glutelins, since a large part of the hydrophilic proteins are carried into the must, during beer manufacturing. These results highlight the potential of BSG as an exceptional source of protein, with broad applications in the food industry.

3.3.4.2. Foaming capacity (FC) and stability (FS)

Proteins have the ability to form a thin and resistant film at the interface between air and water, resulting in the formation of foams when dispersed in an aqueous medium (McClements, 2004). This ability of proteins to remain at the interface and kinetically stabilize large amounts of air is crucial to foaming capacity (FC) and foam stability (FS). In this study, FC varied between 165 and 181% (Figure 5-b), with a small, but significant difference among treatments. EAHP, EUS and EAHPUS showed higher FC, indicating that these concentrates were more capable of unfolding, adsorbing at the air-water interface, and reducing interfacial tension (Stone et al., 2015) when compared to EC.

Furthermore, FS (Figure 5-b) was also increased for all treatments (EAHP, EUS and EAHPUS), when compared to CE. After 120 min, the FS for EUS and EAHPUS decreased significantly when compared to EAHP, with this reduction being more drastic in the case of EAHPUS. However, even after 120 min, CE still presented the lowest FS when compared to the other treatments.

The improvement in foam formation and stability in protein concentrate obtained with ultrasound (US) and/or alkaline hydrogen peroxide (AHP) is probably related to the structural changes induced by these treatments. Fragmentation and disorder in morphology, together with modifications in protein secondary structures, suggest greater flexibility in EAHP, EUS and EAHPUS protein concentrates. These changes allowed protein particles to disperse more efficiently at the air-water interface (Shevkani et al., 2015), allowing the encapsulation of air bubbles and, consequently, contributing to increased foam formation properties and stability of proteins.

3.3.4.3. Emulsion capacity (EC) and stability (ES)

Emulsifying capacity indicates the amount of oil that a protein can emulsify in relation to the total weight of the emulsion, under specific conditions. It was observed that different extraction methods resulted in significant changes in emulsion capacity, ranging from 825 to 1125 g oil/g protein (Figure 5-c). The EAHP, EUS and EAHPUS concentrate showed a similar emulsifying capacity, superior to that observed in the EC treatment.

On the other hand, ES was investigated in a 50/50 oil-in-water emulsion. It was found that, in all cases, ES decreased over time. However, the EAHP, EUS and EAHPUS concentrate showed a higher ES (Figure 5-c), especially after 60, 90 and 120 minutes, compared to the EC treatment. This suggests a greater resistance to the collapse of emulsions and an effective dispersion of oil droplets throughout the aqueous phase, attributed to the resistance of the viscoelastic film at the interface and the charge repulsion and steric hindrance between the droplets (Stone et al., 2015).

The improvement in EC and ES of protein concentrate obtained with US and/or AHP is probably linked to the structural changes induced by these treatments, mainly in relation to the secondary structures of proteins, characterized by an increase in relatively loose and disordered structures. These structural modifications may have improved the interfacial properties, together with a greater exposure of hydrophobic groups on the surface of the proteins, generating a balanced structure in hydrophobic and hydrophilic terms, which adsorbed well to the interface, as was also observed in FC and FS. It is worth mentioning that the combined treatment (EAHPUS) did not result in additional improvement when compared to treatments with US alone (EUS) or

with AHP (EAHP).

3.3.4.4. Instrumental color

The visual aspects and color parameters (L*, a*, b*, C*, h* and ΔE) of the protein concentrate are presented in Table 1.

Table 1. Color parameters of BSG protein concentrate.

Parameters	EC	EAHP	EUS	EAHPUS
Visual aspects				
L*	52.538 ± 0.276 ^{c}	86.029 ± 0.029 ^{a}	52.787 ± 0.421 ^{c}	85.682 ± 0.040 ^{b}
a*	8.463 ± 0.179 ^{a}	0.295 ± 0.012 ^{d}	7.59 ± 0.086 ^{b}	0.437 ± 0.006 ^{c}
b*	18.405 ± 0.439 ^{c}	20.327 ± 0.177 ^{b}	18.766 ± 0.13 ^{c}	20.726 ± 0.262 ^{a}
C*	22.093 ± 0.475 ^{a}	20.328 ± 0.178 ^{d}	22.243 ± 0.153 ^{a}	20.730 ± 0.258 ^{b}
°h	67.472 ± 0.043 ^{d}	89.201 ± 0.035 ^{a}	67.983 ± 0.088 ^{c}	88.796 ± 0.016 ^{b}
ΔE	--	34.486 ± 0.292 ^{a}	1.885 ± 0.310 ^{b}	34.104 ± 0.286 ^{a}

Significant differences were observed between the protein concentrate due to the different extraction methods. The higher L* values indicated that the EAHP and EAHPUS concentrate are clear compared to EC and EUS. On the other hand, the highest values of the a* coordinate for EC and EUS indicated the predominance of the red color, while the lowest values of b* indicated that they are less yellow. Furthermore, the higher C* values suggest a greater color intensity compared to EAHP and EAHPUS. For EAHP and EAHPUS, the hue angle (h*) indicated a greater propensity for yellow tones, while EC and EUS tended towards red tones.

The differences between the parameters L*, a* and b*, when considered together, express the total color difference (ΔE). It is widely accepted that a ΔE value of less than three units indicates that there are no noticeable differences in color to human eyes (Camelo-Silva et al., 2024; Martínez-Cervera et al., 2011). In this study, the differences between EUS and EC are not noticeable, demonstrating that the cavitation generated by ultrasound technology was able

to improve the extraction yield, modify the secondary structures of proteins and improve their techno-functional properties, without causing an apparent change in the color of the EUS protein concentrate.

On the other hand, the differences between EAHP and EAHPUS, when compared to EC, are extremely noticeable. These results are probably attributed to the decomposition of AHP, which generates OH^- anions and can cause bleaching due to peroxide activation, generating the perhydroxyl ion HOO^- (Ho et al., 2019). These ions are responsible for the oxidation of pigments, mainly quinones, resulting from phenolic oxidation (Aïder et al., 2012). This effect is known and widely used in the literature for bleaching purposes (Aider et al., 2024, 2023; Yoshida and Prudencio, 2020).

It is important to highlight that changes in the color of protein concentrate, especially those obtained with AHP, are not undesirable. The AHP bleaching process makes it possible to include these concentrate as additives in light-colored products, such as pasta and bakery products, aiming to increase the protein content and add nutritional value, without major changes in its chromatic parameters, an important characteristic for the organoleptic acceptance of the products by the consumer.

4. CONCLUSIONS

Our study investigated the effects of different strategies using ultrasound (US) and/or alkaline hydrogen peroxide (AHP) to extract proteins from BSG and evaluated the impact on the extraction yield, structural and techno-functional properties of the protein concentrate. BSG has been shown to be a protein-rich byproduct containing a variety of essential and non-essential amino acids. Extractions using AHP (EAHP), or US (EUS) induced significant structural changes, which made the BSG matrix more accessible and improved the protein extraction yield when compared to extraction using conventional method (EC). The combination of these treatments (EAHPUS) proved to be even more effective, resulting in greater disintegration of the BSG matrix and greater protein extraction yield, when compared to the other treatments.

Regarding structural properties, SEM images revealed changes in the morphology of EAHP, EUS and EAHPUS protein concentrate, showing fragmentation and disordered arrangement. The FTIR spectra of these

concentrate also indicated changes in the secondary structures of the proteins, evidenced by a reduction in more ordered structures, such as α-helix and β-sheet, and an increase in partially ordered (β-turn) and disordered (random coil) structures. Furthermore, X-ray diffraction spectra corroborated these changes, suggesting a smaller size of the protein concentrate crystals. It is worth noting that these structural modifications indicated an increase in the flexibility and degree of unfolding of the protein concentrate and were more pronounced in the EAHP and EAHPUS concentrate, due to the oxidizing properties of AHP.

Regarding techno-functional properties, it was observed that water holding capacity was improved in EUS and reduced in EAHP and EAHPUS, compared to EC. There was no significant effect on oil holding capacity. EUS concentrate showed no visible differences in color compared to EC, while those treated with AHP (EAHP and EAHPUS) exhibited a noticeable change in color. On the other hand, foaming capacity, and stability as well as emulsion capacity and stability were improved in EUS, EAHP, and EAHPUS compared to EC. The increase in protein flexibility and unfolding may explain these improvements in techno-functional properties. Therefore, our results highlight the potential of using ultrasound and/or alkaline hydrogen peroxide to improve the extraction yield, structural and techno-functional properties of BSG proteins.

Declaration of competing interest

The authors declare no conflict of interest.

Acknowledgments

This study was financed in part by the São Paulo Research Foundation (FAPESP) – Grant n°2022/05272-8 and by the Coordenação de Aperfeiçoamento de Pessoal de Nível Superior - Brasil (CAPES) - Finance Code 001.

Communauté Urbaine du Grand Reims, Département de la Marne, Région Grand Est and European Union (FEDER Champagne-Ardenne 2014-2020, FEDER Grand Est 2021-2027) are acknowledged for their financial support to the Chair of Biotechnology of CentraleSupélec and the Centre Européen de Biotechnologie et de Bioéconomie (CEBB).

5. REFERENCES

Agrawal, D., Gopaliya, D., Willoughby, N., Khare, S.K., Kumar, V., 2023. Recycling potential of brewer's spent grains for circular biorefineries. **Curr Opin Green Sustain Chem** 40, 100748. https://doi.org/10.1016/J.COGSC.2022.100748

Aïder, M., Martel, A.A., Ferracci, J., de Halleux, D., 2012. Purification of Whole Brown Flaxseed Meal from Coloring Pigments by Treatment in Hydrogen Peroxide Solutions: Impact on Meal Color. **Food Bioproc Tech** 5, 3051–3065. https://doi.org/10.1007/S11947-011-0632-5/TABLES/3

Aider, M., Ndiaye, M., Karim, A., 2023. Optimization of canola meal bleaching by hydrogen peroxide, protein extraction and characterization of their functional properties. **Future Foods** 8, 100282. https://doi.org/10.1016/J.FUFO.2023.100282

Aider, M., Zaddem, M., Karim, A., 2024. Digital monitoring and response surface methodology optimization of wheat bran bleaching by hydrogen peroxide and its incorporation into wheat Flour. **Future Foods** 9, 100327. https://doi.org/10.1016/J.FUFO.2024.100327

Alonso-Riaño, P., Melgosa, R., Trigueros, E., Illera, A.E., Beltrán, S., Sanz, M.T., 2022. Valorization of brewer's spent grain by consecutive supercritical carbon dioxide extraction and enzymatic hydrolysis. **Food Chem** 396, 133493. https://doi.org/10.1016/J.FOODCHEM.2022.133493

Alonso-Riaño, P., Sanz, M.T., Benito-Román, O., Beltrán, S., Trigueros, E., 2021. Subcritical water as hydrolytic medium to recover and fractionate the protein fraction and phenolic compounds from craft brewer's spent grain. **Food Chem** 351, 129264. https://doi.org/10.1016/J.FOODCHEM.2021.129264

Andrade, J., Pereira, C.G., Almeida Junior, J.C. de, Viana, C.C.R., Neves, L.N. de O., Silva, P.H.F. da, Bell, M.J.V., Anjos, V. de C. dos, 2019. FTIR-ATR determination of protein content to evaluate whey protein concentrate adulteration. **LWT** 99, 166–172. https://doi.org/10.1016/J.LWT.2018.09.079

AOAC, 2007. Association of Official Analytical Chemistry, 18th ed, **In: Official methods of analysis to AOAC International**. Gaithersburg.

Arantes da Fonseca, Y., Gurgel, L.V.A., Baêta, B.E.L., Dragone, G., Mussatto, S.I., 2023. Reduced-pressure alkaline pretreatment as an innovative and sustainable technology to extract protein from brewer's spent grain. **J Clean Prod** 416, 137966. https://doi.org/10.1016/J.JCLEPRO.2023.137966

Assandri, D., Pampuro, N., Zara, G., Cavallo, E., Budroni, M., 2020. Suitability of Composting Process for the Disposal and Valorization of Brewer's Spent Grain. **Agriculture** 2021, Vol. 11, Page 2 11, 2. https://doi.org/10.3390/AGRICULTURE11010002

Bacic, A., Stone, B., 1981. Chemistry and Organization of Aleurone Cell Wall Components From Wheat and Barley. **Functional Plant Biology** 8, 475–495. https://doi.org/10.1071/PP9810475

Barretto, T.L., Sanches, M.A.R., Pateiro, M., Lorenzo, J.M., Telis-Romero, J., da Silva Barretto, A.C., 2022. Recent advances in the application of ultrasound to meat and meat products: Physicochemical and sensory aspects. **Food Reviews International** 39, 4529–4544. https://doi.org/10.1080/87559129.2022.2028285

Bayomie, O.S., Romdhana, H., 2023. Cleaner green protein production from vegetable byproducts: Energy recovery and water reuse strategies. **Sustain Prod Consum** 40, 389–397. https://doi.org/10.1016/J.SPC.2023.07.004

Camelo-Silva, C., Mota e Souza, B., Vicente, R., Arend, G.D., Sanches, M.A.R., Barreto, P.L.M., Ambrosi, A., Verruck, S., Di Luccio, M., 2024. Polyfunctional sugar-free white chocolate fortified with Lacticaseibacillus rhamnosus GG co-encapsulated with beet residue extract (Beta vulgaris L.). **Food Research International** 179, 114016. https://doi.org/10.1016/J.FOODRES.2024.114016

Cui, Q., Wang, L., Wang, G., Zhang, A., Wang, X., Jiang, L., 2021. Ultrasonication effects on physicochemical and emulsifying properties of Cyperus esculentus seed (tiger nut) proteins. **LWT** 142, 110979. https://doi.org/10.1016/J.LWT.2021.110979

Dakhili, S., Abdolalizadeh, L., Hosseini, S.M., Shojaee-Aliabadi, S., Mirmoghtadaie, L., 2019. Quinoa protein: Composition, structure and functional

properties. **Food Chem** 299, 125161. https://doi.org/10.1016/J.FOODCHEM.2019.125161

de Paiva Gouvêa, L., Caldeira, R., de Lima Azevedo, T., Galdeano, M.C., Felberg, I., Lima, J.R., Grassi Mellinger, C., 2023. Physical and techno-functional properties of a common bean protein concentrate compared to commercial legume ingredients for the plant-based market. **Food Hydrocoll** 137, 108351. https://doi.org/10.1016/J.FOODHYD.2022.108351

Deb, S., Kumar, Y., Saxena, D.C., 2022. Functional, thermal and structural properties of fractionated protein from waste banana peel. **Food Chem X** 13, 100205. https://doi.org/10.1016/J.FOCHX.2022.100205

Dnyaneshwar Patil, N., Bains, A., Kaur, S., Yadav, R., Ali, N., Patil, S., Goksen, G., Chawla, P., 2024. Influence of dual succinylation and ultrasonication modification on the amino acid content, structural and functional properties of Chickpea (Cicer arietinum L.) protein concentrate. **Food Chem** 445, 138671. https://doi.org/10.1016/J.FOODCHEM.2024.138671

El-Kadiri, I., Khelifi, M., Aider, M., 2013. The effect of hydrogen peroxide bleaching of canola meal on product colour, dry matter and protein extractability and molecular weight profile. **Int J Food Sci Technol** 48, 1071–1085. https://doi.org/10.1111/IJFS.12065

Farjami, T., Sharma, A., Hagen, L., Jensen, I.J., Falch, E., 2024. Comparative study on composition and functional properties of brewer's spent grain proteins precipitated by citric acid and hydrochloric acid. **Food Chem** 446, 138863. https://doi.org/10.1016/J.FOODCHEM.2024.138863

Fasolin, L.H., Pereira, R.N., Pinheiro, A.C., Martins, J.T., Andrade, C.C.P., Ramos, O.L., Vicente, A.A., 2019. Emergent food proteins – Towards sustainability, health and innovation. **Food Research International** 125, 108586. https://doi.org/10.1016/J.FOODRES.2019.108586

Fontana, I.B., Peterson, M., Cechinel, M.A.P., 2018. Application of brewing waste as biosorbent for the removal of metallic ions present in groundwater and surface waters from coal regions. **J Environ Chem Eng** 6, 660–670. https://doi.org/10.1016/J.JECE.2018.01.005

Gholizadeh, H., Naserian, A.A., Xin, H., Valizadeh, R., Tahmasbi, A.M., Yu, P., 2014. Detecting carbohydrate molecular structural makeup in different types of cereal grains and different cultivars within each type of grain grown in semi-arid area using FTIR spectroscopy with uni- and multi-variate molecular spectral analyses. **Anim Feed Sci Technol** 194, 136–144. https://doi.org/10.1016/J.ANIFEEDSCI.2014.05.007

González-García, E., Marina, M.L., García, M.C., 2021. Impact of the use of pressurized liquids on the extraction and functionality of proteins and bioactives from brewer's spent grain. **Food Chem** 359, 129874. https://doi.org/10.1016/J.FOODCHEM.2021.129874

Hadidi, M., Boostani, S., Jafari, S.M., 2022. Pea proteins as emerging biopolymers for the emulsification and encapsulation of food bioactives. **Food Hydrocoll** 126, 107474. https://doi.org/10.1016/J.FOODHYD.2021.107474

Hagen, S.R., Frost, B., Augustin, J., 1989. Precolumn Phenylisothiocyanate Derivatization and Liquid Chromatography of Amino Acids in Food. **J AOAC Int** 72, 912–916. https://doi.org/10.1093/JAOAC/72.6.912

Ho, M.C., Ong, V.Z., Wu, T.Y., 2019. Potential use of alkaline hydrogen peroxide in lignocellulosic biomass pretreatment and valorization – A review. **Renewable and Sustainable Energy Reviews** 112, 75–86. https://doi.org/10.1016/J.RSER.2019.04.082

Huang, Z., Qu, Y., Hua, X., Wang, F., Jia, X., Yin, L., 2023. Recent advances in soybean protein processing technologies: A review of preparation, alterations in the conformational and functional properties. **Int J Biol Macromol** 248, 125862. https://doi.org/10.1016/J.IJBIOMAC.2023.125862

Ibbett, R., White, R., Tucker, G., Foster, T., 2019. Hydro-mechanical processing of brewer's spent grain as a novel route for separation of protein products with differentiated techno-functional properties. **Innovative Food Science & Emerging Technologies** 56, 102184. https://doi.org/10.1016/J.IFSET.2019.102184

Kadam, S.U., Tiwari, B.K., Álvarez, C., O'Donnell, C.P., 2015. Ultrasound applications for the extraction, identification and delivery of food proteins and

bioactive peptides. **Trends Food Sci Technol** 46, 60–67. https://doi.org/10.1016/J.TIFS.2015.07.012

Kapoor, R., Karabulut, G., Mundada, V., Feng, H., 2024. Unraveling the potential of non-thermal ultrasonic contact drying for enhanced functional and structural attributes of pea protein isolates: A comparative study with spray and freeze-drying methods. **Food Chem** 439, 138137. https://doi.org/10.1016/J.FOODCHEM.2023.138137

Kavalopoulos, M., Stoumpou, V., Christofi, A., Mai, S., Barampouti, E.M., Moustakas, K., Malamis, D., Loizidou, M., 2021. Sustainable valorisation pathways mitigating environmental pollution from brewers' spent grains. **Environmental Pollution** 270, 116069. https://doi.org/10.1016/J.ENVPOL.2020.116069

Kinsella, J.E., 1979. Functional properties of soy proteins. **J Am Oil Chem Soc** 56, 242–258. https://doi.org/10.1007/BF02671468

Li, Q., Yang, H., Coldea, T.E., Andersen, M.L., Li, W., Zhao, H., 2022. Enzymolysis kinetics, thermodynamics and structural property of brewer's spent grain protein pretreated with ultrasound. **Food and Bioproducts Processing** 132, 130–140. https://doi.org/10.1016/J.FBP.2022.01.001

Li, W., Yang, H., Coldea, T.E., Zhao, H., 2021. Modification of structural and functional characteristics of brewer's spent grain protein by ultrasound assisted extraction. **LWT** 139, 110582. https://doi.org/10.1016/J.LWT.2020.110582

Lima Moraes dos Santos, A., de Sousa e Silva, A., Sales Morais, N.W., Bezerra dos Santos, A., 2023. Brewery Spent Grain as sustainable source for value-added bioproducts: Opportunities and new insights in the integrated lignocellulosic biorefinery concept. **Ind Crops Prod** 206, 117685. https://doi.org/10.1016/J.INDCROP.2023.117685

Ling, B., Ouyang, S., Wang, S., 2019. Effect of radio frequency treatment on functional, structural and thermal behaviors of protein isolates in rice bran. **Food Chem** 289, 537–544. https://doi.org/10.1016/J.FOODCHEM.2019.03.072

Locali-Pereira, A.R., Caruso, Í.P., Rabesona, H., Laurent, S., Meynier, A., Kermarrec, A., Birault, L., Geairon, A., Le Gall, S., Thoulouze, L., Solé-Jamault,

V., Berton-Carabin, C., Boire, A., Nicoletti, V.R., 2024. Pre-treatment effects on the composition and functionalities of pigeon pea seed ingredients. **Food Hydrocoll** 152, 109923. https://doi.org/10.1016/J.FOODHYD.2024.109923

Lu, Z.X., He, J.F., Zhang, Y.C., Bing, D.J., 2019. Composition, physicochemical properties of pea protein and its application in functional foods. **Critical reviews in food science and nutrition**, v. 60, n. 15, p. 2593-2605, 2020. https://doi.org/10.1080/10408398.2019.1651248

Lynch, K.M., Steffen, E.J., Arendt, E.K., 2016. Brewers' spent grain: a review with an emphasis on food and health. **Journal of the Institute of Brewing** 122, 553–568. https://doi.org/10.1002/JIB.363

Malik, M.A., Saini, C.S., 2018. Rheological and structural properties of protein isolates extracted from dephenolized sunflower meal: Effect of high intensity ultrasound. **Food Hydrocoll** 81, 229–241. https://doi.org/10.1016/J.FOODHYD.2018.02.052

Martínez-Cervera, S., Salvador, A., Muguerza, B., Moulay, L., Fiszman, S.M., 2011. Cocoa fibre and its application as a fat replacer in chocolate muffins. **LWT - Food Science and Technology** 44, 729–736. https://doi.org/10.1016/J.LWT.2010.06.035

McClements, D.J., 2004. Protein-stabilized emulsions. **Curr Opin Colloid Interface Sci** 9, 305–313. https://doi.org/10.1016/J.COCIS.2004.09.003

Miano, A.C., Ibarz, A., Augusto, P.E.D., 2017. Ultrasound technology enhances the hydration of corn kernels without affecting their starch properties. **J Food Eng** 197, 34–43. https://doi.org/10.1016/J.JFOODENG.2016.10.024

Mir, N.A., Riar, C.S., Singh, S., 2021. Rheological, structural and thermal characteristics of protein isolates obtained from album (Chenopodium album) and quinoa (Chenopodium quinoa) seeds. **Food Hydrocolloids for Health** 1, 100019. https://doi.org/10.1016/J.FHFH.2021.100019

Pabbathi, N.P.P., Velidandi, A., Pogula, S., Gandam, P.K., Baadhe, R.R., Sharma, M., Sirohi, R., Thakur, V.K., Gupta, V.K., 2022. Brewer's spent grains-based biorefineries: A critical review. **Fuel** 317, 123435. https://doi.org/10.1016/J.FUEL.2022.123435

Paz, A., Outeiriño, D., Pérez Guerra, N., Domínguez, J.M., 2019. Enzymatic hydrolysis of brewer's spent grain to obtain fermentable sugars. **Bioresour Technol** 275, 402–409. https://doi.org/10.1016/J.BIORTECH.2018.12.082

Pereira, G.N., Cesca, K., Cubas, A.L.V., Bianchet, R.T., Junior, S.E.B., Zanella, E., Stambuk, B.U., Poletto, P., de Oliveira, D., 2021. Non-thermal plasma as an innovative pretreatment technology in delignification of brewery by-product. **Innovative Food Science & Emerging Technologies** 74, 102827. https://doi.org/10.1016/J.IFSET.2021.102827

Qadir, N., Wani, I.A., 2023. Protein concentrates from plain, aromatic and pigmented rice cultivars: Functional, thermal and morphological characterization. **Food Chemistry Advances** 3, 100499. https://doi.org/10.1016/J.FOCHA.2023.100499

Qin, F., Johansen, A.Z., Mussatto, S.I., 2018. Evaluation of different pretreatment strategies for protein extraction from brewer's spent grains. **Ind Crops Prod** 125, 443–453. https://doi.org/10.1016/J.INDCROP.2018.09.017

Ravindran, R., Sarangapani, C., Jaiswal, S., Lu, P., Cullen, P.J., Bourke, P., Jaiswal, A.K., 2019. Improving enzymatic hydrolysis of brewer spent grain with nonthermal plasma. **Bioresour Technol** 282, 520–524. https://doi.org/10.1016/J.BIORTECH.2019.03.071

Ribeiro Sanches, M.A., Camelo-Silva, C., da Silva Carvalho, C., Rafael de Mello, J., Barroso, N.G., Lopes da Silva Barros, E., Silva, P.P., Pertuzatti, P.B., 2021a. Active packaging with starch, red cabbage extract and sweet whey: Characterization and application in meat. **LWT** 135, 110275. https://doi.org/10.1016/j.lwt.2020.110275

Ribeiro Sanches, M.A., Camelo-Silva, C., Tussolini, L., Tussolini, M., Zambiazi, R.C., Becker Pertuzatti, P., 2021b. Development, characterization and optimization of biopolymers films based on starch and flour from jabuticaba (Myrciaria cauliflora) peel. **Food Chem** 343, 128430. https://doi.org/10.1016/j.foodchem.2020.128430

Rodriguez, L.M., Camina, J.L., Borroni, V., Pérez, E.E., 2023. Protein recovery from brewery solid wastes. **Food Chem** 407, 134810. https://doi.org/10.1016/J.FOODCHEM.2022.134810

Rosas Ulloa, P., Ulloa, J.A., Ulloa Rangel, B.E., López Mártir, K.U., 2023. Protein Isolate from Orange (Citrus sinensis L.) Seeds: Effect of High-Intensity Ultrasound on Its Physicochemical and Functional Properties. **Food Bioproc Tech** 16, 589–602. https://doi.org/10.1007/S11947-022-02956-4/FIGURES/2

Saldanha do Carmo, C., Silventoinen, P., Nordgård, C.T., Poudroux, C., Dessev, T., Zobel, H., Holtekjølen, A.K., Draget, K.I., Holopainen-Mantila, U., Knutsen, S.H., Sahlstrøm, S., 2020. Is dehulling of peas and faba beans necessary prior to dry fractionation for the production of protein- and starch-rich fractions? Impact on physical properties, chemical composition and techno-functional properties. **J Food Eng** 278, 109937. https://doi.org/10.1016/J.JFOODENG.2020.109937

Sanches, M.A.R., Augusto, P.E.D., Polachini, T.C., Telis-Romero, J., 2023. Water sorption properties of brewer's spent grain: A study aimed at its stabilization for further conversion into value-added products. **Biomass Bioenergy** 170, 106718. https://doi.org/10.1016/J.BIOMBIOE.2023.106718

Shevkani, K., Singh, N., Kaur, A., Rana, J.C., 2015. Structural and functional characterization of kidney bean and field pea protein isolates: A comparative study. **Food Hydrocoll** 43, 679–689. https://doi.org/10.1016/J.FOODHYD.2014.07.024

Silva, A.M.M. da, Almeida, F.S., Silva, M.F. da, Goldbeck, R., Sato, A.C.K., 2023. How do pH and temperature influence extraction yield, physicochemical, functional, and rheological characteristics of brewer spent grain protein concentrates? **Food and Bioproducts Processing** 139, 34–45. https://doi.org/10.1016/J.FBP.2023.03.001

Singh, P., Krishnaswamy, K., 2022. Sustainable zero-waste processing system for soybeans and soy by-product valorization. **Trends Food Sci Technol** 128, 331–344. https://doi.org/10.1016/J.TIFS.2022.08.015

Sow, L.C., Nicole Chong, J.M., Liao, Q.X., Yang, H., 2018. Effects of κ-carrageenan on the structure and rheological properties of fish gelatin. **J Food Eng** 239, 92–103. https://doi.org/10.1016/J.JFOODENG.2018.05.035

Spies, J.R., 1949. Determination of Tryptophan in Proteins. Hoppe Seylers Z. **Physiol. Chem** 21, 156.

Stone, A.K., Karalash, A., Tyler, R.T., Warkentin, T.D., Nickerson, M.T., 2015. Functional attributes of pea protein isolates prepared using different extraction methods and cultivars. **Food Research International** 76, 31–38. https://doi.org/10.1016/J.FOODRES.2014.11.017

Sun, W., Zhang, Z., Li, X., Lu, X., Liu, G., Qin, Y., Zhao, J., Qu, Y., 2024. Production of single cell protein from brewer's spent grain through enzymatic saccharification and fermentation enhanced by ammoniation pretreatment. **Bioresour Technol** 394, 130242. https://doi.org/10.1016/J.BIORTECH.2023.130242

Sun, X., Ohanenye, I.C., Ahmed, T., Udenigwe, C.C., 2020. Microwave treatment increased protein digestibility of pigeon pea (Cajanus cajan) flour: Elucidation of underlying mechanisms**. Food Chem** 329, 127196. https://doi.org/10.1016/J.FOODCHEM.2020.127196

Telles, A.C., Kupski, L., Furlong, E.B., 2017. Phenolic compound in beans as protection against mycotoxins. **Food Chem** 214, 293–299. https://doi.org/10.1016/J.FOODCHEM.2016.07.079

Wagner, E., Pería, M.E., Ortiz, G.E., Rojas, N.L., Ghiringhelli, P.D., 2021. Valorization of brewer's spent grain by different strategies of structural destabilization and enzymatic saccharification. **Ind Crops Prod** 163, 113329. https://doi.org/10.1016/J.INDCROP.2021.113329

Wang, J.S., Wang, A.B., Zang, X.P., Tan, L., Xu, B.Y., Chen, H.H., Jin, Z.Q., Ma, W.H., 2019. Physicochemical, functional and emulsion properties of edible protein from avocado (Persea americana Mill.) oil processing by-products. **Food Chem** 288, 146–153. https://doi.org/10.1016/J.FOODCHEM.2019.02.098

Wang, L., Dong, J. lin, Zhu, Y. ying, Shen, R. ling, Wu, L. gen, Zhang, K. yi, 2021. Effects of microwave heating, steaming, boiling and baking on the structure and

functional properties of quinoa (Chenopodium quinoa Willd.) protein isolates**. Int J Food Sci Technol** 56, 709–720. https://doi.org/10.1111/IJFS.14706

White, J.A., Hart, R.J., Fry, J.C., n.d. An evaluation of the Waters Pico-Tag system for the amino-acid analysis of food materials. **Journal of Automatic Chemistry of Clinical Laboratory Automation** 8, 170–177.

Withana-Gamage, T.S., Wanasundara, J.P., Pietrasik, Z., Shand, P.J., 2011. Physicochemical, thermal and functional characterisation of protein isolates from Kabuli and Desi chickpea (Cicer arietinum L.): a comparative study with soy (Glycine max) and pea (Pisum sativum L.). **J Sci Food Agric** 91, 1022–1031. https://doi.org/10.1002/JSFA.4277

Yeasmin, F., Prasad, P., Sahu, J.K., 2024. Effect of ultrasound on physicochemical, functional and antioxidant properties of red kidney bean (Phaseolus vulgaris L.) proteins extract. **Food Biosci** 57, 103599. https://doi.org/10.1016/J.FBIO.2024.103599

Yoshida, B.Y., Prudencio, S.H., 2020. Alkaline hydrogen peroxide improves physical, chemical, and techno-functional properties of okara. **Food Chem** 323, 126776. https://doi.org/10.1016/J.FOODCHEM.2020.126776

Yu, L., Yang, W., Sun, J., Zhang, C., Bi, J., Yang, Q., 2015. Preparation, characterisation and physicochemical properties of the phosphate modified peanut protein obtained from Arachin Conarachin L. **Food Chem** 170, 169–179.

Zhang, J., Li, K., Liu, S., Huang, S., Xu, C., 2022. Alkaline hydrogen peroxide pretreatment combined with bio-additives to boost high-solids enzymatic hydrolysis of sugarcane bagasse for succinic acid processing. **Bioresour Technol** 345, 126550. https://doi.org/10.1016/J.BIORTECH.2021.126550

4. CONCLUSÃO GERAL

O bagaço de malte (BSG) apresenta um vasto potencial devido a sua composição rica principalmente em proteínas, celulose, hemicelulose e compostos bioativos. Embora tenha sido explorado em várias aplicações promissoras, como na obtenção de proteínas vegetais e produção de bioetanol, ainda há desafios a serem superados, especialmente em relação ao gerenciamento pós-geração e etapas de pré-tratamento eficientes. A otimização das etapas de secagem, armazenamento e pré-tratamento é essencial para o seu aproveitamento, garantindo a viabilidade desses processos e a maximização dos rendimentos dos produtos.

Em relação as propriedades de adsorção de água do BSG obtido do processo cervejeiro à base de malte de cevada (“Lager” – BSGL) e de trigo (“Weiss” – BSGW), os resultados mostraram comportamentos distintos em temperaturas específicas, com mudanças significativas em temperaturas de secagem. O aumento da umidade relativa e a redução da temperatura levaram a um aumento na umidade de equilíbrio. As propriedades de ligação à água foram ligeiramente prejudicadas pelos maiores teores de proteína observados em BSGW. O modelo GAB foi eficaz na descrição das isotermas de adsorção, fornecendo informações sobre a umidade da monocamada em uma ampla faixa de temperatura. As análises termodinâmicas evidenciaram que os processos de adsorção foram impulsionados pela entalpia e não ocorreram espontaneamente. Uma umidade relativa de 40% foi identificada como ideal para o armazenamento dos BSGs.

Por sua vez, o processamento alcalino com peróxido de hidrogênio (AHP) afetou a composição química, estrutura e propriedades reológicas do BSG. A concentração de AHP e o tempo de processamento melhorou a remoção de proteínas, lignina e extrativos do BSG, aumentando a celulose e hemicelulose no material pré-tratado. Mudanças morfológicas foram observadas, incluindo afinamento das paredes celulares e redução do tamanho das partículas. As suspensões de BSG apresentaram comportamento não newtoniano, com aumento da resistência ao fluxo devido ao incremento da concentração de AHP, BSG e, principalmente, tempo de processamento.

As diferentes estratégias com ultrassom (US) e/ou peróxido de hidrogênio alcalino (AHP) melhoraram o rendimento de extração e afetaram as propriedades estruturais e tecno-funcionais dos concentrados proteicos. A utilização de AHP (EAHP) ou US (EUS), e sua combinação (EAHPUS), resultou em uma matriz BSG mais acessível e em um melhor rendimento de extração proteica em comparação com o método convencional (EC). As mudanças observadas em EAHP, EUS e EAHPUS indicaram alterações nas estruturas secundárias das proteínas, com um aumento perceptível em estruturas parcialmente desordenadas e desordenadas. Além disso, houve um aprimoramento das propriedades tecno-funcionais, destacando-se a capacidade e estabilidade de emulsão e espuma, sendo atribuídas ao aumento da flexibilidade e desdobramento das proteínas.

Portanto, o peróxido de hidrogênio alcalino (AHP) e/ou ultrassom de alta intensidade (US) são abordagens promissoras para melhorar a extração de proteínas e aumentar a acessibilidade do BSG pré-tratado para facilitar sua sacarificação subsequente. Esses avanços não apenas contribuem para a estabilização e aproveitamento sustentável do BSG, mas também viabilizam futuras aplicações alimentícias e/ou em biorrefinarias, impulsionando a conversão do BSG em produtos de valor agregado.

REFERÊNCIAS

VILELA, C. A. A., ARTUR, P. O. Drying of Curcuma longa L. in different shapes. **Food Science and Technology**, v. 28, n. 2, p. 387–394, 2008.

AGRAWAL, D., GOPALIYA, D., WILLOUGHBY, N., KHARE, S. K., & KUMAR, V. (2023). Recycling potential of brewer's spent grains for circular biorefineries. **Current Opinion in Green and Sustainable Chemistry**, 40, 100748.

BHARGAVA, N., MOR, R. S., KUMAR, K., & SHARANAGAT, V. S. Advances in application of ultrasound in food processing: A review. **Ultrasonics sonochemistry**, v. 70, p. 105293, 2021.

BOREL, L. D., LIRA, T. S., RIBEIRO, J. A., ATAIDE, C. H., & BARROZO, M. A. Pyrolysis of brewer's spent grain: Kinetic study and products identification. **Industrial Crops and Products**, v. 121, p. 388–395, 2018.

CABRERA, E., MUÑOZ, M. J., MARTÍN, R., CARO, I., CURBELO, C., & DÍAZ, A. B. Alkaline and alkaline peroxide pretreatments at mild temperature to enhance enzymatic hydrolysis of rice hulls and straw. **Bioresource Technology**, v. 167, p. 1–7, 2014.

CHIELLE, D. P., BERTUOL, D. A., MEILI, L., TANABE, E. H., & DOTTO, G. L. Spouted bed drying of papaya seeds for oil production. **LWT - Food Science and Technology**, v. 65, p. 852–860, 2016.

CORREA, P. C., BAPTESTINI, F. M., VANEGAS, J. D., LEITE, R., BOTELHO, F. M., & OLIVEIRA, G. H. D. Kinetics of water sorption of damaged bean grains: Thermodynamic properties. **Revista Brasileira de Engenharia Agrícola e Ambiental**, v. 21, n. 8, p. 556–561, 2017.

FREITAS, M. L. F., POLACHINI, T. C., DE SOUZA, A. C., & TELIS-ROMERO, J. Sorption isotherms and thermodynamic properties of grated Parmesan cheese. **International Journal of Food Science and Technology**, v. 51, n. 1, p. 250–259, 2016.

HALDAR, D.; PURKAIT, M. K. A review on the environment-friendly emerging techniques for pretreatment of lignocellulosic biomass: Mechanistic insight and advancements. **Chemosphere**, v. 264, p. 128523, 2021.

HASSAN, S. S.; WILLIAMS, G. A.; JAISWAL, A. K. Emerging technologies for the pretreatment of lignocellulosic biomass. **Bioresource Technology**, v. 262, p. 310–318, 2018.

HO, M. C.; ONG, V. Z.; WU, T. Y. Potential use of alkaline hydrogen peroxide in lignocellulosic biomass pretreatment and valorization – A review. **Renewable and Sustainable Energy Reviews**, v. 112, p. 75–86, 2019.

KUMAR, B., BHARDWAJ, N., AGRAWAL, K., CHATURVEDI, V., & VERMA, P. Current perspective on pretreatment technologies using lignocellulosic biomass: An emerging biorefinery concept. **Fuel Processing Technology**, v. 199, p. 106244, 2020.

KUMARI, D.; SINGH, R. Pretreatment of lignocellulosic wastes for biofuel production: A critical review. **Renewable and Sustainable Energy Reviews**, v. 90, p. 877–891, 2018.

MELLO, L. R. P. F.; MALI, S. Use of malt bagasse to produce biodegradable baked foams made from cassava starch. **Industrial Crops and Products**, v. 55, p. 187–193, 2014.

MORENO, Á. H., AGUIRRE, Á. J., MAQUEDA, R. H., JIMÉNEZ, G. J., & MIÑO, C. T. Effect of temperature on the microwave drying process and the viability of amaranth seeds. **Biosystems Engineering**, v. 215, p. 49–66, 2022.

PABBATHI, N. P. P., VELIDANDI, A., POGULA, S., GANDAM, P. K., BAADHE, R. R., SHARMA, M., GUPTA, V. K. Brewer's spent grains-based biorefineries: A critical review. **Fuel**, v. 317, p. 123435, 2022.

POLACHINI, T. C., MULET, A., TELIS-ROMERO, J., & CARCEL, J. A. Acoustic fields of acid suspensions containing cassava bagasse: Influence of physical properties on acoustic attenuation. **Applied Acoustics**, v. 177, p. 107922, 2021.

ROSA, D. P., CANTÚ-LOZANO, D., LUNA-SOLANO, G., POLACHINI, T. C., & TELIS-ROMERO, J. Mathematical modeling of orange seed drying kinetics. **Ciência e Agrotecnologia**, v. 39, n. 3, p. 291–300, 2015.

SARAVANAN, A., KUMAR, P. S., JEEVANANTHAM, S., KARISHMA, S., & VO, D. V. N. Recent advances and sustainable development of biofuels production from lignocellulosic biomass. **Bioresource Technology**, v. 344, p. 126203, 2022.

GALLEGO-JUÁREZ, J. A., HOLMES, M., POVEY, M., SALAZAR, J., CHÁVEZ, J., TURÓ, A., & BENEDITO, J. **Ultrasound in food processing: Recent advances**. Ed. John Wiley & Sons, 544p., 2017.

WOLF, M.; PAULINO, A. T. Full-factorial central composite rotational design for the immobilization of lactase in natural polysaccharide-based hydrogels and hydrolysis of lactose. **International Journal of Biological Macromolecules**, v. 135, p. 986–997, 2019.

YOSHIDA, B. Y.; PRUDENCIO, S. H. Alkaline hydrogen peroxide improves physical, chemical, and techno-functional properties of okara. **Food Chemistry**, v. 323, p. 126776, 2020.

APENDICE A - SUGESTÃO DE TRABALHOS FUTUROS

Caracterizações que ainda poderiam ser realizadas no concentrado proteico (CP) do bagaço de malte visando aprofundar sua análise e compreensão, proporcionando uma melhor compreensão das propriedades físicas, químicas e funcionais desse material.

- **Purificação com membrana de diálise**: Realizar a purificação do CP utilizando membranas de diálise para remover impurezas e componentes de baixo peso molecular, garantindo maior pureza e concentração de proteínas no produto;

- **Composição química**: Determinar a composição química do CP em termos de celulose, hemicelulose e lignina para compreender a proporção de componentes presentes e sua influência nas propriedades do concentrado;

- **Perfil de solubilidade e carga eletrostática**: Avaliar o perfil de solubilidade do CP em diferentes pHs e determinar sua carga eletrostática (potencial zeta) para entender sua estabilidade em dispersões aquosas e sua capacidade de interagir com outras substâncias;

- **Tamanho molecular por SDS-PAGE**: Utilizar a eletroforese em gel de poliacrilamida (SDS-PAGE) para determinar o impacto dos diferentes tratamentos no tamanho molecular das proteínas presentes no CP;

- **Propriedade gelificante**: Avaliar a capacidade do CP de formar géis em diferentes condições de processamento, como temperatura e pH, para entender seu potencial em aplicações de gelificação e espessamento;

- **Dicroísmo circular**: Análise alternativa para avaliar a estrutura secundária das proteínas no CP, permitindo a identificação de elementos estruturais como α-hélices e folhas β, além de comparar com os resultados obtidos pela técnica de FTIR;

- **Análises térmicas (TGA, DTG e DSC):** Realizar análises térmicas, como termogravimetria (TGA), análise termogravimétrica diferencial (DTG) e calorimetria diferencial de varredura (DSC), para investigar a estabilidade térmica e as transições de fase do CP.

- **Perfil de aminoácidos**: Determinar o perfil de aminoácidos do CP para avaliar sua qualidade nutricional e comparar com as recomendações dietéticas, informações importantes para formulação de produtos alimentícios e suplementos nutricionais.

Caracterizações que poderiam ser feitas no bagaço de malte desproteinizado e pré-tratado visando compreender aas mudanças estruturais ocorridas durante o pré-tratamento.

- **Determinar a composição química** do bagaço pré-tratado em termos de celulose, hemicelulose e lignina para avaliar a remoção de proteínas e o impacto do pré-tratamento nas frações de biomassa.

- **Distribuição de tamanho de partículas por difração a laser** para investigar possíveis alterações na morfologia e granulometria do bagaço após o tratamento.

- **Hidrólise enzimática do bagaço desproteinizado** para avaliar a susceptibilidade à degradação enzimática e potencial de produção de açúcares fermentescíveis.

- **Cinética de liberação de açúcar e perfil desses açúcares** para determinar a eficiência do pré-tratamento na conversão da biomassa em açúcares utilizáveis para processos fermentativos.

Análise energética/econômica para avaliar se os custos energéticos associados ao uso do ultrassom reduzem significativamente o tempo de processamento ou

contribuem para uma redução substancial no uso de produtos químicos durante as etapas de pré-tratamento, rendimento/extração de proteínas, sacarificação do BSG desproteinizado;

Estudar o pré-tratamento assistido por ultrassom utilizando diferentes catalisadores como outros álcalis, ácidos, enzimas e agentes oxidantes;

O desenho de um processo ampliado assistido por ultrassom para tratar maior volume de suspensões;

Aplicações do bagaço de malte, concentrado proteicos e fibra lignocelulósica:

Considerando aplicações em alimentos, o processo de extração de proteínas da BSG resulta em dois principais ingredientes: uma **fração rica em proteínas** e outra **rica em fibras**. Essas frações têm potencial para serem utilizadas na produção de produtos de panificação, como massas, extrusados e pães, enriquecidos com fibras e/ou proteínas. O uso dessas frações pode impactar as propriedades nutricionais, texturais, reológicas e sensoriais, quando comparados aos produtos tradicionais.